OCS Study
BOEM 2013-01130

High-resolution Aerial Imaging Surveys of Marine Birds, Mammals, and Turtles on the US Atlantic Outer Continental Shelf—Utility Assessment, Methodology Recommendations, and Implementation Tools

Final Report

U.S. Department of the Interior
Bureau of Ocean Energy Management
Headquarters

OCS Study
BOEM 2013-01130

High-resolution Aerial Imaging Surveys of Marine Birds, Mammals, and Turtles on the US Atlantic Outer Continental Shelf—Utility Assessment, Methodology Recommendations, and Implementation Tools

Final Report

Authors

Caleb Gordon
Michael Kujawa
Jason Luttrell
Donald MacArthur
Julia Robinson-Willmott
Chris Thaxter

Prepared under BOEM Contract M10PC00099
by
Normandeau Associates, Inc.
102 NE 10th Avenue
Gainesville, FL 32601

Published by
U.S. Department of the Interior
Bureau of Ocean Energy Management
Headquarters

Herndon, VA
April 2013

DISCLAIMER

This Final Report was prepared under contract between the Bureau of Ocean Energy Management (BOEM) and Normandeau Associates, Inc. The document has been technically reviewed by the BOEM and has been approved for publication. Approval does not signify that the contents necessarily reflect the view and policies of BOEM, nor does mention of trade names or commercial products constitute endorsement or recommendations for use. It is, however, exempt from review and in compliance with BOEM editorial standards.

AVAILABILITY

The report may be downloaded from the boem.gov website through the Environmental Studies Program Information System (ESPIS). You will be able to obtain this report also from the National Technical Information Service in the near future at this address:

U.S. Department of Commerce
National Technical Information Service
5285 Port Royal Road
Springfield, Virginia 22161
Phone: (703) 605-6040
Fax: (703) 605-6900
Email: bookstore@ntis.gov

CITATION

Suggested Citation:

Normandeau Associates, Inc. 2012. High-resolution Aerial Imaging Surveys of Marine Birds, Mammals, and Turtles on the US Atlantic Outer Continental Shelf—Utility Assessment, Methodology Recommendations, and Implementation Tools for the US Dept. of the Interior, Bureau of Ocean Energy Management. Contract # M10PC00099. 378 pp.

ABOUT THE COVER

Cover photos courtesy of Normandeau Associates, Inc.

Preface and Acknowledgments

This report details the objectives, structure, scope, results, and conclusions of the US Department of the Interior, Bureau of Ocean Energy Management (BOEM) contract #M10PC00099, titled "Pilot Study of Aerial High-definition Surveys for Seabirds, Marine Mammals and Sea Turtles." This project was awarded by BOEM (then Bureau of Ocean Energy Management, Regulation, and Enforcement, BOEMRE) to Normandeau Associates, Inc. (then Pandion Systems, Inc.) on 22 Sep 2010 with an expected period of performance of two years from the award date. The objectives of this study, as stated in the contract, were as follows:

> to develop and test a methodology for conducting surveys of birds, marine mammals, and sea turtles in the offshore environment using state of the art survey techniques that are efficient and provide high quality, reproducible data.

This objective was largely inspired by pioneering European offshore wind-wildlife studies using high-resolution aerial imaging survey methodologies. Several such studies are cited in the original Request for Proposal (RFP) and in the contract, including an article by Drs. Chris Thaxter and Niall Burton (2009) of the British Trust for Ornithology (BTO), who reviewed European high-resolution aerial imaging survey methodologies as applied to offshore wind-wildlife studies in the late 2000s, as a follow up to a workshop held in the UK in 2009 on these methodologies, sponsored by the Collaborative Offshore Wind Researches Into the Environment (COWRIE) consortium.

BOEM's desire to "build on the European experience" was specified in the contract's scope of work, which also further defined the project's objectives and scope to specifically include high-resolution aerial imaging surveys and several other criteria and qualifiers as follows: "[BOEM] seeks to establish a safe, effective, affordable and scientifically valid sampling protocol for high-[resolution] aerial transect surveys to determine seasonal and annual variation in distributions and abundances of birds along the Atlantic coast of the United States from the shoreline to 30 miles offshore and to test the utility of the technique for surveys of marine mammals and sea turtles, as well as birds."

These objectives were translated into a set of tasks and expected project outcomes (deliverables) in the contract as follows:

Tasks (not including administrative, meeting, reporting)

- Evaluate aircraft for safety and effectiveness offshore
- Evaluate high [resolution] cameras and mounting systems
- Develop protocols for camera control and operation
- Evaluate and recommend [onboard] data recording systems
- Propose a valid survey sampling grid or grids and estimate the cost per square mile surveyed
- Develop software to automate data analysis
- Evaluate effectiveness of high-[resolution] aerial transects for surveys of [birds], marine mammals, and sea turtles.

Deliverables (including specified sections of final project report)

- Evaluation of, and recommendations for, specific candidate technologies for conducting aerial high-resolution wildlife imaging surveys, including aircraft, cameras, mounts, digital recorders, and camera control and calibration systems (see tasks listed above).
- Protocol(s), including cost estimates for all stages up to and including data analysis, for conducting aerial high-resolution imaging surveys for the purpose of characterizing seasonal and annual distribution and abundance of birds, marine mammals, and sea turtles from the coast to 30 miles offshore, and from the Maine/Canada border to Miami, FL.
- Software (and accompanying user's manual) to automate digital survey data extraction and image processing to the extent possible, particularly to separate out "zero" frames, and identify potential animals in the captured imagery.
- Evaluation of the effectiveness of digital high-resolution imaging surveys for detecting and identifying birds, mammals, and sea turtles in marine environments, and for characterizing their seasonal and annual distribution patterns, in comparison to the effectiveness of conventional, visual observer based surveys using boats and low flying aircraft.

Our approach to satisfying these objectives, performing these tasks, and producing these deliverables was three-pronged, as follows:

1) Assemble a project team containing world-leading experts in the various specialized fields of study entailed in the study's scope. The specific personnel and organizations that comprised the project team are described below, and collectively encompassed all of the technological and biological facets of the project including aviation (manned and unmanned aircraft systems), high-resolution imaging and image processing, marine biology (birds, marine mammals, sea turtles), and European experience with high-resolution imaging surveys as applied to offshore wind-wildlife studies. The collective expertise of our team enabled us to develop state-of-the-art high-resolution imaging systems for use in experimentation. Our team's expertise also enabled us to perform the evaluation and recommendation components of this study, with experts in their respective fields gathering and synthesizing current information from technical literature and current commercial practice, and then evaluating experimental results to assess effectiveness and develop recommendations.

2) Conduct experimental surveys. The experimental field studies we conducted offshore of Oak Island, North Carolina during May 2011 (Operations House [Op House] see Chapter 1) served as the core of this study, providing the data from which most of the evaluations, protocols, and software deliverables of this study were derived. We applied an experimentalist paradigm to these field surveys, performing offshore aerial high-resolution wildlife imaging survey trials with a variety of imaging treatment combinations (e.g., image resolution, camera tilt, flight altitude), alongside control surveys conducted with conventional survey methodologies using expert visual observers aboard a boat (vessel) and a low flying aircraft. We also conducted a variety of smaller scale imaging survey trials using an unmanned aircraft system (UAS).

3) Manually review high-resolution imagery. We conducted a comprehensive, manual review of all of the imagery gathered during the imaging experiments with the manned aircraft (Op House flight trials) described above, to discover and extract all images of animals captured in the surveys along

with all relevant metadata. This review, and the resulting archive of animal images, provided essential raw material for the development of automated animal recognition software, and also served as the basis for our evaluations of the effectiveness of the specific high-resolution imaging configurations we tested during our experiments. These evaluations, in turn, served as the basis for the development of the high-resolution imaging protocols we present in this report, which are intended to provide practical, feasible, and complete sets of instructions and cost estimates for conducting safe, cost-effective, and scientifically optimized study designs for the characterization of marine bird, sea turtle, and mammal distribution and abundance patterns on the US Atlantic Outer Continental Shelf (AOCS), using aerial high-resolution imaging surveys.

Project Team, Roles, and Contributions: We acknowledge the contributions of many individuals and organizations to this project. These individuals are listed in below, along with the institutional affiliation and project role of each.

Project Personnel with Institutional Affiliation and Project Role.

Name	Organization	Role
Lisa Algarin	BSEE	Contract Officer
Mary Jo Barkaszi	ECOES Consulting, Inc.*	Op House visual-observer survey manager, marine mammal and sea turtle expert, contributing author
Wes Biggs	Normandeau	Bird observer
Richard Brown	ECOES Consulting, Inc.	Mammal/turtle observer
Niall Burton	BTO	Contributing ornithologist
Jenny Carter	Normandeau	Administrative manager, document production, editing
Randall “RJ” Clark	Pinnacle 1 Aviation	Aviation coordinator, contributing author
Stephen Cluff	Boulder Imaging	Target detection algorithm developer
Emily Cochran	Normandeau	Image analysis
Ed Coffman	Orion Aviation	Aviation service provider
Timothy Cole	NOAA	Project liaison, technical contributor to protocol section
Stephen Earsom	USFWS	Project liaison, technical contributor to protocol section
Natalie Elorza-Welling	Normandeau	Image analysis
Greg Forcey	Normandeau	Contributing ornithologist, statistical and modeling analysis
Caleb Gordon	Normandeau	Project manager, lead scientist and ornithologist, lead author, Op House director, bird observer

Project Personnel with Institutional Affiliation and Project Role.		
Name	**Organization**	**Role**
Charles Grandgent	Normandeau	Information technology engineer/designer
Jennifer Grindle	Normandeau	Image analysis
Alexis Hampton	Normandeau	Administrative coordinator
Eric Haney	Normandeau	Bird observer
Rachel Hardee	ECOES Consulting, Inc.	Mammal/turtle observer, sea turtle expert image analyst
Christy Harrington	A.I.S Observers, Inc.	Mammal/turtle observer
Mitch Harris	Normandeau	Bird observer
David Hartgrove	Normandeau	Bird observer
Robert Hasevlat	Normandeau	Safety coordinator
Stan Huddles	Orion Aviation	Pilot
Carlos Jorquera	Boulder Imaging	Chief image acquisition/processing engineer
Binab Karmacharya	Normandeau	Contributing wildlife biologist and author, image analyst, statistical and modeling analysis
Adam Kent	Normandeau	Contributing ornithologist, image analysis
Chelsea Kosobucki	Normandeau	Image analysis
Michael Kujawa	Gemini Renewables	Technical manager, contributing author
Jie Kulbida	Boulder Imaging	Target detection algorithm developer
Jason Luttrell	Boulder Imaging	Image acquisition/processing engineer, contributing author, Op House imaging manager, target detection algorithm developer
Donald MacArthur	IA Tech, Inc.	Unmanned aircraft system engineer, contributing author
Erica MacArthur	IA Tech, Inc.	Unmanned aircraft system engineer, contributing author
Allison MacConnell	A.I.S Observers, Inc.	Mammal/turtle observer
Jeff Martin	ECOES Consulting, Inc.*	Op House technical equipment coordinator
Christina Maurice	Normandeau	Image analysis
Jerry Morris	Orion Aviation	Pilot

Project Personnel with Institutional Affiliation and Project Role.		
Name	**Organization**	**Role**
Christian Newman	Normandeau	Project director
Cameron Radford	Orion Aviation	Pilot
Ron Shrek	Orion Aviation	Pilot
Luke Szymanski	AIS Observers, Inc.	Op House vessel-based-visual survey coordinator
Chris Thaxter	BTO	Contributing ornithologist and author
Michelle Vukovich	Normandeau	Contributing wildlife biologist and author, image analyst
Julia Willmott	Normandeau	Project coordinator, contributing ornithologist and author, Op House coordinator, visual observer survey crew manager, bird observer, image analysis manager, data analysis
James Woehr	BOEM	Contracting officer's representative
Renée Zenaida	Normandeau	Lead editor, document production

* Currently with Continental Shelf Associates, Inc.

Additional Acknowledgements: In addition to the people and institutions whose contributions to this project are described in the table above, the project team wishes to acknowledge several additional individuals and institutions that made valuable contributions to this project, as follows:

- The staff of all subcontractors' institutions for administrative and technical support
- The owner, crew, and captain of the Voyager
- Stuart Clough (APEM, Ltd) and Ib Krag Petersen (NERI) for information about the offshore digital imaging survey methodologies used by their respective organizations
- Additional project liaisons, including Michael Rasser, David Bigger, Tre Glenn, Kimberley Skrupky, Sally Valdes, and Brian Hooker of BOEM; Emily Silverman and Tim Bowman of USFWS
- Assistance in developing the glare mitigation tool (formula for calculating angular deviation from the glint spot) was provided by Dr. R. Scott Schappe, Department of Physics, Lake Forest College, and Dr. Neal White, Department of Mathematics, University of Florida
- Keith Willmott provided assistance with geospatial data analysis from Op House imaging surveys, as well as assistance with statistical comparisons of animal density data for the three-platform methodological comparisons from the Op House survey data.
- Additional administrative and managerial staff of Normandeau Associates

Guide to the structure and origin of the content of this report: The main body of this report contains a diversity of different types of content—reflecting the diverse nature of the tasks and specific deliverables that were outlined in the contract. Herein, we provide a brief guide to the nature of the

different sections, as well as the different project team members who were the primary contributors to each original content section.

Introduction (Chapter 1)—This section was written by Normandeau, except for the subsection titled, Review of European Chronology of Transition to Digital Surveys and Regulatory Acceptance of Digital Data for Offshore Wind Ecological Studies (section 1.2),which was contributed by BTO's Dr. Chris Thaxter.

Experimental Design and Execution (Chapter 1)—This section describes the design and execution of all fieldwork performed over the course of the study, including experimental and supplemental imaging flights with the manned aircraft-based imaging system and associated control visual observer based surveys by vessel and low flying aircraft (Op House), as well as all imaging flights conducted with the UAS. The write-up of the Op House section was developed by Normandeau, while the write-up of the UAS-based section was developed by Don and Erica MacArthur, IATech, Inc.

Technical Analysis and Evaluations (Chapter 3)—This section presents our evaluations and recommendations regarding the different technological elements of high-resolution survey systems. Each subsection corresponds to a different task in the contract (as noted below), and was developed by different technological specialists, as follows:

> *Introduction (section 3.1)—Normandeau Associates*
>
> *Aircraft Evaluation (section 3.2, contract task 2)—Michael Kujawa, Gemini Renewables, and Randall Clark, Pinnacle 1 Aviation (manned aircraft, section 2.2), Donald and Erica MacArthur, IATech, Inc. (unmanned aircraft, section 2.3).*
>
> *Camera and Mounting System Evaluation (section 3.3, contract task 3): Jason Luttrell, Boulder Imaging (manned aircraft, section 3.3.2), Donald and Erica MacArthur, IATech, Inc. (unmanned aircraft, section 3.3.3).*
>
> *Camera Control and Calibration Procedures (section 3.4, contract task 4): Jason Luttrell, Boulder Imaging (manned aircraft, section 3.4.2), Donald and Erica MacArthur, IATech, Inc. (unmanned aircraft, section 3.4.3).*
>
> *Evaluation of Onboard Data Recording Systems (section 3.5, contract task 5): Jason Luttrell, Boulder Imaging (manned aircraft, section 3.5.2), Donald and Erica MacArthur, IATech, Inc. (unmanned aircraft, section 3.5.3).*

Protocols for Conducting High-resolution Wildlife Imaging Surveys in Support of Offshore Wind Development on the Atlantic Outer Continental Shelf (Chapter 4)—In this chapter, we present a set of three protocols, each corresponding to a different spatial scale (entire AOCS, regional, and project scales), for conducting aerial high-resolution wildlife imaging surveys on the AOCS for birds, marine mammals, and sea turtles. These protocols are included as per the specifications of task 6 of the contract, and include total project cost estimates up to and including data analysis. They are intended to be complete, pragmatic, feasible, and optimized for cost effectiveness, resting upon the results of the analyses and evaluations of candidate technologies and methodological choices presented in the other sections of this report. In addition to the protocols themselves, this chapter

includes a discussion of sun glare, including anticipated impacts of sun glare on high-resolution imaging surveys on the AOCS, and an originally developed analytic tool for mitigating these impacts in conjunction with a specialized camera mount. This chapter also includes a discussion of selected statistical and survey design methodological issues based on European experience, contributed by Chris Thaxter of the BTO. All of the other subsections of this chapter were developed by Normandeau Associates.

Target Detection Algorithm (Chapter 5)—In this chapter, we present a narrative description of the development, testing, and evaluation process for the target (animal) detection algorithm(s) that were developed for this project, and included along with this report as a deliverable, as per task 7 of the contract. The original algorithms were developed by image processing software engineers at Boulder Imaging, ground-truthed using the raw material from the manual review of experimental images that were gathered during the Op House flight trials by the project team. The image capture during Op House was also performed directly by Boulder Imaging personnel, and the manual image review process was performed by Normandeau Associates' image analysts at their image analysis laboratory in Gainesville, FL, coordinated and supervised by Julia Willmott (see Table 2–1). The text of this section was developed primarily by Jason Luttrell and Stephen Cluff of Boulder Imaging (software development, section 5.2.2), Normandeau. The supplemental materials (Supplemental Volumes II, and III) associated with this section include the target detection algorithms, produced by Boulder Imaging, upon their pre-existing, proprietary Quazar software platform, a Quazar user's manual, produced by Boulder Imaging, and an image gallery, containing all of the images of animals discovered in the Op House imagery that were of decent or better quality. The image gallery was produced by Julia Willmott of Normandeau Associates (Supplemental Volume I).

Evaluation of Effectiveness of High-definition Aerial Image Gathering for Conducting Surveys of Marine Birds, Turtles, and Mammals (Chapter 6)—This chapter corresponds to task 8 in the contract, and presents a biological analysis of the effectiveness of aerial high-resolution imaging for conducting offshore surveys of marine birds, mammals, and turtles for the purpose of characterizing seasonal and annual patterns of distribution and abundance of these animals on the AOCS. This chapter is divided into five subsections, as follows

Introduction (section 6.1) Normandeau Associates

Review of European Experience (section 6.2) Chris Thaxter, BTO.

Comparison of Digital and Visual Observer-based Methods for Surveying Birds, Turtles, and Mammals in Marine Environments (section 6.3) Normandeau Associates.

Impacts of Selected High-resolution Imaging Parameters on Image Quality and Animal Identification Capability (section 6.4) Normandeau Associates.

Taxonomic Guide to the Utility of High-resolution Aerial Wildlife Imaging Surveys on the Atlantic Outer Continental Shelf (section 6.5) Normandeau Associates, and Mary Jo Barkaszi, Continental Shelf Associates.

Summary

We conducted a two-year study intended to develop and test high-resolution digital aerial imaging survey methodologies in order to evaluate their effectiveness, and to provide protocols and other tools for implementing this new methodology for the purpose of characterizing the seasonal and annual patterns of abundance and distribution of marine birds, mammals, and sea turtles on the US Atlantic Outer Continental Shelf (AOCS). Factors contributing to BOEM's interest in this new survey methodology include 1) significant and growing interest in offshore wind energy development on the US AOCS, which necessitates broad scale environmental risk/impact studies over this vast and difficult-to-access region; 2) scarcity of existing baseline data on birds, marine mammals, and sea turtles on the US AOCS; 3) significant concerns regarding the safety, cost, and data quality of conventional marine wildlife survey methodologies; and 4) pioneering high-resolution aerial imaging studies in Europe, which suggest that this new methodology holds a great deal of potential for providing the wildlife data needed to support the development of an offshore wind energy industry.

The overarching conclusion of this study is that high-resolution digital aerial imaging does, indeed, represent a safe, scientifically robust, and cost-effective solution to the offshore wildlife data collection needs of BOEM and the US offshore wind energy industry. This conclusion is broken down in terms of specific consideration of three criteria, as follows:

- **Cost**. High-resolution digital aerial imaging (aircraft based) survey costs are approximately equal to or significantly less expensive than (vessel based) conventional, visual observer based marine wildlife surveys. The cost savings of aerial surveys relative to vessel based is most significant for large survey areas ($\geq$ 150 km^2), but this also holds for survey areas roughly the size of single, commercial scale offshore wind energy facilities ($\approx$ 150 km^2), primarily due to the slow speed of vessels compared with aircraft. These cost comparisons are inclusive of the entire survey effort up to and including data analysis.
- **Safety**. Although vessel based surveys could be regarded as safer than aerial surveys, among the more efficient and cost-effective aerial surveys, high-resolution digital aerial imaging surveys are safer than are conventional, visual observer based aerial surveys. This difference owes entirely to higher flight altitudes (450 to 1,000 m for digital, 50 to 150 m for observer based), which allow more time for corrective response or escape of onboard personnel from the vehicle in the event of aviation errors or aircraft malfunctions.
- **Effectiveness.** The advantages of high-resolution digital aerial imaging surveys over conventional methods are most significant with respect to this criterion, though some exceptions exist. Summaries of conclusions for different aspects of this criterion are listed below:
    - Digital methods yield more accurate density calculations, with one exception
        - Counts not distorted by animals' attraction to, or repulsion from vehicle—direct methodological comparisons demonstrated that aerial visual observer surveys miss 75% of sea turtles, presumably because most turtles dive prior to being observed when aircraft fly at the lower altitudes required for visual observation

        - Survey swath calculated precisely from image, not subject to observers' error-prone distance estimations
        - No observer swamping or search image effects
        - Interobserver variability can be reduced through post-hoc multiple observer quality assurance/quality control (QA/QC) image review
        - Baleen whales may represent an exception, where rarity, long submersion times, and long distance visibility of intermittent cues (blows, flukes, breaches) may give visual observer based methods an advantage
    - Digital methods using 2.5 cm image resolution or finer yield more reliable determination of animals' taxonomic identity among aerial survey methods, but vessel based methods may retain an advantage for species-level determinations for the most difficult to distinguish sets of taxa
        - Determinations are made post-hoc in digital surveys, using a pre-observer image archive, not requiring near-instantaneous judgments by observers
            - Morphometric measurements of animals inform determinations
            - Different images can be compared directly to one another
            - Identification reference manuals can be consulted
            - Multiple-observer QA/QC image review enables measurement of agreement levels, consistency and reliability of determinations, reduction or elimination of sources of observer error
        - Vessel based visual observer methods are advantageous for the most difficult species-level determinations, because vessel based observers may integrate multiple live cues for identification, including sound, behavior, continuous viewing for an interval of time, not available for aerial visual or image based determinations.
        - Taxonomic determination depth from images depends on image clarity, and is generally only competitive with, or better than visual observer based methods at image resolutions of 2.5 cm or finer, particularly 1.5 cm or finer

In addition to these broad, overarching summary conclusions, this study yielded two other types of general outcomes. The first consists of a variety of more technologically oriented conclusions and recommendations based on the technology-focused review and evaluation components of this study. These elements are summarized in the "Summary of Technology Evaluation Components" subsection below. The second consists of a variety of tools that were developed in order to facilitate the implementation of aerial high-resolution wildlife imaging surveys on the AOCS. These elements are summarized in the "Summary of New Tools for High-resolution Imaging" subsection below.

Summary of Technology Evaluation Components

Aircraft. The type of aircraft that is optimal for conducting offshore aerial high-resolution wildlife imaging surveys may vary depending on the size of the area to be surveyed, and the regulatory landscape for the use of unmanned aircraft systems (UAS). However, under most circumstances, a

small, fixed wing aircraft will be the most cost-effective solution. The aircraft should possess a belly hatch sufficiently large to accommodate the cameras and mounts described below, although external mounting is also possible. The plane must be sufficiently large to safely and comfortably accommodate all of the imaging system hardware plus three people (two pilots, one camera operator). Lower accident rates, longer endurance, greater fuel efficiency, and widespread availability are also important attributes. A number of commercially available fixed-wing manned aircraft are evaluated and compared with respect to a wide range of suitability criteria in section 3.2. Helicopters are significantly more expensive for an equivalent payload capacity and survey area, and hence only potentially competitive for very small surveys. UAS represent a promising technology for future applications, particularly because of the potential safety and cost benefits of unmanned operation, but current US federal use restrictions and certification processes preclude feasible and cost-effective use of UAS for conducting offshore aerial high-resolution wildlife imaging surveys

Cameras. The most suitable camera type for conducting offshore aerial high-resolution wildlife imaging surveys is an area-scan camera, equipped with a high quality lens for optical magnification sufficient to achieve image resolutions of 2.5 cm or finer (ideally 1.5 cm or finer). The use of polarized light filters is not recommended, as such filters do not significantly improve image quality, and because very fast exposure times require maximum use of available ambient light. The size of the image, in megapixels, is an extremely important factor in optimal equipment selection. More megapixels is better, as larger images enabling wider survey swaths for a given image resolution level, or finer resolution imaging for a given survey swath width. The use of a mechanical shutter is recommended for reducing image smear effects, and fast exposure times (generally less than the time it takes for the aircraft to travel the distance of one pixel imaged on the water's surface, equals 100 to 200 microsecond exposure times in our experiments) are essential for producing low blur images. Line-scan cameras offer some advantages in terms of cost per megapixel and color definition of images, but their increased sensitivity to vibrational effects relative to area-scan cameras significantly limits their effectiveness.

Mounts. Gyrostabilization and in-flight camera angle adjustability are both essential requirements for mounting high-resolution cameras in survey aircraft for conducting offshore aerial high-resolution wildlife imaging surveys on the AOCS. Gyrostabilization significantly reduces vibrational effects, improving image clarity and quality. In-flight camera angle adjustability enables in-flight sun glare mitigation (directing the camera away from the sun's reflection on the water's surface), which is essential on the US AOCS, where adjustable angle mounts roughly double the amount of low-glare daylight survey time compared to any fixed angle mount. This is a distinct difference between the US and the northwestern European areas where high-resolution imaging has been pioneered. In northwestern Europe, higher latitudes and correspondingly lower angles of insolation reduce the importance of adjusting camera angles in flight for sun glare mitigation. Internally mounted imaging systems are preferable to externally mounted imaging systems because of increased protection from moisture and increased operator access and adjustability during flight, although a wide range of camera angles may be more difficult to achieve in internally mounted systems.

Optimal imaging configuration. Depending on the extent to which species-level identifications of imaged animals is important, and depending on the visual and morphometric similarities among the co-occurring species of interest in a given survey area, image resolutions of 2.5 cm or finer are generally recommended, where image resolution is defined as the length of a side of a roughly

square single image pixel on the surface of the water being imaged below the aircraft. Image quality is not a simple function of image resolution; hence, many factors are important to consider when selecting an optimal imaging configuration for offshore aerial high-resolution wildlife imaging surveys (see above under Cameras). Optimal flight altitude will generally range from 450 m, which is a general minimum to avoid distorting counts by disturbing animals, up to 1,000 m, above which image quality degradation and interference due to clouds is likely to be unacceptable. We have demonstrated that images of acceptable quality can be generated from flight altitudes as high as 1,000 m, which is likely to be useful as improvements in camera technology generate larger image sizes, enabling wider imaging swaths. However, we also note that image quality generally degrades with increasing flight altitude, because higher flight altitude imaging either entails coarser image resolution for the same optical magnification, or higher optical magnification to achieve the same image resolution as a lower altitude flight. Higher optical magnification may result in increased image blur due to magnification of vibrational effects. Analysis of our experimental imagery revealed that camera angles as acute as 44° away from straight down can be implemented without significant degradation of image quality from pixel distortion. This suggests that effective protocols can be implemented using higher flight altitudes and angled cameras to achieve wider survey swaths, either by using multiple-camera mounts to generate wide composite-image survey swaths, or through advancements in camera technology (increased image sizes) that enable high-resolution imaging of wider swaths with one, or a few cameras.

Summary of New Tools for High-resolution Imaging

Automated animal detection algorithms. We generated two algorithms that can be used to automate the detection of animals in high-resolution marine wildlife survey imagery. These algorithms were both generated using Boulder Imaging's Quazar software as a platform, and the algorithms, themselves, as well as a Quazar user's manual, are submitted as supplemental volumes (Supplemental Volumes I, II, and III) to accompany this report. One algorithm, the blob detector, exclusively uses exposure contrasts to detect animals against the background of the ocean's surface. The other uses color-related attributes (hue, saturation, value) to discern animals and distinguish them from a background of water. Based on our evaluation of the performance of these algorithms on our experimental survey imagery, they should be regarded as preliminary versions, requiring significant additional research and development before they constitute effective and operational tools for automated image data processing. The blob detector is prone to high false negative rates (missed animal detections), and the color-related algorithm is prone to high false positive rates (failure to eliminate very many empty frames). Furthermore, significant improvement would need to be made in processing speed in order for either or both of these algorithms to run in real time during imaging surveys, which is necessary for large survey areas where complete capture of raw imagery is precluded because of data volume constraints. Because of the labor effort entailed in manual image data review, we conclude that an effective automated animal detection algorithm is an essential ingredient for conducting cost-effective high-resolution marine wildlife imaging surveys, particularly at spatial scales greater than the size of single commercial offshore wind energy projects. We also conclude that quality control checks, consisting of manual review of subsets of survey imagery to determine false positive and false negative rates of the automated animal detection algorithms, are a vitally important component of conducting scientifically valid and robust marine wildlife surveys using high-resolution aerial imagery.

Protocols for conducting high-resolution aerial wildlife imaging surveys on the AOCS. We developed protocols for conducting aerial high-resolution marine wildlife imaging surveys on the AOCS, intended as a guide to the basic hardware, staffing, methodological, and budgetary requirements entailed in conducting such surveys. These protocols describe the specific imaging hardware, survey platform, survey pattern and frequency, task structure, labor breakdown by staffer type, and annualized total costs under a variety of specified costing assumptions for complete imaging survey studies extending from survey planning and design up to and including data analysis and reporting. All of the recommended elements of these protocols were selected based on optimizing safety and cost effectiveness for the anticipated scientific objectives of the study, based on the reviews and evaluations of the different methodological components detailed in the other sections of this report and the collective technical expertise of the project team. Surveys of differently sized areas are likely to be driven by different scientific objectives with correspondingly different data gathering requirements. These differences, in turn, dictate different optimal survey protocols; hence, we developed three distinct protocols corresponding to three distinct spatial scales that may be of interest, as follows:

1) AOCS scale. This protocol is intended to cover the entire federally regulated portion of the US AOCS where offshore wind development is most desirable based on the wind resources, and most plausible using existing turbine foundation technology. This area extends from Maine to Florida, from the states' seaward boundaries (generally 3 n.m. from shore) up to the 30 m isobath, and measures 210,000 km^2. At this scale, coarse scale broad baseline data gathering objectives are most likely, which drove our selection of semiannual survey frequency, 10% subsampling, and 2 cm image resolution. This protocol was developed specifically for implementation using either of two existing US federal government wildlife survey aircraft fleets. The estimated annual cost of implementing this protocol is $1.9 to $2.2 million.
2) Regional scale. This protocol is intended to cover subsets of the whole AOCS region described above corresponding to single BOEM planning regions (e.g., northeast, midatlantic, southeast), or to the portions of the AOCS offshore of single states, or consortia of states, measuring on the order of 25,000 km^2. At this scale, data gathering objectives are likely to be finer than at the AOCS scale, but still somewhat broad in scope, along the lines of a regional baseline study. This drove our selection of quarterly survey frequency, 10% subsampling, and 1 cm image resolution. This protocol was developed assuming that a single charter aircraft would be used to conduct the surveys. The estimated annual cost of implementing this protocol is roughly $880,000.
3) Project scale. This protocol is intended to cover individual, commercial scale offshore wind energy facilities sited within the AOCS region described above, measuring on the order of 150 km^2. At this scale, data gathering objectives are likely to be more refined, and compliant with individual leasing and permitting environmental risk/impact analysis requirements. This drove our selection of 8 times per year survey frequency, 20% subsampling, and 1 cm image resolution. This protocol was developed assuming that a single charter aircraft would be used to conduct the surveys. The estimated annual cost of implementing this protocol is roughly $370,000.

One plank on which all of the recommended protocols in this report rest, and a critical consideration for any high-resolution offshore wildlife imaging survey protocol on the AOCS, is the avoidance of

sun glare. Within the protocols chapter (Chapter 4), we describe a glare threshold, above which images are rendered useless for animal detection. We determined this threshold based on analysis of our experimental imagery, and we define it as a 67° angular deviation of the camera angle from the glint spot, which is the camera orientation at which the camera would be pointed directly at the sun's reflection on the water's surface at a given geoposition at a given moment in time. In section 4.2, we demonstrate that using fixed camera angles, the amount of low glare daylight hours available for surveys is heavily restricted on the US AOCS, but can be roughly doubled by using a mount that can allow the cameras to be alternated between 44° rear tilt and 44° forward tilt in flight, with aircraft flying transects alternating between east to west, and west to east. All of our protocols were developed assuming that this particular mount configuration is used for sun glare mitigation. In the protocols chapter (Chapter 4), we also present an originally developed glare mitigation planning tool, consisting of a formula for calculating angular deviation from the glint spot (ADGS) for any geoposition at any time, using easily accessible input data on solar position, flight direction, and camera tilt.

Taxonomic guide to the utility of high-resolution aerial wildlife imaging surveys on the AOCS. A final tool presented in this report is a guide to diurnal high-resolution aerial imaging data gathering expectations and prospects for the bird, marine mammal, and sea turtle fauna of the US AOCS. This guide is intended to inform readers about the specific taxa for which they should, and shouldn't expect to obtain useful data using high-resolution aerial imaging survey methodology, as well as various behavioral and appearance factors of the animals that influence the nature and quality of the data that can potentially be obtained. Although high-resolution aerial imaging survey data cannot satisfy all of the data gathering requirements for birds, marine mammals, and sea turtles associated with offshore wind energy development on the AOCS, the taxonomic breadth of the this technique is a compelling and attractive feature. In the taxonomic guide, we identify 84 species of birds, 35 cetaceans, and five sea turtles, comprising all of the species in these groups that occupy any portion of the region of interest for any portion of the year, for which high-resolution aerial imaging surveys are expected to provide useful data. In many cases, the application of this new survey technique has the potential to radically improve scientific understanding of the biology of these animals on the AOCS. We excluded bird species such as most shorebirds and all songbirds that do not stop, rest, or feed within marine environments, even if they may pass through the AOCS as migrants, because the highly ephemeral occurrence of these species in this region renders effective image survey data gathering unlikely.

Table of Contents

List of Figures

List of Tables

Acronyms and Abbreviations

ADGS	angular deviation from the glint spot
agl	above ground level
ATC	Air Traffic Control
AIC	Akaike's information criterion
AMAPPS	Atlantic Marine Assessment Program for Protected Species
AOCS	Atlantic Outer Continental Shelf
BTO	British Trust for Ornithology
BOEM	Bureau of Ocean Energy Management
BOEMRE	Bureau of Ocean Energy Management, Regulation, and Enforcement
BSEE	Bureau of Safety and Environmental Enforcement
COA	Certificate of Authorization
CV	coefficient of variation
COWRIE	Collaborative Offshore Wind Researches into the Environment
COP	construction and operations plan
DVR	digital video recorder
ESA	Endangered Species Act
ESAS	European Seabirds at Sea
FAA	Federal Aviation Administration
FPN	fixed pattern noise
GAM	general additive model
GCS	ground control system
HPDVR	High-Performance Digital Video Recorder
HSV	hue-saturation-value
IFR	Instrument Flight Rules
JNCC	Joint Nature Conservation Commission
MMPA	Marine Mammal Protection Act
MP	megapixel
MW	megawatt
MBTA	Migratory Bird Treaty Act
MTF	modulation transfer function
NERI	National Environment Research Institute
NEPA	National Environmental Policy Act
NMFS	National Marine Fisheries Service–NOAA
NOAA	National Oceanic and Atmospheric Administration
NJDEP	New Jersey Department of Environmental Protection
PD	peak density

PIC	pilot in command
P1A	Pinnacle 1 Aviation
QA	quality assurance
QC	quality control
RGB	red-green-blue
RFP	Request for Proposal
SAP	site assessment plan
SSD	solid state drive
SAC	Special Airworthiness Certificate
SPA	Special Protection Area
STC	Supplemental Type Certificate
UPS	uninterruptible power supply
UAS	unmanned aircraft system
USFWS	US Fish and Wildlife Service
VFR	visual flight rules
WWT	Wildlife and Wetlands Trust

1 Introduction

1.1 Study Context and Background

Having been delegated responsibility for alternative energy activities on the Atlantic Outer Continental Shelf (AOCS) by the Energy Policy Act of 2005, the Bureau of Ocean Energy Management (BOEM) is challenged with assessing the potential environmental impacts of programmatic and project-specific offshore wind energy development in this region under the National Environmental Policy Act (NEPA). The availability of viable offshore wind energy technology and experience from a maturing offshore wind energy industry in Europe, and a strong, demonstrated interest in the development of offshore wind on the AOCS from Maine to Florida, has produced a need for BOEM to assemble scientifically valid and robust data sets on protected wildlife resources in this region. Limitations in wildlife data availability, and in the quality of available wildlife data, constrain BOEM's ability to complete the environmental studies mandated by NEPA in a timely and satisfactory manner. These wildlife data quantity and quality limitations, therefore, currently represent an obstacle to the development of a US offshore wind energy industry. BOEM, through this and other projects, is seeking solutions for filling existing marine wildlife data gaps with robust, valid, scientific data through innovations that improve the accuracy, reliability, cost effectiveness, and safety of marine wildlife data gathering efforts.

Three wildlife taxa of particular interest for conservation in AOCS marine communities are birds, marine mammals, and sea turtles. Many species of marine birds, mammals, and turtles are highly valued and iconic, and many have experienced significant recent anthropogenic population declines, resulting in significant levels of conservation concern and corresponding legal protection. Virtually all North American bird species that potentially occur on the AOCS are protected by the Migratory Bird Treaty Act (MBTA), and two bird species potentially occurring on the AOCS are also protected by the Endangered Species Act (ESA)—Roseate Tern, Piping Plover—and a third species, Red Knot, is currently a candidate for ESA listing. Seven species of marine mammals that occur on the AOCS, all whales, are protected under the ESA—Northern Right Whale, Blue Whale, Fin Whale, Sei Whale, Humpback Whale, Sperm Whale—and an eighth species, the False Killer Whale, is currently a candidate for ESA listing. All marine mammals are protected under the Marine Mammal Protection Act (MMPA) as well. All five species of sea turtles that occur in the AOCS region are protected under the ESA—Leatherback Sea Turtle, Green Turtle, Loggerhead Sea Turtle, Hawksbill Sea Turtle, and Kemp's Ridley Sea Turtle.

The primary hypothesized potential impacts of offshore wind energy development on birds are 1) fatalities from collisions with wind turbine rotors and towers, which is hypothesized to be most severe if birds do not tend to avoid offshore wind energy facilities, and 2) displacement of birds from essential feeding or transit areas that may occur if birds do tend to avoid offshore wind energy facilities (Drewitt and Langston 2006). A growing number of post-construction bird monitoring studies from European offshore wind facilities have begun to yield significant insights into behavioral, taxonomic, and other correlates of fatality and displacement impacts on birds from offshore wind energy facilities (e.g., Desholm and Kahlert 2005, Larsen and Guillemette 2007, Krijgsveld et al. 2011, Plonczkier and Simms 2012). However, the state of scientific knowledge in this area is still rudimentary, and there is a particularly acute need for data from the US AOCS to

make precise predictions and risk assessments regarding the potential impacts of US offshore wind energy development.

For marine mammals and sea turtles, collisions of animals with turbine towers are not expected to be a significant potential impact (Wilson et al. 2010), but potential adverse impacts from pile driving sound (Nedwell et al. 2007, Thomsen 2010), collisions with vessels resulting from increased vessel traffic (Laist et al. 2001, Wilson et al. 2007), and electromagnetic field impacts (Gill et al. 2005, Wiltschko and Wiltschko 2005) have all been hypothesized as potential adverse impacts. Very little information is currently known about the prevalence or severity of these impacts.

For birds, marine mammals, and sea turtles, a variety of positive effects have also been hypothesized, including localized habitat enhancement and concordant food enrichment (e.g., artificial reef effect) (Inger et al. 2009, Degraer et al. 2010), and mitigation of the adverse impacts of anthropogenic climate change through the combustion-free generation of electricity (Allison et al. 2008). The study of cumulative impacts has also been identified as an important area of future research (Langston et al. 2010). For all of these potential positive and negative impacts of offshore wind energy development on birds, marine mammals, and sea turtles, little more than hypotheses are currently available in technical literature, underscoring the acute need for robust scientific analyses based on empirical data to address the potential impact issues associated with offshore wind energy development on the AOCS.

One of the most significant barriers to understanding these potential impacts is a scarcity of baseline data, owing to the general difficulty and expense of conducting wildlife studies at sea compared with on land. A variety of geospatial data sets for marine birds, mammals, and sea turtles do exist, and several recent initiatives by the US federal government have resulted increased availability of this data (O'Connell et al. 2009, 2011; NOAA 2012a). Nonetheless, gaps in our knowledge of the spatiotemporal distributions of marine wildlife on the AOCS are much greater than they are for terrestrial wildlife, and even less is known about behavioral factors that influence the potential for impacts from offshore wind (e.g., flight altitudes, avoidance behaviors, susceptibility to disturbance and displacement). Field studies of marine wildlife are needed to fill these gaps.

The general scarcity of marine wildlife data is compounded by concerns about the quality of existing data, which derive from well-known sources of error that are inherent in conventional marine wildlife survey methodologies that rely on expert visual observers aboard vessels or low flying aircraft to gather data on marine wildlife. Such methods have been in use for several decades, and have recently been applied to offshore wind environmental baseline studies in the US (Paton et al. 2010; NJDEP 2010). Vessel-based visual observer surveys have well-known limitations including slow survey speed, which makes coverage of large areas difficult and costly; vessel-animal attraction and repulsion effects, which distort density estimates and result in missed detections; and observer effects (e.g., interobserver skill variability and distance estimation error), which further distort density estimates (Shoop and Kenney 1992; Hammond 1995). Low altitude, aerial, visual observer-based surveys provide a faster, and hence less expensive, alternative for surveying large areas. However, there are significant safety concerns with use of low flying aircraft in a marine environment (altitudes of 50 to 150 m are necessary for visual identification of birds). Similar to marine vessels, the activity of low flying aircraft distorts animal counts by disturbing animals—causing them to dive or flee before many are counted by the observers (Shoop and Kenney 1992;

Henkel et al 2007; Buckland et al. 2012). Furthermore, and perhaps most importantly, the accuracy of animal identifications and density estimates resulting from aerial, observer-based surveys is affected by well-known observer biases including observer swamping, observer variability in identification ability, observer error in distance estimation, and search image effects (Laursen et al. 2008; Thaxter and Burton 2009). The lack of a pre-observer data archive in observer-based surveys makes observer biases difficult or impossible to quantify or eliminate from survey data.

High-resolution aerial imaging surveys have emerged recently in Europe as a potential solution to the limitations of conventional marine wildlife survey methods. Over the past five years, this new methodology has been applied extensively in environmental studies in support of offshore wind energy development in Europe (Thaxter and Burton 2009). Based on early European results, BOEM identified this new survey methodology as possessing great potential for filling existing data gaps and overcoming current methodological problems. Although this technique holds great promise, it is still very new—and reliable, consistent, and optimized protocols have not been established. Also, specific consideration has not been given to the application of this methodology on the US AOCS, which possesses some unique features relative to northern Europe, including generally lower latitude with concordant higher angles of insolation and some distinct faunal and environmental elements. This study was undertaken primarily for the purpose of exploring some of these unknowns, and piloting the application of high-resolution aerial imaging marine wildlife surveys on the AOCS in the interest of developing a cost-effective method to gather robust, valid, and accurate data on the spatiotemporal abundance patterns of marine birds, mammals, and turtles on the US AOCS in support of an American offshore wind energy industry.

1.2 Review of European Chronology of Transition to Digital Surveys and Regulatory Acceptance of Digital Data for Offshore Wind Ecological Studies

1.2.1 Introduction

The pioneering European experience using high-resolution imaging surveys to gather data for offshore wind-wildlife studies lays the foundation for the adaptation and application of this new and rapidly evolving survey methodology to the nascent US offshore wind energy industry. In the remainder of this section, we provide a synthesis, contributed by Dr. Chris Thaxter of the British Trust for Ornithology (BTO), of the European context in which this new survey technology emerged, and the evolution of its acceptance in UK scientific and regulatory communities. In the five years since these techniques were introduced, high-resolution imaging surveys have become almost universally applied to offshore wind-wildlife studies. Dr. Thaxter is an ornithologist, and is an internationally recognized scientific leader in the field of marine bird survey methodology. He was the lead author of the article on high-resolution aerial imaging methodology that stimulated and inspired the current study (Thaxter and Burton 2009), and currently performs research and quality control review on high-resolution aerial imaging survey data and methods on behalf of BTO for offshore wind-wildlife studies in the UK.

1.2.2 Visual Boat-based Methods

The earliest offshore boat surveys for counting and recording birds at sea highlighted an increasing need for standardised survey protocols (Powers 1982). The need for robust baseline data was made

more urgent after subsequent oil spills and the development of gas and oil exploration in the North Sea in the 1970s. Consequently, early standardized methods were developed using strip transect approaches, building on Canadian Wildlife Service methods (Brown et al. 1975), and formed the basis of surveys conducted by the European Joint Nature Conservation Commission (JNCC) since 1979 (Blake et al. 1984; Tasker et al. 1987). However, these methods were then refined to include corrections for birds a greater distance from the boat that might be missed during counts. Therefore, line-transect methodology was adopted, leading to establishment of a European Seabirds at Sea (ESAS) database storing large amounts of standardized pelagic data on seabird numbers and distribution for northwestern European waters. A slightly revised line-transect technique is still used today (Camphuysen and Leopold 1994; Durinck et al. 1994; Stone et al. 1995; Skov et al. 1995; Pollock et al. 2000; Maes et al. 2000; Taylor and Reid 2001; Seys 2001; Skov et al. 2002) to answer questions on species vulnerability to anthropogenic changes to the marine environment (Tasker et al. 1990; Carter et al. 1993; Webb et al. 1995; Begg et al. 1997; Maes et al. 2000), but also resulted in ecological research and atlases summarizing seabird distribution patterns. Although the ESAS data are relatively patchy in UK coverage, are at fairly coarse spatial resolution, and are mostly 10 years or more old (Langston 2010), they represent the most comprehensive data set on distribution and relative abundance (Stone et al. 1995). Today, the ESAS database is being analysed as part of work to identify offshore Special Protection Areas (SPAs) and other collaborative projects (JNCC 2012).

1.2.3 Visual Aerial-survey Methods

The use of aerial survey techniques offshore in Europe for describing aggregations of seabirds increased in the 1960s, particularly in Denmark (Joensen 1968, 1973, 1974), to characterize the overall numbers and distributions of seabirds rather than provide robust statistical comparisons over space and time. These aerial survey methods were further developed and refined during the 1980s (Laursen et al. 1997), covering the Baltic Sea, for wintering seaducks (Durink et al. 1994), and UK waters (Dean et al. 2003). Such methods varied by species and weather conditions but followed strip transect protocols out to 100 m. As with boat survey methods, these methods have been further refined to include correction for detection bias closer to the aircraft, surveying swathes of sea out to 1,000 m either side, and has been deployed in the UK (e.g., JNCC, BTO, WWT), Denmark, and Germany (BioConsult, FTZ/University Kiel). Furthermore, in the UK, aerial surveys have been conducted side by side with boat-based surveys, for example, to cover coastal areas that are difficult or less efficient to reach by boat (e.g., Barton et al. 1994).

German and Dutch surveys were first conducted as part of the international waterfowl census (Bräger 1990), but are increasingly used to survey marine areas for seabirds and marine mammals (Diederichs et al. 2002).

1.2.4 Context for Many Current Offshore Surveys in Europe: Renewable Energy

It has long been recognized that to mitigate human-induced climate change, developed economies need to reduce reliance on fossil fuels and reduce carbon emissions. Following the Kyoto protocol in 1997, most industrial nations agreed to reduce greenhouse gas emissions by an average of 5% (compared to 1990) by 2012. As part of this, the UK government invested in more ambitious programs of renewable energy development to avoid reliance on fossil fuels, and in particular has seen a marked expansion of renewable energy developments in the offshore environment. In 2007, the UK signed an EU commitment to obtain 20% of energy from renewable sources by 2020, which

constitutes 15% of UK energy. The renewable sources include wave, tidal, and solar power; however, wind energy is becoming an important source. This has led to an ever pressing need for more standardized baseline data collection to characterize and understand species distribution and population estimates. Such data are required as part of environmental impact assessments (EIAs) for all developments proposed. In the UK there have been several Rounds of wind farm developments and extensions, with additional developments in Scotland. The first of these (Round 1) was launched in 2001 to deliver 1 GW of energy; and the first UK Round 1 offshore wind farm was completed in 2003 (North Hoyle, Wales). Earlier in 2003, bids for Round 2 were invited by consortia to produce up to 8 GW. In 2008, the next round of developments (Round 3) was more extensive, and in 2008 bidding began for seven large zones to generate up to 32 GW of energy. Further agreements for wind farms in Scottish territorial waters were set out in 2009, and in 2010 extensions to existing Round 1 and 2 zones were announced.

The most recent aerial and boat-based methods described above have traditionally been used to provide baseline information on the distribution and population estimates of species in areas likely to be affected by such developments (Camphuysen et al. 2004; Maclean et al. 2009). However, the evolution of survey techniques for seabirds and marine mammals offshore has recently seen a shift toward high-resolution imaging technology based methods, both video-based and still images.

1.2.5 High-resolution Methods

High-resolution imagery methods have not totally replaced existing visual methods. However, there has been a clear recognition of their advantages (Thaxter and Burton 2009). The first trials of high-resolution techniques were conducted between 2007 and 2009 by HiDef, Ltd.—testing video-based methods at Shell Flats, Rhyl Flats, Norfolk coast, Moray, Hastings, Isle of Wight, and Bristol Channel (Mellor et al. 2007; Mellor and Maher 2008; Hexter 2009a, 2009b); and by APEM, Ltd.—testing high-resolution aerial still photography at Carmarthen Bay, Barrow-in-Furness, Morecambe Bay, Liverpool Bay, Jumbles Reservoir, and the River Kent. Further work by the Danish National Environment Research Institute (NERI, University of Aarhus) was conducted at Horns Reef, Samsø, Aalborg Bay, and Kamfers Dam lake, Kimberly, South Africa (Groom et al. 2007, 2011, in press) with additional trials for gull and tern colonies in Denmark, and for cliff-nesting seabirds in nothwest Greenland (Boertmann et al. 2009).

On behalf of the Collaborative Offshore Wind Research Into the Environment (COWRIE), a workshop was held in Peterborough, UK in 2009 bringing together regulators (JNCC), developers of the technology, and users to discuss the new approaches and its recent use in offshore surveys, and in particular the pressing need to identify protocols for its use. The workshop culminated in a report that split these protocols into camera specification and survey design parameters (Thaxter and Burton 2009). The report highlighted that the protocols needed to retain flexibility. This flexibility was closely related to the stated survey aims (i.e., characterization of species, species distribution, species-specific data, or robust population estimates) and the costs to the surveyor, which would impact survey design. Following the workshop, additional comparisons between visual and high-resolution methods have also been conducted, including the focus on design- and model-based population estimates (Burt et al. 2009, 2010). Model-based estimates are the focus of recent work (Petersen et al. 2011; Buckland et al. 2012), and such data, along with visual-based data sets, are currently being used in combined habitat association models to produce predicted spatial surfaces in at-sea distributions of species.

1.2.6 Regulatory Acceptance of Digital Methods

Visual-based methods are still used in offshore surveys. One of the disadvantages of aerial and boat-based methods is the potential flushing of birds due to disturbance. Another disadvantage of boat methods is the time needed to travel to an offshore area and then conduct the survey is much longer, making coverage of an area in shorter time periods to minimise double counting very difficult. Nevertheless, in the UK visual aerial and boat-based surveys are still being conducted as part of Round 3 and extension surveys. The main reasons for their continued use is that regulators agree that some uncertainty remains in the quality of species identification obtained from high-resolution methods (Thaxter and Burton 2009 provide a list of species groupings currently used in high-definition surveys based on previous JNCC groupings). Therefore, visual methods are being used to provide species-specific information, while high-resolution methods are being used alongside as a more robust characterisation of numbers of individuals of particular species groups (or some more easily identified species). The two can be used together to provide a more accurate assessment of species distribution and abundance. Moreover, the technology being used in high-resolution methods is improving continuously. Already increases have been seen in resolution that can improve picture clarity, and hopefully species identification. From the workshop in 2009, a minimum 5 cm benchmark was agreed on for ground pixel resolution; however, images are currently being collected under 3, 2, and now 1 cm resolutions. It is expected that such improvements will improve the high-resolution method, but for now, visual methods are still required to provide the baseline species-specific information required for EIAs.

2 Experimental Design and Execution

2.1 Introduction

High-resolution aerial imaging survey experiments comprised a core component of this pilot study. Whereas previous studies using offshore high-resolution aerial wildlife imaging have selected and applied a single imaging methodology, or a small range of methodologies, our approach was based on experimentation as a means to study the impacts of different methodological choices on survey effectiveness, and to develop recommendations for survey protocols specifically optimized and adapted for application to wildlife studies in support of offshore wind energy development in the US.

The manned aircraft-based system was used as the primary vehicle for this experimentation, because aviation permitting processes were much more expedient and flexible, and payload constraints were not as severe as with the unmanned aircraft system (UAS) system. The manned aircraft-based imaging flight experiments were conducted during an intensive, two-week period in May 2011, during which two survey aircraft, a survey boat, and 22 project-related personnel were based in Oak Island, North Carolina for the purpose of conducting offshore experiments in the coastal waters nearby. This intensive experimentation period with the manned aircraft-based imaging system is described in section 2.2 of this chapter, and is referred to throughout the report as Operations House (Op House).

Experimentation with the UAS was more limited in scope, and was oriented more toward proof-of-concept tests of the viability of UAS as a vehicular platform for conducting offshore aerial high-resolution wildlife imaging surveys. These UAS flight tests were conducted with a smaller project team consisting entirely of personnel from the UAS specialist subcontractor, IATech, Inc., and are described in section 2.3 of this chapter.

This chapter is intended to describe the design and execution of all imaging flight trials conducted over the course of this study. Evaluations of experimental results, as well as recommended survey protocols and other materials derived from the flight experiments, are presented in subsequent chapters of this report.

2.2 Manned Aircraft System (Operations House Experiments)

2.2.1 Equipment Selection, System Construction, and Pretesting

Planning discussions were held from the initiation of the contract (October 2010) through April 2011 between the project manager (C. Gordon), technology manager (M. Kujawa), aviation specialist (R. Clark, Pinnacle 1 Aviation), and imaging specialists (C. Jorquera and J. Luttrell, Boulder Imaging) to coordinate all planning, equipment selection and pretesting, and logistical planning for the Op House experiments

In April 2011, Boulder Imaging shipped two cameras to the Raleigh Executive Jetport in Sanford-Lee County, North Carolina for integration into the aircraft-mounted imaging system by Aeroservices, Inc., an aviation services subcontractor arranged by the project's aviation specialist. The cameras are as follows (also see section 3.3):

- Area-scan: Imperx IGV-B4820
- Line-scan: Dalsa Spyder Color 4K

The two cameras were selected, one of each type (area-scan and line-scan), following a battery of tests at the Boulder Imaging laboratory. (section 3.3). The tests showed that the chosen cameras would meet the required performance. Imaging results confirmed the test results for both cameras, although only the area-scan camera was able to capture usable images both before and after addition of a gyrostabilizer to eliminate the impacts of high frequency engine vibrations.

The first camera mount and enclosure specified, adapted, and installed by Aeroservices proved successful at isolating the area-scan camera from low frequency vibrations, but was insufficient for doing the same with the line-scan camera. Neither camera was protected from high frequency jitter with this mount (Figure 2–1).

Figure 2–1. Low frequency vibration isolation components mount ring and vibration isolation coils (top left), camera mount plate, isolation coils, and mount ring (top right), and protective cover plate for mount enclosure (bottom) prior to installation on aircraft for Operations House imaging experiments.

The fine resolution and shutter speed of the line-scan camera recorded every vibration in detail (**Figure 2–2**), and thus generated images noted for their random waviness. By the end of integration week (week prior to Op House), it was decided to discontinue testing of the line-scan camera unless vibration damping could be achieved (see gyroscopic stabilization discussion in section 3.3). Efforts were then focused on optimizing the area-scan camera performance, which demonstrated an ability to obtain good imagery despite the high frequency vibration.

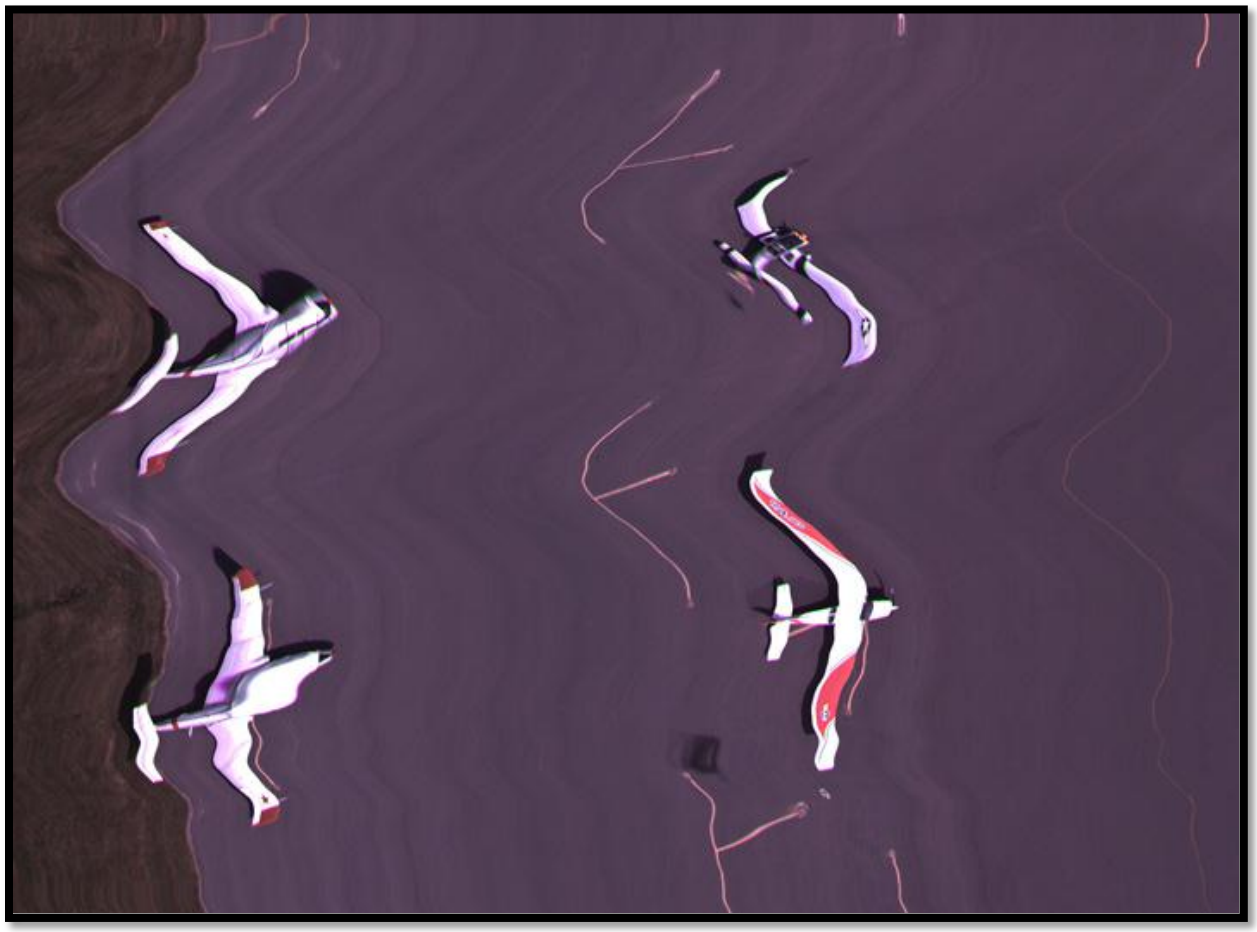

Figure 2–2. Image of airplanes on tarmac at Raleigh NC taken during integration testing prior to Operations House with line-scan camera, showing vibration effect. Some amelioration of this effect was achieved at the end of the Operations House experimentation period using a gyroscopic stabilizer (see section 3.3).

To meet experimental requirements, Aeroservices drilled out two holes on the axle of the camera mount rod to allow hard-point, manual rotation of the external camera mount to angles of 43.8º (the farthest outward facing angle in a large array system) and 15.2º (an arbitrary intermediate angle that would allow evaluation of low-oblique angle image capture).

The rotation angles were designed to point backward, shielding the camera from atmospheric moisture and direct exposure from aerodynamic turbulence.

A series of test altitudes was devised and flown that included flight heights from 450 m to 1,200 m altitude, covering all three angles (0º, 15.2º, 43.8º).

Figure 2–3. Installation of camera mount system on the Cessna 337 Skymaster in Raleigh NC prior to Operations House, showing external airframe reinforcement plates and camera mount attachment bolts (top left), camera interior in preparation for mount installation (top right), inner mount axle and support strut (middle left), and fully installed mount with windshield (middle right), rear view of fully installed mount system with two mounted cameras (bottom left), and gyroscopic stabilizer installed during final week of Operations House experimental flights (bottom right).

Initial camera flight tests were conducted 3 to 6 May 2011 in the local area of Raleigh Executive Jetport near Sanford NC, using a set of test targets determined by Boulder Imaging and M. Kujawa.

Aeroservices continued to provide technical support because the team operated out of their facility for the week.

After two days of certification flights, restricted category approval was obtained from the Federal Aviation Administration (FAA), which allowed great flexibility in the flight profiles of any trial performed with the Cessna 337 Skymaster (Skymaster) during integration trials tests and Op House. The external mount configuration was selected because it had already received FAA flightworthiness approval.

In early May 2011, Aeroservices, subcontractor to Pinnacle 1 Aviation (P1A), performed extensive modifications to the Skymaster to mount and ensure the robustness of the external components.

Before the integration trials began technology manager, M. Kujawa, traveled to Sanford NC to observe, discuss, and analyze the unfolding process and the equipment being added to the Skymaster, and to anticipate as much as possible conditions that would be encountered during the flight trials.

Figure 2–4. Cessna 337 Skymaster Undergoing Modifications in Hanger at Sanford-Lee County Airport, North Carolina, May 2011.

The week of pre-Op House integration tests performed at the Sanford facility consisted of the following preparations for the full flight tests scheduled for Op House:

- Powering and unpowering the equipment with and without aircraft power.
- Obtaining power from the aircraft through an inverter.
- Obtaining power through an onboard UPS.
- Synching the GPS signal of the Quazar with the GPS from the aircraft Garmin.
- Flight trials with both or only one camera operating.
- Focusing the camera lenses for different altitudes using an ISO 12233 target (4 × 5 feet) mounted on a frame and carried by truck to planned altitude distances near the runway.

- Repeated attempts to deal with morning humidity during the focusing sessions spurred a decision to obtain focus settings only when ground level humidity is low, then use a glue gun (or a locking ring) to fix the setting in place.
- Exploration of impacts of various gain, depth of field, exposure time, frame rates, and presence or absence of an image doubling teleconverter on image quality.
- Discovery of an as-yet seemingly intractable occurrence of high frequency blurring when using the line-scan camera.
- Stabilization of the area-scan camera settings so that workable images could be acquired at the onset of Op House trials.
- Establishment of reliable procedures to safely remove the onboard Quazar hard drives and back them up nightly.
- The necessity of making numerous takeoffs and landings revealed an instability in mechanical hard drives that indicated that multiple drive failures were possible. A decision was reached to convert all onboard hard drives to solid state drives (SSDs) (section 3.5).
- The weight of a full Quazar unit is substantial for one person to handle. Equipment movements must always be done with proper shock-absorbing cases.

2.2.2 Op House Personnel

A team of 22 people were engaged full- or part-time, and housed by the project in Oak Island NC from 9 to 21 May 2011 (Table 2–1).

Table 2–1.

Personnel Housed by Project at Oak Island NC for Op House Field Work, Conducted 9 to 21 May 2011

Person	Organization	Project Role
Caleb Gordon	Normandeau	Project manager, lead scientist, bird observer
Julia Willmott	Normandeau	Project coordinator, bird survey crew manager, bird observer
Michael Kujawa	Gemini Renewables	Technical manager
Mary Jo Barkaszi	ECOES Consulting, Inc.	Control survey manager
Jeff Martin	ECOES Consulting, Inc.	Technical equipment coordinator
Luke Szymanski	A.I.S. Observers, Inc.	Visual survey coordinator
Allison MacConnell	A.I.S. Observers, Inc.	Mammal/turtle observer
Christy Harrington	A.I.S. Observers, Inc.	Mammal/turtle observer
Rachel Hardee	ECOES Consulting, Inc.	Mammal/turtle observer
Richard Brown	ECOES Consulting, Inc..	Mammal/turtle observer
Stan Huddles	Orion Aviation	Pilot

Person	Organization	Project Role
Cameron Radford	Orion Aviation	Pilot
Ron Shrek	Orion Aviation	Pilot
Jerry Morris	Orion Aviation	Pilot
Wes Biggs	Normandeau	Bird observer
David Hartgrove	Normandeau	Bird observer
Eric Haney	Normandeau	Bird observer
Mitch Harris	Normandeau	Bird observer
Carlos Jorquera	Boulder Imaging	Chief image acquisition/processing engineer
Jason Luttrell	Boulder Imaging	Image acquisition/processing engineer
Ed Coffman	Orion Aviation	Aviation service provider
Randall "RJ" Clark	Pinnacle 1 Aviation	Aviation coordinator

Most of the people listed were present during the entire experimentation period. Some were present at oak island during only part of that time. Other personnel associated with Op House, but not housed by the project (i.e., boat captain and crew, Gainesville-based project coordination and administration staff) are not listed.

2.2.3 Op House Vehicles

- Two Cessna 337 Skymaster twin engine, fixed wing aircraft and a 40-foot deep sea charter fishing vessel, collectively referred to as platforms, were reserved and employed during the entire Op House period to execute all planned experimental image gathering trials and accompanying control surveys.
- Aircraft were based at, and flew their Op House operations out of, the Cape Fear Regional Jetport in Oak Island NC.
- The vessel (The Voyager) was based at, and performed Op House surveys out of, the South Harbour Village Marina in Oak Island NC.
- Two 15-seat vans were rented to move all personnel from houses to field departure sites during Op House.
- Health and safety plans for each platform were developed and relevant information forms created.
- Floatation devices were secured for all personnel on all platforms.
- In each platform, and at Op House, marine band radios were installed for interplatform communication.
- An antenna for the marine band radio was erected at the Op House base command house (larger of the two rental properties: A Little R & R; section 2.2.4).
- GPS devices were installed in each platform.
- The boat was equipped with dry sacks for stashing damp-sensitive equipment.

- The boat was stocked with sunscreen, and all personnel organized with the necessary equipment for onboard safety including nonslip footwear, sunglasses, and waterproof clothing.
- It was ensured that each platform had adequate first aid equipment and necessary knowledge.
- All required field equipment was acquired and deployed to appropriate platforms.

2.2.4 Op House Food and Accomodations

- Two properties were rented from Oak Island Accommodations to accommodate all Op House personnel during the experimentation period: A Little R & R (accommodations for up to 12 people, used as Op House base command, pictured in Figure 2–5) and The Lighthouse (accommodations for up to eight people).

Figure 2–5. The rental property A Little R&R in Oak Island NC served as Op House base command.

- Internet services at both houses were prearranged, but service was lacking at both houses, requiring the purchase and installation of wireless routers at both houses to facilitate internet connections, and the hiring Jeff Martin of ECOES Consulting, Inc., to stay on through the duration of Op House as technical equipment manager.
- A dedicated aviation-tracking computer was installed at Op House for aircraft safety monitoring. Procedures for tracking both aircraft at all times were developed, reviewed with Op House base command platform monitoring personnel, and emergency contact numbers were posted on the wall next to this dedicated computer.
- Four dedicated data entry computers for visual observation data and one for high-resolution imagery data were installed in Op House.
- Extension cables and powerstrips provided by ECOES Consulting, Inc., were located in Op House to facilitate daily data entry and image review.

- All household supplies supplied for food preparation, bathrooms, and other basic domestic necessities were purchased and distributed between rental properties.
- Both houses were provisioned with first aid kits and other items required by the health and safety plan.
- Sufficient food stuffs (accommodating a variety of dietary requirements) and equipment were purchased and stored for breakfasts and the making of packed-lunches at both houses.
- Sufficient snacks and drinks were purchased and adequately stored at the airfield and on the boat.
- A flexible evening meal plan was organized covering the various dietary requirements of all personnel.
- Sufficient food and drink was purchased for all personnel for evening meals, including condiments.
- A flexible schedule for meal preparation and consumption that coordinated all daily experimental schedules and subsequent data recording was designed.
- Arrival and departure airport pick-ups were organized.
- In the interests of time and logistics, it was decided that evening meals should be prepared by the project coordinator (J. Willmott), and that all personnel should eat together, to enable discussion and facilitate coordinated data entry.
- At the conclusion of Op House, all remaining food and domestic items were distributed to R. Hardee and R. Brown for delivery to a homeless shelter in Wilmington NC, or were distributed to other members of the project team.

2.2.5 Op House Fieldwork Preparation

- An Op House orientation meeting was held on the evening of 9 May, prior to the first surveys. Observers, project coordinators, pilots, and boat captains were all included in this initial meeting.
    - The basic goals and plan of the Op House field work were laid out, the command structure explained, and an intimation given of how changes and modifications to the set schedule were to be expected. Emphasis was placed on the need for flexibility in every single aspect of the operation from domestic arrangements to scientific experimentation by each individual involved.
    - Domestic organization, house rules, and health and safety issues were discussed. Information was given on emergency contact numbers and emergency facility locations, and forms distributed that needed to be completed before the first field day. An overview of daily expectations for visual observers was also made, stressing that given the relatively short time frame for all experimentation requirements, daily data entry had to be completed, and delivered to the coordinator, before the end of each day, despite anticipated fatigue.
    - Written protocols were provided for individual review prior to the extensive training and experimentation the following day. This information covered field techniques and data gathering and recording for all visual observers and environmental data recorders.

  - By the end, all observers understood the primary and secondary goals of the project and how they differed from other surveys.
- On 10 May field personnel training included chart and map illustration of various transect and platform combinations.
  - Training was given on how to use GPS devices and digital voice recorders, fill out field data sheets, and complete necessary computer data entry. Individual training was given on using range finders and inclinometers, and protocols explained for field work for each platform and taxonomic group.
  - Lists of expected bird, mammal, and turtle taxa were distributed, and taxonomic familiarity and identification ability compared. Target and most common species were discussed and time given for practice and questions arising.
  - Pilots and boat captain presented an on-site/on-platform briefing of the safety requirements and explained what was expected in/on their specific platforms. For each platform, careful emphasis was placed on procedures in the event of an emergency.
- On 10 May, the camera plane performed a reconnaissance flight to find suitable reference targets to enable calibration for each flight and camera combination covering the duration of the experimental trials.
- Land-based personnel were trained in radio operation, flight monitoring via internet, and interpreting the boat float-plan in the event of an emergency. Reassurance was given to all that there was the ability for constant contact among all platforms.

2.2.6 Operations House Execution, Experimental, and Control Trials Conducted

Operations House Experiment Execution

Experimental image-gathering flights and associated visual observer-based control surveys were conducted 11 to 20 May 2011, as described in Table 2–2 and Table 2–3. This schedule was developed using predetermined experimental priorities and control survey design planning, modified by day-to-day decision making by the project manager in consultation with all Op House personnel, on the basis of evolving weather and technical constraints and considerations. All platforms departed on coordinated tracks, each observer on each platform had reviewed platform and taxa protocols, familiarized themselves with the complexities of equipment handling and data recording, and completed data entry for review and comment.

Vessel-based survey configuration is depicted in Figure 2–6. Vessel-based visual observer surveys were conducted from a sport fishing vessel called Voyager. For each survey, two marine mammal/turtle observers and two avian observers, one of each covering opposite sides of the vessel were stationed on board. Observers were equipped with binoculars, range finder, GPS, data sheets, and digital voice recorder. The boat captain and crew performed all navigation, and also arranged for and performed chumming at certain intervals and locations. The objective of chumming was to attract numerous animals to the vicinity of the boat for the purpose of obtaining a sufficient quantity of photographs. The objective of transect surveys was to obtain standard boat-transect visual observer data, hence chumming was never performed during transect surveys.

Figure 2–6. Animal observer crew boarding Voyager for a survey operation during Operations House.

Aircraft-based visual observations were conducted from a Cessna 337 Skymaster (Skymaster) aircraft (Figure 2–7). Stationed on the aircraft were two marine mammal/turtle observers and two avian observers, one of each covering opposite sides of the aircraft. Observers were equipped with binoculars, data sheets, inclinometer, GPS, and digital voice recorder. Two pilots were aboard for each flight to provide extra safety assurance. The second pilot also recorded meteorological and position information during all flights. Such flights always accompanied camera-plane transect surveys, but never accompanied target flyovers, such as reference object flyovers, chum boat flyovers, or bird island flyovers. While accompanying the camera plane, the visual observer plane flew roughly 500 m behind, to obtain information on the same surveyed area, as close to simultaneously as possible within aircraft operational safety limits.

Figure 2–7. Bird and marine mammal observers receiving safety training and orientation from pilot before boarding the visual observer plane during Operations House.

Aircraft-based high-resolution image gathering flights were conducted from a Skymaster aircraft equipped with a mount containing one or more cameras, and onboard data storage and processing equipment (i.e., camera-plane configuration) (Figure 2–8). One image gathering engineer, who monitored the in-flight image gathering process, calibrated equipment, and directed aircraft activity based on in-flight image monitoring was stationed on the aircraft. On most flights, a second non-pilot was also onboard, to consult with the imaging engineer regarding project-related biological or other technical considerations of the image gathering. Two pilots were aboard for each flight, to provide extra safety assurance. The second pilot also recorded meteorological and position information during all flights. Such flights were accompanied by a visual observer plane during transect surveys, but never during target flyovers, such as reference object flyovers, chum boat flyovers, or bird island flyovers. On all camera-plane flights, experimental image gathering was preceded by visual confirmation of correct equipment calibration and function by the onboard image gathering engineer. The next step on each image gathering flight was a flyover of a set of reference objects, consisting of a series of docks and other objects along the coast, that had been determined and selected on 10 May, to provide a consistent set of objects of varying size, coloration, and patterning, whose images could be compared across all image gathering flights for the purposes of evaluating and comparing image quality with different image gathering equipment configurations.

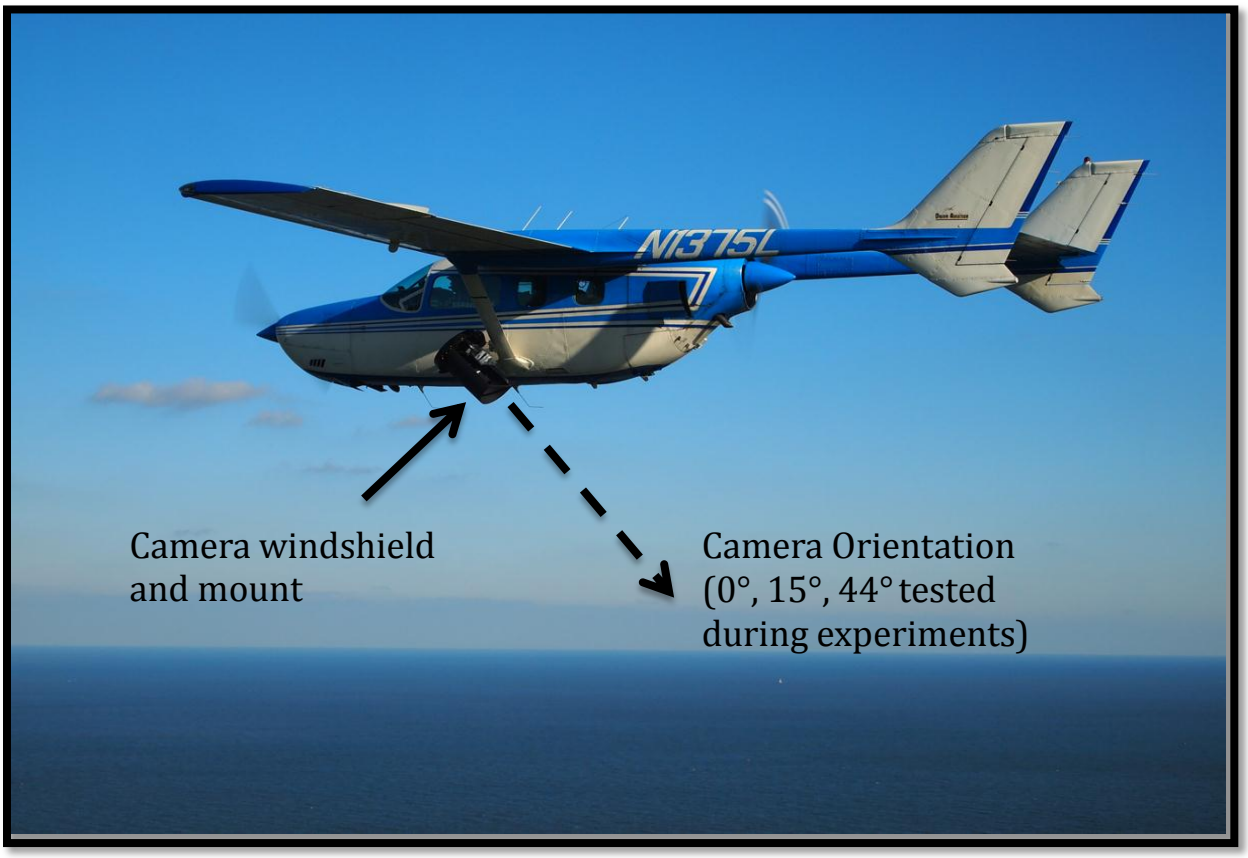

Figure 2–8. Operations House camera plane showing camera mount oriented at 44˚ angle.

General survey design and platform coordination—The following survey design was created to accomplish the project's multiple image gathering and experimental survey goals in the most efficient manner possible. On some days, this plan was varied based on technical and/or biological considerations. The specific platform operation schedule is described in detail in Table 2–2, and the image gathering experimental configurations that were performed are described in Table 2–3.

The boat generally made an early morning transect across the AOCS to a predetermined point beyond the 30 m isobath of the AOCS. After arrival at the predetermined point, the boat would then chum to attract birds. This was to give the camera plane some definite identified and quantified images to capture after completing an unchummed transect (Figure 2–9).

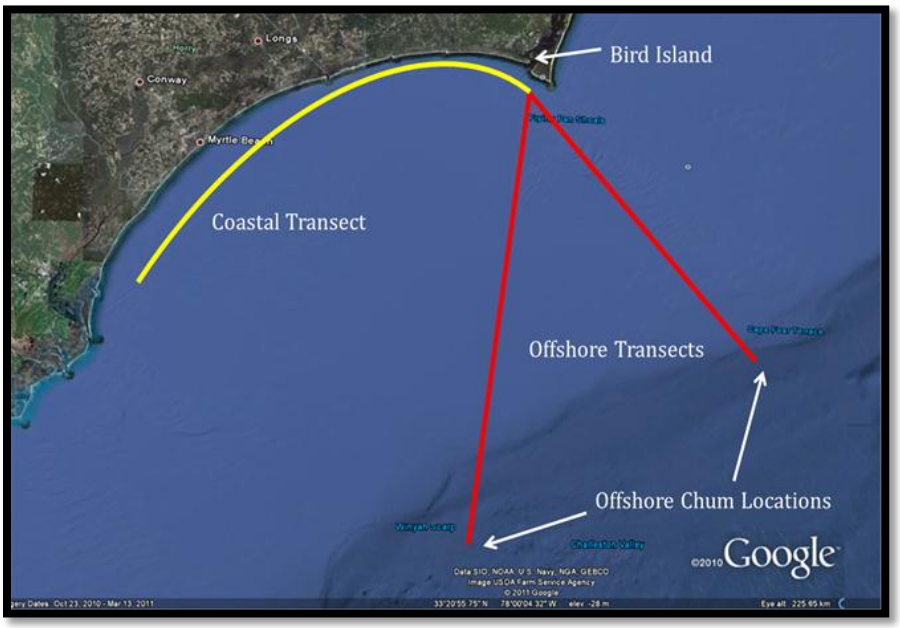

Figure 2–9. Area of boat and plane operation for Operations House image gathering experimental trials and associated control surveys conducted 10 to 20 May 2011.

Figure 2–10. Survey route planning meeting at Operations House base command among boat captain, pilots, and biological survey manager.

While the boat completed its outbound transect, the camera plane conducted some reference object flyovers and then set out on a coastal transect (see Figure 2–9) in tandem with the visual observer plane. The visual observer plane remained at least 500 m behind the camera plane and at a lower altitude (ca. 150 m). At the conclusion of the coast transect, both aircraft landed and refueled. After confirming the boat position and status, both aircraft would then normally fly (in the same transect formation) along AOCS traversing the offshore transect previously followed by the boat. Once within sight of the boat, and early enough to avoid disturbing any of the animals, the observer plane returned to base, performing an additional transect sample on the way back, while the camera plane conducted boat flyovers. At the conclusion of the chum flyovers, both the camera plane and the boat platforms performed transect surveys on their return to the harbor.

Table 2–2.

Schedule of All Operations Performed by All Three Survey/Image Gathering Platforms During Operations House from 10 to 20 May 2011, based out of Oak Island NC.

	Observer Boat			**Observer Plane**			**Camera Plane**		
Date	*Start Time*	*End Time*	*Activity*	*Start Time*	*End Time*	*Activity*	*Start time*	*End Time*	*Activity*
9 May 2011			At Docks			Arrived at airport			Arrived at airport
10 May 2011	13:37	17:25	Orientation trip	13:50	14:47	Orientation trip	8:14	8:40	Testing
							11:38	12:34	Testing
							14:18	14:44	Testing
11 May 2011	8:43	16:37	Offshore transect and chumming	10:13	11:36	Short coastal and short offshore transect with camera plane	10:04	11:45	Coastal transect and short offshore
				13:19	14:17	Offshore transect with camera plane	13:11	14:41	Offshore transect and chum boat flyovers
				16:07	17:37	Coastal Transect with camera plane	16:00	17:39	Coastal transect
12 May 2011	8:10	16:18	Offshore transect and chumming	9:42:04	11:15:02	Coastal Transect with camera plane	9:30	11:46	Coastal transect
				12:54	13:22	Offshore transect with camera plane	12:37	14:09	Offshore transect and chum boat flyovers
				15:26	16:51	Coastal Transect with camera plane	15:21	16:53	Coastal transect
13 May 2011	8:32	16:00	Coastal chumming **non-transect**	9:27	10:49	Coastal transect with camera plane	9:17	11:33	Coastal transect
							14:49	16:20	Offshore chum boat flyovers

	Observer Boat			**Observer Plane**			**Camera Plane**		
Date	*Start Time*	*End Time*	*Activity*	*Start Time*	*End Time*	*Activity*	*Start time*	*End Time*	*Activity*
				15:29	16:48	Coastal transect with camera plane	15:30	17:00	Coastal transect
14 May 2011	8:45	14:00	Coastal chumming **non-transect**	9:10	10:29	Coastal transect with camera plane	8:49	10:52	Coastal transect and chum boat flyovers
				11:50	13:02	Frying Pan Shoals **bird recon mission**	11:52	13:23	Coastal transect
15 May 2011	9:14	16:07	Offshore transect and chumming	9:50	11:06	Coastal transect with camera plane	9:15	11:29	Coastal transect with bird island flyovers
				12:53	13:16	Offshore transect with camera plane	12:28	14:32	Offshore transect, chum boat flyovers and bird island flyovers
16 May 2011	7:22	17:09	Offshore transect and chumming	10:13	11:13	Coastal transect with camera plane	9:21	11:34	Coastal transect with bird island flyovers
				12:49	13:15	Offshore transect with camera plane	12:26	14:39	Offshore transect and chum boat flyovers
17 May 2011			**Did not sail**				12:51	13:07	First day with stabilizer, quick flight to test bracket security
			N/A	14:08	15:04	Coastal transect with camera plane	13:40	15:30	Coastal transect with bird island flyovers
18 May 2011	7:10	16:10	Offshore transect and chumming				9:00	9:20	Bird Island flyovers
				12:25	12:38	Circle Bird Island with camera plane	12:00	12:30	Bird Island flyovers
				12:39	13:40	Offshore transect with camera plane	12:30	13:00	Offshore transect and chum boat flyovers
							19:00	19:30	Bird Island flyovers

	Observer Boat			Observer Plane			Camera Plane		
Date	*Start Time*	*End Time*	*Activity*	*Start Time*	*End Time*	*Activity*	*Start time*	*End Time*	*Activity*
19 May 2011	7:02	16:55	Offshore transect and chumming				7:05	8:02	Bird Island flyovers
							8:39	8:56	Equipment test runs
				11:39	12:14	Offshore transect with camera plane	9:18	9:55	Bird Island flyovers
							11:30	13:39	Offshore transect and chum boat flyovers
20 May 2011	7:05	16:46	Offshore transect and chumming				9:39	10:25	Bird Island flyovers
				12:30	13:39	Offshore transect with camera plane	12:25	14:15	Offshore transect and chum boat flyovers

Table 2–3.

Complete Inventory of Image Gathering Flight Experimental Trials and Segments Performed during Operations House, 10 to 20 May 2011, Out of Oak Island NC (Experimental Transect Surveys (Non-chummed) are Listed in Red, While Target Flyovers [Chummed Boat, Reference Object, or Bird Island] Are Listed in Black)

Day	Segment Type	Time of Day	Location	Altitude (m)	Resolution (cm)	Swath Width (m)	Polarizer	Gyrostabilizer	Camera Angle (degrees)	Camera
5/11/11	Reference object flyovers	10:00–10:13	Docks	600	2	98	Yes	No	0	Area-scan
	Transect	10:13–11:00	Coastal	600	2	98	Yes	No	0	Area-scan
	Short transect	11:00–11:45	Offshore	600	2	98	Yes	No	0	Area-scan
	Reference object flyovers	13:00–13:05	Docks	450	1	49	Yes	No	15	Area-scan
	Transect	13:05–13:52	Offshore	450	1	49	Yes	No	15	Area-scan
	Target flyovers	13:53–14:07	Chum boat	450	1	49	Yes	No	15	Area-scan
	Transect	14:07–14:30	Offshore	450	1	49	Yes	No	15	Area-scan
	Reference object flyovers	15:00	Coast	450	1	50	No	No	15	Area-scan

Day	Segment Type	Time of Day	Location	Altitude (m)	Resolution (cm)	Swath Width (m)	Polarizer	Gyrostabilizer	Camera Angle (degrees)	Camera
	Reference object flyovers	15:02	Docks	450	1	50	No	No	15	Area-scan
	Reference object flyovers	15:00–16:30	Coast	450	1	50	No	No	15	Area-scan
	Transect	16:07–17:29	Coast	450	1	50	No	No	15	Area-scan
	Reference object flyovers	17:29–17:39	Coast	450	1	50	No	No	15	Area-scan
5/12/11	Reference object flyovers	9:30–9:40	Ocean and docks	1,000	2.5	121	Yes	No	15	Area-scan
	Transect	9:40–11:46	Coast	1,000	2.5	121	Yes	No	15	Area-scan
	Reference object flyovers	12:40–12:50	Docks	1,000	2.5	121	Yes	No	15	Area-scan
	Transect	12:54–13:20	Offshore	1,200–600 (Clouds)	3–1.5	146–73	Yes	No	15	Area-scan
	Target flyovers	13:20–13:30	Chum boat	600	1.5	73	Yes	No	15	Area-scan
	Transect	13:30–14:00	Offshore	600	1.5	73	Yes	No	15	Area-scan
	Reference object flyovers	15:10–15:20	Docks	425	1.5	73	No	No	44	Area-scan
	Transect	15:21–16:51	Coast	425	1.5	73	No	No	44	Area-scan
	Reference object flyovers	16:51–16:55	Docks	425	1.5	73	No	No	44	Area-scan
5/13/11	Reference object flyovers	09:17–09:25	Docks	1,000	2.5	121	No	No	15	Area-scan
	Transect	09:25–10:45	Coast	1,000	2.5	121	No	No	15	Area-scan
	Transect	10:45–10:50	Coast	600–450 (Clouds)	1.5–1	73–50	No	No	15	Area-scan
	Reference object flyovers	10:50–11:33	Docks	1,000	2.5	121	No	No	15	Area-scan
	Target flyovers	14:59–15:25	Chum boat	1,200	3	146	No	No	15	Area-scan
	Transect	15:25–16:08	Coast	1,200	3	146	No	No	15	Area-scan
	Transect	16:08–16:17	Coast	1,000	2.5	121	No	No	15	Area-scan
	Transect	16:17–16:23	Coast	600	1.5	73	No	No	15	Area-scan
	Transect	16:23–16:45	Coast	1,200	3	146	No	No	15	Area-scan
	Reference object flyovers	16:48–17:00	Docks	1,200	3	146	No	No	15	Area-scan
5/14/11	Reference object flyovers	08:49–09:10	Docks and ocean	1,000	2.5	121	No	No	15	Area-scan
	Transect	09:10–10:25	Coast	1,000	2.5	121	No	No	15	Area-scan
	Target flyovers	10:25–10:36	Chum boat	1,000	2.5	121	No	No	15	Area-scan
	Reference object flyovers	11:45–12:13	Ocean	300–450	1	49	No	No	44	Area-scan
	Target flyovers	12:13–13:00	Chum boat	300–450	1.5	73	No	No	44	Area-scan
	Target flyovers	13:00–13:15	Chum boat	600	2.1	102	No	No	44	Area-scan

Day	Segment Type	Time of Day	Location	Altitude (m)	Resolution (cm)	Swath Width (m)	Polarizer	Gyrostabilizer	Camera Angle (degrees)	Camera
5/15/11	Target flyovers	9:15–09:30	Bird Island	332	1	49	No	No	44	Area-scan
	Reference object flyovers	09:30–09:45	Docks	433	1.5	73	No	No	44	Area-scan
	Reference object flyovers	09:45–09:50	Ocean	433	1.5	73	No	No	44	Area-scan
	Transect	09:50–11:06	Coast	433	1.5	73	No	No	44	Area-scan
	Reference object flyovers	11:06–11:10	Docks	400	1.4	69	No	No	44	Area-scan
	Target flyovers	11:10–11:29	Bird Island	433	1.5	73	No	No	44	Area-scan
	Target flyovers	12:28–12:45	Bird Island	731	2.5	121	No	No	44	Area-scan
	Reference object flyovers	12:45–12:50	Docks	731	2.5	121	No	No	44	Area-scan
	Transect	12:50–13:16	Offshore	731	2.5	121	No	No	44	Area-scan
	Target flyovers	13:20–13:55	Chum boat	433	1.5	73	No	No	44	Area-scan
	Reference object flyovers	14:00–14:32	Bird Island	433	1.5	73	No	No	44	Area-scan
5/16/11	Target flyovers	09:20–09:55	Bird Island	733	2.5	121	No	No	44	Area-scan
	Target flyovers	09:55–10:00	Bird Island	900	3	146	No	No	44	Area-scan
	Reference object flyovers	10:00–10:13	Docks	733	2.5	121	No	No	44	Area-scan
	Transect	10:13–11:13	Coast	733	2.5	121	No	No	44	Area-scan
	Reference object flyovers	11:13–11:25	Docks	900	3	146	No	No	44	Area-scan
	Target flyovers	11:25–11:34	Bird Island	900	3	146	No	No	44	Area-scan
	Reference object flyovers	12:26–12:45	Docks	733	2.5	121	Yes	No	44	Area-scan
	Transect	12:45–13:14	Offshore	733	2.5	121	Yes	No	44	Area-scan
	Target flyovers	13:14–13:54	Chum boat	733	2.5	121	Yes	No	44	Area-scan
	Target flyovers	2:00–14:15	Barge	733	2.5	121	Yes	No	44	Area-scan
	Target flyovers	14:15–14:40	Bird Island	733	2.5	121	Yes	No	44	Area-scan
5/17/11	Reference object flyovers	12:51–12:59	Docks	**No data gathered. Equipment Test Flight**						Area-scan
	Target flyovers	12:59–13:07	Water tower							Area-scan
	Target flyovers	13:40–14:00	Bird Island	600	1.5	73	No	Yes	15	Area-scan
	Reference object flyovers	14:00–14:05	Docks	600	1.5	73	No	Yes	15	Area-scan
	Transect	14:05–15:04	Coast	600	1.5	73	No	Yes	15	Area-scan
	Reference object flyovers	15:04–15:10	Docks	600	1.5	73	No	Yes	15	Area-scan
	Target flyovers	15:10–15:15	Water tower	600	1.5	73	No	Yes	15	Area-scan

Day	Segment Type	Time of Day	Location	Altitude (m)	Resolution (cm)	Swath Width (m)	Polarizer	Gyrostabilizer	Camera Angle (degrees)	Camera
	Target flyovers	15:15–15:23	Bird Island	600	1.5	73	No	Yes	15	Area-scan
	Target flyovers	15:23–15:30	Bird Island	1,000	2.5	121	No	Yes	15	Area-scan
5/18/11	Target flyovers	09:00–09:15	Bird Island	600	1.5	73	No	Yes	15	Area-scan
	Target flyovers	09:15–09:30	Bird Island	1,000	2.5	121	No	Yes	15	Area-scan
	Target flyovers	09:30–09:50	Bird Island	1,200	3	146	No	Yes	15	Area-scan
	Reference object flyovers	09:50–10:00	Docks	1,200	3	146	No	Yes	15	Area-scan
	Reference object flyovers	10:00–10:12	Docks	1,000	2.5	121	No	Yes	15	Area-scan
	Target flyovers	10:12–10:15	Water tower	1,000	2.5	121	No	Yes	15	Area-scan
	Target flyovers	10:17	Water tower	1,200	3	146	No	Yes	15	Area-scan
	Target flyovers	10:20	Water tower	600	1.5	73	No	Yes	15	Area-scan
	Target flyovers	10:25	Lighthouse	600	1.5	73	No	Yes	15	Area-scan
	Target flyovers	10:30	Lighthouse	1,000	2.5	121	No	Yes	15	Area-scan
	Target flyovers	12:00–12:20	Bird Island	1,000	2.5	121	No	Yes	15	Area-scan
	BirdIsland3_1000m_15Tilt	12:20–12:38	Bird Island	1,000	2.5	121	No	Yes	15	Area-scan
	Transect	12:39–13:08	Offshore	1,000	2.5	121	No	Yes	15	Area-scan
	Target flyovers	13:08–13:22	Chum boat	1,000	2.5	121	No	Yes	15	Area-scan
	Target flyovers	3:30–15:50	Bird Island	433	1.5	73	No	Yes	44	Area-scan
	Target flyovers	3:50–16:00	Bird Island	719	2.5	121	No	Yes	44	Area-scan
	Target flyovers	16:00–16:15	Bird Island	863	3	146	No	Yes	44	Area-scan
	Reference object flyovers	16:15	Docks	863	3	146	No	Yes	44	Area-scan
	Reference object flyovers	16:15	Docks	719	2.5	121	No	Yes	44	Area-scan
	Reference object flyovers	16:15	Docks	433	1.5	73	No	Yes	44	Area-scan
	Target flyovers	16:40	Water tower	433	1.5	73	No	Yes	44	Area-scan
	Target flyovers	16:40	Water tower	719	2.5	121	No	Yes	44	Area-scan
	Target flyovers	16:40	Water tower	863	3	146	No	Yes	44	Area-scan
	Reference object flyovers	18:45	Circle	719	2.5	121	No	Yes	44	Area-scan
	Target flyovers	19:00	Bird Island	863	3	146	No	Yes	44	Area-scan
	Target flyovers	19:15	Bird Island	719	2.5	121	No	Yes	44	Area-scan
	Target flyovers	19:30	Lighthouse	719	2.5	121	No	Yes	44	Area-scan

Day	Segment Type	Time of Day	Location	Altitude (m)	Resolution (cm)	Swath Width (m)	Polarizer	Gyrostabilizer	Camera Angle (degrees)	Camera
5/19/11	Reference object flyovers	7:15	Circle	719	2.5	121	No	Yes	44	Area-scan
	Target flyovers	7:30	Bird Island	863	3	146	No	Yes	44	Area-scan
	Target flyovers	7:45	Bird Island	719	2.5	121	No	Yes	44	Area-scan
	Reference object flyovers	9:00	Docks	863	2	97	No	Yes	44	Area-scan
	Target flyovers	9:30	Bird Island	863	3	146	No	Yes	44	Area-scan
	Target flyovers	9:45	Bird Island	719	2.5	121	No	Yes	44	Area-scan
	Target flyovers	10:00	Bird Island	433	1.5	73	No	Yes	44	Area-scan
	Transect	11:30–12:14	Offshore	863	3	146	No	Yes	44	Area-scan
	Target flyovers	12:15–13:01	Chum boat	863	3	146	No	Yes	44	Area-scan
5/20/11	Reference object flyovers	9:39	Docks	433	1.5	61	No	Yes	44	Line-scan
	Reference object flyovers	10:00	Docks	433	1.5	61	No	Yes	44	Line-scan
	Target flyovers	10:20	Bird Island	433	1.5	61	No	Yes	44	Line-scan
	Reference object flyovers	10:30	Ocean	433	1.5	61	No	Yes	44	Line-scan
	Transect	12:25–13:09	Offshore	433	1.5	61	No	Yes	44	Line-scan
	Target flyovers	13:09–13:41	Chum boat	433	1.5	61	No	Yes	44	Line-scan

Visual Observer and Meteorological Data Processing

All visual observer animal survey data, as well as meteorological and position data from all survey platforms were transcribed from voice recordings, recorded onto field sheets, and data were entered each night on four dedicated laptops. These data consisted of boat-bird surveys, boat-mammal/turtle surveys, observer plane-bird surveys and observer plane-mammal/turtle surveys.

Data entry was performed in pairs for efficiency and an element of quality control.

All platform GPS data were also collected and stored. Platform-relevant environmental data were also recorded and stored. These data were collected nightly, archived nightly on dedicated USB storage devices and nightly copied onto the Normandeau coordinator's laptop for review. These data were later stored on three computers, on Sharepoint, and on three USB drives.

During the first several days of Op House, quality assurance and quality control (QA/QC) review of the previous day's visual observer survey data was performed by the project manager and coordinator. Errors and missing data were identified for subsequent correction and completion. These QA/QC reviews resulted in several adjustments to nightly data entry supervision and protocols, including the development of a nightly data entry checklist, to ensure that data entry was performed completely and correctly by all observers each night.

During, and subsequent to Op House, an Access database was developed for analyses of the visual observer data in comparison with animal density/abundance data that was subsequently derived from the analyzed camera plane images. All of the visual observer data were QA/QC reviewed, cleaned, verified, and entered into this database. This includes GPS data by time and platform, field data by time and platform, transect times and types by time and platform, and environmental data by time and platform.

Op House High-resolution Image Data Storage and Processing

- Twenty terabytes of hard drive storage were purchased with eSATA connection facility to back up and store, and subsequently to facilitate analyses of the camera images.
- Nine terabytes of image data were collected in the field during Op House. All image data had associated GPS information, with the exception of pre-field study experimental images.
- All image data were copied onto secondary hard drives for back up. One complete copy of all image data resided with Normandeau in Gainesville FL, and another complete copy resided with Boulder Imaging in Boulder CO.
- Quazar software (Boulder Imaging) was loaded onto Normandeau computers in Gainesville to facilitate image analyses.
- Software user orientation began during Op House and continued afterward.
- Initial, cursory review of the gathered images was conducted on a nightly basis during Op House (Figure 2–11), and continued afterward, resulting in the identification of various images of animals gathered during experimental flights. This review was conducted for the sole purpose of obtaining an immediate indication of whether or not the image gathering was generally successful, and to perform on-the-fly decision making during Op House regarding more or less promising image gathering configurations for experimentation.

- Systematic review of the images was initiated immediately by Normandeau (manual image review and animal identification) and by Boulder Imaging (target recognition software development) subsequent to Op House (Supplemental Volumes I–III).

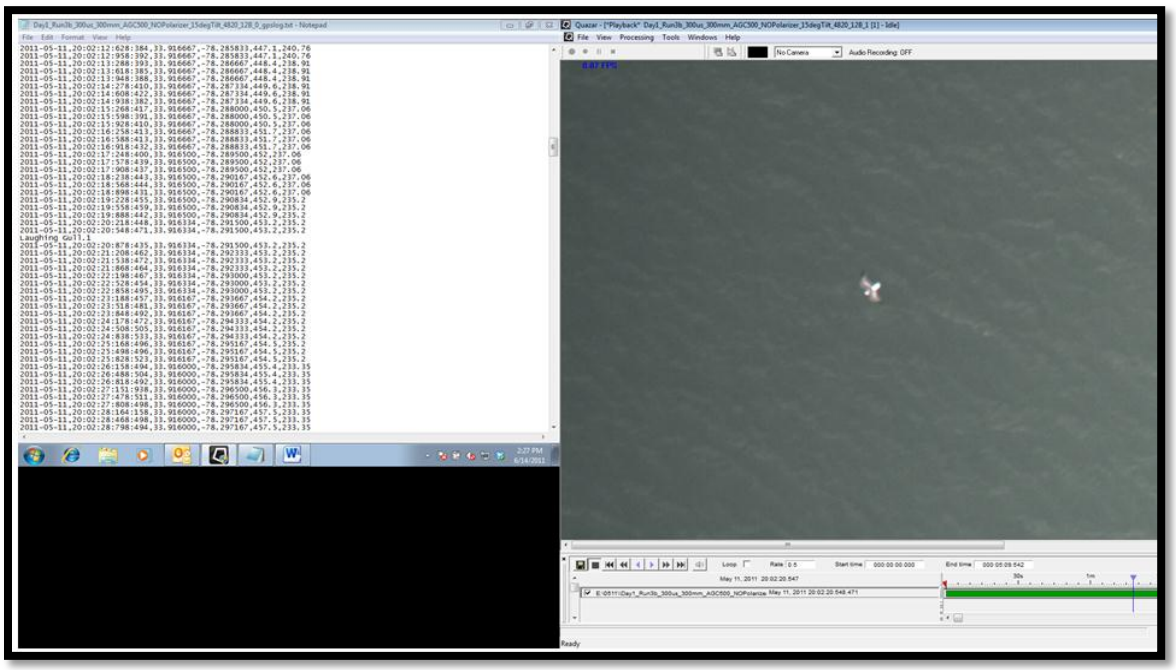

Figure 2–11. Screen shot of image analysis computer during initial image reviews conducted during Operations House using Quazar software. Images (at right) were visually scanned for animals (e.g., Laughing Gull shown in image), and then accompanying text files (at left) were annotated to mark locations of photographed animals.

2.3 Unmanned Aircraft System

2.3.1 Experimental Design

The testing and experimentation with the UAS-based high-resolution imaging system were developed and conducted by the UAS specialist subcontractors on the project team, Donald and Erica MacArthur of IATech, Inc., working in coordination with technology development manager, M. Kujawa, and project manager and lead scientist, C. Gordon. This testing consisted of preliminary laboratory and bench testing of equipment, followed by a series of four field tests, described in this section.

2.3.2 System Construction and Pretesting—January to August 2011, Gainesville, Florida

Estimated Payload Weight

During preliminary system design and requirement meetings, an integrated payload weight analysis was performed (camera, lens, housing, DVR, power conditioning, mount). As with any aircraft,

overall payload weights are critical. With smaller aircraft systems, payload weight and center of gravity will determine whether or not an aircraft will fly.

Table 2–4.

Payload Weight Matrix for the Pelican Aircraft System

Payload Component	Weight Budget (lbs)
Camera	1.8
Lens	1.7
Housing	5.0
DVR (single board computer, hard drive)	2.2
Power Conditioning	1.6
Mounts	2.3
TOTAL	**14.6**

Camera Mounting System

The camera mounting system was fixed and shock mounted to the airframe. Mechanically speaking, this is the easiest and safest solution for a payload of this size. The mounts that were used have some vibration isolation and compliance to mitigate some of the high frequency jitter from the aircraft. These mounts are designed for avionic and marine applications and provided sufficient damping for our application. Because we chose to power the aircraft using electric motors rather than internal combustion engines, this greatly reduced vibration and thus improved the image quality (section 3.3.3).

Camera Interface

The camera was interfaced to a single board computer through a USB 2.0 connection. A custom program was written to send commands to the camera that would actuate the shutter at specified time intervals. During pretesting, we found the speed of the USB 2.0 connection sufficient to capture image data sets with adequate overlap from image to image. The camera was powered using the battery power provided with the camera. This was believed to be the best option for powering the camera instead of trying to recreate a custom battery solution and powering circuit. The rest of the imaging system was powered by a series of lithium polymer batteries with a voltage regulator to condition the power going to the computer and hard drive.

Camera and Optics Testing

A series of images was collected with the camera/lens configuration and used to evaluate the camera and lens based on ISO 12233 standard chart (ANSI 2000). This chart is the I3A/ISO standard for measuring the resolution of digital still imaging cameras. The target is designed to measure visual resolution, limiting resolution, and offers a method to obtain spatial frequency response data.

This ISO 12233 image was purchased and is a very high-resolution image compared to the laser jet printed image that is available for download online. Some example images taken at different lenses and ISO settings are shown in Figure 2–12 to Figure 2–15.

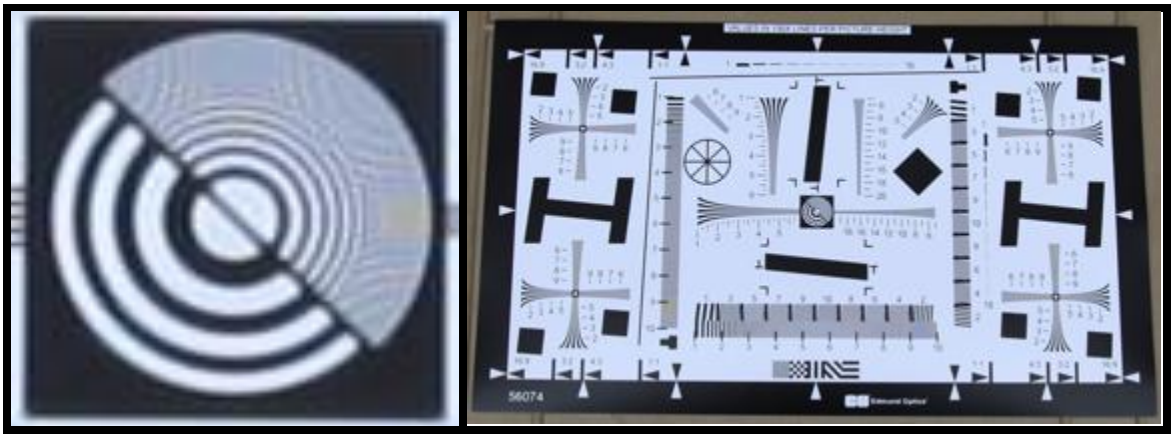

Figure 2–12. ISO 12233 test image photographed with the UAS-based imaging system during laboratory pretesting, using a variable focus lens (24 mm setting) with ISO 4.0.

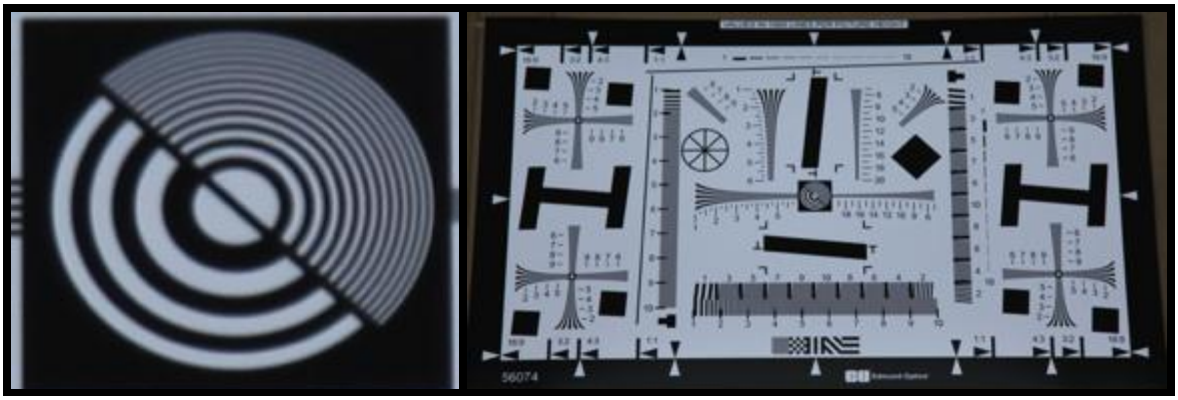

Figure 2–13. ISO 12233 test image photographed with the UAS-based imaging system during laboratory pretesting, using a variable focus lens (104 mm setting) with ISO 4.0.

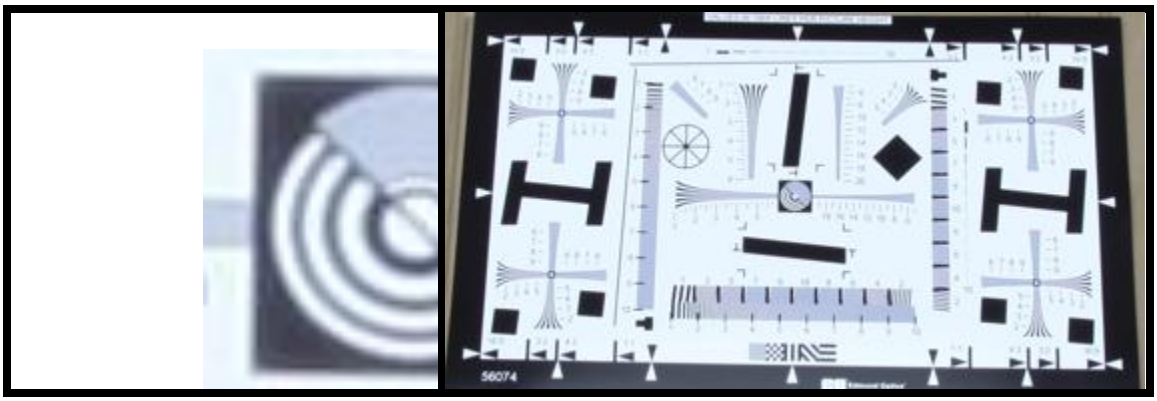

Figure 2–14. ISO 12233 test image photographed with the UAS-based imaging system during laboratory pretesting, using a variable focus lens (24 mm setting) with ISO 22.0.

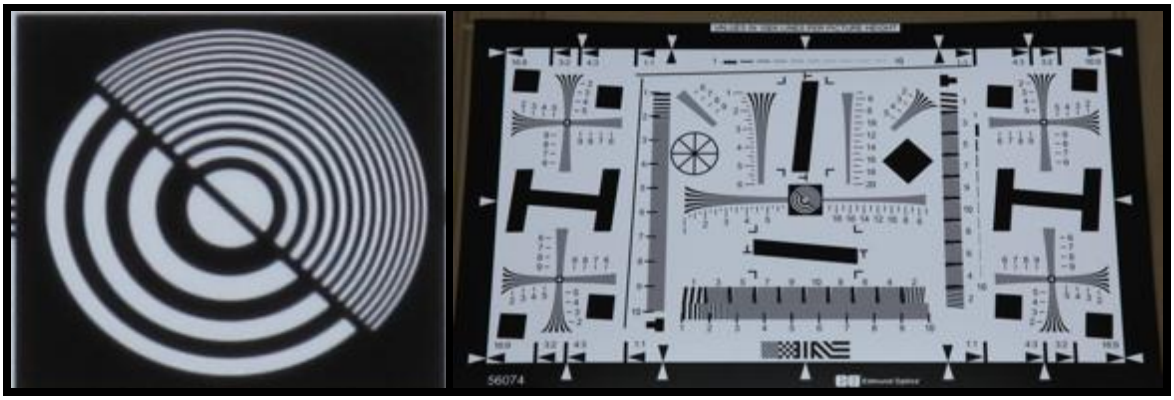

Figure 2–15. ISO 12233 test image photographed with the UAS-based imaging system during laboratory pretesting, using a variable focus lens (104 mm setting) with ISO 22.0.

The system components that were installed in the aircraft during all subsequent field tests are shown in Figure 2–16. This system was tested on the benchtop prior to installation in the aircraft. The bench power supply was replaced with a DC battery pack and power regulation circuitry that powered the image capture system. The image capture process was automated or programmed to capture three frames per second or more depending on storage capacity of the hard disk, and the camera system was configured for outdoor operation.

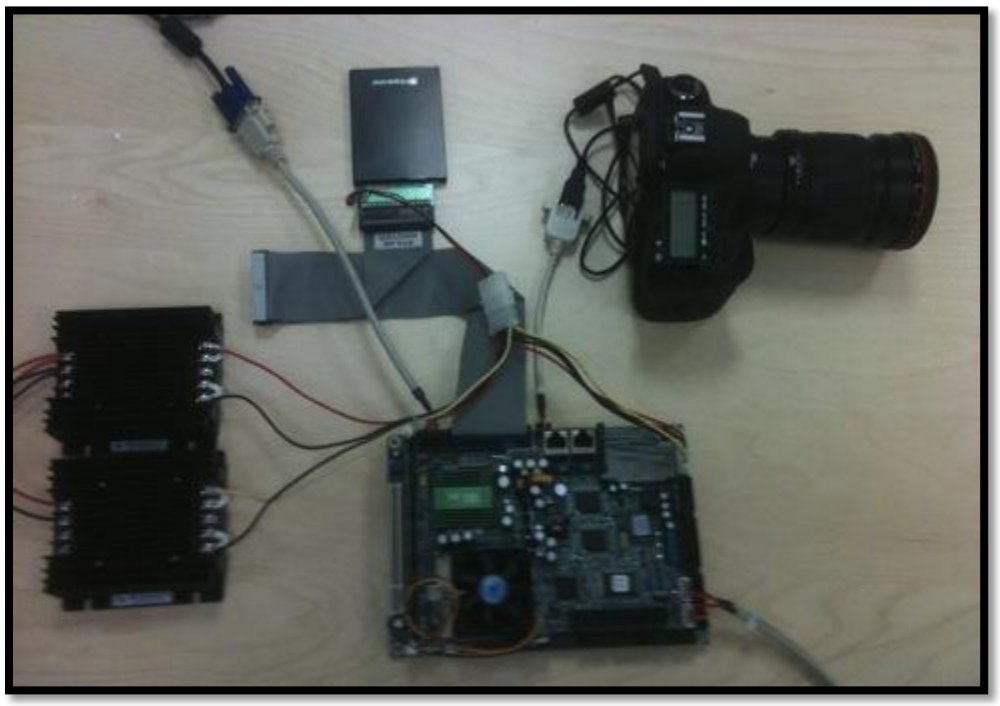

Figure 2–16. Image capture system with DC power supply, prior to installation in aircraft for field testing.

In Figure 2–17, a block diagram of the system components is shown. In addition to the aircraft avionics, additional computation hardware was necessary to automate the camera image collection process. The single board computer ran a master program that actuated the camera shutter, synced the image data to the pose of the aircraft, and stored the data. There was also the ground control station (GCS) that the operator/pilot used to command and control the aircraft. The GCS consisted of a laptop, joystick, and antennas.

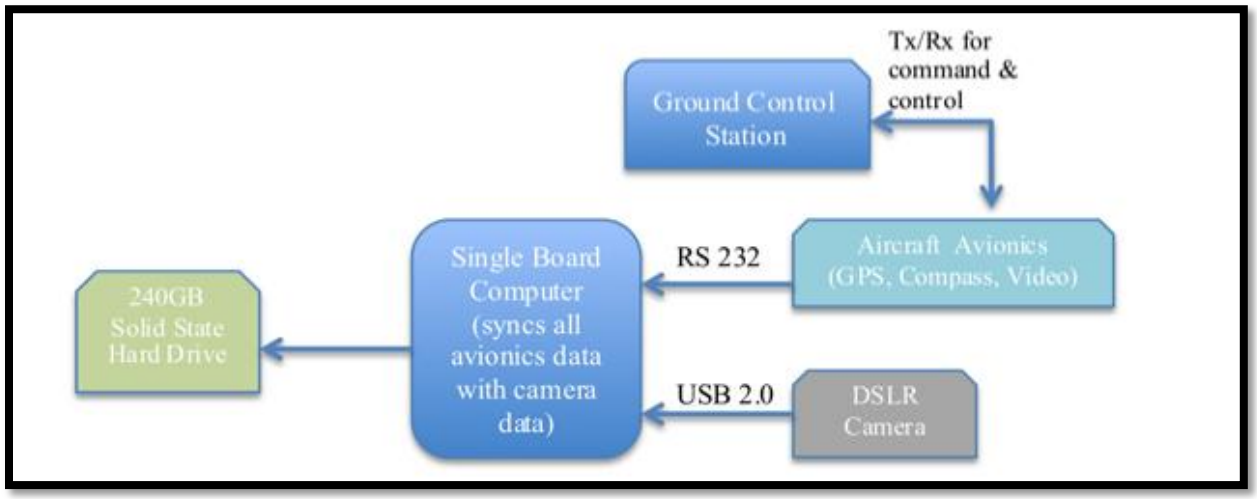

Figure 2–17. Block diagram of system components for automated image capture and aircraft command and control in the UAS-based high-resolution imaging system.

For this system, the required interconnections with aircraft systems and peripherals were as follows:

- Camera/DVR
  - USB 2.0
- DVR/Autopilot
  - Serial RS232
- DVR/IMU+GPS
  - Serial RS232
- DVR/SSD
  - SATA 2.0

(DVR: digital video recorder, IMU: inertial mobility unit, SSD: solid state disk)

A ground test was performed to test and document the maximum duration of in-flight operation under internal power. The results are summarized below:

Table 2–5.

Maximum Runtime Results from Pretesting Conducted in Gainesville FL in August 2011

Parameter	Value
Operating voltage	12 Volt
Operating current	Max: 3.15 A
Battery capacity required for 1-hour mission	3S1P LiPo @ 3.2Ah
Current battery configuration	3S1P LiPo @ 9Ah
Current mission capacity	2.8-hour runtime

The following experiments were performed in the laboratory to ensure proper operation prior to remotely piloted flight tests:

1) Test full range of cameras, optics, and vectoring and automated operations in-flight.

   We designed the payload mounting structure to accommodate a range of camera angles measured from the vertical downward direction.

2) Test full range of relevant remote control maneuvers in flight.

   This was regularly tested to check for proper radio communication and any drop outs that may occur during flight.

3) Test video streaming link speed in flight.

   The onboard video camera was used for operator navigation purposes. This video downlink was tested in flight to have a of 1 to 2-mile line of sight. Due to the large file size and limited communication bandwidth, the high-resolution images were stored onboard the aircraft and retrieved after the flight.

4) Test full range of camera, optics, and automated operations in flight.
5) Test and document instrument response to altitude changes.
6) During each mission, basic parameters were recorded such as roll, pitch, yaw, position, and altitude.
   a. Test and document response time to control inputs and results (at varying altitudes).
   b. Test and assess effectiveness of method used to maintain synchronization between frame capture rate and airspeed.

Test Matrices

Prior to conducting field tests, we developed a set of test matrices to ensure successful execution and data gathering during all field tests. These test matrices are described for individual imaging system components below.

a. Cameras

Test Case	Description	Requirements	Pass/Fail	Comments
a.1.	Maximum frame rate	20% image overlap during cruise		
a.2.	Exposure settings—ISO value	Shortest exposure time while maintaining image contrast		
a.3.	Battery capacity	Internal battery capacity exceeds mission duration		

b. Lenses

Test Case	Description	Requirements	Pass/Fail	Comments
b.1.	Focal length allows for desired spatial resolution at mission altitude	1 cm, 2 cm, 5 cm ground pixel spatial resolution		
b.2.	Polarization filters (vertical, horizontal)	Reduce glint, glare, sky reflection effects		
b.3.	Color filters	Increase image contrast		

c. Mounts

Test Case	Description	Requirements	Pass/Fail	Comments
c.1.	Camera angle (vertical/oblique)	Observe reduction in glint, glare effects		
c.2.	Camera angle (vertical/oblique)	Increase coverage area while maintaining image quality		
c.3.	Vibration isolation	Improve image quality through passive vibration mounts		

d. Control systems

Test Case	Description	Requirements	Pass/Fail	Comments
d.1.	Automated exposure control	Unattended image capture		
d.2.	Syncing image and metadata	Unattended syncing of images with metadata		

e. Digital Voice Recorder

Test Case	Description	Requirements	Pass/Fail	Comments
e.1.	Automated exposure control	Unattended image storage		
e.2.	Syncing image and metadata	Unattended storage of images with metadata		
e.3.	Capacity	Storage capacity exceeds mission requirements (mission duration × frame rate × image size)		

2.3.3 Flight Trials Conducted

Following all system development and pretesting, flight testing was conducted with the UAS-based high-resolution imaging system in four stages, outlined in Table 2–6 and detailed in text below.

Table 2–6.

Summary of Flight Testing Conducted with UAS-based Aerial High-resolution Imaging System

Flight Test Stage	Dates	Location	Ground Substrate	Flight Altitudes (agl)	Vehicle
1: Preliminary test of imaging equipment	1–4 Sept 2011	Lake Santa Fe FL	Lake (water)	370 m	Manned aircraft
2: Initial UAS imaging test	5–9 Sept 2011	Gainesville FL	Land	30–160 m	UAS
3: High altitude UAS imaging test	Week of 3 Oct 2011	Camp Roberts CA	Land	200–500 m	UAS
4: Over water UAS imaging test	Jan–Feb, 2012	Near Cedar Key FL	Gulf of Mexico (water)	60–140 m	UAS

Flight Testing Stage 1

Lake Renegade manned plane aerial payload tests were conducted to collect synchronized image, position, velocity, and orientation data from the imaging system: camera/IMU/GPS sensors, prior to integration of the system within the UAS. The Lake Renegade manned aircraft (Figure 2–18) provided an ideal platform for these tests because of its rear-mounted propeller and engine. This provided a clear, unobstructed view from the passenger seat.

Experimental Setup:

- Computer initiated camera shutter and all data was transferred and databased
- Flown at ~370 m agl due to cloud ceiling
- Flown at ~80 knots
- Area of Lake Santa Fe FL
- Environmental: Scattered clouds with smoke and fog
- Camera and IMU/GPS handheld
    - Camera: Canon Mark II with 200 mm lens
- Observations:
    - Camera exposure/shutter speed needed adjustment
    - Image jitter due to manual holding of camera payload

Figure 2–18. Lake Renegade manned aircraft flown over Lake Santa Fe near Gainesville FL during stage 1 flight testing of the imaging system developed for UAS-based aerial high-resolution imaging surveys, September 2011.

Some sample images are provided in Figure 2–19 and Figure 2–20. These images were taken once per second from the onboard camera imaging system. See section 3.3.3 also.

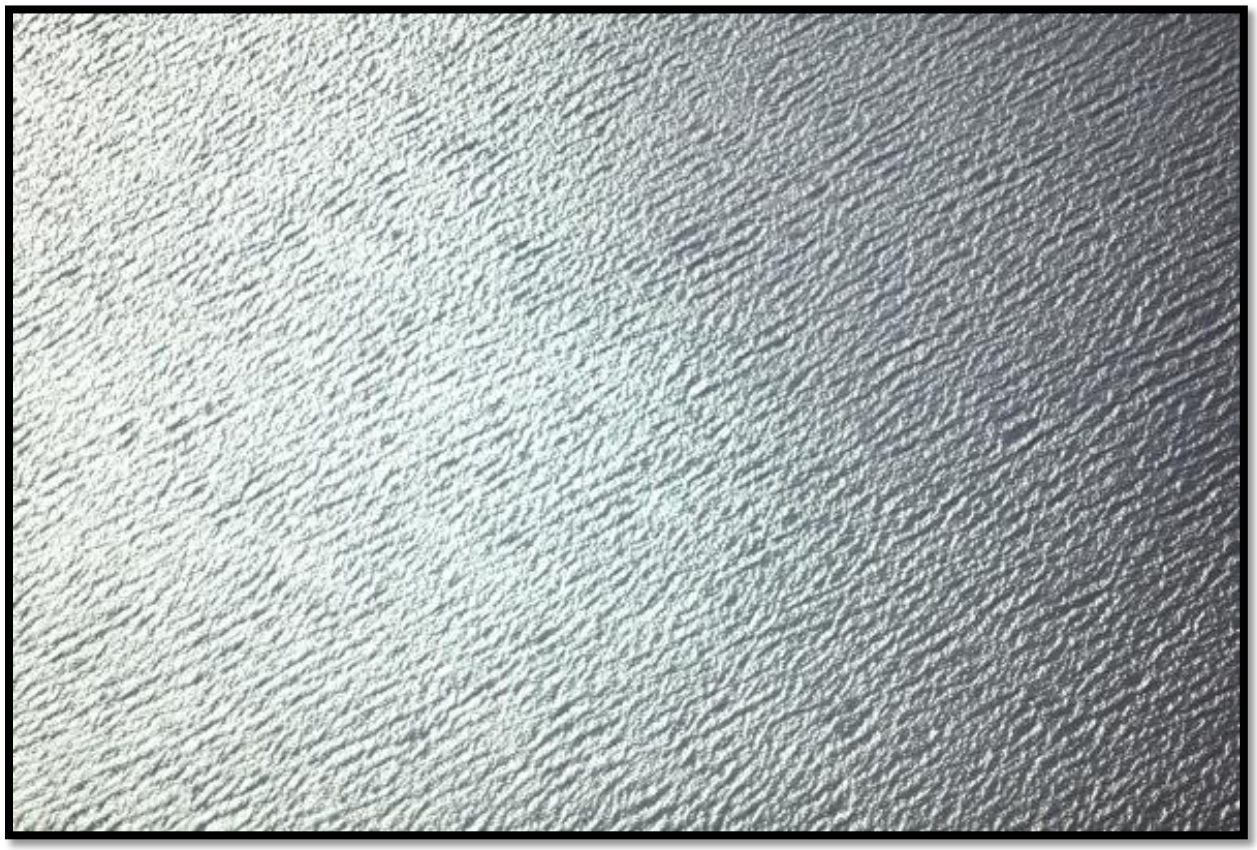

Figure 2–19. A sample image of the surface of Lake Santa Fe FL taken during stage 1 flight testing of the imaging system developed for UAS-based deployment, September 2011.

Figure 2–20. A sample image of the water and shoreline of Lake Santa Fe FL taken during stage 1 flight testing of the imaging system developed for UAS-based deployment, September 2011.

Flight Testing Stage 2

Our preliminary imaging system testing was conducted in Gainesville FL over land and at low altitudes. During these experiments we were evaluating the performance of the aircraft and of the camera imaging system during its first test after integration of the imaging equipment into the UAS. Details of the experimental setup are listed below, and the aircraft is shown in Figure 2–21.

- Flight Elevation: 100 to 500 feet over land
- Flight Speed: 35 to 40 mph
- Environmental: Early evening flight during very overcast conditions
- Testing of camera, single board computer, solid state hard drive onboard the aircraft.

Figure 2–21. Pelican aircraft at flying field in Gainesville FL during stage 2 flight testing, September 2011.

Some sample images from the stage 2 UAS-based imaging flight tests are provided in Figure 2–22 and Figure 2–23. These images were taken once per second from the onboard camera imaging system.

Figure 2–22. Eight sample images of the ground surface near Gainesville FL taken during stage 2 flight testing of the imaging system developed for UAS-based deployment, September 2011.

From our initial over land field experiments, we were able to create a composite or stitched image that provides a merged aerial image. Based on these experiments, we found that there was sufficient overlap from image to image using a once per second sampling rate. These results will vary with flight speed and prevailing wind conditions.

Figure 2–23. Composite image of the ground surface near Gainesville FL, created by stitching together four separate images taken during stage 2 flight testing of the imaging system developed for UAS-based deployment, September 2011.

Flight Testing Stage 3

High altitude flight tests were performed at Camp Roberts CA in restricted military airspace during the week of 3 October 2011. The objective of these tests was to collect synchronized image, position, velocity, and orientation data from the camera/IMU/GPS sensors at higher altitudes, including the altitudes of interest for offshore wind-wildlife imaging surveys (safely above the rotor swept zone of commercial marine wind turbines). UAS flight tests at these altitudes were only permissible within military airspace for this project, due to lengthy and difficult FAA permitting processes for flying UAS within US civilian airspace (see section 3.2.3).

Experimental Setup:

- The system was initially flown at low altitudes (200 m above ground level [agl])
- Gradually increased the flight height (up to 513 m agl)
- Flying at ~35 to 40 knots (kts)
- With heavier winds, sometimes flying at a slower speed
- Weather: calm in the mornings with increasing winds (10+ kts) in the afternoon, there was some rain and storms to work around
- Camera, IMU/GPS, embedded DVR equipped on aircraft
- Camera: Canon 18MP with 55 mm lens

During the stage 3 field tests, winds ranged from 5 to 10 mph with 20 mph gusts. During the heaviest winds, the aircraft was still able to penetrate the wind and collect survey images.

Our GCS is used to send and receive commands to and from the aircraft. This is used to remotely pilot the aircraft and provides the pilot with a video downlink at all times. A sample screenshot of our GCS interface is shown in Figure 2–24.

Figure 2–24. Sample screenshot from the ground control station (GCS) interface used during stage 3 flight testing of the UAS-based high-resolution imaging system at Camp Roberts CA, October 2011.

Stage 3 field testing produced imagery of the ground surface containing an image quality evaluation target, as well as other objects of known size and visual appearance that were useful for evaluating the effectiveness of the UAS-based high-resolution imaging system. A selection of representative images captured during stage 3 flight testing is presented in Figure 2–25, Figure 2–26 and Figure 2–27 below. The flight altitude profile of a single stage 3 test flight is shown in Figure 2–28.

Figure 2–25. Image of the ground surface at Camp Roberts CA, taken during stage 3 flight testing of the UAS-based imaging system, October 2011. Flight altitude = 513 m agl.

Figure 2–26. Image of the ground surface at Camp Roberts CA, taken during stage 3 flight testing of the UAS-based imaging system, October 2011. Flight altitude = 272 m agl.

Figure 2–27. Image of the ground surface at Camp Roberts CA, taken during stage 3 flight testing of the UAS-based imaging system, October 2011. Flight altitude = 436 m agl. The black and white image quality evaluation target is visible just below the runway in this image. The dimensions of the target are 457 × 366 cm.

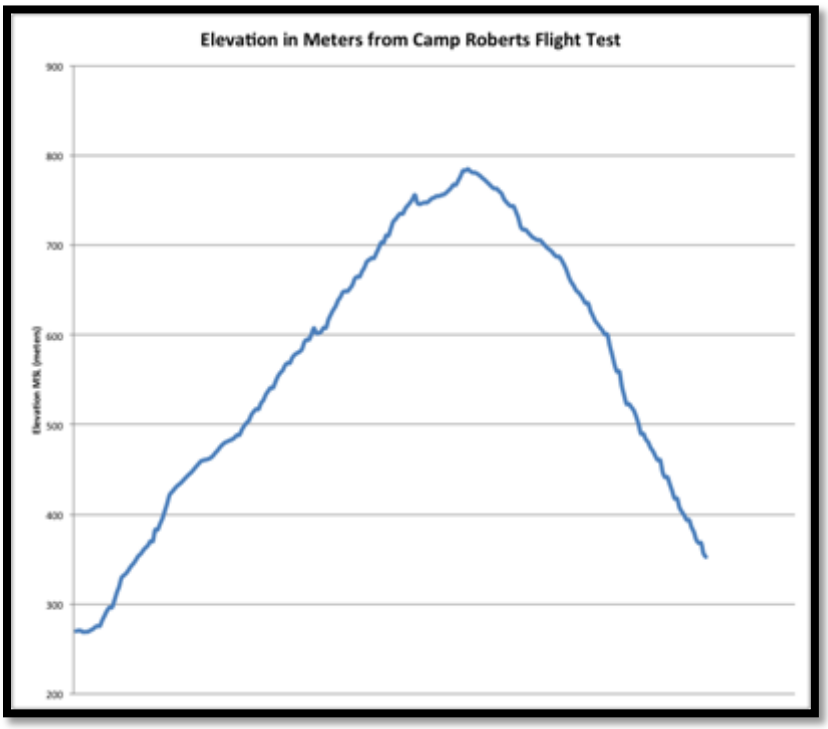

Figure 2–28. Flight elevation profile for a stage 3 test flight of the UAS-based imaging system conducted at Camp Roberts CA during October 2011.

Flight Testing Stage 4

Lower altitude flight tests were performed near Cedar Key FL over the surface of the water of the Gulf of Mexico, from 0 to 1 km from the shore, during January and February 2012. The objective of these tests was to collect synchronized image, position, and orientation data from the aircraft in a marine environment. Higher altitude flights at this location were precluded by FAA permission restrictions on UAS flights within US civilian airspace.

Experimental Setup:

- The system was flown at low altitudes (20 m agl)
- Gradually increased the flight height (up to 140 m agl)
- Flying at ~35 to 40 kts
- Weather was very clear and calm with light winds (3 to 5kts)
- Camera, IMU/GPS equipped onboard aircraft

Stage 4 flight testing of the UAS-based imaging system produced overwater images that were useful for evaluating the effectiveness of the imaging equipment for conducting offshore wildlife imaging surveys, including several images of birds and a possible marine mammal. Representative images gathered during the stage 4 flight testing are presented in Figure 2–29, Figure 2–30, and Figure 2–31 (see also section 3.3.3). The flight altitude profile of a stage 4 flight test is shown in Figure 2–32.

Figure 2–29. Image of the water's surface of the Gulf of Mexico near Cedar Key FL, taken during stage 4 flight testing of the UAS-based imaging system, January to February 2012. Flight altitude = 80.5 m agl.

Figure 2–30. Image of a boat and the water's surface of the Gulf of Mexico near Cedar Key FL, taken during stage 4 flight testing of the UAS-based imaging system, January to February 2012. Flight altitude = 141.5 m agl.

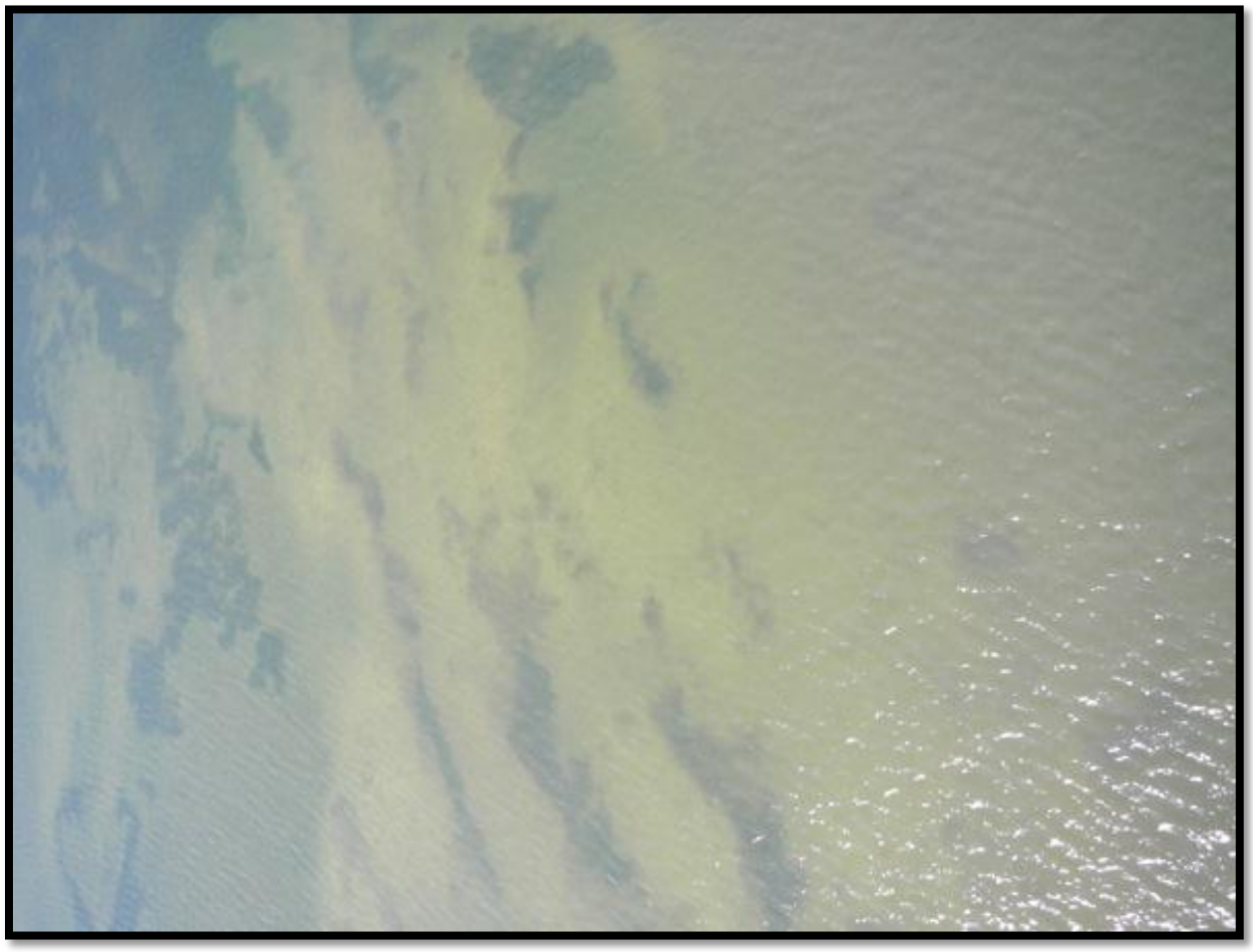

Figure 2–31. Image of shallow water in the Gulf of Mexico near Cedar Key FL, with the shallow sea floor visible below the water's surface, taken during stage 4 flight testing of the UAS-based imaging system, January to February 2012. Flight altitude = 83.1 m agl.

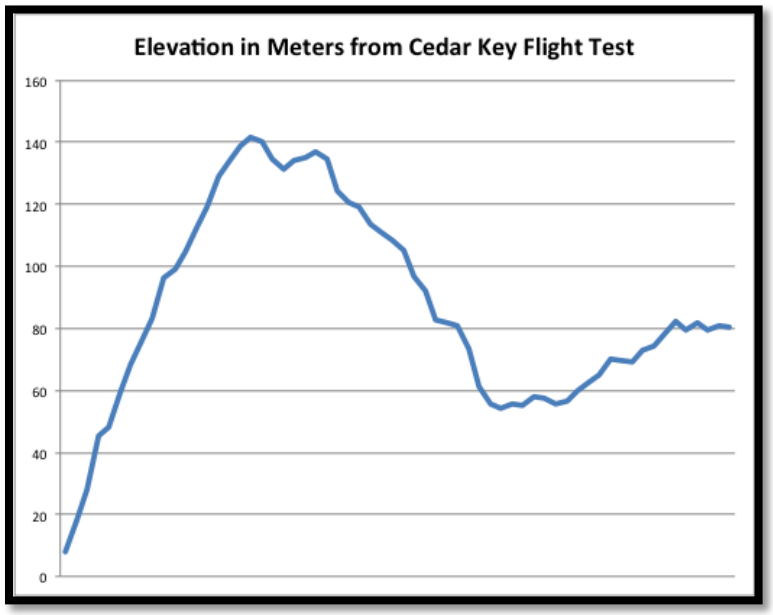

Figure 2–32. Flight elevation profile for a stage 4 test flight of the UAS-based imaging system conducted over the Gulf of Mexico near Cedar Key FL, during January to February 2012.

3 Technical Analyses and Evaluations

3.1 Introduction

The objective of this project is highly methodological—to optimize and adapt a new survey method through a pilot study; and the method of interest—high-resolution aerial imaging—is highly technological in nature. For this reason, the evaluation, development, and implementation of technology for conducting offshore high-resolution aerial wildlife imaging surveys comprised a core component of this project, and is outlined in this chapter.

In particular, the contract specified four areas of technology to be addressed in separate tasks, as follows:

- Task 2: Evaluate aircraft for safety and effectiveness offshore
- Task 3: Evaluate high-definition cameras and mounting systems
- Task 4: Develop protocols for camera control and operation
- Task 5: Evaluate and recommend data recording systems

Each of these four technological components is addressed in a separate subsection of this chapter.

All of the technology-related work in this project was performed directly by subcontracted technical experts, working under the direction of the technology manager, M. Kujawa, and Normandeau. The subcontracted technology experts, and their respective areas of expertise and project roles were as follows:

- Aviation (aircraft and integration of imaging equipment)
    - Manned aircraft systems: Randall Clark, Pinnacle 1 Aviation (P1A)
    - Unmanned aircraft systems (UAS): Donald and Erica MacArthur, IATech, Inc.
- Imaging (cameras, optics, data recording, storage, and transfer)
    - Manned aircraft systems: Carlos Jorquera and Jason Luttrell, Boulder Imaging
    - UAS: Donald and Erica MacArthur, IATech, Inc.

The technology-related sections of this report contain both broad-based evaluations of existing technologies based on reviews of available information, and also focused evaluations of the specific technologies we implemented during flight experiments, based on analysis of our experimental results. The aircraft and camera/mount evaluation sections contain significant depth, as these technology choices are more pivotal for the design of aerial high-resolution wildlife imaging surveys, while the camera control and data recording system sections are more brief, with an emphasis on description of the systems implemented, and evaluation of performance during the experimentation that was conducted over the course of this study.

As a final point of introduction to the technical analysis section of this report, we note that technology is rapidly changing, particularly with respect to imaging equipment. Future technological

advances can impact optimal high-resolution aerial imaging survey design in many ways, but in particular, we anticipate significant future improvements in aerial imaging survey protocols with the development of digital cameras capable of recording larger images (more pixels). Early in the design of this project, the project team identified increasing the survey swath width over that typically implemented in the pioneering European offshore high-resolution wildlife imaging surveys of the late 2000s as a critical need for successful implementation of offshore aerial high-resolution imaging surveys in US waters. This is primarily driven by the large areal extent of the AOCS that is desirable for offshore wind development (USDOE 2008). Although the implementation of multiple camera arrays was initially envisioned as a potential solution to this need, recent rapid advances in digital camera image size capacity suggests that camera technology development may present a more efficient and economical solution for surveying wider swaths.

3.2 Aircraft Evaluation

3.2.1 Introduction

The objective of the aircraft evaluation, as defined in task 2 of the contract, was to "collect relevant data and information to evaluate the suitability of various aircraft for safe, effective, and efficient conduct of aerial surveys offshore on the AOCS." Three broad criteria were used to define suitability as follows:

1) Safety
2) Effectiveness
3) Cost

This evaluation was conducted in two stages. In the first stage, a desktop analysis was conducted in which all possible candidate aircraft were evaluated based on available literature, technical specifications from manufacturers, and expert opinion to identify aircraft likely to be most suitable for the purpose of conducting aerial high-resolution marine wildlife imaging surveys. The desktop review was also used to select a subset of aircraft to be used in field testing for this project. The second stage of aircraft evaluation consisted of post-field testing evaluation of the performance of the aircraft used for this project.

An initial review of candidate aircraft for conducting high-resolution marine wildlife imaging surveys revealed significant potential utility of both manned and unmanned aircraft systems, hence one of each was selected for field testing. The aircraft evaluation section of this report is correspondingly divided into separate sections for manned and unmanned aircraft systems.

3.2.2 Manned Aircraft Evaluation

The evaluation of candidate manned aircraft under the project was led by the subcontracted aviation technical expert on the project team, R. Clark of P1A, in coordination with the technology task manager, M. Kujawa, and under the direction of Normandeau.

Desktop Evaluation and Flight Test Aircraft Selection

The desktop evaluation of aircraft was initiated with an exhaustive literature review. Information on the technical specifications and performance of candidate aircraft gathered was compiled and combined with the professional opinion and experience of aviation experts to systematically evaluate

all candidate manned aircraft under the three broad suitability criteria—safety, effectiveness, and cost. To supplement the direct experience and opinion of aviation expertise on the project team, M. Kujawa and C. Gordon conducted a series of interviews with pilots and aerial imaging practitioners, as well as representatives from US federal government agencies involved in conducting aerial wildlife surveys. A summary of this information is presented in Table 3–1 and Table 3–2, and is discussed in the text of this section.

Table 3–1.

Detailed Evaluation of Candidate Manned Aircraft on the Basis of Many Specifications and Aircraft Characteristics that Influence Suitability for Conducting Offshore Aerial High-resolution Wildlife Imaging Surveys—All Candidate Manned Aircraft Are Fixed Wing Aircraft Except for the Jet Ranger Bell Helicopter

Aircraft*	Cessna 337E Skymaster	Piper Navajo	Piper Aztec PA 23-250F (Non Turbo)	Vulcanair/ Partenavia P68 Observer 2	Diamond DA42 MPP	Twin Otter, De Havilland DHC-6-300	Cessna 208B Grand Caravan	King Air 100	Cessna 206 Turbo Stationair	Kodiak 100	Beaver, De Havilland DHC-2	Jet Ranger Bell 206BIII Helicopter
Power Plant (No)	2	2	2	2	2	2	1	2	1	1	1	1
Power Plant (Type)	Piston	Piston	Piston	Piston	Piston	Turbine	Turbine	Turbine	Piston	Turbine	Piston	Turbine
Cruise Airspeed (mph)	175	215	150	184	155	173	165	295	130	150	140	100
Climb Rate (fpm)	1,180	1,445	1,400	1,100	1,700	1,600	1,115	2,140	1,050	1,371	1,020	1,260
Useful Load (lbs)	994	2,800.00	1,600.00	1,499.00	1,025.00	5,200.00	3,734.00	1,540.00	811	3,535.00	2,100.00	1,038.00
Cabin Size	Small	Medium	Small	Medium	Small	Very Large	Large	Medium	Small	Large	Medium	Small
Gen/Alt Output (V/A)	28/60 × 2	317 KW × 2	28/60 × 2	28/70 × 2	28/61 × 2	28/200 × 2	28/200	> 400 KW	28/60	28/300	28/60 Min	28/150
Range (nautical miles [nm]; approx.)	922	1,093	1,300	1,598	784	775	900	1,000	570	1,032	455	374
Production Dates (All Models)	1963–1982	1964–1984	1952–1981	1972–Present	2004–Present	1965–1988	1984–Present	1969–1983	1962–Present	2007–Present	1947–1967	1967–2009
Compatible with 12-Camera Array	N	Y	Y	Unknown	Unknown	Y	Y	Y	Y	Y	Y	Y
Marine Survey History (Y/N)	Y	Y	Y	Y	Y	Y	Y	Y	Y	Y	Y	Y
Maximum Seating (Crew + Pax)	6	8	6	6	4	20	12	7	6	10	7	5

Aircraft*	Cessna 337E Skymaster	Piper Navajo	Piper Aztec PA 23-250F (Non Turbo)	Vulcanair/ Partenavia P68 Observer 2	Diamond DA42 MPP	Twin Otter, De Havilland DHC-6-300	Cessna 208B Grand Caravan	King Air 100	Cessna 206 Turbo Stationair	Kodiak 100	Beaver, De Havilland DHC-2	Jet Ranger Bell 206BIII Helicopter
Availability (Units in Service)	~ 3,000	~ 2,000	> 4,000	450	< 750	> 500	~ 2,000	416	> 5,000	< 50	> 1,000	> 7,000
Wing Type	High	Low	Low	High	Low	High	High	Low	High	High	High	N/A
Landing Gear F = fixed R = retractable	R	R	R	F	R	F	F	R	F	F	F	F (SKID)
Cost Of Operation† ($/hour)	110	185	129	79.348	42.064	334.6	335	500	76	239	129	335
Endurance (hours)	~ 5.0	7.5	4.5	10	10	7	5.1	~ 6.5	4.5	5.9	5	4
Fuel Burn (gph)	23	37	27	16.6	8.8	70	53	100	16	50	27	28

*Production information and statistics available at www.airliner.net.

Table 3–2.

Summary of Desktop Evaluation of Candidate Manned Aircraft on the Basis of the Three Principal Criteria (Safety, Effectiveness, and Cost) that Influence Suitability for Conducting Offshore Aerial High-resolution Wildlife Imaging Surveys

Manned Aircraft	Safety	Effectiveness	Cost	Total
Cessna 337	**4**	**3**	**5**	**12**
Piper Navajo	**4**	**4**	**4**	**12**
Piper Aztec	**4**	**5**	**3**	**12**
Vulcanair P68 Observer 2	**4**	**3**	**5**	**12**
Diamond DA42 MPP	**4**	**2**	**5**	**11**
Twin Otter, De Havilland DHC-6-300	**5**	**5**	**1**	**11**
Cessna 208B Grand Caravan	**3**	**5**	**3**	**11**
King Air XXX	**5**	**4**	**1**	**10**
Cessna 206	**2**	**3**	**5**	**10**
Kodiak 100	**3**	**4**	**3**	**10**
Beaver, De Havilland DHC-2	**1**	**4**	**3**	**8**
Jet Ranger Bell 206BIII helicopter	**2**	**2**	**2**	**6**

Higher scores indicate higher suitability. All candidate manned aircraft are fixed wing aircraft except for the Jet Ranger Bell Helicopter. Each aircraft's scores for each criterion were derived from a combination of many individual specifications and factors, presented in more detail in Table 3–1 and in the text.

Discussions with Other Airborne Imaging and Surveying Practitioners

The project team contacted a variety of practitioners of aerial wildlife surveys in the process of evaluating candidate aircraft, as well as other aerial high-resolution imaging equipment configurations and techniques. In the case of commercial practitioners, limited information was available for use in the current project, because much of the technical information about survey methodologies they use is privileged, confidential information. The organizations and persons contacted via meetings, telephone, email, and Skype were:

- Steve Earsom, USFWS pilot
- Tim Bowman, USFWS; pilot, Sea Duck joint venture director
- Dr. Ib Krag Petersen, Danish National Environmental Research Institute (NERI)
- Mark Robinson and John Martin, UK-based HiDef Aerial Surveying, Ltd.
- Dr. Stuart Clough, UK-based APEM, Ltd.
- Tim Cole, NOAA, AMAPPS project

It is important to note that all three European high-definition aerial wildlife survey organizations use through-the-floor imaging devices that are mounted within the interior of the aircraft. All US-based

video and digital imaging efforts are also carried out using cameras peering out from within the aircraft. The helicopter-based Block Island RI offshore survey has been carried out using a camera looking out through the aperture afforded by removing the door behind the pilot (M. Kujawa, pers. comm.).

US Fish and Wildlife (Steve Earsom, Tim Bowman)

Discussions with S. Earsom and T. Bowman focused on US government use of manned aircraft for high-definition aerial wildlife surveys, in particular USFWS breeding waterfowl surveys and winter sea duck surveys on the AOCS, focusing on lessons learned and equipment and methodology employed. Attention was also given to the use of the Kodiak 100 turbine driven, single engine aircraft as a potential candidate survey aircraft. S. Earsom noted that flight safety statistics have shown that single engine, turbine driven aircraft have the lowest accident rates of all general aviation aircraft. Currently USFWS uses the Kodiak 100 to conduct their continental scale waterfowl surveys (waterfowl breeding population and habitat surveys, offshore wintering sea duck surveys), and all are fitted with floats for increased safety and flexibility in marine operations.

NOAA, Atlantic Marine Assessment Program for Protected Species (AMAPPS) project (Tim Cole)

Discussions with Tim Cole, a NOAA biologist involved with the large-scale AOCS wildlife surveys of the Atlantic Marine Assessment Program for Protected Species (AMAPPS) project, focused on the survey objectives and methodologies currently being applied to the AMAPPS project. Although this project entails exclusively visual observer-based surveys, the De Havilland Twin Otter aircraft being used for the aerial surveys are potentially suitable for conducting digital aerial imaging surveys, particularly because they possess belly hatches in which cameras could be mounted. The possibility of adapting these aircraft to supplement the current AMAPPS methodology and help accomplish AMAPPS project objectives was discussed, and a specific protocol for conducting large scale marine aerial high-resolution imaging surveys was developed, presented in Chapter 4.

Criterion 1: Safety

A number of subcriteria were identified within the safety criterion that contributed to the suitability of candidate aircraft for conducting offshore aerial high-resolution wildlife imaging surveys. These subcriteria are presented in Table 3–1 and described below.

- Power Source

Aircraft of the size of interest have either one or two engines, using either piston or turbine power. A single engine aircraft has its engine mounted on the centerline. Except for a single mass-produced design, all dual engine aircraft have engines mounted left and right of center. The lone exception to this standard two engine arrangement is the Skymaster, which features dual center-mounted in-line engines mounted fore and aft of the main wing. One engine pushes and the other pulls.

In general, multiengine aircraft have a higher safety advantage over single engine aircraft, particularly for piston engines. Depending on payload, in the case of a single engine failure over water, the aircraft can be safely flown to a suitable airport on the remaining engine. Turbine engines

are historically more reliable than piston engines, although usually at the price of higher operating costs. Operating time between failures is significantly higher in turbine engines than piston.

Both European commercial high-resolution aerial survey companies (APEM, Ltd. and HiDef Aerial Surveying, Ltd.) employ twin engine aircraft when performing marine wildlife surveys (S. Clough, APEM Ltd., pers. comm.; Mark Robinson, HiDef Aerial Surveying, Ltd., pers. comm.).

Twin engine aircraft also provide redundancy in electrical power generation because each engine is typically driving an alternator or generator. Given the increased electrical loads produced by the onboard imaging equipment, this ensures adequate electrical power margins for both organic aircraft power requirements and the imaging system components.

Traditionally, government agencies have required their aircraft operating over water for extensive periods to be equipped with at least two engines. However, with ever improving engine technology and powerplant maintenance, aircraft engines today rarely encounter failure if properly maintained. In addition, turbine engines (turbo-prop) are becoming more common in larger single engine aircraft such as the Cessna 2088 Grand Caravan, Kodiak Quest, and Pilatus PC-12. For example, the turbine PT-6 engine has a long history of reliability. However, turbine engines also result in higher operating costs.

- Long Aircraft Production Runs

Long production runs result in valid safety and performance data derived from many thousands of hours of performance and many years of flight operations. A long production history also typically equates to a larger pool of qualified and experienced pilots in that aircraft. This ensures that a sufficient number of qualified, experienced pilots will be available to fly the aircraft if a survey is undertaken.

Continuous use over decades means that there are facilities where pilots regularly go to gain or maintain currency and qualifications with a particular aircraft model. Further, it means that there is a standing cadre of aircraft service providers with personnel who are familiar with the aircraft, its components and maintenance, and with access to parts.

Criterion 2: Effectiveness

A number of subcriteria were identified within the broad effectiveness criterion that contributed to the suitability of candidate aircraft for conducting offshore aerial high-resolution wildlife imaging surveys. These subcriteria are presented in Table 3–1 and described below.

- Cruise airspeed—miles per hour (ground speed)

The distance covered per hour greatly impacts the flight time necessary for a survey, which in turn strongly influences the amount of fuel burned and the cost per square mile surveyed. It is important to note that flight speed also interacts with imaging specifications, as more image blur tends to be introduced at higher speeds.

- Climb rate—feet per minute

The climb rate to survey altitude may impact flight time, although this impact is expected to be minimal at the survey altitudes considered.

- Useful load—in pounds

This aircraft characteristic limits the amount of equipment and number of technicians and observers that can be onboard the survey aircraft. Weight and balance distribution is also an important feature impacting the safe and effective operation of various aircraft with certain imaging payloads.

- Cabin size—in cubic feet

This is a limiting factor for the size of any equipment and number of technical personnel for a survey flight. This also may limit the available floor area for mounting camera systems and support equipment.

- Generator/alternator output—in volt/amperes

The power output criterion is only important as a minimum threshold above which power is sufficient for operating all imaging system equipment as well as all organic aircraft functions.

- Endurance—hours

This aircraft characteristic governs the maximum flight time possible before returning for refueling. Greater aircraft endurance increases the survey efficiency—and thereby lowers the cost—of imaging surveys. It is important to note that endurance interacts with payload and speed, which impact fuel consumption rates.

- Range—nautical miles

A function of useable fuel and flight speed, this characteristic reflects the maximum distance the aircraft can fly between refueling stops.

- Production dates—time in manufacture

This information is provided to indicate when the aircraft was produced from the factory. However, whether or not an aircraft is still in production is not a relevant factor in this experiment.

- Maximum seating—crew and passenger

Related to cabin size, this criterion refers specifically to available room for passengers and equipment, and is an indication of aircraft interior design flexibility.

- Availability—units in service; ease of access to multiple aircraft of the same make and model

Pilots have flexibility in scheduling if the same type of aircraft is flown; substitute aircraft can be found more easily if more of the same model of aircraft are available and operation and mounting configurations and procedures are understood. The use of rare, limited availability aircraft models carries additional risk that surveys will not be able to be performed in the times and places desired, hence we regard high availability of aircraft models as a positive factor contributing to effectiveness for aerial offshore wildlife imaging surveys.

- Wing type—High/low/middle

This feature is more relevant to survey methods employing visual observers viewing wildlife through cabin windows. A low wing aircraft obviously has significant obstacles to the observer as they view targets below the aircraft. Low wing aircraft also have a wing spar passing through the cabin floor, which can limit the available locations for belly camera ports..

- Landing gear—fixed/retractable

Retractable landing gear ensures that there will be no obstructions in the field of view beneath the fuselage of the aircraft.

- Fuel burn rate—gallons per hour (gph)

This aircraft characteristic interacts both with endurance and cost of aircraft operation. Its importance will vary with fuel prices. For example, fuel increased in price by 25% per gallon the year after the flight experiments for this study were designed and planned. Note: Another consideration regarding fuel is availability. Turbine engines require jet fuel, while piston engines use 100LL Avgas. While Avgas is readily available in the US, it is becoming increasingly difficult to obtain in more remote parts of the world. This could be a consideration depending on the location of the survey.

Criterion 3: Cost

The cost criterion was the simplest to evaluate, as a function of price per hour offered by aviation service providers for different aircraft.

Quantitative Candidate Aircraft Ranking and Selection for Field Tests

All candidate aircraft were evaluated on the basis of their combined scores for all criteria and subcriteria described above, and presented in the aircraft evaluation matrices (Table 3–1 and Table 3–2). In the scoring process, heavy weight was given to the recommendation provided by the project team's aviation expert, R. Clark. Specific information on the specifications and subcriteria affecting suitability (Table 3–1) were distilled into an overall score ranging from 1 to 5 for each of the three broad criteria, with 5 being the most positive score, and 1 the lowest. All scores are presented in Table 3–2. The scores for each of the three criteria were summed to produce an overall score for each candidate manned aircraft.

These scores were used to select a manned aircraft for field experimentation. This scoring matrix and the explanatory text above and below is also intended to serve as a general comparative guide for the selection of aircraft for conducting aerial imaging surveys in the future. Several of the candidate aircraft that received the highest scores are discussed individually below.

Cessna 337 Skymaster—The Cessna 337 Skymaster (Skymaster) was selected for field testing under this project, as it was one of the highest ranking candidate aircraft in total suitability score (12, see Table 3–2) and readily available to the project. The high level of suitability of this aircraft resulted from a variety of factors including lower operating costs, history of use in aerial marine surveys, and its broad availability (approximately 3,000 manufactured). This latter factor also contributed to the score of 4 in the safety category because maintenance would be assured, as would be the availability of a significant number of certified pilots.

The Skymaster has an in-line twin engine arrangement that is unique among commercially available aircraft. An engine-out situation is not accompanied by a period of asymmetric thrust.

Physically, the Skymaster has high wing placement, which permitted a side mount for the field tests, and retractable landing gear, thus avoiding blind spots below the aircraft. The range and endurance of the Skymaster meshed well with the fairly short range, regularly changing flight profiles that were explored during the field tests for this project. We noted that this flexibility was particularly important for the variation in imaging parameters that was necessary for this project's field tests, but may not be a requirement for imaging surveys that employ a more invariant imaging methodology.

During this project, aircraft technicians explored the feasibility of installing a belly hatch in the test aircraft. However, it was determined that very limited floor area was available without major modifications to existing structures and components within the belly of the aircraft.

Piper Navajo—Thousands of the the Piper Navajo (Navajo) and its derivatives have been produced. It is about 20% faster than the Skymaster, but because speeds in excess of 170 mph result in increased image blur challenges, speed capability above 170 mph may not add much marginal value. The Navajo is capable of carrying more than twice as much load as the Skymaster and incorporates a much larger cabin, factors that may be critical when considering surveys with large sensor arrays. Lastly, an external cargo pod is available for this aircraft providing additional options for internal camera mounting.

Piper Aztec—At least twice as many Piper Aztecs (Aztec) have been produced compared to Skymasters. The Aztec cruise speed is at least 20 mph higher than the Skymaster, and fuel efficiency is slightly lower.

An additional drawback to this otherwise very popular and reliable piston powered aircraft is that its wings are mounted low. That posed a significant problem for an outboard camera mount such as was used for the field experimentation for this project.

Finally, the Aztec does not possess the nimble flying characteristics of the Skymaster.

Vulcanair/Partenavia P68 Observer2—The Vulcanair/Partenavia P68 Observer 2 (P68) is an Italian-made aircraft designed from the ground up to serve as an observational aircraft. It is the platform

used by the two leading offshore wind aerial high-resolution imaging wildlife survey companies doing surveys for the UK Round 3 offshore wind farms—APEM, Ltd. and HiDef Aerial, Ltd. It is one of the two most fuel-efficient aerial survey aircraft considered, and has a range 50% greater than the Skymaster. The P68 is routinely flown 10 hours per day performing imaging work in UK offshore waters. It is a dual engine aircraft, which commends it to offshore work.

A major downside, given the safety and availability criteria of long-term serial production and extensive production runs, is that only about 50 of the aircraft have been manufactured. This would pose an operational risk (not enough planes and/or qualified pilots) for survey applications.

Were it not for the short production and operational history of this aircraft, plus its relative scarcity in the US, the P68 may have been the aircraft selected for the flight experiments conducted under the current project.

Lastly, there is no certificated P68 cargo pod, restricting the applicability of this aircraft for surveys with large, multisensor arrays.

Diamond DA42MPP—The Diamond DA42MPP (DA42) is a purpose-built survey plane that originates in Germany. It is the most fuel efficient of all the aircraft considered. Additionally nearly 1,000 of the aircraft have been manufactured.

The much smaller cabin means that space would be tight for the equipment and the technician in imaging survey applications.

The DA42 was first certified for EU operation in 2004, recent relative to the other candidate aircraft. Due to financial problems with the supplier of one of the four types of engines the aircraft has been equipped with, production was suspended from 2008 to 2009. Thus, there is no long-term experience with this aircraft, particularly in the US, where sales first began in 2009. This aircraft has been successfully used to support airborne surveillance operations using a gimbaled sensor.

De Havilland DHC-6-300 Twin Otter—Approximately 750 De Havilland DHC-6-300 Twin Otters (Twin Otter) were produced of this larger, high wing, twin turbine-propeller aircraft. NOAA possesses a small fleet of these aircraft, which are currently used in visual observer-based offshore wildlife surveys—including the AMAPPS project. The cost of operation is roughly three times that of the Skymaster. This cost ruled out the use of Twin Otters in the field experiments for the current study. However, we developed a protocol for using the NOAA fleet of these aircraft to conduct large-scale offshore wildlife imaging surveys on the AOCS, assuming that the planes are already available for use at no additional cost (Chapter 4).

Cessna 208B Grand Caravan—This larger Cessna aircraft, the Cessna 208B Grand Caravan (Caravan) has the requisite horsepower, adequate flight speed, and sufficient range (close to 900 miles with a cargo pod). Numerous Caravans have been produced in the past couple of decades, and are available worldwide. Of note, the newer design Kodiak 100 closely resembles the Caravan in appearance and performance. The Caravan has a spacious cabin, which could easily accommodate a technician and a full suite of image recording and control equipment. The fuel consumption rate is more than double that of the Skymaster, typical of turbine powered aircraft. Like the Kodiak, the

Caravan is powered by a single, turbine engine with an excellent operational history. The worldwide availability of the Caravan, combined with its proven ruggedness, versatility, and reliability make it a first choice in single engine aircraft.

King Air XXX—The King Air 100 (King Air) and its derivatives are frontrunners as offshore aerial high-resolution imaging survey aircraft, particularly for cases in which an aircraft larger than a Skymaster is needed. The King Air is powered by twin turbine engines (turbo-propeller).

The aircraft model designation XXX is used here because, as noted above, fewer than 200 of the Model 100s were produced, yet a high degree of commonality remains through several decades of evolution of this aircraft series, which continues to the present (King Air 2012).

The King Air series possesses more than sufficient electrical power (> 1 MW) to drive any foreseeable sensor array as well as the onboard control and recording electronics (King Air 2012). Its cruise speed, above 300 mph, exceeds the maximum suitable imaging speed for many sensors, but where sensors capable of obtaining low-blur images at this speed are possible (extremely short exposure times), the high speed of the King Air presents an additional advantage. In addition, the higher speed of the King Air enables the aircraft to move quickly between the survey area and its home base or refueling site.

There is a commercially available, certified cargo pod available for the King Air series aircraft. It affords at least 12 inches of ground clearance, should this be required for a large, multisensor array configuration. The King Air is also becoming a popular choice for modification and deployment in support of military airborne surveillance missions, a testament to its versatility and reliability as a workhorse aircraft.

Cessna 206—We do not regard the Cessna 206 (206) as a strong candidate for an offshore wildlife imaging survey platform, because the single piston engine confers a relatively low safety score.

Kodiak 100—A turbine driven aircraft, the Kodiak 100 (Kodiak) has only been in production for a few years. It is currently used by the USFWS to conduct breeding waterfowl surveys, as well as wintering sea duck surveys on the AOCS. Because it has a single engine, there is no built-in redundancy for assuring safe operation/landing in the event of an engine failure. Nonetheless, similar to the Caravan, high reliability of this aircraft's turbine engine has been demonstrated operationally. Furthermore, because the USFWS already possesses a fleet of these planes, which are intended for conducting wildlife surveys, they may be uniquely suitable for conducting offshore wind-wildlife imaging surveys on the basis of low cost and high availability. We have developed a protocol for using this aircraft in large-scale AOCS surveys, presented in Chapter 4 (protocols chapter). This protocol assumes that the aircraft are modified to create a belly hatch for mounting cameras inside the aircraft.

De Havilland DCH-2 Beaver—The De Havilland DCH-2 Beaver (Beaver) is perhaps the quintessential bush plane, most frequently used in regions with long distances between settlements and little infrastructure for air traffic. More than 1,600 were manufactured from 1947 to 1967. Many are still flying in the US and abroad. It has ample load capacity and cabin volume. Its shortcomings are that it has a maximum airspeed of 140 mph, significantly below the frontrunning aircraft.

Another negative is fixed landing gear (or floats), which potentially impact viewing angles for the sensors. It is also a single engine aircraft. Finally, its range is significantly below that of the frontrunning aircraft, meaning extra time allotted for refueling, moving into staging position, etc.

Jet Ranger Bell 206BIII—The Jet Ranger Bell 206BIII (Jet Ranger) is the only helicopter included in this evaluation. An enormous number of this aircraft type has been produced (more than 7,000). There is vast experience with the technology, its maintenance, and operations. Helicopters, in general, are some of the costliest aircraft to operate. There is only one turbine engine, which would be a disqualifier under the multiple engine criterion in Europe. Finally, the cruise speed and range of most utility helicopters rule them out for use for the distances required in the performance of offshore marine wildlife imaging surveys, although use of helicopters may be economical for surveying very small areas (e.g., project-sized areas, Chapter 4).

Post Field-testing Evaluation of Cessna 337 Skymaster Performance

The Skymaster was selected as the manned aircraft survey platform for the field tests, consisting of imaging flight experiments conducted by the project team from 10 to 20 May 2011 offshore of Oak Island NC. Section 2.2 of this report presents a full description of the specific flight trials and imaging experiments that were conducted during this period. In the current section of this report, we present a post-hoc evaluation of the performance of the Skymaster that was used in these field tests, with respect to the suitability of this aircraft as a platform for future offshore high-resolution wildlife imaging surveys.

Vibrations

Field tests revealed that the Skymaster's in-line engines produced high frequency vibrations that were transmitted through the low frequency isolation mount to the cameras, affecting image quality. The effects of these vibrations on image quality is illustrated and discussed in Chapter 1 of this report. This was most likely not a particularly problematic feature of the Skymaster, but rather a function of using an external side mount for the camera (see Figure 2–3), which exacerbated vibrational effects because of the lever effects produced by the mount. Thus, even though the external camera mount shielded the sensors from wind buffeting, the mount was subjected to intense shaking during flight. The addition of a small gyrostabilizer (KS-8; Kenyon Laboratories, Higganum CT) attached directly to the sensor mount proved effective in significantly reducing the vibrations.

The success with the gyrostabilizer confirmed that it would be an essential component in any external camera mounting system. In the case of internally or pod-mounted cameras, less severe vibration effects would be expected, but further evaluation of vibration effects would be required. The use of gyroscopic stabilizers is likely to produce significant imaging benefits even in internally or pod-mounted imaging systems.

Reliability

The two Skymasters functioned perfectly during the entire period of field trials. One aircraft carried the cameras, and the other carried visual observers to gather data using conventional visual observer-based survey methodology for direct, methodological comparisons (section 2.2). Both the observer aircraft and camera aircraft had 100% reliability and availability throughout the period with zero incidents, malfunctions, or mishaps. Endurance, speed, and visibility were all sufficient for conducting the survey experiments.

Useful Load

The Skymaster successfully carried a two-sensor imaging array, a Quazar High-Performance Digital Video Recorder (HPDVR) (Boulder Imaging, Louisville CO), an inverter, an uninterruptible power supply (UPS), a control computer, an imaging technician, and the project's technology manager, as well as two pilots. A switchover to aircraft power after several days obviated the need for a UPS and inverter. The hard drives were removed from the HPDVR and replaced with solid state drives (SSDs) as an alternate data recording system (section 3.5), further lightening the load. The storage capacity for the SSDs was sufficient for several hours of recording with two cameras, indicating that at least two such data recording systems would be required for a morning or afternoon recording session during a future survey. The weight saved with the removal of the UPS and the inverter during flight would be more than the inclusion of a second, or possibly even a third data recording system if needed.

The Skymaster is not likely to be a good candidate for imaging surveys with large, externally mounted multiple camera arrays, as even more additional load would be required. Furthermore, additional air resistance due to the presence of a larger externally mounted sensor array would slow the aircraft and increase the fuel consumption rate, reducing range and endurance of the aircraft. An external cargo pod is commercially available for the Skymaster; however, initial research indicates the dimensions (primarily depth) are too small for a multicamera array.

Air Speed

The Skymaster consistently maintained an airspeed of 165 mph throughout the imaging flight trials. The sensors used during these trials are able to gather images with minimal motion blur up to an estimated 170 mph (section 6.4). An important point of consideration for future surveys is that alternative aircraft capable of higher speeds may be desirable when sensors capable of capturing low-blur images at higher flight speeds are available (section 6.4).

Sufficiency and Quality of Power Supply

The Skymaster has two alternators capable of delivering far more power than was required for the flight trials (~250 kW available). In its original configuration, the onboard imaging control and power supply equipment featured an inverter and an UPS. All aircraft power, which was anticipated as the backup power, was routed through the UPS. After the first week of flight trials, the inverter and UPS were eliminated from the power supply chain, and power was taken directly from the aircraft power supply, which was found to be cleaner power than that available from the UPS-driven inverted power.

Maneuverability

The Skymaster performed well with respect to the flight maneuverability required for conducting offshore aerial high-resolution wildlife imaging surveys. The range of flight profiles explored during the course of the flight trials was extensive, allowing both a thorough testing of the imaging system capabilities and limitations, as well as characterizing the suitability of the Skymaster for conducting the necessary flight maneuvers. Maneuvers that were used included:

- 100-m incremental altitude changes from 600 m to 1,200 m above sea level (asl) to test the impacts of changing distances to a ground target

- Spiral flights, changing direction in 10-degree increments to capture image data and gain a better understanding of the temporal behavior of glare fields

- Level flights at altitudes ranging form 435 m to 1,000 m at airspeeds ranging from 145 mph to 167 mph, using different oblique and 0 angles for the sensors

- Repeated passage over a desired ground target, such as Bird Island in the Cape Fear River and a boat in the Gulf Stream, to test the piloting ability to accurately image a ground target using only visual cues and GPS guidance

- Time to reach desired altitude and entry into a reference transect, to develop an understanding of flight time required to and from active scanning flight to account for this time when planning flight times for offshore surveys.

Summary of Lessons Learned

The Skymaster proved to be an extremely reliable, economical, and flexible platform with which to conduct myriad flight profiles that allowed for a wide range of methodological experimentation. In addition to serving the purpose of this experimental study, such reliability and flexibility indicates that the Skymaster is a highly suitable platform for conducting a wide range of offshore aerial high-resolution wildlife imaging surveys in the future.

Specific lessons learned during the flight trials vis à vis aircraft suitability include the following:

- The crude aerodynamic design of the bespoke fairing enclosing the flight trial camera mounts caused a 10% reduction in cruise airspeed. A better design for the fairing, and therefore for a larger sensor array, may allow for attaining a cruise airspeed that achieves the maximum imaging speed of 170 mph. Use of a slightly more powerful aircraft, such as the Navajo, would ensure that the faster airspeed would be maintained, whatever aerodynamic loads were imposed by the presence of one or multiple larger and heavier sensor array(s). Such drag effects could be eliminated with the use of internally mounted cameras, and reduced with the use of a highly aerodynamic pod for external camera mounting.

- A minimum of 20 seconds must be added to the total survey time for each turn required in the flight transect pattern. The turns, plus distance from airfield to transect pattern entrance point, may add several hours to the total temporal length of a survey, depending on the survey size.

- Any custom-designed mount must be affixed to the airframe using vibration isolation mounts. The use of small diameter, unstiffened cantilevered axles should be avoided wherever possible because they are very effective at transmitting high frequency engine vibrations to camera mounts.

- Onboard power from the engine alternator can be cleaner and more reliable than that from an UPS-inverter configuration.

3.2.3 Unmanned Aircraft System (UAS) Evaluation

The evaluation of candidate UAS aircraft was led by UAS experts subcontracted for the project, Donald MacArthur and Erica MacArthur of IATech, Inc., working in coordination with the technology task manager, M. Kujawa, under the direction of Normandeau.

Desktop Evaluation and Flight Test Aircraft Selection

The desktop evaluation of UAS aircraft suitability for conducting offshore high-resolution aerial wildlife imaging surveys was in some ways parallel to, but in other ways different from, our evaluation of candidate manned aircraft. Some of the differences stem from the much newer market history and availability of UAS compared with manned aircraft, but the primary difference is with respect to various operational constraints and considerations that are unique to UAS. Most importantly, heavily restrictive current federal aviation policies preclude the use of UAS as a platform for conducting offshore high-resolution aerial wildlife imaging surveys over the AOCS, as is desired for the purpose of providing data for offshore wind environmental studies. Nonetheless, at a technical level, the capacity exists for conducting such surveys with UAS technology, and the potential cost and safety benefits of UAS-based surveys compared to manned aircraft surveys warrant the consideration of UAS as a platform for this application. Much of this section focuses on the unique aspects of UAS as a potential offshore high-resolution aerial wildlife imaging survey platform, and the challenges that must be overcome for UASs to be a viable option for this application.

In Table 3–3, we highlight several candidate UASs that would potentially be suitable for conducting offshore aerial high-resolution wildlife imaging surveys. The three selected UASs in this table span a spectrum of size and payload capacity. Smaller UASs, such as the Pelican and ScanEagle, are potentially suitable for smaller surveys (e.g., project scale, Chapter 4), and current permitting constraints make it more likely that such applications could be permitted on a fairly near horizon. By contrast, larger UASs, such as the Predator, are more suitable candidates for conducting larger scale surveys, but more extensive modifications of existing aviation regulations would be required to be able to conduct them.

Table 3–3.

Unmanned Aircraft System (UAS) Specifications and Other Characteristics Used in the Evaluation of Suitability for Offshore High-resolution Wildlife Imaging Surveys

Evaluation Characteristics	Unmanned Aircraft System (UAS) Type		
	ScanEagle	Predator	Pelican
Wing Span	10.2 ft	55 ft	10 ft
Length	4.5 ft	27 ft	6 ft
Endurance	24 hrs	40 hrs	60 min
Fuel	Gas	Gas	Battery
Range	55 nm	200 mi	1 mi
Cruise Speed	55 mph	115 mph	60 mph
Ceiling	19,500 ft	25,000 ft	400 ft

Evaluation Characteristics	Unmanned Aircraft System (UAS) Type		
	ScanEagle	Predator	Pelican
Launch Method	Catapult	Runway	Runway, launcher, water
Recovery	SkyHook	Runway	Runway, water
Basic Sensors	EO/IR cameras and more	EO/IR cameras and more	DSLR camera
Cost	$250K	$1.4M	$100K

Insitu's ScanEagle has a strong history of performing marine missions, and can be both launched and retrieved via boat/ship. General Atomics' Predator UAV is an extremely capable unmanned aircraft, and can fly at high altitude and for long durations. IATech's Pelican UAS is designed to be a lower cost option able to be launched from land or sea and accommodate large sensor payloads, such as the camera payload for this application. Because of its suitability to perform proof of concept experiments at relatively low costs, we selected the Pelican UAS for use in the field experiments for this project.

Criterion 1: Safety

Safety of operation is perhaps the strongest potential benefit of using UAS for offshore aerial wildlife imaging surveys, as no pilots' lives are at risk in the event of an aircraft failure. Nonetheless, there is a risk of human death or injury from UAS operation, particularly when UAS are flown over areas with high densities of people. In the case of offshore wildlife surveys, such risk is likely to be negligible, as the density of people (e.g., on boats) is extremely low over most of the AOCS. In this section, we present a discussion of general safety considerations in UAS operation.

When performing unmanned aircraft operations, safety and risk mitigation is paramount. Whether designing an entire aircraft or designing a series of flight experiments, controlling or eliminating hazards is an integral part of the process. Some examples to reduce risk include:

- Use of a highly reliable engine in the UAS design can reduce the risk of loss of propulsion.
- Confining test flights to an unpopulated area eliminates risk to people on the ground.
- Designing a series of tests with a gradual buildup in risk reduces the chance of sudden unexpected failures.

The incorporation of safety and warning devices/procedures is also essential. Such systems are implemented when a simple change in design cannot eliminate a hazard. Examples of these safety systems that are commonly implemented in UAS are:

- Back-up batteries
- Redundant communication links in the case of failure of the primary link
- Software return-home routine in the case of a loss of link
- Independent flight termination system

Warning systems are very useful to the operator on the ground and are displayed through the ground control system interface. Some warning systems that are included are:

- Engine performance safety (e.g., such as over temperature alerts)
- Aircraft strobe lights to make the UAS easier to see
- Low fuel or battery warning lights or messages

In addition to the safety and warning systems, sufficient documentation of procedures and training are critical to the safe operation of UAS. Documentation of safety-critical procedures, training requirements, as well as general operation of the system is essential. Safety procedures can include preflight checklists, cautions and warnings, emergency procedures, operating limits, operator qualification procedures, and required personal protective equipment (e.g., ear plugs).

Criterion 2: Effectiveness

Effectiveness is affected by payload limitations/constraints on onboard storage system, camera, lens, including endurance tradeoffs.

With the need to be able to ultimately gather images over water some distance offshore comes the need to be able to safely launch, perform the mission, and recover the system from a moving vessel or boat. The ability to safely launch the aircraft in varying wind conditions becomes crucial. This can be highly dependent on overall system weight and thus a limitation on the overall payload of the aircraft. Launching mechanisms can be employed to assist in the takeoff, but can add complexity to the system operation. Launching systems are used quite successfully with systems such as the ScanEagle (shown in Figure 3–1), but require a significant sized vessel to accommodate the launcher.

Figure 3–1. Boeing-Insitu ScanEagle taking flight from launcher onboard a ship.

The limitation on longevity and endurance of these small aircraft systems is directly correlated to the maximum flight weight. As the payload weight increases the endurance decreases. When a consumable fuel is used from propulsion, the aircraft inherently reduces weight over the course of the flight. Despite this fact, battery and fuel powered aircraft are limited to a maximum takeoff weight, which relates directly to payload weight and endurance. Given a specific payload weight, a given aircraft will only have a corresponding fuel capacity and still be able to takeoff. The endurance of the aircraft will have to be sufficient to allow for coverage of a moderate amount of transects for the survey area before landing to refuel. Given the large size of prospective survey areas, it is conceivable for both propulsion style aircraft to be used effectively for this application.

Operator Supervision Constraints

FAA regulations presently ban unmanned aerial vehicles in national airspace except for use by the Departments of Defense and Homeland Security. The primary problem is that UAVs in their two main forms (i.e., remotely piloted vehicles and drones) do not have see-and-avoid capability. Pilots constantly monitor radio chatter, transponder traces on electronic displays, and the visual airspace around their aircraft. No stable, proven, and reliable means is presently available that can impart this level of situational awareness into a machine, even one that is remotely piloted. The constant line-of-sight surveillance operator supervision systems and procedures described below are largely directed at addressing this need, and imparting a safe level of see-and-avoid capability to UAS operation. This aspect of UAS operation is strongly related to the permitting constraints discussed below, and also affects operational cost, as constant surveillance by UAS operators, including boat-based monitoring, add significant operational costs, resulting in the disappearance of some of the potential cost benefits of UAS compared to manned aircraft survey platforms. The greatest potential benefits of UAS system operation for the purpose of offshore wildlife imaging surveys could be achieved if

UAS were permitted to operate without constant line-of-sight surveillance by operators, as is frequently the case in certain UAS applications such as military and border surveillance.

During unmanned aircraft operations with constant line-of-sight operator surveillance, the pilot in command (PIC) and an observer have individual roles and responsibilities. These roles and responsibilities are specifically outlined in the FAA's order 8130.34B Airworthiness Certification of Unmanned Aircraft Systems and Optionally Piloted Aircraft. Pilots are responsible for a thorough preflight inspection of the UAS prior to departure, and they are accountable for controlling the aircraft in the same manner as a manned aircraft. The PIC has the following responsibilities while operating an unmanned aircraft system:

1) One pilot in command must be designated at all times.
2) The PIC of an aircraft is directly responsible, and is the final authority of the operation of that aircraft.
3) The PIC must not perform crew duties for more than one UAS at a time.
4) The PIC is not allowed to perform concurrent duties both as pilot and observer.

The main role of the observer is to perform the see-and-avoid function for the UAS. The observer can either be ground-based or airborne onboard a dedicated chase aircraft. The main task of the observer is to provide the pilot of the UAS with instructions to steer the vehicle clear of any potential collision with other air traffic. The visual observer duties require the ability to maintain visual contact with the UAS at all times while scanning the immediate horizon and environment for any possible conflicting traffic. The observer will at no point allow the UAS to operate outside their line-of-sight. This requirement ensures that any maneuvering information can be reliably provided to the PIC.

The visual limitation will specify a lateral and vertical distance and will be regarded as a maximum distance from the observer and where a determination of a conflict with another aircraft can be made. In general, observers are to be positioned no farther than 1 nautical mile laterally and 3,000 feet vertically from the UAS. The distance is based on the observer's normal unaided vision. However, corrective lenses, spectacles, and contact lenses may be used.

Permitting Constraints

With the growing demand for public use of UAS, the FAA recently developed guidance in a memorandum titled "Unmanned Aircraft Systems Operations in the US National Airspace System—Interim Operational Approval Guidance" (UAS Policy 05-01). In this document, the FAA set out guidance for public UAS use by defining a process for evaluating applications for Certificate(s) of Waiver or Authorization (COAs) for unmanned aircraft to operate in the national airspace. The FAA will issue a COA generally based on the following set of rules:

1) The COA will be based on special provisions unique to each operation. This includes the operator to define the airspace, flight height, and may include the requirement to operate under visual flight rules (VFR) and/or during daylight hours only. In most cases this is valid for a specified time (usually up to one year).
2) Most COAs will require coordination with local air traffic control and may require a transponder onboard depending on the class airspace the operation is performed in.

3) Because UASs cannot currently comply with see-and-avoid rules, the ground observer or accompanying chase plane must maintain visual contact with the UAS at all times when the operating outside of restricted, prohibited, or warning airspace.

The concern is not only that UAS operations might interfere with commercial and general aviation aircraft operations, but that they could also pose a safety problem for other airborne vehicles, and persons or property on the ground. The FAA guidance supports unmanned aircraft flight activity that can be conducted at an acceptable level of safety.

To ensure this level of safety, the operator is required to establish UAS airworthiness either from FAA certification, a Department of Defense airworthiness statement, or by other approved means. Applicants also have to demonstrate that a collision with another aircraft or other airspace user is extremely improbable as well as complying with appropriate cloud and terrain clearances as required.

UAS flight above 18,000 feet must be conducted under Instrument Flight Rules (IFR), on an IFR flight plan, must obtain Air Traffic Control (ATC) clearance, be equipped with at least a Mode C transponder (preferably Mode S), operating navigation lights and / or collision avoidance lights, and maintain communication between the PIC and ATC. UAS flights below 18,000 feet have similar requirements, except that if operators choose to operate on other than an IFR flight plan, they may be required to precoordinate with ATC.

Unmanned aircraft systems operating as civil aircraft, just as manned aircraft, have a variety of uses in the public sector; their application in commercial or civil use is equally diverse. This is a quickly growing and important industry. Under FAA policy, operators who wish to fly an unmanned aircraft for civil use must obtain FAA airworthiness certificate the same as any other type aircraft.

The FAA is currently only issuing Special Airworthiness Certificates (SAC) in the experimental category. Experimental certificates are issued with accompanying operational limitations (14 CFR § 91.319) that are appropriate to the applicant's operation. The FAA has issued experimental certificates for UASs for the purposes of research and development, marketing surveys, or crew training. UAS issued experimental certificates may not be used for compensation or hire.

Federal Aviation Administration (FAA) Restrictions—Future Expectations

According to one verbal response from an FAA policy and regulatory leader, traditional rulemaking averages are between eight and 10 years, and they are "working toward having an initial rule out in mid 2011 for public comment with a final rule issued in late 2012; five years from when it was started." Moreover, an emphasis on safety has been a growing trend as the FAA continues to issue COAs. The waiting time and uncertainty about new rules (whether FAA will relax or not) should be weighed carefully.

In response to our inquiry, a senior FAA analyst delineated a general time frame and specific guidelines for applicants to receive a COA and a SAC:

- The FAA asks for 60 days to process the COA.
- The actual time required to process depends on the complexity of the mission and UAS.

- The COA includes special provisions unique to each operation. Most are issued for a specified time period (up to one year, in some cases) and for a specified location.
- To make sure the UAS will not interfere with other aircraft, a ground observer or an accompanying chase aircraft must maintain visual contact with the UAS.
- Local law enforcement and state universities must use a COA.
- Currently, any law enforcement organization must follow the COA process if they wish to conduct demonstration flights.

Requirements for application of COA include:

- Statement of specific criteria used to show the adequacy of the safety element and how the safety element complies with the specific criteria
- Specific operating limits
- Engineering design and analysis that demonstrate the fitness of the proposed element for its intended use.

Criterion 3: Cost

The potential cost savings of using UAS instead of manned aircraft for offshore aerial high-resolution wildlife imaging surveys are significant for two primary reasons. Firstly, UAS can be significantly smaller and lighter for the same imaging payload, meaning lower fuel costs. Secondly, fewer personnel are required for operation, further lowering the hourly cost of operation. A general comparison of UAS to manned aircraft costs is presented in Table 3–4.

Table 3–4.

Cost Comparison of Manned and Unmanned Aircraft Systems As Platforms for Offshore Aerial Imaging Surveys.

Cost Factor	Manned Aircraft	Unmanned Aircraft System
Pilot labor	Higher due to additional flight ratings and number of pilots	Lower due to reduced flight ratings and number of pilots
Pilot training	Offshore additional flight ratings	No additional flight ratings required
Number of pilots required	Two pilots required for over-water surveys	One pilot and one observer required
Fuel	Greater payload, cost would be higher	Lower if not negligible fuel cost
Payload cost	Possibly higher cost due to faster airspeed • Higher frame-rate and data recording Possibly higher cost due to higher altitude • Higher powered optics and stabilization required	Possibly lower cost due to slower airspeed • Lower frame rate and data recording Possibly lower cost due to lower altitude • Lower powered optics and stabilization required
Loss of aircraft	Minimum of two lives at risk in the event of aircraft loss Higher cost of aircraft Higher cost of payload	No lives at risk in the event of aircraft loss Lower cost of aircraft Lower cost of payload

Post Field-test Evaluation

A series of flight experiments was performed to determine effectiveness of the Pelican UAS as a high-resolution imaging platform in different environmental conditions, payload performance, and overall system integration. These experiments are fully described in section 2.3.

Our overall conclusion is that significant improvement would be required for the Pelican to serve as an effective platform for conducting offshore aerial high-resolution wildlife imaging surveys. Below is a summary of certain lessons learned, upon which this conclusion is based.

- Imaging payload is too heavy for hand launch from a boat. The imaging payload consisted of a digital SLR camera with lens, SSD, and computer system that was able to take successive images at altitude and store them on board on the SSD (see sections 2.3, 3.2.3). For a land-based takeoff (i.e., with landing gear) the payload weight was within acceptable limits. To accommodate a hand-launched aircraft (i.e., from a boat) the overall aircraft and payload weight would have to be decreased.

- Imaging equipment needs to be improved over that used in the field trials with the Pelican for this project, hence there is uncertainty regarding the ability of the Pelican to accommodate an effective imaging payload. The Pelican-based imaging system was not able to capture images of sufficient quality to effectively serve the purpose of offshore marine wildlife data gathering, even when flying at low altitudes within the rotor swept zone of commercial marine wind turbines (see camera evaluation section 3.3.3). Using an imaging payload significantly larger and heavier than that used in the UAS, the manned aircraft flight experiments for this study were able to capture very high quality images of marine wildlife, flying at altitudes as high as 1,000 m. It is unclear whether or not the Pelican UAS could accommodate the type of highly specialized imaging equipment necessary to gather images of sufficient quality for the purpose of conducting marine wildlife imaging surveys, flying at altitudes safely above the rotor swept zone of commercial marine wind turbines.
- For UAS to serve as an effective platform for conducting offshore aerial wildlife imaging surveys, FAA rules for the use of UAS in civilian airspace must be relaxed. Under current rules, time periods on the order of two years are required to obtain permission to fly at the altitudes required for marine wildlife imaging surveys (minimum 200 m, ideal 400 to 1,000 m). Furthermore, constant line-of-sight operator surveillance requirements negate much of the potential cost savings of using UAS for the purpose of conducting offshore wildlife imaging surveys, as compliance with this requirement entails the extensive use of either boats or manned chase planes, which would introduce costs surpassing those of manned aircraft-based imaging surveys.
- If current UAS permitting and use restrictions are relaxed, and if an adequate imaging system is integrated within a UAS capable of carrying it, it is possible that a UAS, most likely larger than the Pelican, may provide a highly cost-effective platform for conducting high-resolution offshore wildlife imaging surveys in the future.

3.3 Camera and Mounting System Evaluation

3.3.1 Introduction

The objective of the evaluation of cameras and mounts, as defined in task 3 of the contract, was to "evaluate existing high definition cameras (including video) and mounting systems for effectiveness in a marine environment, convenience of use and in-flight maintenance, and compatibility with the aircraft selected in task 2." With these criteria in mind, we evaluated candidate cameras and mounting systems in two stages: pre-experimental desktop analysis and post-experimental performance evaluation, parallel to the pre- and post-experimental aircraft evaluation stages (section 3.2).

In the pre-experimentation analysis, all possible candidate cameras and mounts were evaluated based on available literature and technical specifications from manufacturers, to identify the cameras and mounts likely to be most suitable for the purpose of conducting aerial high-resolution marine wildlife imaging surveys. The desktop review was also used to select a subset of cameras and mounts to be used in field testing for this project. In the case of imaging systems to be used in flight tests in the manned aircraft, desktop evaluation was supplemented with laboratory testing to select the most promising imaging equipment for flight testing. The second stage of camera and mount

evaluation consisted of post-field testing evaluation of the performance of the cameras and mounts utilized during the field tests for this project.

Because of the different operational constraints and engineering personnel involved with the execution of imaging experiments on manned versus unmanned aircraft, separate evaluations of cameras and mounts were conducted for application to manned and unmanned aircraft platforms, presented in separate subsections of this chapter. The manned aircraft imaging equipment evaluation focused on applying the most highly specialized imaging equipment available for industrial and scientific applications, to achieve the best quality images possible with no consideration of imaging payload size or weight limitations. By contrast, the imaging equipment evaluation for the UAS-based experiments focused on smaller, lighter weight, less specialized imaging systems that could be integrated into the small payload Pelican UAS (section 3.2.3), including camera models that were available on the retail market at the time of the experiments.

3.3.2 Evaluation of Imaging Systems for Manned Aircraft

The evaluation of candidate imaging systems for use with manned aircraft platforms under the project was led by the subcontracted imaging and image processing technical experts on the project team, C. Jorquera and J. Luttrell of Boulder Imaging, in coordination with the technology task manager, M. Kujawa, under the direction of Normandeau.

Desktop and Lab-based Evaluation and Flight Test Imaging Equipment Selection

Camera/Sensor Analysis

Method

Prior to lab evaluation of imaging technologies, literature and technical specifications were reviewed for applicable technologies. After the initial research phase, three camera models were chosen as candidates to undergo a thorough lab-based qualification. Of these cameras, one was a line-scan sensor and the other two were area-scan sensors. A test methodology was chosen to evaluate/compare technologies, which included a set of camera test parameters and method(s) for evaluating each test parameter. After all analyses were performed, two camera models were chosen for inclusion in experimental flight trials.

Sensor Type

Two fundamental camera sensor types exist: area-scan and line-scan sensors. Area-scan sensors are those associated with typical cameras. An area-scan sensor exposes an entire frame each time an image is captured. The speed of area-scan cameras is measured in frames per second: the number of fullframe exposures the camera can generate each second.

The second type of camera sensor is the line-scan sensor, which is traditionally used for industrial automated inspection applications. A line-scan sensor only exposes a single line of pixels each time an image is generated. For this reason, either the camera must be in motion over the image target, or the image target must be in motion under the camera sensor. Line-scan cameras do not generate what would conventionally be called video frames. These cameras produce a continuous stream of single lines, based on the line rate at which the camera is imaging. Assuming the camera line rate is synchronized with target motion, the net result is a single, continuous image. This continuous image

is typically broken into distinct frames to better facilitate analysis and processing. This process of splitting the continuous image into frames is arbitrary; systems may simply split the continuous image up in a way that is convenient for processing and viewing.

Sensor Type Comparison

Area-scan and line-scan cameras have very different properties. Both were included in the evaluation/experimental trials because they each have significant potential benefits and tradeoffs. Below is a list of applicable benefits for each camera type.

Area-scan Benefits

- For each camera, multiple images of the same scene can be produced. For aerial survey purposes, multiple images of individual animals can be acquired. This can more simply be thought of as video. Line-scan technology provides a single, continuous image, so each animal can only be imaged a single time with each camera.
- Line-scan technology is very susceptible to low-frequency horizontal vibration in the camera system, which can produce visible waviness in acquired imagery (as the camera moves from side-to-side). Area-scan sensors are far less susceptible because they image an entire scene at the same time. Vibration affects all pixels identically, so individual lines of pixels will not be shifted relative to others.
- Line-scan technology is also very susceptible to low-frequency vertical vibration. If a camera moves vertically, a line-scan system can re-image a previously imaged line, or skip over lines in the scene if motion is in the opposite direction. Either situation causes loss of data in a line-scan system. Area-scan systems, for the reasons noted above, do not suffer from this concern.
- Area-scan systems need not be synchronized with speed of the aircraft. A frame rate simply must be chosen, based on various considerations (e.g., how many images of each animal are desired, data-processing rate of the system, exposure times).

Line-scan Benefits

- Line-scan sensors typically have the ability to generate much better images under low light conditions. This is achieved through the use of larger, more sensitive pixels, and sensors with multiple lines that image the same portion of the scene and are added to increase sensitivity. Even though aerial surveys are performed in daylight, aircraft speed causes exposure times to be very low. A line-scan system can potentially provide good quality images at very high aircraft speeds.
- Line-scan sensors are available in much larger widths than area-scan sensors. The net benefit is that very large area surveys could be conducted with fewer cameras using line-scan technology.
- Color accuracy is typically higher with line-scan cameras. Conventional area-scan cameras use Bayer color sensors, on which each pixel is sensitive to only a single color. Color line-scan sensors use technology to provide more than one color component for each pixel, producing more accurate color rendition and higher pixel sharpness.
- Area-scan sensors are susceptible to an imaging problem known as image smearing, which can cause artifacts in imagery. Line-scan cameras are not susceptible to this problem.

Chosen Cameras

The following cameras were chosen for evaluation:

- Imperx IGV-B4820—area-scan sensor
- Imperx IGV-B4020—area-scan sensor
- Dalsa Spyder3 Color 4k 9 KHZ CL—line-scan sensor

Camera Test Parameters

The following camera test parameters were chosen to serve as the basis for camera evaluation:

Table 3–5.

Parameters Used for Camera Evaluation

Parameter	Definition	Dependent On	Effects
Signal to noise ratio—pixel-rate random noise	Random variation in pixel signal level	Design of camera sensor drive circuits, and post-processing systems	Sensitivity, image quality
Signal-to noise—fixed pattern noise (FPN)	Low level stationary noise patterns in the image	Drive circuitry design and image post-processing	Sensitivity, image quality
Linearity	Signal deviation from ideal linear transfer function	Camera drive electronics and image post processing	Useful dynamic range and grey scale of image. color grey scale accuracy
Dynamic range	Ratio of highest image signal level to the lowest signal level detectable by the camera	Camera design operating parameters of the image sensor	Sensitivity and high light level performance
Dark current	Signal that accumulates when no incident photons are present. Shows up as bright points in the image.	Operating temperature of the image sensor. Clocking speed of sensor	Sensitivity, image quality

Parameter	Definition	Dependent On	Effects
Image smear	Error signal that can result from bright specular highlights in the captured image	Exposure time, camera design and image sensor architecture	Ability to image bright shiny objects without artifacts. Image quality
Anti-blooming protection	Ability of camera to image bright objects without signal spilling into adjacent rows	Image sensor characteristics, setting of the camera sensor drive electronics, choice of IR-cut filter	Ability to image bright shiny objects without artifacts. Image quality
Modulation Transfer Function (MTF)—camera electronics	Ability of camera electronics to provide sufficient bandwidth to resolve adjacent pixel values accurately.	Image sensor drive and post-processing electronics—settling time of camera signal between adjacent pixels	Ability of camera to handle color separation properly. Accuracy of captured image. Color Image Quality
Modulation Transfer Function (MTF)—optics and image sensor	Ability of optics chain to resolve image detail at sensor plane	Internal camera optics, external lens optics	Image sharpness—ability to resolve fine detail
Optical distortion	Spatial Deviation of camera image from ideal coordinates	Lens spatial distortion, Image Sensor alignment in camera	Spatial accuracy of the acquired image. Ability to tile adjacent cameras
Electronic shutter range	Shutter speed range of camera	Camera electronics design	Motion blur, motion artifacts
Motion blur	Blur of image due to relative motion between image and sensor during capture	Shutter performance, ground tracking speed	Sharpness of image along the axis of relative motion
Operating temperature	Operating temperature of camera under steady-state operation	Design of camera electronics and thermal management	Dark Current performance and long-term reliability

Parameter	Definition	Dependent On	Effects
Physical properties—camera size, weight, power consumption	Self explanatory	Manufacturer specifications	Key will be to measure power dissipation in all operating modes that will be used in the Pandion application

Camera Test Methodology

Signal to Noise Ratio—Pixel-rate Random Noise: The pixel-rate random noise floor is a function of the camera design and the image sensor characteristics. The standard deviation over a fixed region of interest was recorded to compare the random noise performance between models.

Quantitative Measurement Variable: **Standard Deviaton**

Signal to Noise Ratio—Fixed Pattern Noise: Fixed pattern noise can result from many potential sources in the camera design architecture. We isolated the fixed pattern noise component from the random noise by implementing temporal averaging of sequential frames.

Quantitative Measurement Variable: **Standard Deviaton**

Linearity: We recorded the signal as a function of exposure time, to quantify the linearity of the camera system. Varying the exposure time provides a more accurate and simple method for quantifying linearity, as opposed varying the scene illumination.

Quantitative Measurement Variable: **Deviation of Signal from Ideal Linear Function.**

Dynamic Range: Dynamic range is a measure of the linear operating span of the camera—from the highest possible to the lowest possible signal levels. We recorded the ratio of the maximum scene brightness capability of the camera to the RMS noise floor of the camera, to determine the dynamic range.

Quantitative Measurement Variable: **Decibels**

Dark Current: Dark current is an error signal that accumulates in each pixel due to a small level of electron leakage into the pixel during image capture. Dark current is a linear function of exposure time and the operating temperature of the image sensor. The exposure time for this application is very short, which minimizes the effect of dark current in this application. We recorded the performance for each camera model for use in the section process, as the image sensor operating temperature will vary between camera models.

Quantitative Measurement Value: **Percentage of Dynamic Range.** The percentage of dynamic range occupied by dark current was measured at very long integration times.

Image Smear: We captured an image of a brightly illuminated square box, with dimensions of roughly 10% of the total vertical frame, to quantify image smear performance. Image smear is related to exposure time, with the shortest exposure time being the most prevalent contributor to smear. We investigated smear performance under the minimum exposure time that was used for the application. High smear can result in faint vertical columns that correspond with the horizontal location of the bright object in the image.

Quantitative Measurement Variable: **Percentage of Signal Added by Smearing.** A scene that produces smearing was characterized in order to measure the percentage of smearing transferred to adjacent rows.

Anti-Blooming Protection: The resistance to blooming is a function of the image sensor operating parameters and clocking accuracy of the camera design. We subjected the camera to a worst case scene with bright specular reflection highlights, to ensure that the anti-blooming characteristics were sufficient for the real condition for the application.

Quantitative Measurement Variable: **Unitless Ratio of Onset of Blooming Exposure over Full Capacity Exposure.**

Modulation Transfer Function—Camera Electronics: The integral color filter array of the image sensor, under incident monochromatic light illumination, was used to confirm that the camera had sufficient spatial bandwidth to provide maximum scene detail and accurate color processing.

Quantitative Measurement Variable: **Pass/Fail** (adjacent pixel settling time will be evaluated for color processing artifacts)

Modulation Transfer Function: Optics and Image Sensor: A resolution chart was used to quantify the onset of aliasing in each color plane, to verify that each imaging system had resolution performance at or above the stated specifications. This is a lumped measurement of both the camera optical performance and the lens optics.

Quantitative Measurement Variable: **Pass/Fail**.

Optical Distortion: We captured an image of a high-spatial-accuracy rectangular grid to assess the pincushion distortion and run-out distortion of the imaging system. Pincushion distortion is primarily a function of the lens, and the run-out distortion is a function of the image sensor flatness and coplanarity with respect to the camera lens mount.

Quantitative Measurement Variable: **Spatial Offset Map** in units of microns or millimeters, to map deviation of image coordinates as a function of spatial position.

Electronic Shutter Range: We exercised the full exposure range of the electronic shutter of the cameras, while looking for any potential artifacts that might occur at the low end of the shutter range. This confirmed the useful exposure range, for comparison to the exposure range stated in the camera specification document provided by the manufacturer.

Quantitative Measurement Variable: **Milliseconds**.

Motion Blur: Motion blur is a function of the exposure time and the relative motion between the imaging system and the target. We tested each camera configuration against the ground tracking speed requirements of the application, using a moving target in the laboratory.

Quantitative Measurement Variable: **km/hour:** Minimum ground tracking speed for onset of blur, at minimum acceptable exposure time.

Operating Temperature: We recorded the steady state operating temperature of the case of each camera. Fifteen minutes of operation in free air was sufficient for each camera to attain its steady state operating temperature. These measurements were made in the ambient environment of Boulder Imaging's laboratory for two reasons: for comparison among models and for verification of the operating temperature value provided in the camera manufacturer's specification document.

Quantitative Measurement Variable: **Degrees C**

Physical Properties—Camera Size, Weight, and Power Consumption: We measured the mass and verified the physical footprint of each camera. Power consumption was measured as the product of the power supply voltage and current consumption, for all operating modes of the camera.

Camera Test Results

Signal to Noise Ratio—Pixel-Rate Random Noise

Test Procedure:

A sequence of images was gathered at low exposure time (200µs) with 50% analog gain under completely dark lighting conditions (metal foil covering lens opening). Frames were averaged and then subtracted from a single raw image to subtract out fixed pattern noise. Standard deviation was calculated over the resulting image. Standard deviation was divided by sqrt (Num_Averaged_Frames) as the frame averaging operation adds random noise that must be compensated for.

Camera	Standard Deviation
Imperx IGV-B4820	9.5
Imperx IGV-B4020	7.26
Dalsa Spyder3	9.9

Signal to Noise Ration—Fixed Pattern Noise (FPN)

Test Procedure:

A sequence of images was gathered at low exposure time (200µs) with 50% analog gain under completely dark lighting conditions (metal foil covering lens opening). Thirty frames were averaged to average random noise rate. Standard deviation of the resulting image was measured directly to determine the fixed pattern noise (FPN).

Camera	Standard Deviation
Imperx IGV-B4820	5.0
Imperx IGV-B4020	3.17
Dalsa Spyder3	5.08

Linearity

Test Procedure:

Images were captured in regular intervals at exposure times ranging from very low (200 µs) until the camera sensor saturated. Analog gain was set at 50%. The camera was set up under constant lighting conditions using techniques that diffused the light evenly across the sensor. After collecting multiple data points, the result was charted. A second order best fit polynomial curve was applied to the scatter chart. The second order coefficient was then recorded, providing a measurement of the linearity of the sensor response to increasing exposure times.

Camera	Linearity (Value, Chart)
Imperx IGV-B4820	.000004

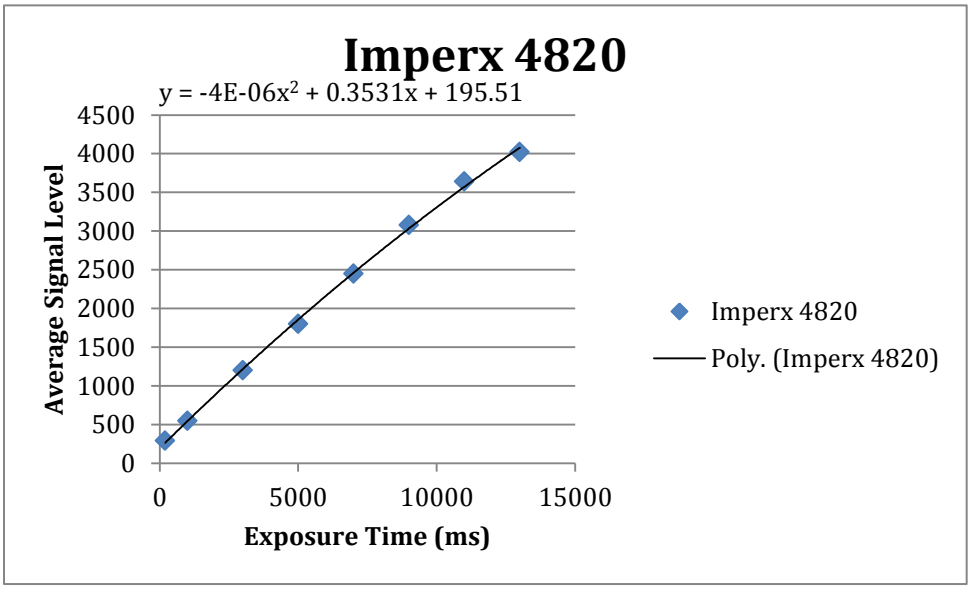

Camera	Linearity (Value, Chart)
Imperx IGV-B4020	.000001

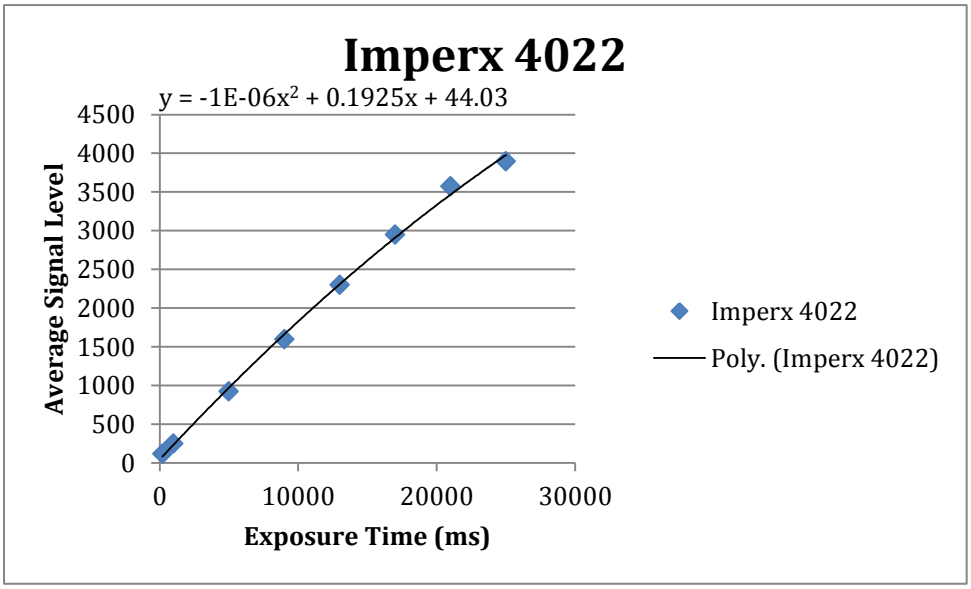

Dalsa Spyder3	.0003

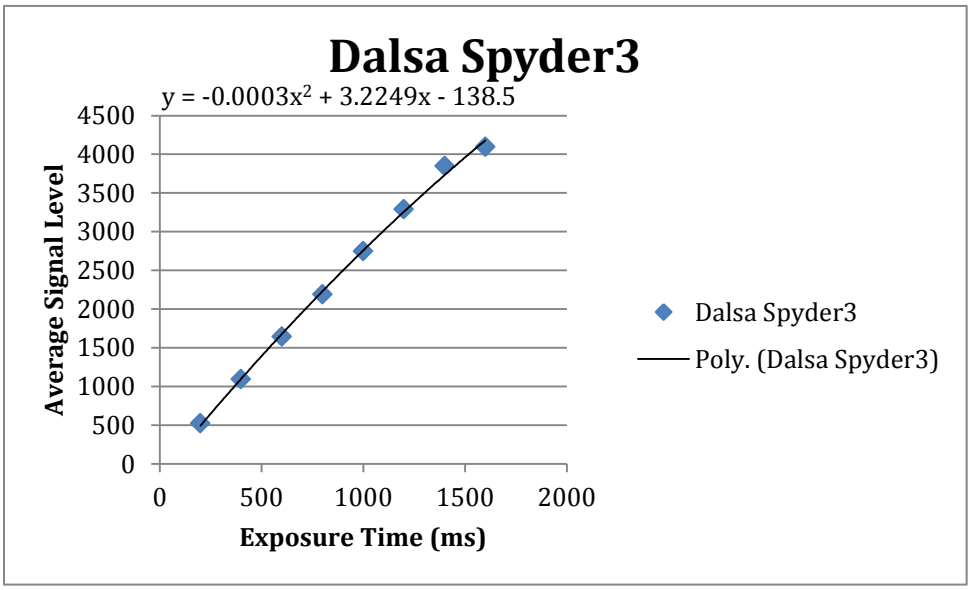

Dynamic Range

Test Procedure:

Images were captured in regular intervals at exposure times ranging from very low (200 µs) until the camera sensor saturated. Analog gain was set at 50%. The camera was set up under constant lighting conditions using techniques that diffused the light evenly across the sensor. To measure the entire dynamic range, the highest possible signal level is determined, and divided by the pixel-rate random noise. This value is then converted into decibels.

Camera	Decibels
Imperx IGV-B4820	52 dB
Imperx IGV-B4020	55 dB
Dalsa Spyder3	52 dB

Dark Current

Test Procedure:

A single dark frame was gathered from each camera using the maximum exposure time of the camera. The average signal level of the resultant frame was compared against the maximum signal level to determine the percentage of dynamic range that dark current accounted for at that exposure time. The maximum exposure times were much different between the area and line-scan cameras.

Camera	Percentage of Dynamic Range at Exposure Time
Imperx IGV-	3.5% at 330 µs
Imperx IGV-	.9% at 330 µs
Dalsa Spyder3	.8% at 3.3 µs

Image Smear

Test Procedure:

A constant scene was imaged with both area-scan cameras. The scene contained a bright light in the center with black objects surrounding it. The vertical smearing generated by the light was measured as a percentage of average smeared region/maximum signal of light source.

Camera	Percentage of Smeared Region
Imperx IGV-B4820	27%
Imperx IGV-B4020	17%
Dalsa Spyder3	No smearing on line-scan sensors

Anti-blooming Protection

Test Procedure:

Lab testing indicated that blooming was not likely to present a problem in field tests, but we were unable to create conditions similar to flight over water perfectly in the lab. Blooming requires very bright reflections that completely saturate the sensor. Blooming effects were evaluated primarily on the basis of the results of the field experiments.

Modulation Transfer Function (MTF)—Camera Electronics

Test Procedure:

A sequence of images was gathered with all cameras in a controlled environment imaging a resolution test chart. Various sets of optics were used to isolate the camera electronics from the optics. Resulting images were analyzed quantitatively.

Camera	Pass/Fail
Imperx IGV-B4820	Pass
Imperx IGV-B4020	Pass
Dalsa Spyder3	Pass

Modulation Transfer Function (MTF)—Optics and Image Sensor

Test Procedure:

A sequence of images was gathered with all cameras in a controlled environment imaging a resolution test chart. The optics chosen for the experiment were used with all three cameras. Resulting images were analyzed quantitatively.

Camera	Pass/Fail
Imperx IGV-B4820	Pass
Imperx IGV-B4020	Pass
Dalsa Spyder3	Pass

Optical Distortion

Test procedure:

Optical distortion was tested after the field experiments were conducted, on the basis of the images gathered during the experimentation.

Electronic Shutter Range

Test procedure:

Electronic shutter speed ranges of the three candidate cameras subjected to lab testing are presented in the table below.

Camera	Electronic Shutter Speed Range
Imperx IGV-B4820	1/67,000 to 1/3 sec
Imperx IGV-B4020	1/67,000 to 1/5 sec
Dalsa Spyder3	3 to 3,300 µs

Motion Blur

Test procedure:

Motion blur was tested after the field experiments were conducted, on the basis of the images gathered during the experimentation.

Operating Temperature

Test procedure:

Previously known operating temperature ranges of the three candidate cameras subjected to lab testing are presented in the table below.

Camera	Temperature Range °C
Imperx IGV-B4820	- 30.0° to + 65.0°C
Imperx IGV-B4020	- 30.0° to + 65.0°C
Dalsa Spyder3	0.0° to 50.0°C

Physical Properties—Size, Weight, Power Consumption

Test procedure:

Various additional physical properties of the three candidate cameras subjected to lab testing are presented in the matrix below.

Camera	Size	Weight	Power Consumption
Imperx IGV-B4820	(60 x 60 x 51) mm	280 g	3.6 W / 6.1 W
Imperx IGV-B4020	(60 x 60 x 51) mm	280 g	4.0 W / 6.5 W
Dalsa Spyder3	(85 x 65 x 50) mm	300 g	< 7 W

Integrated Discussion of Camera Properties Affecting Aerial Imaging Suitability

The suitability of candidate cameras for offshore aerial high-resolution wildlife imaging survey applications is not a simple function of certain camera characteristics considered in isolation, but rather a complex function of all characteristics taken together, including balancing various trade-offs between different characteristics. This section presents an integrated discussion of some of the most important considerations regarding the suitability of cameras for the survey application of interest in this study.

Sensor Width

Sensor width has a direct impact on suitability for offshore wildlife imaging surveys, as it affects how many cameras are necessary to cover a given swath width. The relation is simply: *Transect width = horizontal pixels × image resolution, where image resolution is the width of one pixel on the surface of the ocean.* Sensors with higher pixel density and width will allow a survey over a given area to be performed using fewer imaging sensors.

Although the direct impact is clear, sensor width also has an indirect impact on a number of areas of the imaging system. With higher density, larger pixel width sensors, pixel size decreases. This is a result of physical sensor size itself being limited. This experiment evaluated only commercially available sensors which could be paired with commercially available optics. This resulted in sensors no larger than traditional 35 mm. As a result, increased sensor pixel width means a decrease in pixel size. As pixel size decreases, each pixel has less ability to gather light, so sensitivity will typically decrease. Under aerial survey conditions, exposure time is very limited (to reduce image blur), so decreased sensitivity is a concern. A number of approaches can be used to compensate for decreased pixel sensitivity, including the use of larger aperture optics and the reduction of aircraft speed to allow more exposure time.

While larger sensor pixel width can have a negative effect on light gathering ability of the system, it has a potentially positive effect on the optical side of the system. With higher pixel density (smaller pixels), less optical magnification is required to produce the same resolution imagery. This can result in smaller, more cost-effective optical solutions.

Sensor Speed

This discussion refers only to area-scan cameras, as line-scan cameras are operated at a fixed speed relative to the object being imaged. Area-scan sensors have configurable imaging speed. The sensors used during this experiment could image up to approximately four frames per second. The relatively low imaging speed is due to the large size of the sensors chosen. Selection of sensor speed has an impact on how many images are gathered of each animal. Based on aircraft speed, an estimate can be calculated of the number of images in which an individual animal will appear (allowing some error for movement speed of animals). While it is ideal to operate at as high a frame rate as possible, higher rates put a burden on the image acquisition system to be able to reliably capture all data from the survey. As the number of cameras increases, the storage rates become large very quickly. As a result, sensor speed may need to be limited to facilitate reliable image acquisition.

During the field experiments for this study, image processing (animal detection algorithms) were not run live during survey experimentation. If image processing were run live, as is anticipated in the future, this would put additional processing burden on the system, and would have an impact on sensor speed.

Camera Size

When designing an aircraft-mounted imaging solution, camera size becomes a key concern. Space is always at a premium in aircraft. Furthermore, camera size can have a direct impact on the choice of aircraft for the solution. The cameras evaluated during this experiment were all industrial, machine-

vision type cameras with relatively small footprints. These small cameras can be combined to produce a very large swath survey width.

Exposure

Due to the likely combination of small image resolution (as small as 2 cm) and the relatively high speed of travel for most of the candidate aircraft (up to 170 mph), it was critical for the camera chosen to be capable of very short exposure times, potentially as short as 100 µs. If the exposure were longer than the time it takes the aircraft to move a distance equal to the image resolution, then motion blurring would occur, leading to a degraded effective image resolution. This requirement immediately rules out most of the existing geospatial type cameras, most of which require exposure times longer than 1 frame per second.

Very short exposure times have a number of impacts on the aerial survey system design. Short exposures translate into less available light for the imaging system. To compensate for a short exposure window, the following techniques can be used:

- Choose camera sensors that have high sensitivity (i.e., high quantum efficiency).
- Choose optical solutions that have high light gathering ability at the required focal lengths (i.e., large apertures).
- Avoid using filters that reduce light gathering ability of the imaging system.
- Carefully consider and evaluate the use of camera gain mechanisms, preferring analog gain mechanisms over digital.
- Consider performing surveys during portions of the day that have high light levels.

Dynamic Range

Selecting a camera with a large dynamic range is very important to properly capture images of animals with varying shades of color. This entails gathering images with 12 or more bits per pixel per color. If a wide dynamic range is not used, the result is that within one image, darker animals may look completely black while lighter ones may look white. A large dynamic range may also greatly help in compensating for harsh lighting conditions that can occur due to sunlight reflections off the water surface.

Dynamic range is represented most simply through the bits per pixel of the camera sensor. While this measurement is useful, it is not a true representation of the dynamic range of a camera. A camera with 12 bits per pixel of dynamic range may not be able to actually represent 4,096 different shades of color. It is important to measure the true dynamic range of a sensor to understand how many different levels of color it can actually distinguish.

Lens Analysis

Method

Prior to lab evaluation of optical solutions, literature and technical specifications were reviewed for applicable lens assemblies. A very large range of focal lengths were required for the experimental trials. Tests were to be performed at multiple resolutions, from multiple altitudes, using two different

camera sensors. It was determined that using multiple lens assemblies would not be practical for the experiment, as additional mount-integration work would need to be done for each different type of lens. Therefore, a single lens assembly that could cover all experimental requirements was necessary.

After the initial research phase, only a handful of commercially available lenses were identified as potential solutions for the field experiments. Based on lens performance requirements, a single lens assembly was chosen which would meet all experimental needs.

Lens Test Parameters

Based on experimental treatments, the following requirements were identified for the lens assembly(s):

- Adjustable focal length from 100 to 600 mm
- Aperture of f/2.8 at 300 mm, f/5.6 at 60 0 mm
- Manually adjustable aperture
- Length of assembly at 600 mm < 15 inches
- Maximum diameter of assembly < 4.5 inches
- 35 mm sensor coverage
- Depth of field at 1,200 m, 2 cm resolution of at least 200 m

Chosen Lens Assembly

The following lens assembly was chosen:

- Sigma APO 120-300mm F2.8 EX DG OS HSM Lens
- Sigma 2x Teleconverter(Optionally used to double focal length while maintaining mount compatibility)

Lens Properties Discussion

The choice of optical solution has a significant impact on an aerial survey system. The experimental trials performed represented a tremendous amount of variation in necessary focal lengths, so a solution was pursued that was very multipurpose. This resulted in an optical solution that was relatively large, and was not optimized for ideal performance at any specific focal length.

When designing an optical solution for an aerial survey, the following considerations should be taken into account:

- Because of limited exposure time, a lens with a large aperture should be chosen (f/2.8 at 300 mm is ideal).
- If possible, a fixed focal length lens is preferred, as lens performance of vari-focal solutions is limited.
- Lens size is of high importance, as it has an effect on aircraft and mounting selection.
- Commercially available lenses are viable, but custom lenses may be desirable.

Length of the lens assembly has an indirect effect on the imaging solution as well, and must be taken into consideration. Longer lens assemblies are more susceptible to low and high frequency vibration. As vibrations translate down a lens assembly, longer assemblies will produce larger vibrations at the end of the lens. This translates into imagery with higher levels of blur. To compensate for this, the following techniques can be used:

- Use a shorter lens assembly
- Evaluate mount stabilization techniques
- Shorten camera exposure time, thus providing isolation from movement during exposure.

Mount Analysis

Method

Mounting technologies were continually evaluated based on camera, lens, and aircraft choices. The aircraft used in the imaging experiments (see Chapter 1) was modified with an external camera mount on the left side of the aircraft fuselage, near the pilot's station (Figure 3–2). The mount was the type used for electro-optical/infra-red, gimbal-mounted systems such as those used by airborne law enforcement or military operations. On the test aircraft, the Boulder Imaging Systems high-definition camera was fixed to this mount with an adapter plate and isolation collar, and shielded from the slipstream and elements by a custom fabricated shroud.

Figure 3–2. Cessna 337 Skymaster with side mounted camera system.

This mount was selected and designed to accommodate both cameras with the full 600 mm optical assembly as well as a gyrostabilizer, which we used during a portion of the flight experiments to evaluate the importance of additional stabilization for reducing image blur.

Mount Test Parameters

Mount test parameters studied during the pre-experiment integration phase are listed in Table 3–6. During this phase, test flights were performed at altitudes ranging from 600 m to 1,200 m, at imaging resolutions of 1 cm to 5 cm (see section 2.2.1).

Table 3–6.

Parameters for Mount Evaluation.

Parameter	Definition	Dependent On	Effects
Stability	Resistance to change	Design/type of mount	Sensitivity to turbulence, vibration
Rigidity	Firmly fixed	Design of mount	Repeatable pointing, motion blur.
Pointing Accuracy	Ability to point camera within tolerance to predicted point on the ground	Design of mount	Repeatable pointing.

We note that other mount technologies may be viable, particularly for internally mounted aerial imaging assemblies, but were not evaluated during the field experimentation for this study (e.g., gimbal mounts).

Post field-testing Evaluation of Manned Aircraft Imaging Systems

The imaging equipment selected for field testing with the manned aircraft survey platform is listed in Table 3–7. Field testing consisted of imaging flight experiments conducted by the project team from 10 to 20 May 2011 offshore of Oak Island NC. Section 2.3 of this report presents a full description of the specific flight trials and imaging experiments that were conducted during this period. In this section, we present a post-hoc evaluation of the performance of the imaging equipment that was used in the field tests, with respect to the suitability of this equipment for future offshore high-resolution wildlife imaging surveys.

Table 3–7.

Cameras and Mount Stabilizer Used in Imaging Flight Experiments Conducted by the Project Team Using a Cessna Skyhawk 337 (Manned Aircraft) as the Imaging Survey Platform between 10 and 20 May 2011 Offshore of Oak Island NC

Name of Model	Type of Equipment
Imperx IGV-B4820	Area-scan camera
Dalsa Spyder3	Line-scan camera
Kenyon Laboratories KS 8	Gyroscopic stabilizer

Summary

Based on image analysis conducted subsequent to the field experiments, we concluded that the gyrostabilized, area-scan imaging system used aboard the manned aircraft during the field experiments generated images of sufficient quality to effectively provide the requisite animal distribution, abundance, and seasonality data for offshore wind-wildlife risk/impact studies (Chapter 1). A discussion of the performance of specific imaging system components in these experiments is provided below.

Area-Scan Camera Performance

Performance of the area-scan camera during experimental trials proved to be excellent. Species identification could be reliably performed with gyrostabilized imagery obtained at flight elevations up to 1,200 m. Color reproduction was good, facilitating species identification/differentiation based on color features. Because of the high quality imagery relative to any other image gathering equipment configuration, images from the area-scan camera aboard the manned aircraft imaging platform served as the entire basis for the effectiveness evaluation of this study (Chapter 1), including all considerations of other imaging variables on effectiveness (e.g., image resolution, camera angle, importance of multiple pictures). A selection of animal images gathered with the area-scan camera during the flight experiments with the manned aircraft system is presented in Figure 3–3 through Figure 3–11. A discussion of several important area-scan imaging considerations based on our experimental results is provided below.

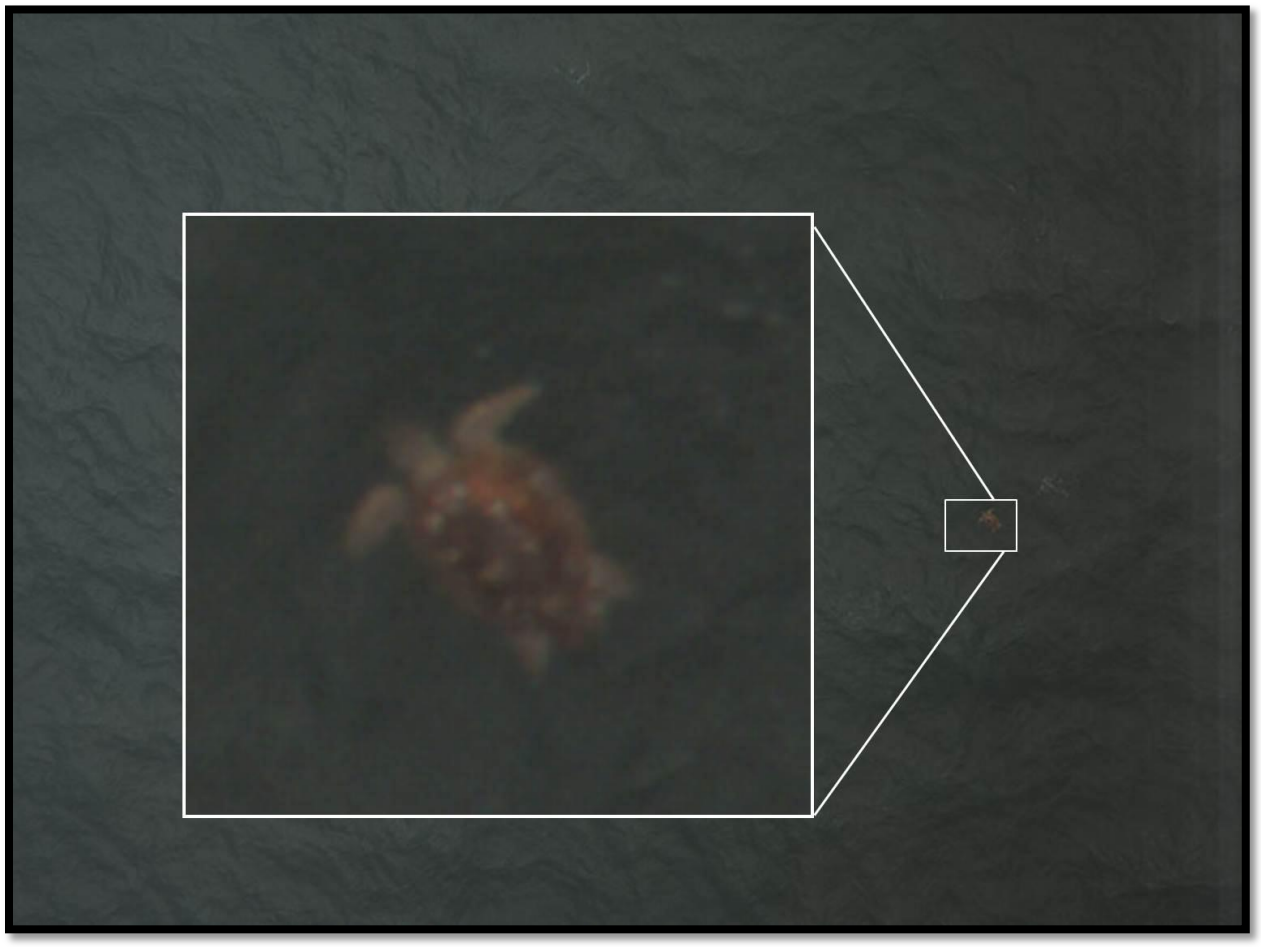

Figure 3–3. Loggerhead Sea Turtle (*Caretta caretta*)—Image captured by a gyrostabilized high-resolution area-scan camera mounted externally to a Cessna 337 Skymaster aircraft during experimental imaging flights conducted by the project team 10 to 20 May 2011 offshore of Oak Island NC. This image has a resolution of 1.5 cm and was taken from a survey flight altitude of 600 m.

Figure 3–4. Royal Tern (*Thalasseus maximus*)—Image captured by a gyrostabilized high-resolution area-scan camera mounted externally to a Cessna 337 Skymaster aircraft during experimental imaging flights conducted by the project team 10 to 20 May 2011 offshore of Oak Island NC. This image has a resolution of 1.5 cm and was taken from a survey flight altitude of 600 m.

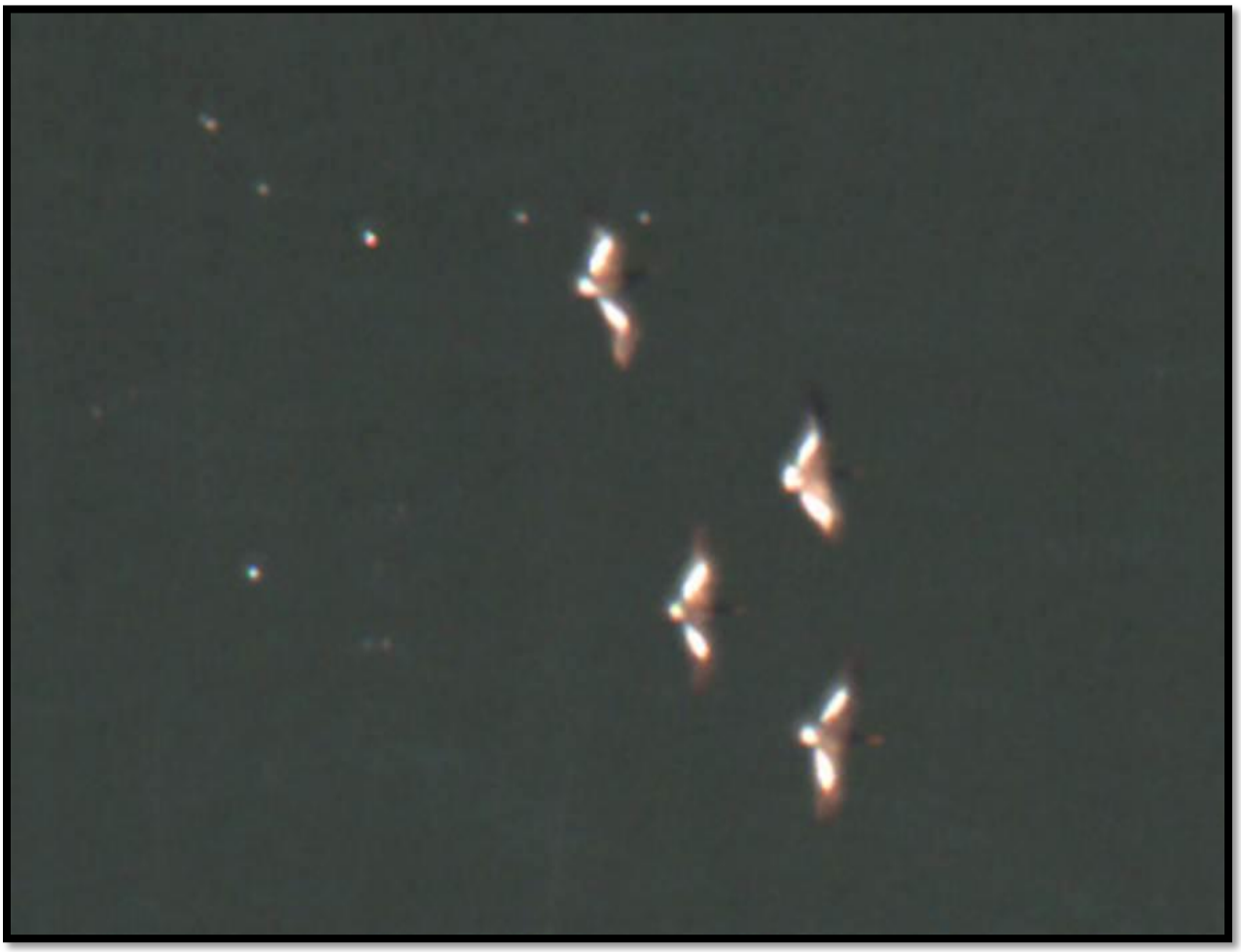

Figure 3–5. American Oystercatchers (*Haematopus palliatus*)—Image captured by a gyrostabilized high-resolution area-scan camera mounted externally to a Cessna 337 Skymaster aircraft during experimental imaging flights conducted by the project team 10 to 20 May 2011 offshore of Oak Island NC. This image has a resolution of 1.5 cm and was taken from a survey flight altitude of 600 m.

Figure 3–6. Immature Northern Gannet (*Morus bassanus*)—Image captured by a gyrostabilized high-resolution area-scan camera mounted externally to a Cessna 337 Skymaster aircraft during experimental imaging flights conducted by the project team 10 to 20 May 2011 offshore of Oak Island NC. This image has a resolution of 2.5 cm and was taken from a survey flight altitude of 1,000 m.

Figure 3–7. Magnificent Frigatebird (*Fregata magnificens*)—Image captured by a gyrostabilized high-resolution area-scan camera mounted externally to a Cessna 337 Skymaster aircraft during experimental imaging flights conducted by the project team 10 to 20 May 2011 offshore of Oak Island NC. This image has a resolution of 1.5 cm and was taken from a survey flight altitude of 433 m.

Figure 3–8. Probable Audubon's Shearwater (*Puffinus lherminieri*)—Image captured by a gyrostabilized high-resolution area-scan camera mounted externally to a Cessna 337 Skymaster aircraft during experimental imaging flights conducted by the project team 10 to 20 May 2011 offshore of Oak Island NC. This image has a resolution of 1.5 cm and was taken from a survey flight altitude of 425 m.

Figure 3–9. Wilson's Storm-Petrel (*Oceanites oceanicus*)—Image captured by a gyrostabilized high-resolution area-scan camera mounted externally to a Cessna 337 Skymaster aircraft during experimental imaging flights conducted by the project team 10 to 20 May 2011 offshore of Oak Island NC. This image has a resolution of 1.0 cm and was taken from a survey flight altitude of 450 m.

Figure 3–10. Osprey (*Pandion haliaetus*)—Image captured by a gyrostabilized high-resolution area-scan camera mounted externally to a Cessna 337 Skymaster aircraft during experimental imaging flights conducted by the project team 10 to 20 May 2011 offshore of Oak Island NC. This image has a resolution of 1.5 cm and was taken from a survey flight altitude of 433 m.

Figure 3–11. Common Tern (*Sterna hirundo*)—Image captured by a gyrostabilized high-resolution area-scan camera mounted externally to a Cessna 337 Skymaster aircraft during experimental imaging flights conducted by the project team 10 to 20 May 2011 offshore of Oak Island NC. This image has a resolution of 1.0 cm and was taken from a survey flight altitude of 450 m.

Mount Performance

In addition to motion over the ground generated by movement of the plane, the imaging platform can contain motion caused by the mounting platform itself. This motion can be low to high frequency, depending on the characteristics of the mount.

Exposure time is generally calculated based on an imaging platform that does not contain any motion. In the field experiment planning and equipment design stages of this project, the speed of the airplane was the sole factor used in computing a safe exposure time for the area-scan camera. This exposure time was calculated to be ~200 µs, and compensates for 2 cm of image blur in the direction the plane is moving. If the imaging platform is responsible for additional motion in the same axis that the plane is moving, image blur may be present in the image. Because the motion of the plane is only in one axis (assuming motion in the other axis is negligible over a window as short as 200 µs), the imaging platform can actually sustain motion in the other axis during imaging (up to 2 cm in our example).

To summarize, the imaging platform is more susceptible to motion (jitter) in the axis that the plane is moving. In the other axis, the imaging platform can tolerate motion up to the imaging platform resolution (2 cm on the ground), without showing noticeable image blur.

It should be clear that stability of the imaging platform is of high importance to gathering image data that does not show noticeable image blur. If an imaging platform does contain motion that cannot be eliminated, the exposure time can be further lowered, allowing some freedom of movement in the axis that the plane is travelling. In any case, the imaging platform cannot move more than the imaging resolution on the ground during exposure (e.g., 2 cm), or image blur will definitely be present. Lowering exposure time to compensate for mount vibration has a significant downside (loss of light), so may not be an option.

Early in the experimentation phase, it was determined that the chosen mount was generating very high levels of vibration (both low and high frequency). On-aircraft observations were sufficient alone to determine that the mount assembly was exhibiting very high levels of motion during flight. This vibration was causing excessive blurring of animals in area-scan imagery, and unacceptable levels of waviness in line-scan imagery. The original, unstabilized mount configuration was used for the initial flight experimental trials, and for later trials, a single electrical gyrostabilizer was attached to the inside of the camera mount assembly. This gyrostabilizer showed a significant improvement/dampening of both high and low frequency vibrations. The two images below (Figure 3–12 and Figure 3–13) show an example of image blur before and after adding the gyrostabilizer. Both images were taken at the same altitude, with the same resolution, of a similar bird (likely the same species).

Figure 3–12. Image of a bird from aerial imaging experiments conducted between 10 and 20 May 2011 offshore of Oak Island NC. This image was produced using a nonstabilized area-scan camera, with a 1,000 m flight altitude and image resolution of 2.5 cm (see text).

Figure 3–13. Image of a bird from aerial imaging experiments conducted between 10 and 20 May 2011 offshore of Oak Island NC. This image was produced using a gyrostabilized area-scan camera, with imaging parameters otherwise identical to that used in Figure 3–12 above (1,000 m flight altitude and image resolution of 2.5 cm). The increased sharpness of this image compared with Figure 3–12 illustrates the importance of gyroscopic stabilization.

These two images are highly representative of the blur caused in imagery as a result of mount vibration. Imagery collected with the original mount design showed relatively high levels of image blur across all configurations. After adding the gyrostabilizer, images collected showed much higher sharpness, as evidenced in Figure 3–13 above.

Based on results from the experiment, gyrostabilization technology is a highly viable solution to compensate for both high and low frequency aircraft/wind vibration.

Lighting Performance

Light levels proved to be of significant importance to performance of the area-scan camera. Exposure times of 200 to 300 µs were used during experimental trials. Lens apertures of f/2.8 to f/5.6 were evaluated. With an aperture level of f/5.6, lighting levels during early morning and evening proved insufficient to acquire high quality imagery. The images below (Figure 3–14 and

Figure 3–15) are representative samples of the challenges of imaging when outside light levels are low.

Figure 3–14. Image of water from aerial imaging experiments conducted 10 to 20 May 2011 offshore of Oak Island NC with a digitally magnified portion of the image shown in the inset in the upper right. This image was taken during relatively high light conditions in the early afternoon.

Figure 3–15. Image of water from aerial imaging experiments conducted 10 to 20 May 2011 offshore of Oak Island NC with a digitally magnified portion of the image shown in the inset in the upper right. This image was taken during relatively low light conditions in the early evening. The reduced image quality of this image compared with Figure 3–14 can be seen in the graininess and color distortion visible in the inset (see text).

During experimentation, analog camera gain levels were continuously adjusted based on lighting conditions. When camera electronics apply a high level of analog gain into imagery, the imagery begins to exhibit noise. This can be observed in the evening light image above (Figure 3–15), where the image is noticeably grainy. This noise will exhibit itself as both blur in the imagery and anomalies in animal color.

These samples were acquired with a lens aperture of f/5.6; with an aperture of f/2.8, imagery would not have exhibited this level of noise. This example does still illustrate an important point, as the system itself was borderline with respect to light levels. Plane speed during acquisition of these images was ~160 mph. If plane speed were increased, lower exposure times would be necessary to compensate. In this case, even optics at f/2.8 aperture may encounter lighting problems during early morning/evening at increased plane speed.

This same phenomenon can exhibit itself under cloud cover. If cover is heavy, camera electronics may need to compensate by applying additional electronic gain to imagery.

During experimentation, the lesson was continually reinforced that light-gathering performance of the imaging solution is of critical importance, particularly when imaging with area-scan cameras.

Image Smearing

Image smearing is a sensor effect in which light from bright objects in the sensor's field of view leaks into the sensor during frame readout. This leak occurs only after the image has been completely exposed. The figure below shows an example of image smearing.

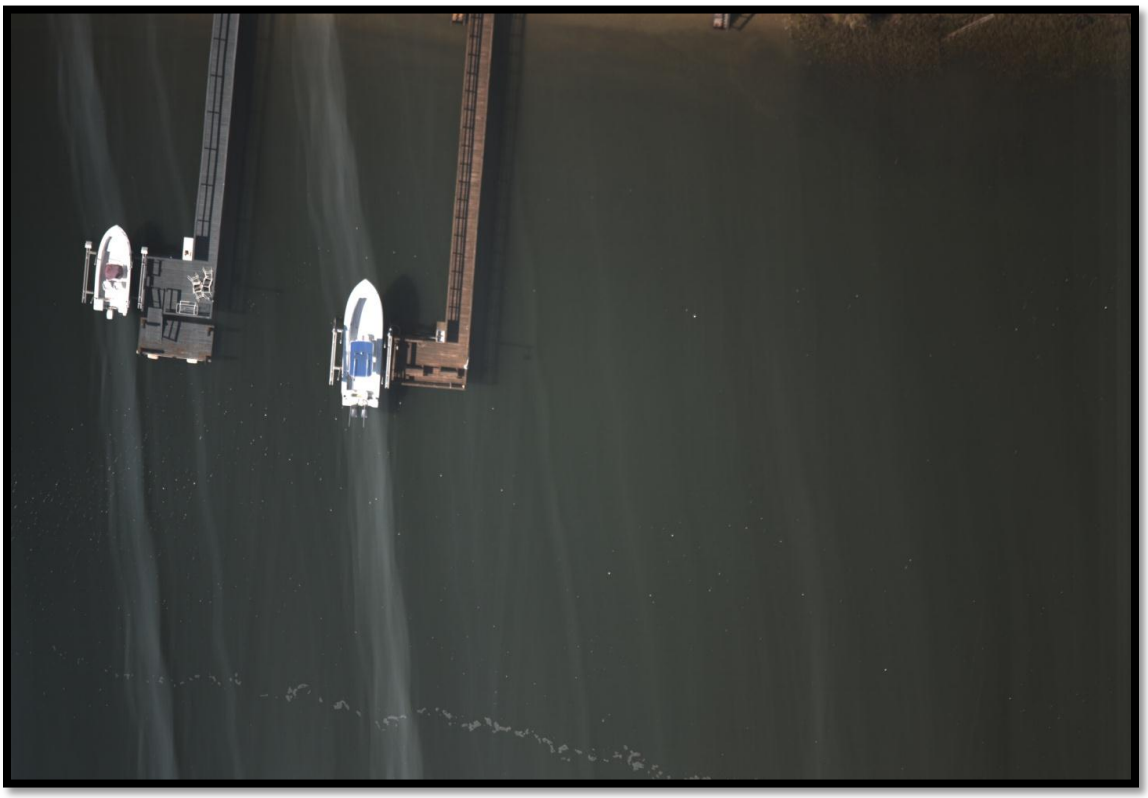

Figure 3–16. Image of boats and docks from aerial imaging experiments conducted 10 to 20 May 2011 offshore of Oak Island NC, showing image smearing effects (whitish vertical streaks in the image). These streaks are an artifact of residual light being let in by the mechanical shutter during digital frame readout and can be eliminated in future applications by using a faster mechanical shutter than was used (see text).

Image smearing can be compensated for by using a mechanical shutter in combination with the electronic shutter in the imaging system. A mechanical shutter closes after exposure is complete, thus preventing light from entering the sensor during frame readout. Although mechanical shutters do not operate quickly enough to close off incoming light during the entire frame readout period, they are fast enough to reduce the amount of image smearing by 30 to 100 times, making image smearing negligible in resultant imagery. Any further surveys should use a mechanical shutter on all cameras, as image smearing is very prevalent when using exposure times < 200 µs.

Exposure Time (Shutter Speed)

Exposure time must be carefully chosen to prevent motion blur across pixels during exposure of each individual frame. Exposure time can be calculated based on ground speed of the imaging platform and imaging resolution. Exposure time is bounded by the amount of time that it takes the imaging platform to move 1 pixel over the ground. If the imager exposes for more than 1 pixel worth of motion, each pixel on the sensor will be exposed to multiple pixels on the ground, and blur will be present.

For example, if the imager is set for 2 cm resolution, and the aircraft (imaging platform) is flying at 350 kph. Each pixel in the image represents exactly 2 cm on the ground. When exposing a frame, if the imaging platform crosses more than 2 cm on the ground, image blur will be present in all pixels in the image. If, for example, during exposure, the imaging platform covered 10 cm on the ground (while imaging at 2 cm resolution), 5 pixels would be blended into each individual pixel on the image, showing significant image blur.

To calculate maximum exposure time for the example above (2 cm resolution, 350 km/hr ground speed), one must calculate the amount of time that it takes the imaging platform to move 1 pixel (2 cm). This can be easily calculated with a ground speed of 350 km/hr:

$$350\ km / 1\ hr = 2\ cm / x.$$

The amount of time the imaging platform takes to move 1 pixel (2 cm) is ~200 µs. Therefore, the maximum exposure time for each frame is 200 µs. If exposure time is set to 200 µs or below, each pixel in the image will contain data for exactly 1 pixel on the ground, with no motion blur present across pixels. Note that, during exposure, the imaging platform is in motion, but each pixel on the sensor is gathering light from an area on the ground the same size as the intended resolution, so no detectable blur is present. Each pixel on the sensor contains data from a position on the ground that is no larger than 2 cm. Because the imaging platform moves 2 cm (in the axis of plane travel) during exposure, what the sensor actually records is an average light intensity over that 2 cm area.

Optical Magnification Level Impacts

Higher magnification levels resulted in more vibrational blur effects in the imagery obtained with the area-scan camera. This is likely to have resulted from two separate but related factors, described below.

1) Long lens assemblies magnify vibrations. Focal lengths above 600 mm entailed using lens assemblies ~2 inches longer than that used to produce imagery below 600 mm. Increased lens assembly length results in the magnification of any vibration-related image distortions

because of the cantilever effect. Length of lens assembly should be considered carefully when designing a survey platform, as shorter lens(s) provide tangible benefits with respect to image blur.

2) High image magnification magnifies vibrations as well as images. Higher zoom levels translate vibrations on the aircraft into larger movement at the ground level. This is the same effect noticed when using high zoom binoculars; even slight motion of the binoculars causes large motion in the object being viewed.

The effects of increased magnification on image blur is illustrated in the pictures presented in Figure 3–17 and Figure 3–18. Both images are taken at the same resolution, yet show drastically different image quality. The first image was taken at 1,200 mm focal length, using an optical setup that was ~2 inches longer than the setup used for the second image. The second figure shows an image taken with a shorter 600 mm optical package (with less zoom). Image blur is very prevalent in the image taken at high zoom with a longer lens assembly.

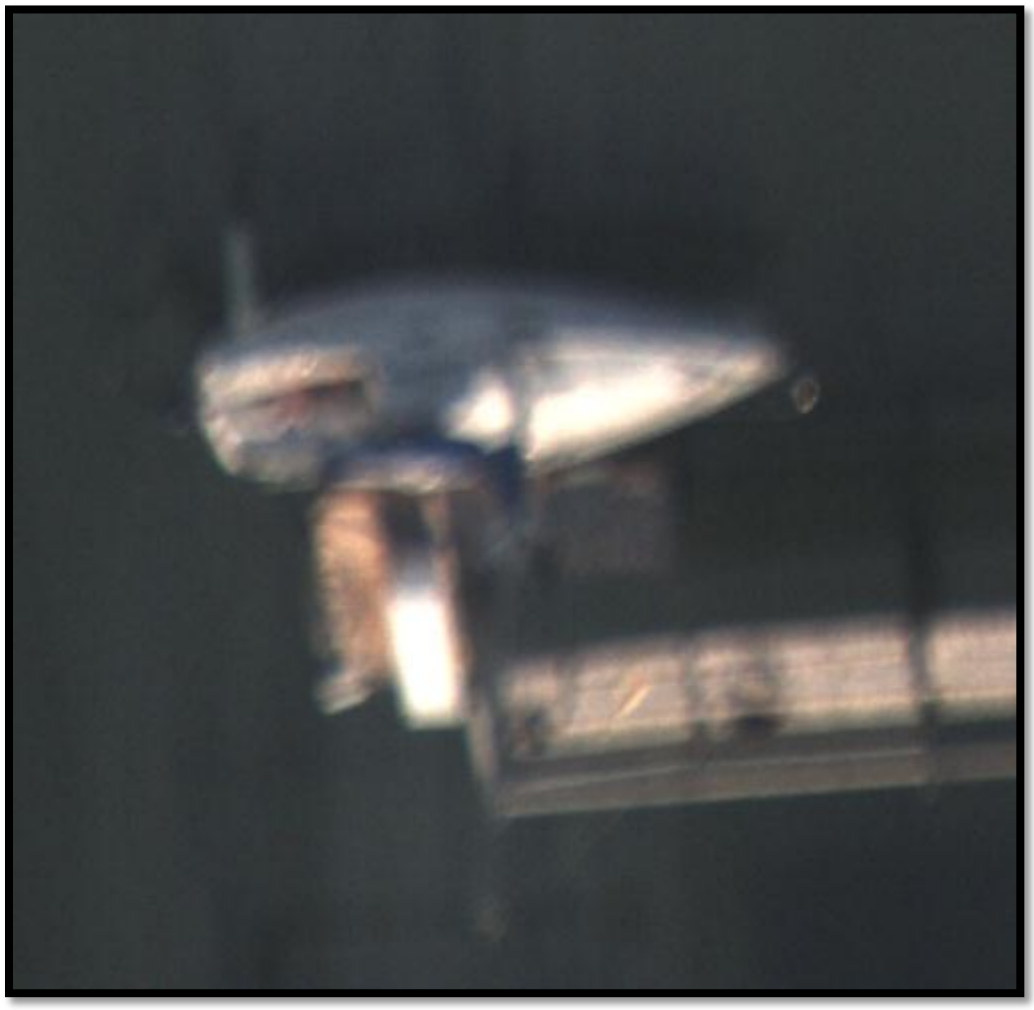

Figure 3–17. Image of a boat and dock taken during aerial imaging experiments conducted between 10 and 20 May 2011, near Oak Island NC. In this image, a 1,200 mm focal length lens is used to provide high magnification to achieve the desired image resolution level (2 cm) at high flight altitude (1,200 m).

Figure 3–18. Image of the same boat and dock as in Figure 3–17, from aerial imaging experiments conducted between 10 and 20 May 2011 near Oak Island NC. In this image, a shorter (600 mm) focal length lens is used in order to achieve the same image resolution level as in Figure 3–17 (2 cm) at a lower flight altitude (600 m). The increased sharpness of this image relative to Figure 3–17 illustrates the increased image blur that can occur with increased image magnification (see text).

Line-Scan Camera Performance

During experimentation, early test results showed significant problems with the use of a line-scan camera onboard the aircraft. Because line-scan cameras image a single line at a time, they are highly susceptible to motion on the platform to which they are mounted. This vibration produced imagery that was unusable, even with the addition of a gyrostabilizer to the mount platform.

Line-scan imagery did show significant advantages in other areas (detailed below), but ultimately cannot be recommended as a viable aerial survey imaging solution.

Horizontal Mount Vibration

While imaging with a line-scan camera, if the mount is moving horizontally with respect to the camera sensor, the imagery will exhibit waviness that is directly representative of the motion of the mount. This phenomenon can be observed in Figure 3–19.

Figure 3–19. Image of a parking lot taken using the line-scan camera on an unstabilized mount (see text) during initial testing flights near Raleigh NC during the first week of May 2011. The waviness in the image illustrates the sensitivity of line-scan cameras to vibrational effects (see text).

Figure 3–19 clearly exhibits the vibration problem. The same phenomenon was observed with all line-scan imagery, regardless of altitude or resolution. The waviness observed in the vehicles is a direct result of the camera mount moving horizontally with respect to the sensor. This effect was

somewhat reduced, but still problematic when the line-scan camera was used with the gyrostabilized mount during the flight experiments offshore of Oak Island NC.

Vertical Mount Vibration

Line-scan cameras are equally susceptible to vibration in both dimensions, but vibration in the vertical dimension (with respect to the sensor) causes an even more significant imaging problem with respect to suitability for wildlife surveys. Vertical movement can cause the camera to point at an area where it has previously already imaged, producing duplicate imaging data over an entire line. If the mount moves the opposite direction, the camera may point beyond portions of the scene that it has not imaged, skipping portions of the scene, as illustrated in Figure 3–20.

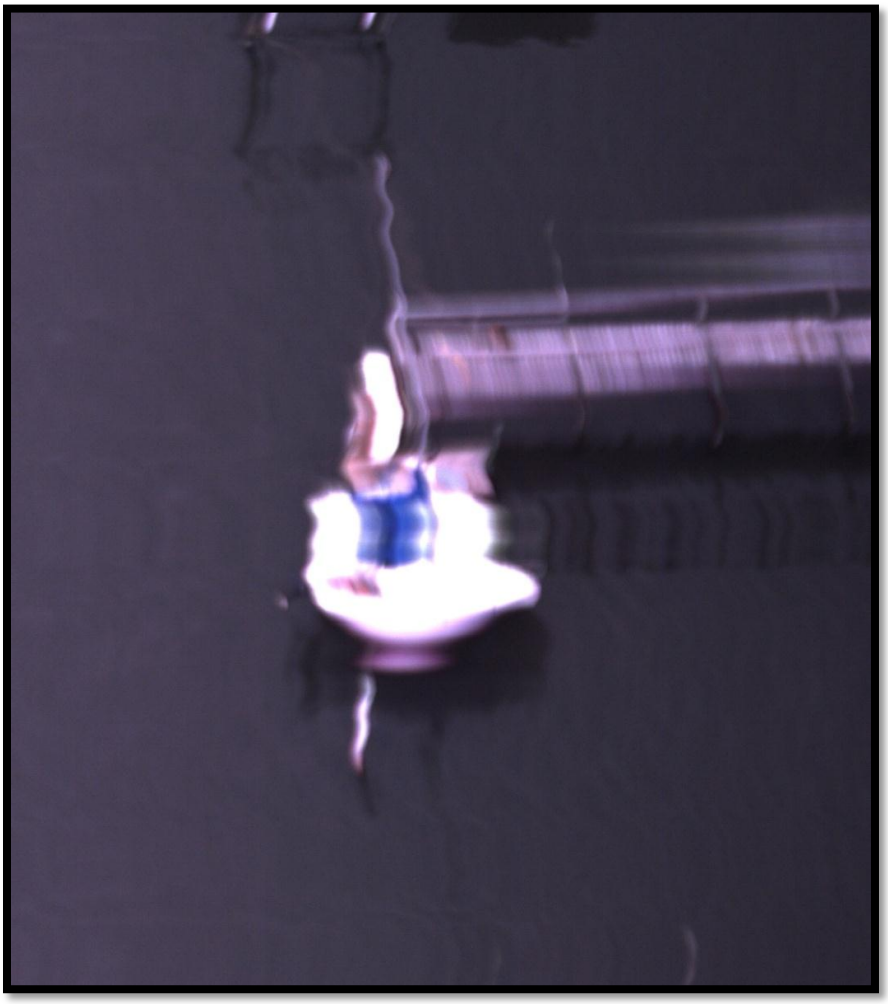

Figure 3–20. Image of a boat and dock from aerial imaging experiments conducted 10 to 20 May 2011 offshore of Oak Island NC taken with the line-scan camera. The duplicated portions of the boat and dock are caused by vertical vibration effects in the camera/mount, and would result in data loss in the case of wildlife imaging surveys (see text).

The upper portion of the boat, and some portions of the dock in Figure 3–20 are replicated over multiple lines, effectively obscuring anything that might have been present in the water in those areas (e.g., an animal). Such distortions effectively create missing data in the imagery, as there is water that is obscured by the imaging anomaly that may have contained animals.

Color Quality

The line-scan camera used was a 2-line sensor, which provides two of three color components for each pixel imaged, compared with a single color component in the area-scan camera. Although line-scan sensor technology is superior to area-scan in this respect, it does not outweigh the disadvantages of line-scan sensors compared with area-scan with respect to vibrational effects and the resulting image distortions.

Light Sensitivity

Light sensitivity of the line-scan camera was higher than that of the area-scan camera, representing another advantage of line-scan sensors, particularly for low lighting conditions. Effective imaging during low light conditions allows higher plane speed and an expanded time window of suitable daylight for imaging. Nonetheless, this advantage does not outweigh the serious disadvantage of line-scan sensors compared with area-scan with respect to vibrational effects and the resulting image distortions.

3.3.3 Unmanned Aircraft System

The evaluation of UAS-based imaging systems under the project was led by the UAS experts that were subcontracted for the project, Donald and Erica MacArthur of IATech, Inc., working in coordination with the technology task manager, M. Kujawa, under the direction of Normandeau. It is important to note that the manned aircraft system was used as the primary experimental system for this project, primarily due to the intensity of permitting restrictions and constraints governing the operation of UAS in US airspace. For this reason, the range of imaging options evaluated and field tested on the UAS was much smaller than it was on the manned aircraft system under this project. The UAS-based portion of this project was intended more as a proof of concept demonstration of UAS technology for offshore aerial high-resolution wildlife imaging surveys. We note that the discussions of imaging technological and methodological issues and experimentation contained within the manned aircraft portions of this report are not unique to manned vehicular platforms (e.g., vibration, resolution, light exposure issues), and hence apply equally well to considerations of unmanned vehicle-based aerial imaging survey design.

Desktop Evaluation and Flight Test Imaging Equipment Selection

Camera/Optics Evaluation

We evaluated the suitability of cameras and lenses based on effectiveness and cost criteria. For the UAS system, we considered only off-the-shelf area-scan camera models and commercially available optics (matrix for the candidate cameras is shown in Table 3–8). The Canon EOS 1DS Mark III was selected for experimentation on the basis of its overall desirability, with a 200 mm lens capable of achieving the desired image resolution levels (2 to 5 cm) at the desired flight altitudes (300 to 600 m).

Table 3–8.

Camera Evaluation Matrix Used to Select the Camera Used for Aerial Imaging Experimentation in the Unmanned Aircraft System (UAS)

Capability	Pixel array (MPXMP)	Gating time (nsec)	Dynamic range (%)	Linear resolution (1 line elements)	Sensor element (CCD, CMOS,..)	Near-IR (Y/N)	Low-UV (Y/N)	Polarizing filters (Y/N)	Quantum efficiency (%)	Weight (kg)	Cost ($)
Area scan											
Nikon D3X	6048x4032	n/a	n/a	6048	CMOS	Y	N	Y	35%	1.22	$7500
Canon EOS-1DS Mark III	5632x3750	n/a	n/a	5632	CMOS	Y	N	Y	31%	1.21	$7000

Mount Evaluation

After evaluating a variety of mounting options, a shock mount containing passive vibration isolators was selected as the optimum for field testing with the Pelican UAS, on the basis of maximum load rating, the frequency rejection at higher frequencies, resistance to humidity/salt, and high shock rating, as well as cost, complexity, and size considerations. The passive vibration isolators are shown in Figure 3–21, as they were mounted on the camera enclosure for the UAS-based field tests.

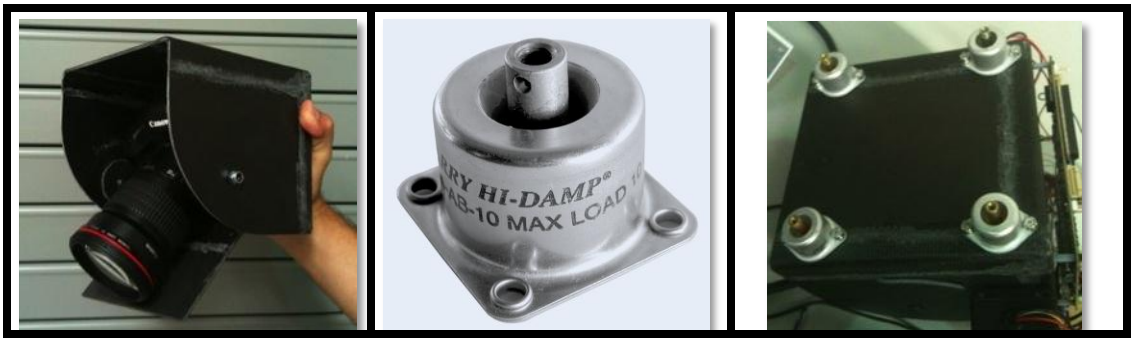

Figure 3–21. Camera and enclosure (left), passive vibration isolator (center), and enclosure with isolators (right) used for UAS-based aerial imaging experiments (see text).

Based on the distributed load for each isolator and the total weight of the payload, the effective natural frequency of the isolators was estimated at ~28 Hz. This implies that high frequency vibration above this frequency is damped from the payload. This improves the image quality and protects the payload from vibration and shock.

Post Field-testing Evaluation of Unmanned Aircraft System-based Imaging Equipment Performance

We performed a series of flight tests to evaluate the effectiveness of the UAS-based high-resolution imaging system. These tests are described in full detail in section 2.3. In the current section of this report, we present a post-hoc evaluation of the performance of the imaging equipment that was used in these field tests, with respect to the suitability of this equipment for future offshore high-resolution wildlife imaging surveys.

Summary

Based on image analysis conducted subsequent to the field experiments, we concluded that the passively stabilized, area-scan imaging system used aboard the UAS during the field experiments was not able to generate images of sufficient quality to effectively provide the requisite animal distribution, abundance, and seasonality data for offshore wind-wildlife risk/impact studies. Despite the insufficiency of the field-tested UAS in this study, it is also evident that collection of high-resolution imagery of sufficient quality for offshore wind-wildlife studies using an UAS platform should be possible in the future, using a UAS with a larger payload capacity capable of carrying more advanced imaging equipment, such as was used in the manned aircraft portion of this study. A discussion of the UAS-based imaging field test results is presented below.

The best quality imagery collected by the imaging system intended for the UAS was obtained during the preliminary flight tests conducted in September 2011, in which this imaging system was mounted in a manned aircraft and flown over Lake Santa Fe, roughly 20 miles east of Gainesville FL (see section 2.3). During these tests, marginally acceptable quality images of objects on the water's surface were produced at image resolutions within acceptable limits (2.5 cm), and at flight altitudes within acceptable limits for conducting offshore wind-wildlife surveys (363 m, Figure 3–22 and Figure 3–23).

Figure 3–22. Shoreline image taken over Lake Santa Fe FL, at 363 m flight altitude using the imaging system designed for UAS-based testing mounted within a manned, fixed wing aircraft during preliminary flight tests conducted during 1 to 4 September 2011. Red boxes are drawn around two red buoys, shown enlarged in Figure 3–23.

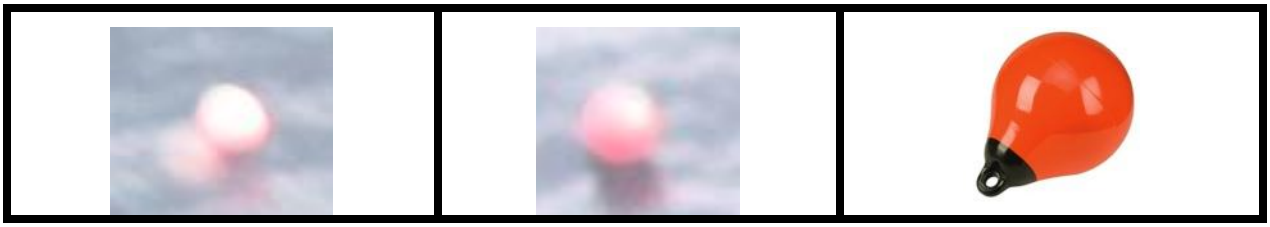

Figure 3–23. Enlargements of the image presented in Figure 3–22, showing the two buoys captured within the image (left, center) along with an illustration of what the buoys look like (right). The buoys are roughly 68 cm in diameter, and the image resolution is approximately 2.5 cm—illustrating marginally suitable image resolution and quality obtained by the imaging system.

One very high quality image of a bird (Black Vulture, *Coragyps atratus*) flying over water was obtained during the preliminary testing at Lake Santa Fe (Figure 3–24). Individual primary flight feathers on the bird can be discerned from this image, indicating that species-level identification of many birds and other marine wildlife would be possible with imagery of this quality and resolution. However, subsequent analysis of the image revealed that the high quality was likely due to the proximity of the bird to the aircraft; the aircraft was flying at 322 m above ground level, and the vulture is estimated to have been flying at 235 m, only 87 m from the aircraft.

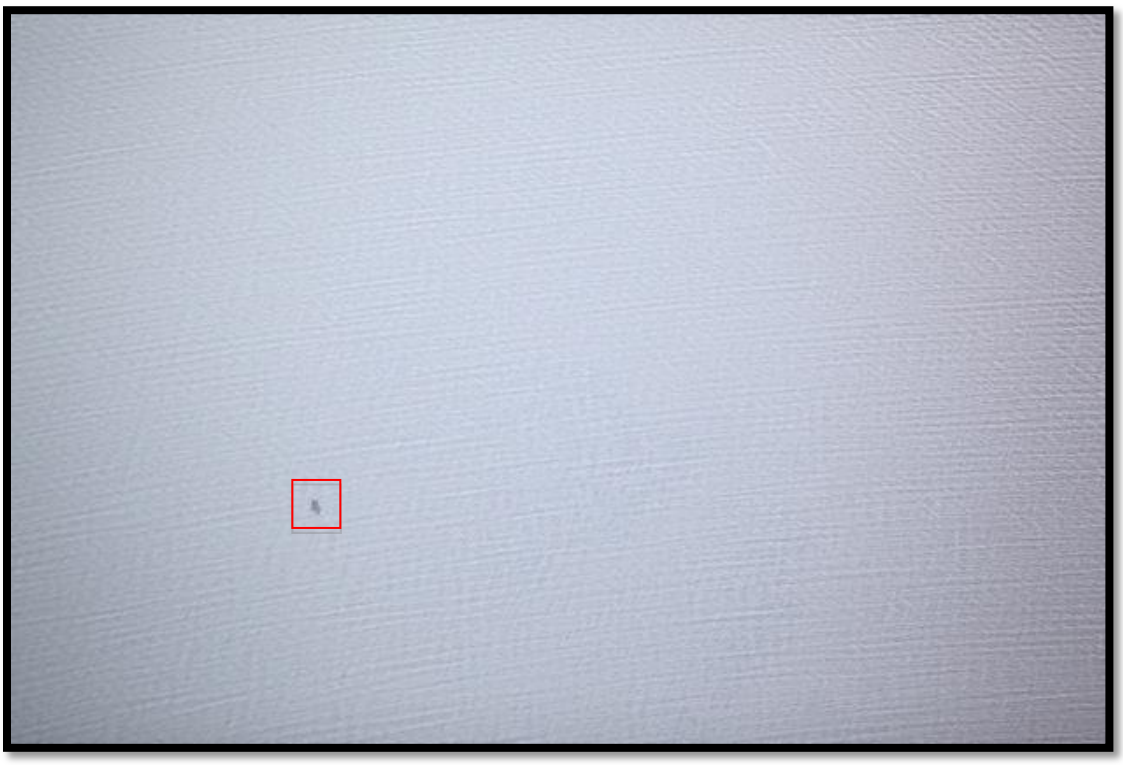

Figure 3–24. Over water image taken over Lake Santa Fe FL at 322 m flight altitude using the imaging system designed for unmmanned aircraft system-based testing mounted within a manned, fixed wing aircraft during preliminary flight tests conducted during 1 to 4 September 2011. A red box is drawn around a Black Vulture, shown enlarged in Figure 3–25.

Figure 3–25. Enlargement of the image presented in Figure 3–24, showing a flying Black Vulture captured within the image. Calculations based on the known size ranges of Black Vultures and the known magnification of the image revealed that this bird was flying at approximately 235 m agl, only 87 m below the aircraft, hence the high quality of the imaged vulture is not necessarily indicative of the quality of animals imaged at, or near, the water's surface.

In subsequent flight tests with the imaging system deployed within the UAS, images of acceptable quality were not able to be obtained at flight altitudes within acceptable limits for application to offshore wind-wildlife studies. Even at low flight altitudes within the rotor swept zone of offshore wind turbines, the images obtained were unsuitable, or marginally suitable for offshore wind-wildlife data gathering purposes. A selection of illustrative examples from these tests is provided in Figure 3–26 through Figure 3–35 below.

Figure 3–26. Image taken during UAS-based imaging flight tests conducted during the week of 3 October 2011 at Camp Roberts CA, from a flight altitude of 272 m agl. A red box is drawn around a black and white image calibration object, located on the ground just above the runway in the image. An enlargement of this object is shown in Figure 3–27.

Figure 3–27. Enlargement of a portion of the image from Figure 3–26, showing the calibration object which measured 457 × 366 cm. The resolution of this image is approximately 2.5 cm.

Figure 3–28. Image taken during unmanned aircraft system-based imaging flight tests conducted during January to February, 2012 in the Gulf of Mexico near Cedar Key FL, at a flight altitude of 80.5 m. A red box is drawn around an object in the water that is possibly a Bottlenose Dolphin, shown enlarged in Figure 3–29.

Figure 3–29. Enlargement of a portion of the image in Figure 3–28, showing a possible Bottlenose Dolphin. Image resolution = 2.5 cm.

Figure 3–30. Image taken during unmanned aircraft system-based imaging flight tests conducted during January to February, 2012 in the Gulf of Mexico near Cedar Key FL, at a flight altitude of 141.5 m. A red box is drawn around the unmanned aircraft system launch-recovery vessel, shown enlarged in Figure 3–31.

Figure 3–31. Enlargement of a portion of the image in Figure 3–30, showing the unmanned aircraft system launch/recovery vessel. Image resolution = 4.38 cm.

Figure 3–32. Image taken during unmanned aircraft system-based imaging flight tests conducted during January to February, 2012 in the Gulf of Mexico near Cedar Key FL at a flight altitude of 64.9 m. A red box is drawn around a flying bird, shown enlarged in Figure 3–33.

Figure 3–33. Enlarged portion of the image in Figure 3–32, showing an image of a flying bird. Image resolution is 2.01 cm.

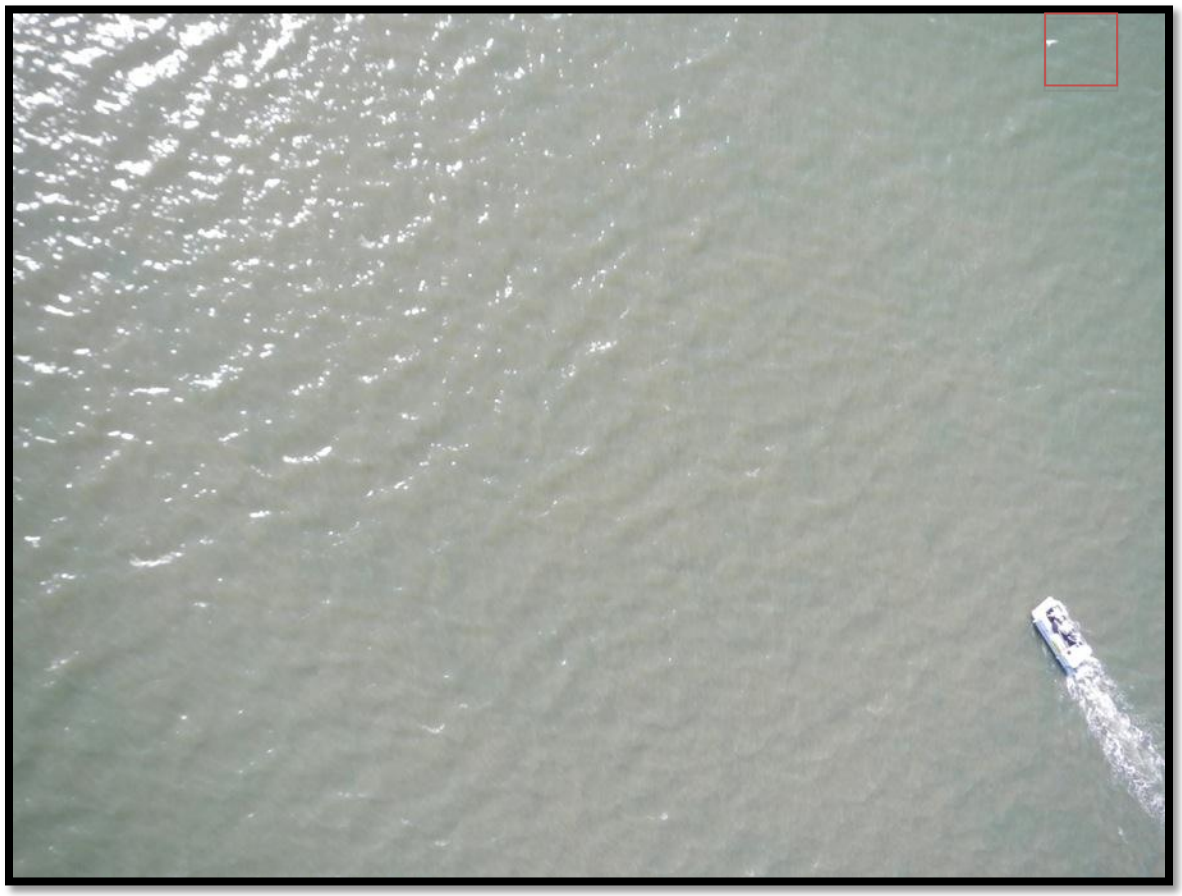

Figure 3–34. Image taken during unmanned aircraft system-based imaging flight tests conducted during January to February, 2012 in the Gulf of Mexico near Cedar Key FL at a flight altitude of 69.8 m. A red box is drawn around a flying bird, shown enlarged in Figure 3–35.

Figure 3–35. Enlarged portion of the image in Figure 3–34, showing an image of a flying bird. Image resolution is 2.19 cm.

3.4 Camera Control and Calibration Procedures

3.4.1 Introduction

In this section, we outline the protocols we developed and implemented for control and calibration of the cameras used in the high-resolution aerial imaging experimental trials we conducted during this study, as per the description of task 4 in the contract. The manned aircraft section was prepared by Boulder Imaging, who developed and implemented the camera control and calibration systems described below during the aerial imaging flight experiments conducted using manned aircraft from 10 to 20 May 2011 offshore of Oak Island NC (see section 2.2 for complete description of manned aircraft system experiments). The UAS section was prepared by IATech, Inc., who developed and implemented the camera control and calibration systems described below during the aerial imaging flight experiments conducted using UAS from September 2011 through February 2012 (see section 2.3 for complete description of UAS-based experiments).

3.4.2 Manned Aircraft System

Control System Overview

The following basic components made up the camera control system:

- Camera remote control for exposure, gain, and offset settings
- Integrated GPS input correlated with image data
- Ability to dynamically control exposure time, with automated adjustment
- Ability to dynamically control camera gain, with automated adjustment
- Synchronized and time-correlated data acquisition from all cameras
- Recording of aircraft altitude
- Recording of aircraft flight speed
- Laptop to log into data recorder

Control System Software

The following software/operating system was required for control system operation:

- Windows 7 Professional running on the recorder
- Boulder Imaging Software suite running on the recorder (Input Configuration Tool, Quazar)

Control System Interconnects

The following interconnects were required for the control system:

- Connection from aircraft GPS system to recorder
- Connections from each camera to the data recorder
- Ethernet connection from recorder in aircraft to laptop in aircraft
- Power connection from aircraft to power inverter
- 110V power connection from power inverter to UPS battery

Control System Diagram

A diagram of the manned aircraft imaging control system is presented in Figure 3–36.

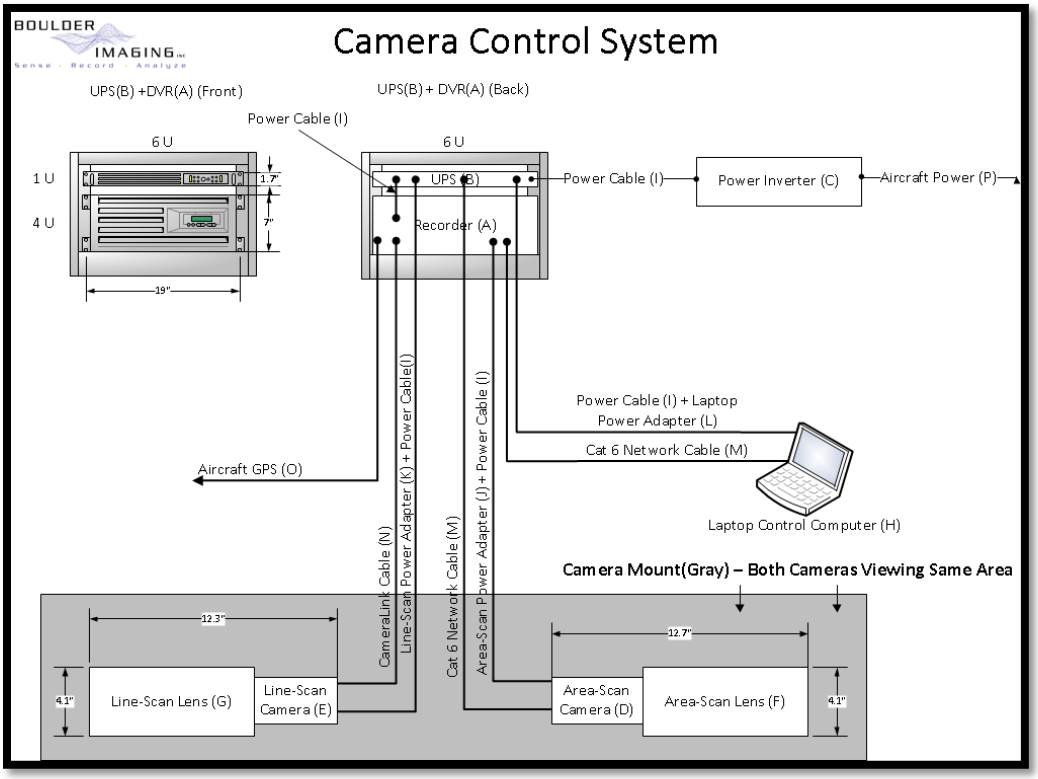

Figure 3–36. Diagram of the Boulder Imaging control system used in the manned aircraft system.

Control System Test Matrix

The testing procedures for the manned aircraft imaging control system are presented in Table 3–9.

Table 3–9.

Control System Matrix.

Equipment	Function	Test
UPS Battery	Powered, proper function	Verify UPS indicator light is Green. Use on-board diagnostics to verify input voltage/battery level
Control System	Operational	Power on system, verify Windows boots without error
Control System	Storage	When recorder starts, verify that automatic storage performance test succeeds

Equipment	Function	Test
Camera	Operational	Verify lights on all cameras indicate cameras are in operational state
Camera	Communication	Start the Input Configuration Tool, Detect Cameras, verify that all cameras are detected
Camera	Video	Configure inputs using the Test version of all camera inputs; start Quazar and perform live acquisition (green button). Verify that video is present on all inputs.
GPS	Signal present/locked	Start Quazar, start the GPS-lock tool, verify visually that the gps signal is locked and present.
Interface	Operational	The above tests will verify that the display/operator interface are functioning properly

Software Error Messages/Correction

The Boulder Imaging Quazar user's guide documents possible software error messages and courses of correction.

Checklist for Operational/Readiness Checks

- Adjust camera mount for proper angle, verify screw tightness
- Check that camera mount assembly is secure
- Check camera(s) securely mounted to plate(s)
- Check lens focus is at proper marking and secure
- Check lens focal length is at proper marking and secure
- Attach/detach polarizer
- Check that polarizer is secure (if installed)
- Check that polarizer is set to proper angle (if installed)
- Check that camera(s) are properly cabled, both power and data
- Check that recorder/cameras are properly plugged into UPS
- Verify that data drives are inserted into the recorder
- Five minutes prior to flight, turn on UPS on while on the ground, verify operational beep code
- Verify camera(s) have powered on before flight
- Verify laptop power supply is plugged into UPS
- Plug in laptop, verify laptop power through LED
- Verify network connection from laptop to recorder

Install/Pretest Control System

During the week of 2 May 2011, control system integration was performed in Sanford NC. The control system was integrated on the aircraft, and all control pathways were verified to be 100% functional. Test flights were performed over approximately 1 week, to continue to exercise the control system, with no malfunctions noted.

Implement Control System during Survey Experiments

Mission completed successfully; data was collected for 10 days with all desired combinations of treatment factors (see section 2.2). Operational readiness checklist was successfully observed on all flights. Camera control system operated as designed over the full course of the experiment.

Control System Performance during Experimentation

As noted above, the control system performed as designed during experimentation, with several deficiencies/areas for improvement noted, as follows:

Recording Naming/Organization

Prior to experimentation, a strategy for naming and separating recordings was not defined. This proved problematic for analyzing data after the experiment. At times, different test runs were combined into the same recording. The names of recordings were often not consistent between days. As two different operators performed experiments in the plane, there were differences between how the two operators named/organized recordings. These problems were able to be resolved with no loss of data using time stamps. However, for future experiments/surveys, a naming convention should be clearly defined before any flight occurs. The onboard operator should adhere strictly to the convention. Future experiments/surveys should also clearly define recording boundaries (where one recording ends and another begins).

Recording Metadata

Each recording that was performed had a set of metadata associated with it. For experimental trials, this included items such as altitude, camera angle, polarizer, focal length, gain settings, etc. Prior to trials, a consistent way to store this metadata along with each recording was not defined. All metadata was able to be properly assigned to each recording with no loss of data. However, for future experiments/surveys, a clear convention for storing metadata for each recording should be defined. Exactly what metadata needs to be gathered/stored should also be defined.

Another problem encountered was that not all teams were acquiring GPS time stamps in the same time zone. Before any future experiment/survey, a single time zone should be chosen and used throughout the experiment.

In-aircraft Hardware Access

During testing, it was discovered that while performing flights, the operator in the aircraft needs to have easy access to the following components of the system:

- Power button to the recorder
- LED lights on the recorder must be visible
- Power/reset button on UPS
- LED panel on the UPS must be visible
- It is helpful if the operator has access to the cables on the rear of the recorder, but not necessary.

Hardware Access—Portability

During experimental testing, all of the hardware in the plane needed to be removed at least once. This included the recorder, UPS, and cameras. For future designs, the ability to remove equipment during a survey should be an important factor. In order to deal with unexpected circumstances, sometimes hardware needs to be modified, tested, rebuilt, etc.

Degree of Imaging Automation

During experimentation, the on-aircraft operator was responsible for many tasks. This was largely due to the experimental nature of the testing. The experiment did show that many of the tasks could be automated for future surveys, but only a low level of automation was achieved during testing.

Imaging Speed Control

Almost all of the experiments were conducted with the area-scan camera, running at maximum frame rate of 3 frames per second. This was not adjusted during the experiment. Approximately 2 days of testing were performed with the line-scan camera; the line rate was manually adjusted from the recorder during flight to match the flight speed.

Camera Calibration System

Camera Calibration System Overview

To achieve high quality imagery at all experimental resolutions/altitudes, the camera system needed to be calibrated for each combination. This calibration occurred each time a change was made in test parameters, and was re-checked periodically to ensure the system remained in calibration.

Camera Calibration Metrics

The following were camera calibration metrics used:

Metric	Description
Vertical pixel size	Vertical resolution of each pixel (cm).
Horizontal pixel size	Horizontal resolution of each pixel (cm).
Focus	The focal point of the lens.
Line-scan rate	Only applicable for line-scan camera(s). The frequency that lines were scanned.

Camera Calibration Procedure

Camera calibration was performed using multiple flight paths over premeasured ground-based targets. The procedure was as follows:

1) Premeasure (or record) on-ground features to be imaged. During experimentation, these targets were resolution charts (during pretest), and on-ground features during test.
2) Perform all pre-flight/in-flight checklists.
3) Perform an initial pass over the ground target(s) to verify system operation, including proper line-scan rate for line-scan camera(s). Perform test recording to persistent storage.
4) Reach target altitude, and make one successful pass over the resolution target.
5) While in the air, analyze recorded video from the pass, checking/calculating the following:
    a. Proper focus—calibration target(s) should be the sharpest object(s) in the image,
    b. Horizontal resolution—using premeasured distance of calibration targets, calculate the horizontal pixel size in the recorded imagery (cm), and
    c. Vertical resolution—using premeasured distance of calibration targets, calculate the vertical pixel size in the recorded imagery (cm).
6) Record all data from the first flight analysis.
7) If system is not properly calibrated, land plane, calculate adjustments to lens parameters necessary to achieve calibration, adjust optics, and recalibrate.
8) Record final calibrations.

Install/Pretest Camera Calibration System

During the week of 2 May 2011, a camera calibration system test was performed in Sanford NC. Initially, calibration was performed on the ground with the cameras on tripods. Resolution targets were set up at distances away from the camera system to represent experimental altitudes (i.e., 600 m, 1,000 m, 1,200 m). All optical setups were calibrated using the on-ground targets and marked with proper focal length/focus point for all experimental combinations.

After all equipment was calibrated, on-ground, flight-based calibration procedures were executed. Flights were performed at all altitude/resolution combinations. During each flight, horizontal/vertical pixel resolutions were checked, as well as focus. If any incorrect measurements were noted, the aircraft landed, adjustments were made, and another test flight was initiated. At the end of the integration phase before experimentation, calibration settings were complete and recorded for all experimental treatment combinations.

Implement Camera Calibration System during Experimentation

During the experimentation phase, the optical calibrations made during the pretest phase were initially used. Test flights were performed during the first day of experimentation, checking the calibration using the procedures detailed above. Small adjustments were made to the optical calibrations, and the new calibration points were marked (focal point/focal length).

Each time a new experimental combination was run, the optics were adjusted to their pre-calibrated positions. During the initial portion of the flight, altitude was reached and system calibration was checked. After day 1, the aircraft never had to return to the ground to adjust calibration. All pre-marked calibration points were correct throughout the rest of the experiment.

Calibration System Performance

The calibration system performed as designed during pretest and experimentation, but several deficiencies and areas for improvement were noted, as follows:

On-Ground Calibration

Calibration procedures were initially performed on-ground for easy of calibration. This procedure proved problematic because water vapor distorts imagery at large distances (all the distances we were working with). It was very hard to verify correct focus as imagery was showing significant anomalies due to water vapor in the path from the camera to the image target. The problems associated with water vapor were not observed when imaging from the aircraft as the water vapor evaporated enough to not cause significant problems when looking down through the vapor column.

Depth of Field

During experimentation, the lenses were tested with apertures ranging from f/2.8 to f/5.6. There was significant concern that depth-of-field would be too low when running at f/2.8. During experimentation, we found that the depth-of-field was sufficiently large at all aperture settings. When running any experimental combination, a depth of field at least 150 m above the ocean surface and 50 m below the ocean surface was easily achievable. At no point during any of the experimentation were animals imaged that were out of focus.

Future experiments/surveys should only take special consideration regarding depth-of-field if the altitude of the flight is well below 600 m, which was not addressed during the experiment

3.4.3 Unmanned Aircraft System

Camera calibration was performed with the camera and the candidate 200 mm lens. The purpose of performing camera calibration is to determine the intrinsic and extrinsic properties of the camera lens. This calibration procedure provides specific properties that are unique to the optics.

We collected a series of 30 images using our 13 × 13 black-and-white checkerboard grid. This particular calibration code requires the use of the checkerboard to perform the computations. Below are the series of images that we used to perform calibration (Figure 3–37). Pictures of the checkerboard were taken at a variety of distances and angles relative to the camera.

Figure 3–37. Calibration images collected with camera payload for unmanned aircraft system-based imaging system.

Once we obtained the image data set, the next step involved extracting the grid corners on each image shown in Figure 3–38. The user manually clicks the corners of the grid (boundary) in a clockwise fashion and the number of squares in the grid is calculated. In addition, the user provides the size of each grid square, which is 30 mm × 30 mm (dX, dY). The corner extraction algorithm proceeds by then extracting every corner in the image as shown in the example below (Figure 3–38). The origin is in the upper left hand corner. This is performed for each image in the data set.

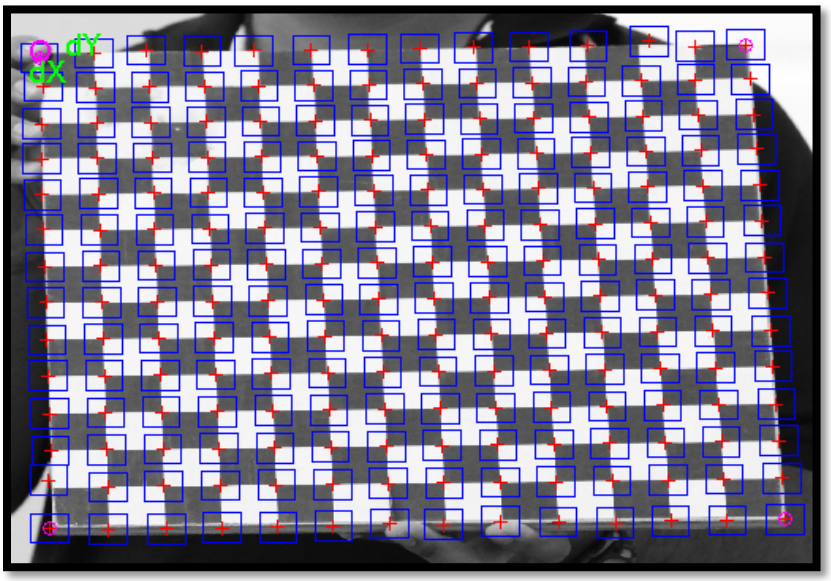

Figure 3–38. Grid corner extraction performed by the camera calibration code for the unmanned aircraft system-based system.

Once the corner extraction procedure has been performed on the entire data set, the extrinsic parameters of the camera are determined. The extrinsic parameters are the relative position of the grids relative to the camera. The three-dimensional plot below in Figure 3–39 illustrates this.

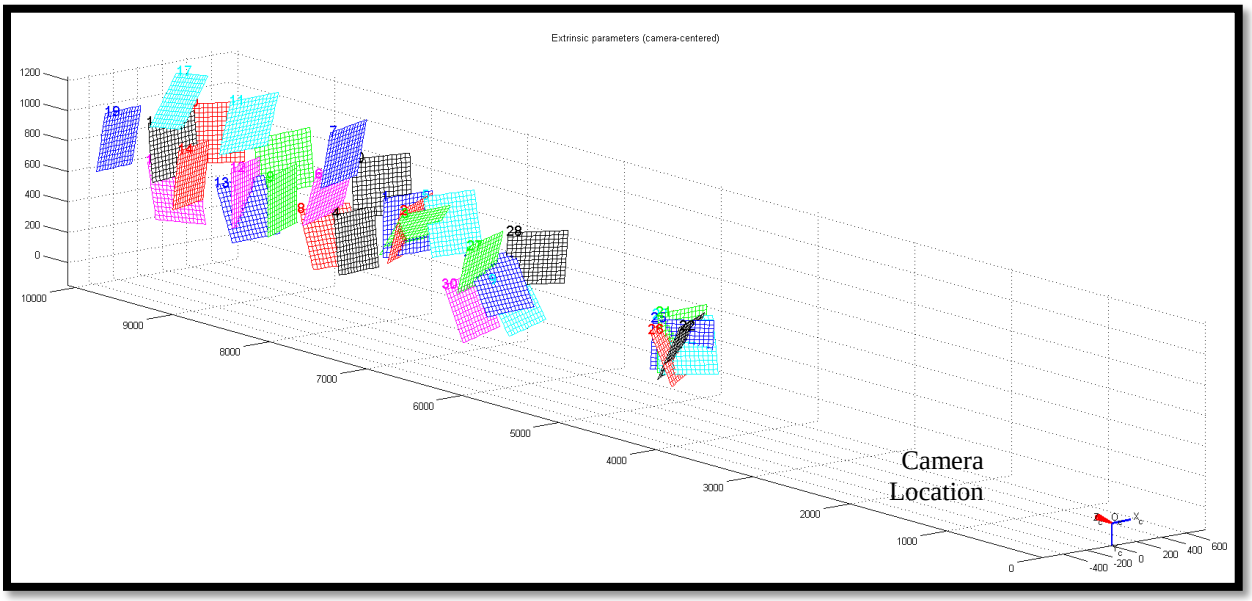

Figure 3–39. A three-dimensional plot of the position of the grids relative to the camera location.

The focal length, principal point, skew, distortion, and image size are calculated as a result of this calibration procedure and is summarized in Table 3–10.

Table 3–10.

Intrinsic Camera Parameters as Calculated through the Camera Calibration Code for the Unmanned Aircraft System-based Imaging System.

Parameter	Calibration Code
Focal length (mm):	fc = [28237.865376327696000 ; 29006.989983521682000]
Principal point (pixels):	cc = [2594.608445753900500 ; 4149.304955046088300]
Skew coefficient:	alpha_c = 0.000000000000000
Distortion coefficients:	kc = [1.559331885057325;-27.053611229686489; 0.128779415949645; 0.005715087739262;0.000000000000000]
Focal length uncertainty:	fc_error = [702.619910994141260 ; 747.007853927368610]
Principal point uncertainty:	cc_error = [0.000000000000000 ; 0.000000000000000]
Skew coefficient uncertainty:	alpha_c_error = 0.000000000000000
Distortion coefficients uncertainty:	kc_error = [0.310320597797559;6.941278717644920;0.015346852046463; 0.004095980535962;0.000000000000000]
Image size (pixels):	nx = 5616 ny = 3744

Another useful part of this analysis is the effect of lens distortion on the pixel image. A preliminary distortion model as well as the radial component and tangential component of distortion is shown in Figure 3–40 through Figure 3–43. Each arrow represents the effective displacement of a pixel induced by the lens distortion. This is important, as the angle of the camera varied from 0 to 45° degrees during imaging tests.

Geometrical distortion pertains to the position of the points in an image plane. In general, geometrical distortion is caused by imperfections in a camera's lens or lens assembly (Weng et al. 1992). We can apply corrections for this type of distortion by modeling these effects. Complete, radial, and tangential distortions are modeled in this analysis.

Radial and tangential distortion can cause inward or outward displacement of an image point from where it should be (Heikkila and Silven 1997). This type of distortion is symmetric about the optical center. A basic diagram depicting the effect distortion has on an image point is shown in Figure 3–40, with tangential and radial distortion components described in Figure 3–42 and Figure 3–43, respectively.

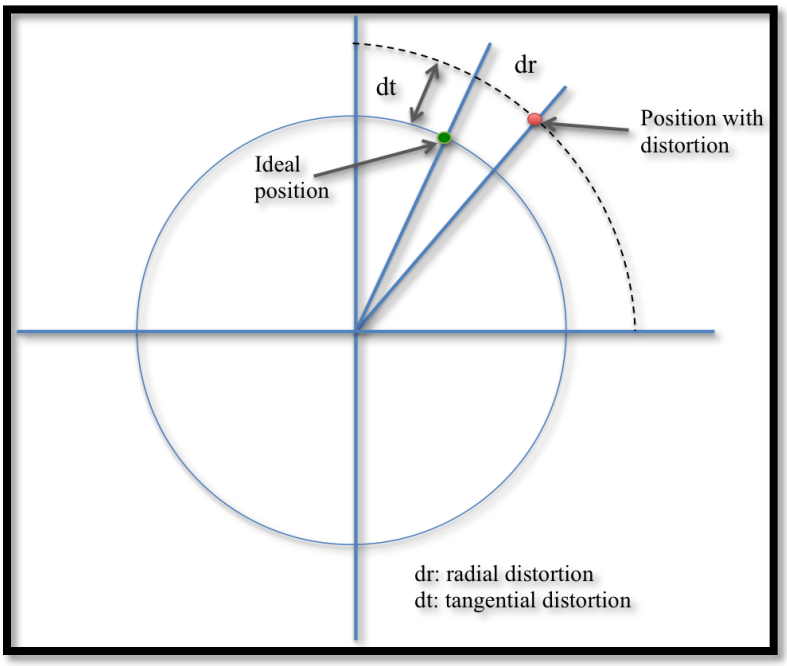

Figure 3–40. Graphic depicting how radial and tangential distortion can affect the position of a point in an image.

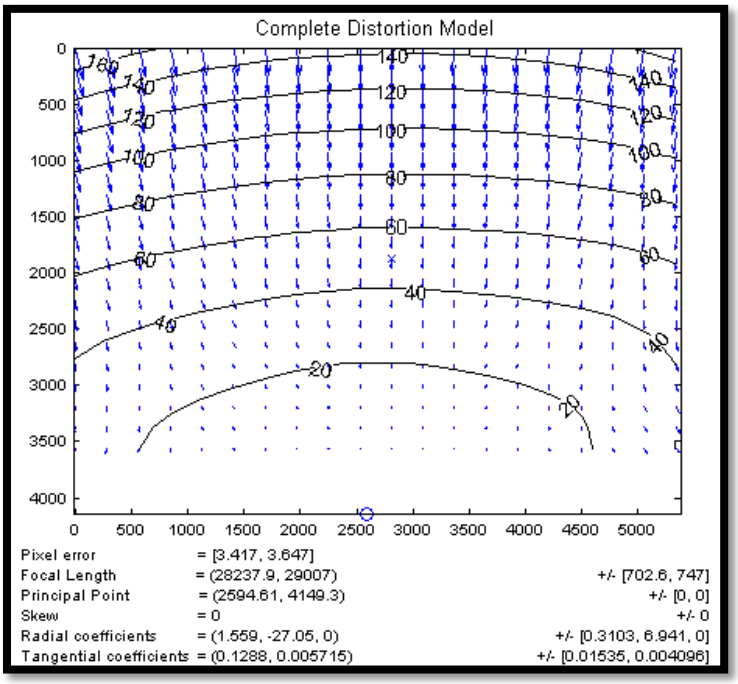

Figure 3–41. Complete distortion model (radial + tangential).

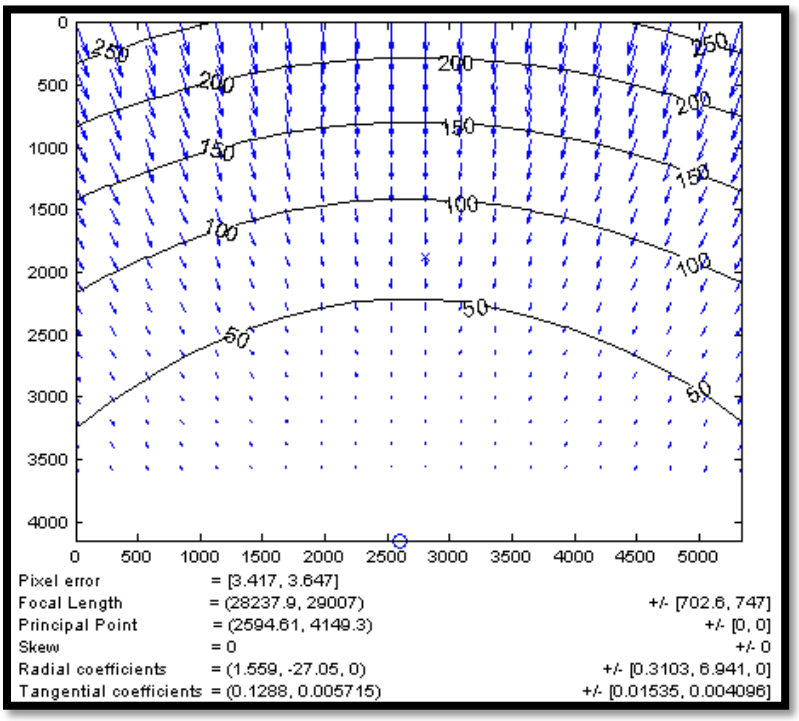

Figure 3–42. Tangential component of the distortion model.

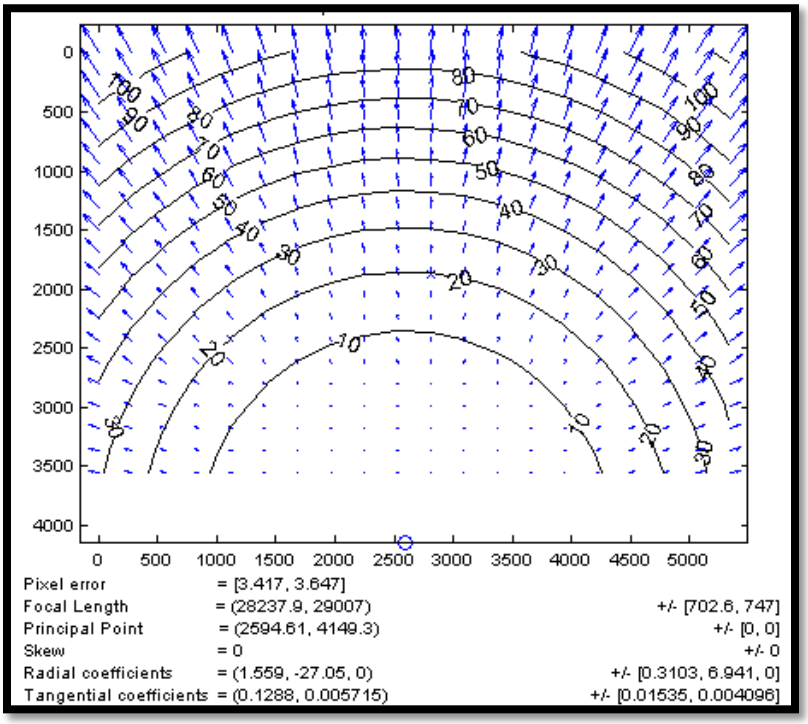

Figure 3–43. Radial component of the distortion model.

3.5 Evaluation of Onboard Data Recording Systems

3.5.1 Introduction

In this section, we describe the on-board data recording systems we developed and used during the high-resolution aerial imaging experimental trials we conducted during this study, as per the description of task 5 in the contract. The manned aircraft section was prepared by Boulder Imaging, who developed and implemented the data recording systems described below during the aerial imaging flight experiments conducted using manned aircraft from 10 to 20 May 2011 offshore of Oak Island NC (see section 2.2) for a complete description of manned aircraft system experiments). The UAS section was prepared by IATech, Inc., who developed and implemented the data recording systems described below during the aerial imaging flight experiments conducted using UAS from September 2011 through February 2012 (see section 2.3 for a complete description of UAS-based experiments).

3.5.2 Manned Aircraft System

Selection Method

To select a data recording system, the first phase was to review literature and technical specifications of data recording systems with applicability to aerial surveys. After a thorough evaluation, a data recording system was selected.

Recording System Requirements

The key features and capabilities assessed and compared include:

Support for High-resolution Imaging: The system had to be engineered to natively interface to and record data from a wide range of high-resolution cameras, including non-broadcast formats (> 16 megapixel (MP) cameras).

Support for Line-Scan Cameras: The system had to be able record and control line-scan cameras simultaneously with area-scan cameras, with potentially very large frame sizes.

Recording from Multiple Inputs: To enable multi-camera imaging, either for large transect widths or multi-spectral imaging, the system had to be able to record from multiple, possibly dissimilar, camera sources. The system had to have native support for Bayer-color, panchromatic, and infrared sensors types. It had to be able to seamlessly interpret image data with 12 bits or more per pixel per color. All inputs also had to be recorded in such a way that they could be precisely time-correlated during playback, for frame-by-frame data review.

Guaranteed Loss-less Data Recording: The system had to be able to record all inputs without any data loss, and completely free of any compression artifacts. This was critical for detailed analysis and for the processing algorithms (automated animal detection).

GPS Input: The system had to be able to record GPS position information with every image frame.

Long Recording Duration at High Rates: The system had to be able to record continuously for a full flight, which for some aircraft could be many hours, at data rates from 120 to possibly more than 600 megabytes per second, depending on the transect widths desired.

Fast Data Transfers: Upon landing, the system needed to support quick transfer of recorded data into other systems.

Resistant to Aircraft Vibrations and Shock: The system had to be sufficiently rugged to tolerate repeated flights and landings without the risk of data loss.

Size, Weight, and Power Considerations: The system had to be able to scale to support recording from multiple cameras within a limited size envelope, reasonable power needs, and reasonable total weight.

Selection of Recording System

After evaluating the data gathered on available recorder systems, Boulder Imaging's Quazar HPDVRs possessed the most complete set of features, allowing the most flexibility and recording power for this application, all at a cost-effective and competitive price (especially as multiple inputs were needed). Therefore, we selected the Quazar VR400R model, as it provided all of the necessary camera and data input interfaces required for this project.

All other recorders evaluated were either constrained to support a single type of camera, or were significantly limited when scaling to a large number of cameras.

Checklist for Recording System Integration and Operation aboard Aircraft

- ☐ Mount UPS battery system
- ☐ Mount power inverter
- ☐ Provide 110V AC to UPS battery system
- ☐ Verify UPS powered/functional
- ☐ Mount control system
- ☐ Provide power cabling from UPS to control system
- ☐ Connect display/control interfaces to control system (laptop/display/keyboard/mouse)
- ☐ Test control system is operational
- ☐ Mount camera(s)
- ☐ Attach camera lens(s)
- ☐ Provide power cabling to cameras from UPS
- ☐ Power cameras, test power through LED
- ☐ Connect camera(s) to control system
- ☐ Connect GPS signal to control system
- ☐ Perform pre-flight checklist

Checklist for Pre-flight Recording System Power-Up, Connectivity, Control Checkout, Readiness, and Operation

- ☐ Ensure 110V power to UPS battery backup. Verify power input using light indicators on UPS and on-device diagnostics.
- ☐ Connect all cameras to the control system using either CameraLink or Cat-6 GigE cables.
- ☐ Power on all cameras. Verify power to each camera using on-camera LED.
- ☐ Connect GPS feed into control system.

- Connect display system to control system.
  - If using laptop, connect laptop GigE cable directly to recorder.
- Connect control interface to control system
  - If using laptop, ensure GigE connection to recorder.
- Power on control system.
- Verify system boots into Windows.
  - If using monitor, visually verify boot process.
  - If using laptop, wait ~2 minutes, then attempt to remote desktop into the control system to verify Windows boot.
- Verify persistent storage functionality.
  - After machine boots, a tool will automatically run that will verify the presence/performance of the storage subsystem. Verify that the automatic test has passed.
- Verify communication with cameras
  - With all cameras powered and connected to the control system, start the Input Configuration tool located on the desktop. Wait for the tool to perform automatic camera detection. When the tool opens, navigate to the Detected Cameras tab, and verify that all cameras are present.
- Verify configuration of inputs
  - With the Input Configuration tool open, navigate to the Inputs tab. Verify that all cameras are listed as inputs to the system, in chronological order.
- Start the Quazar recording application from the desktop.
- Ensure the application starts with no errors, and that all cameras are listed as inputs.
- Verify presence of GPS signal. From the Tools menu in Quazar, select GPS Lock. Verify that a GPS signal is locked.
- System is now ready for recording procedures.

Checklist to Fully Test DVR Functions while Powered on Ground

- Perform pre-flight checklist below
- Perform five 1-minute recording sessions from all cameras to persistent storage. Analyze/verify each recording session.

Install/Test Data Recorder

During the week of 2 May 2011, data recorder integration was performed in Sanford NC. During this integration phase, the data recorder was installed into the aircraft and all necessary aircraft integration was performed. Test flights were conducted over a 1-week period. The data recorder system performed as designed, with the following exceptions:

Mounting Technique

The recorder was not mounted directly to the aircraft, or placed into a rack assembly. The recorder and the rack mount battery backup were secured into the rear of the aircraft using straps.

Vibration Problems

During pretest/system integration, significant problems were observed with respect to vibration on-board the aircraft. Initially, the storage subsystem performed at an acceptable level, but began

showing degradation after a few days of test flights. The drive subsystem began showing low performance levels while in the air, while performance levels remained high on the ground. It was determined that on-aircraft vibration was causing the traditional hard drives to enter an unacceptably low performance level. At that point, the traditional storage subsystem was replaced with a system comprised exclusively of SSD hard drives. The operating system drive was also replaced with an SSD drive. The system performed as designed after this change was implemented.

While SSD hard drives represent a significant increase in cost, their use is essential for aircraft-based data recording, where vibration is expected.

Implement Data Recorder during Survey Experiments

During experimental trials, the data recorder performed as designed. No malfunctions were noted. Approximately 9TB of data was recorded during experimental trials (see section 2.2).

Data Offload

On-board recorder storage was reduced to ~2TB after moving from traditional hard drives to SSD drives. Because of this, recording data was offloaded nightly during the experimentation period to a persistent storage array. This was facilitated through the use of removable hard drives and compatible disk-storage hardware.

Vibration Problems

After three days of experimental trials, the recorder was removed from the aircraft for inspection. After a thorough inspection, multiple components were found to have become loose as a result of vibration. The recorder was completely repaired, and vibration dampening material was added to the aircraft to reduce recorder system vibration. Again, it was shown that vibration is a critical concern for data recording system(s) onboard aircraft.

3.5.3 Unmanned Aircraft System

During the UAS-based high-resolution imaging flight experiments, the camera was interfaced to a single board computer through a USB 2.0 connection (Figure 3–44). A custom program was written to send commands to the camera that would essentially actuate the shutter at specified time intervals. During our experiments (see section 2.3) we found that the speed of the USB 2.0 connection was sufficient in capturing image data sets with sufficient overlap from image to image. The data recording system was powered by a series of lithium polymer batteries with a voltage regulator to condition the power going to the computer and hard drive.

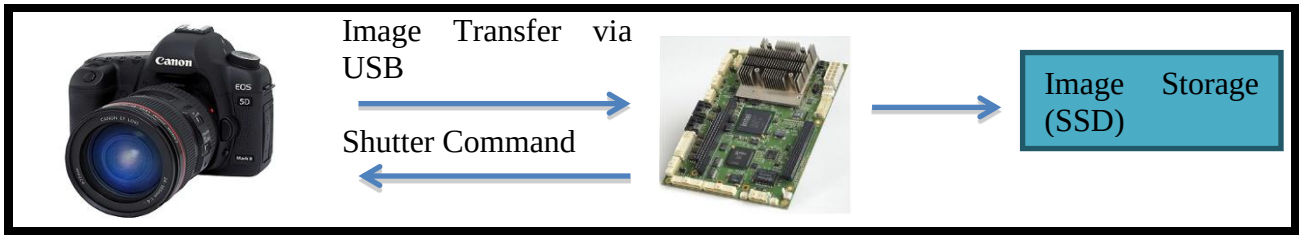

Figure 3–44. A diagram of the imaging system used onboard the unmanned aircraft, showing data transfer process and data recording system.

4 Protocols for Conducting High-resolution Wildlife Imaging Surveys in Support of Offshore Wind Development on the Atlantic Outer Continental Shelf

4.1 Introduction

In this section, we provide protocols for conducting digital aerial high-resolution wildlife imaging surveys covering the AOCS for the purpose of providing the necessary ecological data to support a commercial offshore wind leasing program. These protocols were developed in accordance with the specifications for such protocols described in task 6 of the contract.

Our presentation of recommended protocols is prefaced with discussions of two topics that are central to the selection and development of offshore high-resolution aerial wildlife imaging survey protocols. In subsection 4.2, we discuss the impact of sun glare on imaging surveys, and the importance of taking sun and camera angles into account when designing survey protocols. In this section, we present an empirical analysis of "how much glare is too much?" based on our experience with manual and automated detection of animals from the imagery gathered during our offshore high-resolution imaging experimental trials under a complete spectrum of glare conditions. This analysis resulted in the empirical characterization of a glare threshold. We also analyzed when this threshold is exceeded as a function of the camera angle's relationship to the sun angle, and present a tool, in the form of a simple geometric equation, that can be used to plan survey transect patterns to avoid crossing the glare threshold by implementing simple and pragmatic camera angle adjustments depending on the time of day, year, and geoposition of surveys.

In subsection 4.3, we present a discussion of selected statistical and sampling design considerations in high-resolution offshore wildlife imaging survey methods, largely derived from European lessons learned with such surveys. This subsection is contributed by BTO's Chris Thaxter, who reviewed high-resolution offshore wildlife imaging survey methods in 2009 in the wake of a workshop held by COWRIE to explore this methodological frontier, and who continues to review and to provide quality assurance and quality control services for the application of this methodology to offshore wind environmental studies in the UK.

4.2 Mitigating Glare in Imaging Surveys

4.2.1 Introduction

When sunlight hits the surface of the water, a portion of the light penetrates the water, and a portion is reflected into the atmosphere from the water's surface. When viewed from an airplane, the light reflected from the water surface is referred to as sun glint (Image Science and Analysis Laboratory, NASA-Johnson Space Center 2012). Sun glint can ruin digital aerial imaging survey data by producing glared-out images in which animals that are present at or near the water's surface, and that would normally be visible in aerial images, cannot be detected in the images because all, or most of the image consists of glare produced by the sun glint. This can cause tremendous loss of information in aerial photographic surveys over the ocean (Doerffer et al. 2008, Kay et al. 2009). Imagery lost to glare represents a considerable cost both financially and scientifically (Kay el al. 2009).

Unfortunately, this problem is particularly acute under conditions at which aerial surveys for high-definition imaging might otherwise produce excellent images—clear skies and shallow water (Hedley et al. 2005). The intensity and directionality of reflected sunlight are such that polarized light filters are not an effective solution (see section 3.3). There are techniques suggested for the removal of sun glare in the images (Hochberg et al. 2003; Hedley et al. 2005). However, those techniques were suitable for high-definition images of large spatial scale where study objects are large natural structures like coral reefs and require correction on each image separately. This is not feasible in the scale where hundreds of thousands of images are collected and study objects are individual birds, marine mammals, and turtles. Under such circumstances the best approach is to avoid taking images of the surface of water with excessive sun glint.

Regarding the applicability of European experience to the US, it is important to note that sun glare is a more significant problem at lower latitudes than at higher latitudes because of the more direct angles of insolation. For this reason, sun glare is a more significant challenge in much of the US AOCS than it is in northwestern Europe, where, to date, high-resolution imaging surveying has been most extensively applied for offshore wildlife surveys at relatively high latitudes with low sun angles. The success of applying aerial digital imaging for marine wildlife surveys in the US hinges on developing cost-effective techniques to minimize glare and capture the best images on which all the animals that are present can be detected and identified correctly.

In this chapter, we present a set of tools that can be used to design aerial imaging survey protocols that maximize cost effectiveness by minimizing data losses due to glare. The solution is based on an analysis of the results of the high-resolution imaging experiments performed off the coast of Oak Island NC during May 2011 (see Chapter 1). In this analysis, we address the following questions:

1) How much image glare is too much for animal detection? The answer to this question defines the glare threshold for gathering useful images of marine wildlife.
2) Which camera/sun angles result in images with glare levels above the glare threshold?
3) What are the potential extent and impact of glare losses on the US AOCS, given the seasonal and latitudinal pattern of insolation in this region for a range of potential camera angles and transect patterns?
4) How can glare levels be predicted and excessive glare levels avoided by survey planners using available data on insolation angle, time, and geoposition?

4.2.2 Empirical Basis of Analysis

The raw material for our analysis of glare impacts came entirely from imagery gathered during our high-resolution aerial imaging survey experiments, carried out during the second and third weeks of May 2011 off the coast of Oak Island NC (see Chapter 1). Our analysis of glare impacts and mitigation solutions is based on our review of all of the imagery gathered during the 48 different aerial transect survey segments conducted during this experimentation, which included manual review of more than 200,000 images, most of which were contained within the transect segments (see Chapter 0 for image review description). For the glare analysis, we only used the transect segments because flight directions and camera angles were much more highly controlled on such segments, allowing precise determination of glare impacts and animal detection success as a function of camera and sun angles.

4.2.3 Glare Threshold Characterization

An automated process was used to score all images on a glare scale from 0 (lowest glare) to 10 (highest glare) as a function of the level of overexposure of the image. The scale we used was nonlinear, and was developed based on manual inspection of selected images, and analysis of the extent green pixel exposure in images covering a spectrum of user-defined glare levels. The aerial images we captured with the camera were RGB Bayer color, which means they are a pattern of red, green, and blue pixels. Only green pixels were used to calculate glare because green gives the best representation of the overall sensor response. Approximately half of the pixels in the images were green. The glare scale we used is presented in Table 4–1.

Table 4–1.

Glare Scale Used in the Analysis of Sun Glare Impacts on Successful Animal Detection in High-resolution Aerial Imagery

% Green Pixels above Threshold	Glare Level
< 0.01	0
0.01–0.02	1
0.02–0.03	2
0.03–0.05	3
0.05–1.00	4
1.00–2.00	5
2.00–3.00	6
3.00–4.00	7
4.00–5.00	8
5.00–6.00	9
> 6.00	10

Note: The threshold referred to in the first column is an arbitrarily defined level of high glare for a given pixel as a function of the pixel's green exposure level, and is not equivalent to the glare threshold discussed later, which is defined by actual animal detection success.

Examples of images spanning a complete spectrum of glare levels are shown in Figure 4–1. Although the images in some of the intermediate glare levels do not appear to be glared out overall, it is important to note that glare can cause significant interference with successful animal detection even at relatively low glare levels (e.g., when hundreds of small white glare spots on wave tips can potentially be confused with similarly sized whitish animals, as is the case with the representative images at glare levels 3 through 7, in particular [Figure 4–1]). The same factors that cause difficulties in discerning animals from glare spots to the human eye are likely to present similar

problems for automated animal detection algorithms, because the glare spots will often have similar size, shape, background contrast, and spectral characteristics to light colored birds. It is also important to note that while much of the glare discussion in this chapter centers around glare as a function of sun and camera angles, glare is also exacerbated by waviness on the water's surface.

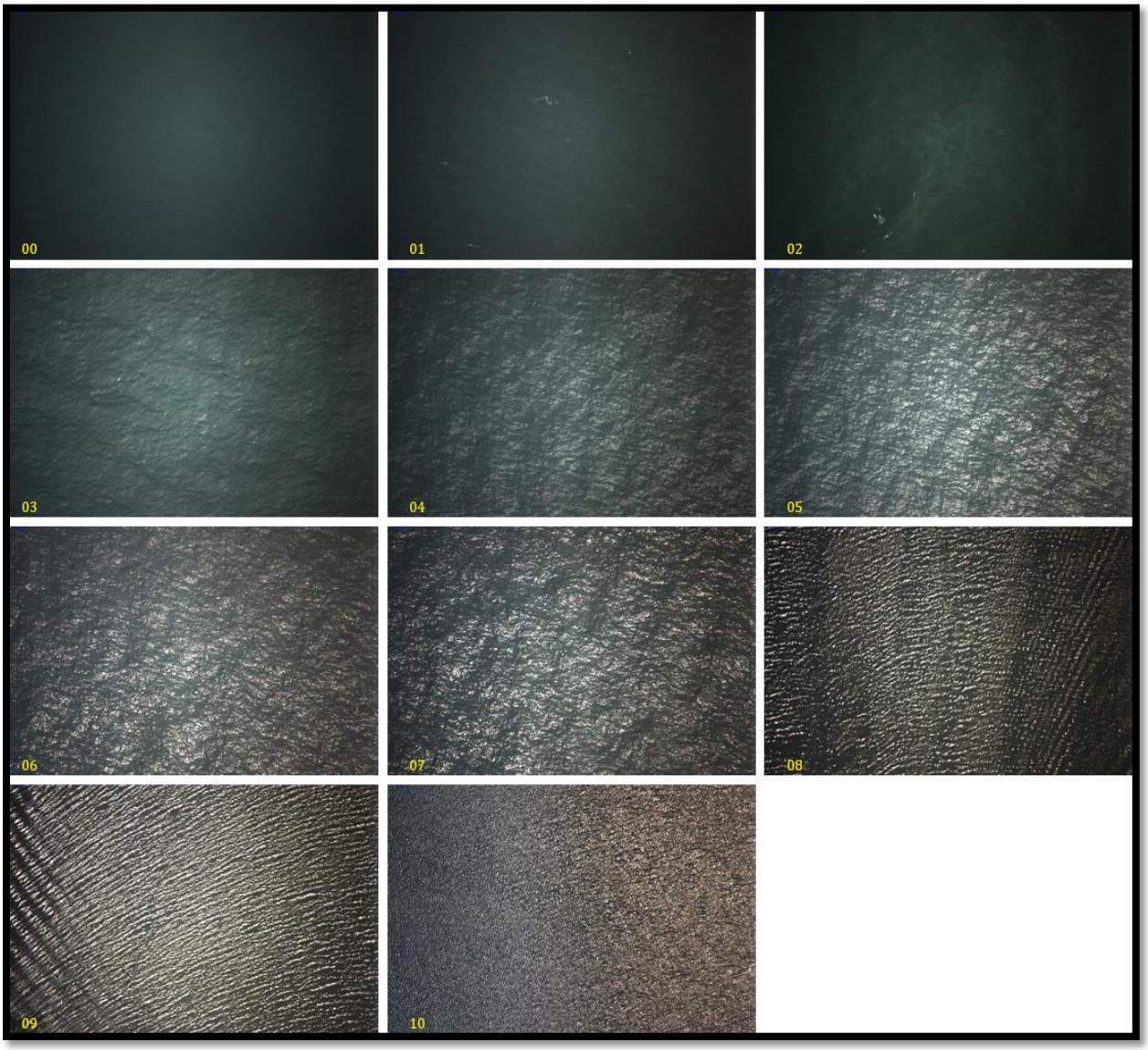

Figure 4–1. Images of the water's surface taken during experimental offshore aerial imaging transect survey segments conducted 10 to 20 May 2011 off of Oak Island NC illustrating a complete spectrum of glare levels from 0 through 10 (see text and Table 4–1). Glare levels are reported in the bottom left corner of each frame.

4.2.4 Impact of Glare Level on Animal Detection: Defining the Glare Threshold

The first step in understanding the impact of glare on survey methodology was to characterize animal detection success as a function of glare level in the image. To do this, we plotted the relationship between number of animals detected and glare levels of the images in which they were detected. This analysis was done using all 48 aerial survey transect segments, containing 180,718 total images. The distribution of image glare scores in this imagery is shown in Figure 4–2. Glare level 0 was the most abundant followed by glare level 4, with a fairly even distribution of rest of the glare levels (Figure 4–2). It is important to note that because the glare scale was nonlinear, the different glare scores do not represent even intervals of green pixel exposure levels (Table 4–1). This scale was developed to serve the purpose of defining the level of glare above which animal detection from the imagery is so degraded as to be of little value (or, the glare threshold), and so the scale is not intended to be linear, but to include increased sensitivity in the vicinity of the threshold.

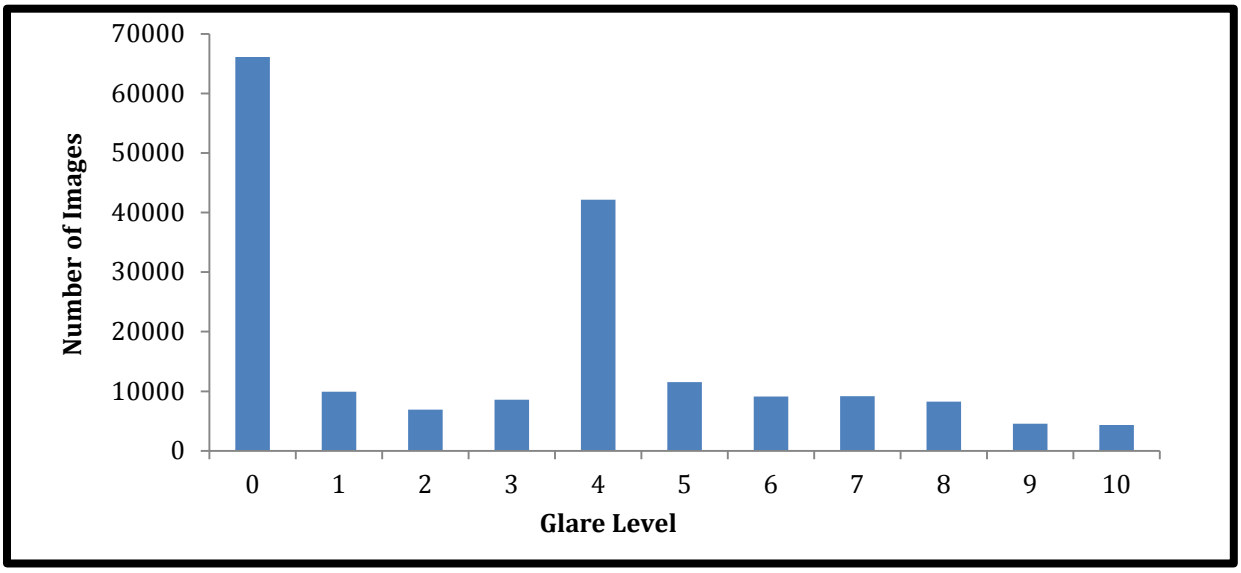

Figure 4–2. Distribution of glare level scores in 180,718 images recorded during experimental offshore aerial imaging transect survey segments conducted 10 to 20 May 2011 off of Oak Island NC. See text and Table 4–1 for glare score definitions.

To characterize the relationship between glare level and animal detection success, we used the results of our systematic manual review of all images for animal detection (see section 5.2) for complete image review procedure and description). Animals were discovered in a total of 6,312 of the 180,718 total images from transect segments reviewed. This included all birds, marine mammals, sea turtles, and large fish (e.g., rays, sharks).

The glare scores of these images are shown in Figure 4–3. This distribution is one illustration of the impact of glare level on the successful detection of animals in images, but it is important to keep in mind that the number of total number of images in each glare level was not equal (see Figure 4–2).

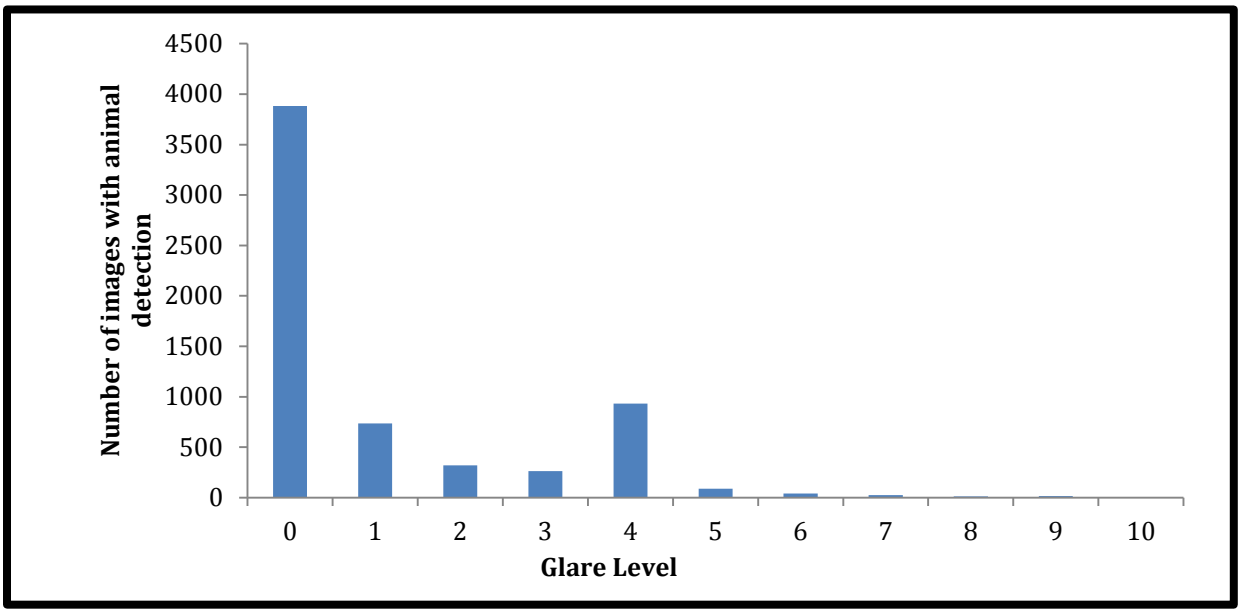

Figure 4–3. Distribution of frames in which animals were detected as a function of glare level, for 180,718 images recorded during experimental offshore aerial imaging transect survey segments conducted 10 to 20 May 2011 off of Oak Island NC, and subsequently manually reviewed for animals. See text and Table 4–1 for glare score definitions. See section 5.2 for description of manual review methodology.

To standardize animal detection success rates for the variation in sample sizes of images in different glare categories, we plotted the distribution of frames with successful animal detections per 1,000 frames reviewed for each glare level (Figure 4–4). This revealed the overall expected inverse relationship between animal detection rate and glare level. This relationship is also presented in Table 4–2, which further shows the percentage of frames containing animals that were successfully detected at each glare level, assuming that the maximum value, observed for glare level 1 (74 frames with animals per 1,000 frames reviewed) is the true value of animal occurrence for all glare scores.

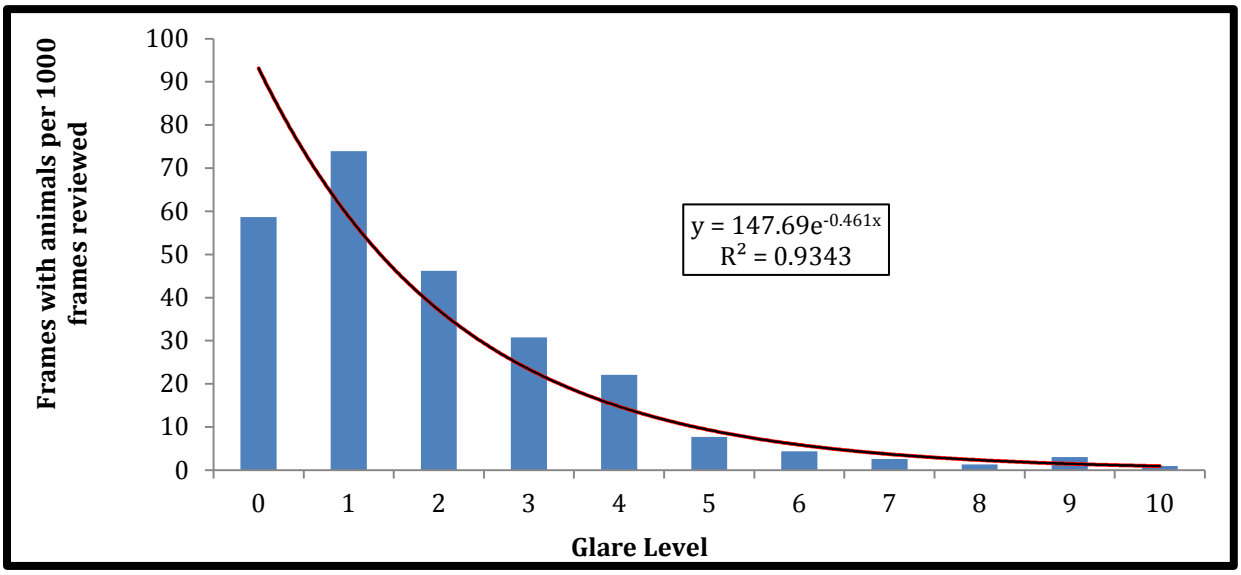

Figure 4–4. Distribution of animal detection rates (frames with animals detected per 1,000 frames reviewed) as a function of glare level, for 180,718 images recorded during experimental offshore aerial imaging transect survey segments conducted 10 to 20 May 2011 off of Oak Island NC and subsequently manually reviewed for animals. See text and Table 4–1 for glare score definitions. (See section 5.2 for description of manual review methodology.) The red line is an exponential regression line characterizing the observed inverse relationship between animal detection rate and glare level, whose equation and r^2 level are presented in the box above the line.

Table 4–2.

Animal Detection as a Function of Glare Level in the Image, Based on Manual Review of 180,718 Images Recorded during Experimental Offshore Aerial Imaging Transect Survey Segments Conducted 10 to 20 May 2011 off of Oak Island NC (See Text and Table 4–1 for Glare Score Definitions, See Section 5.2 for Description of Manual Review Methodology)

Glare Level	Number of Frames	Frames with Animal Detection	Detection per Frame	Detection per 1,000 frames	% Animals Detected[1]	Linearized Animal Detection Rate[2]
0	66,149	3,881	0.059	59	80	80
1	9,939	735	0.074	74	100	100
2	6,910	319	0.046	46	62	62

Glare Level	Number of Frames	Frames with Animal Detection	Detection per Frame	Detection per 1,000 frames	% Animals Detected[1]	Linearized Animal Detection Rate[2]
3	8,588	264	0.031	31	42	21
4	42,180	931	0.022	22	30	0.32
5	11,550	89	0.008	8	11	0.11
6	9,092	40	0.004	4	5.4	0.054
7	9,147	24	0.003	3	4.1	0.041
8	8,251	11	0.001	1	1.4	0.014
9	4,564	14	0.003	3	4.1	0.041
10	4,348	4	0.001	1	1.4	0.014
Overall	**180,718**	**6,312**				

[1] Assuming 74 frames out of every 1,000 actually contained animals
[2] Success in animal detection on linearized glare scale, calculated as % animals detected/ hundredths of green pixel percentage increment contained in glare level category (Table 4–1).

One curious element of this relationship between glare level and animal detection rate is the apparent increase in animal detection between glare levels 0 and 1. The most likely explanation for this portion of the relationship is that animal detection rate is somewhat depressed at the lowest glare levels because of insufficient light availability, which causes degraded image quality and increased image blur (see section 3.3 for complete discussion). Reduced light availability can be caused by overcast conditions or low sun angles. This is essentially the opposite of the glare problem, and is an important consideration for aerial imaging survey planning and design.

A key objective of this analysis was to empirically characterize the glare threshold, defined as the level of glare above which the decline in animal detection success is deemed to be unacceptable. Based on the relationship presented in Figure 4–4 and Table 4–2, we believe that glare levels up to, and including 2, are acceptable, but that glare levels in excess of 2 will produce such depressed animal detection rates that they should be regarded as unacceptable, hence the recommended glare threshold is 2. Thresholds, in general, are often ascribed when a function reaches an inflection point. Below the inflection point, a given increment in the x variable renders a relatively small incremental change in the y variable, while above the inflection point, the same increment in the x variable renders a relatively large change in the y variable. Such an inflection point and natural threshold value is not suggested by the negative exponential shape of the line shown in Figure 4–4, which, at first glance, suggests that incremental changes in animal detection rate are relatively small and smoothly distributed across glare level increments. However, the shape of this function as presented in Figure 4–4 is largely an artifact, as glare intervals are not evenly sized, as discussed above. Glare

levels from 0 to 3 contain very small ranges of green pixel exposure, while glare levels 4 and above contain much larger chunks of the range of green pixel exposure (Table 4–1). In essence, this means that we examined variations in glare much more finely in the lower part of the range (3 and below) than in the higher part of the range (4 and below), where variations in glare were assumed to be unimportant.

Linearizing the glare scale for green pixel exposure reveals that a strong threshold is present between glare scores of 2 and 3 (Table 4–1). Glare scores 2 and 3 each contain very small ranges of green pixel exposure value (Table 4–1), yet animal detection rate drops from 62% to 42% between these categories. By contrast, glare category 4 covers almost 30 times as large an interval of green pixel exposure as does category 3, and yet the drop off in animal detection rate from glare level 3 to glare level 4 is only an additional 12%.

Based on the evidence for a distinct threshold in animal detection success above glare levels of 2, we use 2 as a recommended glare threshold throughout the remainder of our protocol section. However, it is worth noting that some successful animal detections do still occur above this threshold. Under some circumstances, higher glare thresholds may be deemed cost effective, particularly if glare mitigation options are very difficult, or if the animals of interest are detected relatively easily.

4.2.5 Relationship between Camera/Sun Angles and Glare

Sun glare is the specular reflection of sunlight by suitably tilted facets of water surface into the camera; therefore, its intensity depends primarily on imaging geometry, specifically the relationship of the camera angle to the angle of the sun (Melsheimer and Kwoh 2001). Sea state also influences the pattern of sun glint reflection by producing variation in the angular orientation of surface water facets that reflect sun glint at different angles, as can be seen in the complex pattern of sun glint spots in the images in Figure 4–1. However, glare issues are most strongly influenced by the relationship of the camera angle to the sun angle (Kay et al. 2009). Hence, for the sake of simplicity, our analysis of glare impacts and glare mitigation in survey design only incorporates these angular considerations.

For any given geoposition, time of day, and time of year, there is a certain camera angle where the camera will be oriented directly at the reflection of the sun on the water's surface. We define this as the glint spot. In terms of aerial survey methodology, the glint spot is determined by four variables, as follows:

- Camera azimuth
- Camera elevation
- Solar azimuth
- Solar elevation

The camera azimuth is is the horizontal, or x–y orientation of the camera during flight. This corresponds to compass orientation and can range from 0° (true north) to 359° (one degree west of true north). The camera azimuth can be determined for any given aerial transect by combining the flight azimuth, or compass orientation of flight, with the azimuth (orientation) of the camera as

mounted to the aircraft. To illustrate this with an example, if a plane were flying straight to the true north, the flight azimuth would be 0°. If the camera were oriented directly backward, the camera azimuth would be 180°.

The camera elevation is the vertical (z axis) angle at which the camera is tilted. It can range from 90° (camera pointed vertically straight down) to 0° (camera pointed horizontally out toward the horizon). Camera elevation, therefore, corresponds to 90° camera tilt, as described in other sections of this report (e.g., Chapter 1).

Solar azimuth (x–y, or compass orientation) and elevation (z-axis,or vertical orientation) are parallel variables, and can be readily attained for any given geoposition as a function of time of day and time of year. Solar azimuth also corresponds to compass orientation of the location of the sun, and ranges from 0° (true north) to 359° (one degree west of true north). For solar elevation, 0° represents the sun at the horizon, while solar elevation of 90° occurs when the sun is directly overhead.

For the purpose of conducting our glare analysis, we obtained solar azimuth and elevation data from the solar calculator on the National Oceanic and Atmospheric Administration (NOAA) webpage (NOAA 2012b). Although solar azimuth and elevation change as geoposition and time change, the incremental changes in both variables are very small with small scale geopositional movements, and also small increments of time (e.g., a movement of 20 km over a period of 10 minutes in the course of conducting an aerial survey along a transect). Therefore, in the interest of simplicity, we used single solar azimuth and elevation values for each transect segment, and we recommend this practice as a substitute for analyzing continual spatiotemporal variation in solar azimuth and elevation in survey protocol design, as long as spans of space and time represented by single solar position variables are relatively small.

We then calculated camera azimuth from GPS tracks of survey transect flight segments, accounting for the direct, rear orientation of the cameras, and camera elevation from the three different experimental tilt levels at which our cameras were mounted (see Chapter 1) for full description of experimental design and execution). As mentioned above, camera elevation corresponds to 90° camera tilt, as described in other sections of this report. Hence, when the camera was pointing straight down, the camera elevation was 90°. The other experimental camera tilt levels used in our imaging flight trials of 15° and 44° correspond to camera elevations of 75° and 46°, respectively.

For the purpose of conducting our glare analysis, we wanted to carefully examine the variation in camera azimuth and elevation as it impacted image glare, hence we eliminated target flyover flight segments in which flight azimuth, as well as pitch, roll, and yaw of the aircraft, exhibited pronounced variation, and only analyzed transect flights during which aircraft flight direction and orientation were relatively constant. Furthermore, we broke such transect flights into 48 distinct segments, corresponding to portions of the flights with relatively uniform flight direction. For each of these 48 flight segments, we calculated average image glare levels using automated glare scoring of all images, according to the glare score classification presented in Table 4–1. The representative values of all four angular variables of interest, plus average glare scores of each of these transect survey segments are presented in Table 4–3.

Table 4–3.

Angular Variables of Interest for Glare Impact Analysis, Plus Average Glare Scores for 48 Aerial Imaging Transect Survey Segments Conducted 10 to 20 May 2011 off of Oak Island NC.

Transect Number	Camera Azimuth (degrees)	Camera Elevation (degrees)	Solar Azimuth (degrees)	Solar Elevation (degrees)	Average Glare
1	44	46	238	64	0
2	229	46	251	56	0
3	131	75	150	72	0
4	25	46	245	60	0
5	251	46	254	54	0
6	190	75	87	31	0
7	222	75	88	33	0
8	251	75	90	35	0
9	72	75	82	22	0
10	223	46	94	41	0
11	265	46	97	43	0
12	13	46	90	37	0
13	251	46	96	45	0
14	81	46	234	66	1
15	70	46	85	27	1
16	14	75	85	27	1
17	43	75	83	25	1
18	215	46	95	43	1
19	2	75	102	53	1
20	200	46	248	59	2
21	12	75	246	60	2
22	44	75	240	64	2
23	193	75	248	59	2
24	44	75	191	75	2
25	310	75	127	67	3
26	184	46	92	39	3
27	14	46	126	68	3

Transect Number	Camera Azimuth (degrees)	Camera Elevation (degrees)	Solar Azimuth (degrees)	Solar Elevation (degrees)	Average Glare
28	321	46	123	67	3
29	90	75	200	73	4
30	90	75	235	66	4
31	66	75	236	65	4
32	247	75	255	53	4
33	235	75	250	57	4
34	35	46	88	33	4
35	36	46	91	38	4
36	222	75	208	73	4
37	355	90	98	45	5
38	249	46	137	71	5
39	306	75	119	66	5
40	176	90	101	49	6
41	75	75	179	76	6
42	129	75	178	74	7
43	72	46	87	31	7
44	74	46	90	36	7
45	252	75	217	72	7
46	323	75	119	66	7
47	310	75	141	70	8
48	270	75	204	73	9

Only half of the transect segments produced average glare levels below the glare threshold of 2 for successful animal detection, discussed previously. This high frequency of high-glare images is also evidenced by the fact that more than half (54%) of the individual images captured during the transect portions of the experimental flights had glare level above 2 (Figure 4–2and Table 4–2). This occurred despite the application of camera tilts of up to 44° and planning efforts to avoid obtaining excessive high-glare imagery during the execution of the imaging experiments, based on nightly review of results.

This underscores the importance of understanding and avoiding image data loss due to sun glare for designing cost-effective offshore aerial imaging surveys in US waters, where low latitudes compared with Northern Europe result in sun elevations high enough to significantly impact survey success at camera orientations close to vertical.

4.2.6 Glare Mitigation In Survey Design as a Function of Angular Deviation from the Glint Spot

As defined previously, the glint spot is the combination of the four angles discussed above at which the camera is oriented directly at the reflection of the sun on the water's surface. It is logical that the farther a camera is oriented away from the glint spot, the lower the glare level in the imagery will be. To empirically characterize this relationship, we studied variation in observed image glare level as a function of a variable that we term angular deviation from the glint spot (ADGS).

We define ADGS as the angular difference between a camera pointed at a given angle and the angle at which it would be pointing directly at the glint spot. A two-dimensional illustration of this concept is presented in Figure 4–5.

When the camera is pointing directly at the glint spot, ADGS = 0. The farther the camera is pointed away from glint spot in any direction, the larger the ADGS.

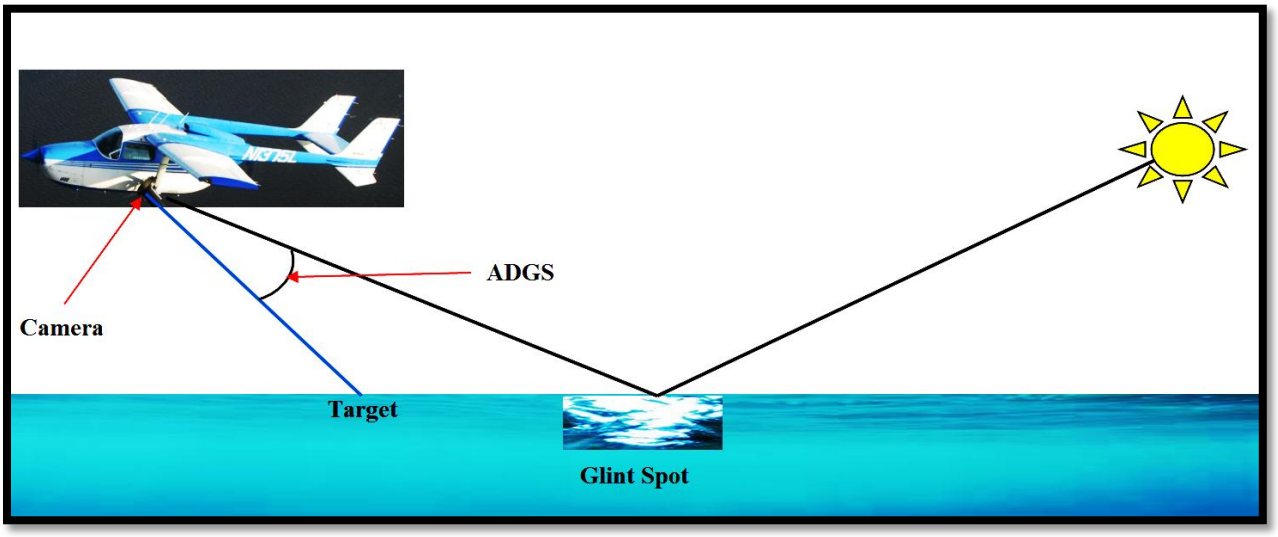

Figure 4–5. Angular deviation from the glint spot (ADGS) can be calculated using spherical geometry for any given combination of the four angular input variables as the dot product of two vectors: the first vector is the line from the origin to the glint spot and second is the line from the origin to target (where the camera is pointing). The product of the two x coordinates plus the product of the two y coordinates plus the product of the two z coordinates is the cosine of the angular difference between two points, hence the ADGS is the arccosine of the dot product of the two vectors. The formula for calculating ADGS is given below (formula developed with the assistance of Drs. R. Scott Schappe, Department of Physics, Lake Forest College and N. White, Department of Mathematics, University of Florida).

$$\alpha = \arccos\left[\sin E_t \cos C_t \sin E_g \cos C_g + \sin E_t \sin C_t \sin E_g \sin C_g + \cos E_t \cos E_g\right]$$

α = Angular deviation from the glint spot (ADGS)
E_t = Camera elevation with respect to vertical = 9° camera tilt
C_t = Camera Azimuth
E_g= Solar elevation with respect to vertical = 9°solar elevation
C_g= Solar Azimuth

The relationship between camera angle, or E_t, was discussed earlier and is written above. The relationship between solar elevation with respect to vertical, or E_g, and solar elevation as conventionally used to describe solar position is written above, and is graphically illustrated in Figure 4–6.

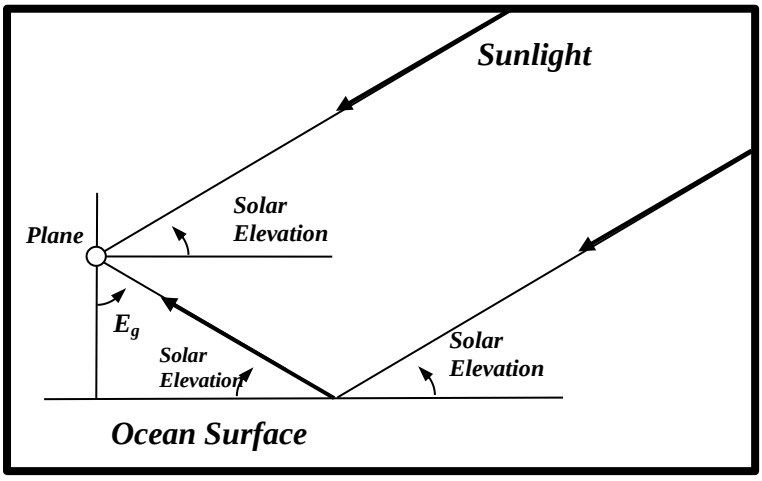

Figure 4–6. Illustration of solar elevation, as conventionally defined to describe solar position, and solar elevation with respect to vertical, or E_g, as defined in this study and in the ADGS formula presented above. Graphic designed by Dr. R S. Schappe, Department of Physics, Lake Forest College.

Using the formula above, we input the four angular variables for each of the 48 transect segments from our May 2011 offshore Oak Island NC imaging experiments to calculate ADGS for each of the segments, and plotted the relationship between ADGS and average glare levels in the segments (Figure 4–7).

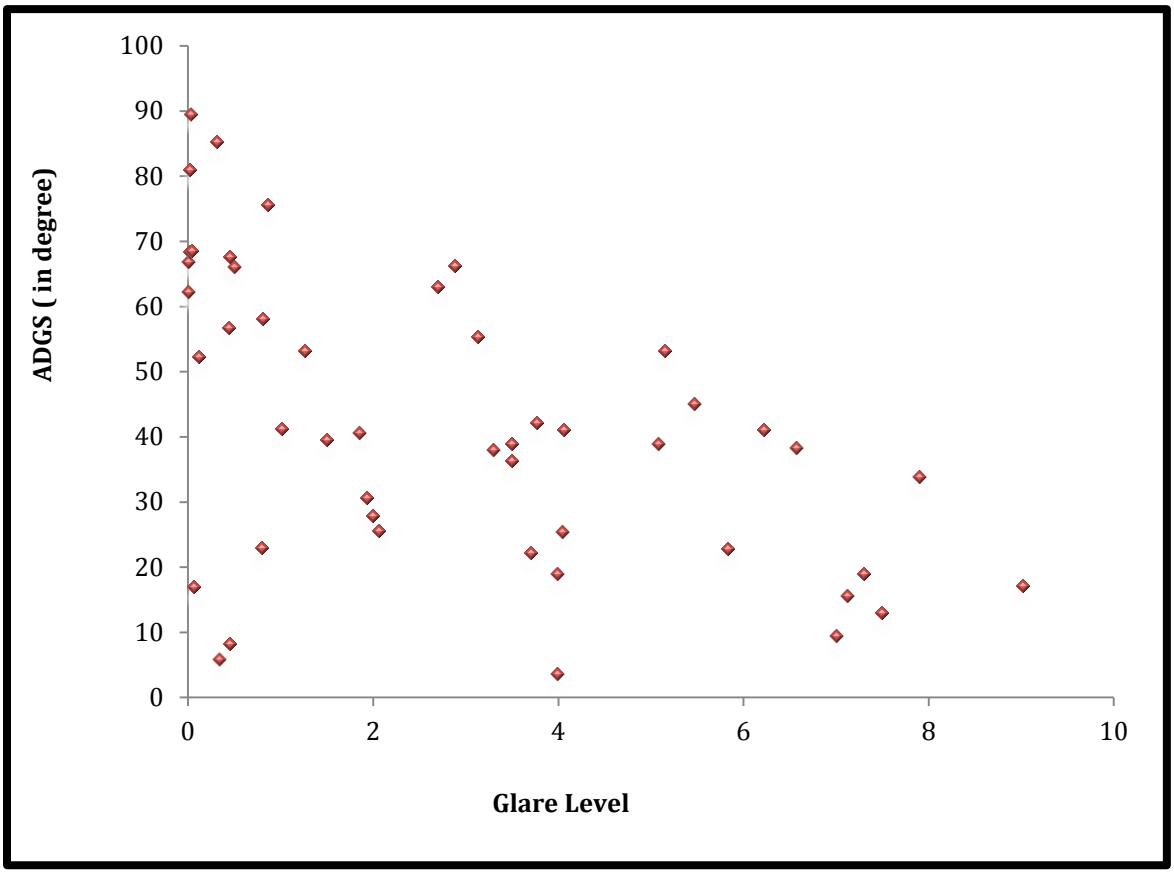

Figure 4–7. Relationship between angular deviation from the glint spot (ADGS) and average image glare level for 48 imaging transect survey segments conducted 10 to 20 May 2011 off of Oak Island NC. Each point represents a single transect survey segment.

The relationship presented in Figure 4–7 revealed that glare levels above the 2 threshold were only obtained when ADGS was below 67°. Hence, we conclude that maintaining ADGS over 67° is necessary in imaging survey design to ensure the collection of usable imagery. As illustrated in Figure 4–7, seven of our 48 transect segments had ADGS above 67°, all of which produced average image glare scores below the threshold value of 2, while 41 transect segments had ADGS below 67°. Of these, 17 produced average image glare scores below the 2 threshold, while 24 produced average image glare scores above 2. In general, we observed an inverse relationship between average glare level and ADGS as expected. However, it is also evident that under some circumstances, it is possible to obtain low glare images even at low ADGS levels. Such cases are represented by points in the lower left hand portion of Figure 4–7. Subsequent analysis of climatological data gathered during the Op House experiments confirmed that such points represent transect survey segments taken during overcast conditions, when sun glare is not produced despite camera angles that are close to where the sun's reflection would be in the absence of clouds. The mitigation of sun glare by cloud cover in offshore wildlife surveying has been noted previously by (Certain and Bretagnolle 2008). This phenomenon suggests a possible means to opportunistically expand the envelope of

methodological options for obtaining low glare images in offshore wildlife imaging surveys. However, we note that it may not always be operationally feasible to alter camera angles, transect patterns, or flight times, dates and places at a fast enough time scale to capitalize on weather-related opportunities for low-glare imaging.

4.2.7 Applying the Glare Threshold in Survey Protocol Design

Our analysis suggests that to obtain imagery useful for environmental risk and impact studies of birds, marine mammals, and sea turtles high-resolution offshore aerial imaging surveys must avoid capturing images with glare values greater than 2, as defined previously. We have also determined that to do so, ADGS of 67° or greater must be maintained.

As discussed previously, ADGS varies across time and space, and is affected by four angular variables: camera elevation, camera azimuth, sun elevation, and sun azimuth. To better understand the variation in ADGS and its impact on aerial imaging protocol design on the US AOCS, we performed series of hypothetical simulations in which we calculated the extent of usuable imaging survey hours achievable for different combinations of survey methodological parameters. In these simulations, usable survey hours were defined as hours of daylight with ADGS of 67° or higher. Sunrise and sunset times, as well as solar elevation and azimuth data were obtained from the NOAA solar calculator (NOAA 2012b). In all simulations, flight directions were directly west to east, alternating with east to west. All flight transects extended from the states' seaward boundaries eastward to the 30 m isobaths, as depicted in Figure 4–8. In all simulations we simplified the variation in solar angle variables by taking a single representative value per hour for the given location and time. In the different simulations, we varied the following parameters:

1) Latitude—Latitude impacts available suitable survey time because of seasonal variation in day length, as well as seasonal variation in sun azimuth and elevation. We used four representative locations along the AOCS, as follows: Bar Harbor ME, Gloucester MA, Ocean City MD, and Oak Island NC. For the calculation of solar azimuth and elevation, the central point of proposed survey transects was used as a representative point (Figure 4–8).
2) Season—Seasonality affects available suitable survey time because of seasonal variation in sunrise and sunset times at different latitudes, and through seasonal variation in solar elevation and azimuth, also as a function of latitude. To examine this variation, we created simulation surveys at four dates of the year for each of the latitudes selected: spring equinox, summer solstice, fall equinox, and winter solstice.
3) Camera angles—Camera angles affect available suitable survey times because they comprise two of the four angular components of ADGS, which determines how closely the camera is oriented toward the glint spot, or the sun's reflection on the water's surface (see earlier text). In our simulations, we examined some simple variations in both camera elevation (or tilt) and camera azimuth (or orientation) as follows. In one set of simulations, we assumed that the camera was always pointing directly downward (90° elevation = 0° degree tilt, see earlier text). This configuration was selected as this is a common and simple way of mounting cameras within aircraft. We also performed a set of simulations in which the camera azimuth was fixed at 180° opposite the flight direction (toward the rear of the aircraft) with a camera elevation of 45° (equivalent to 45° tilt, essentially equivalent to the 44° tilt experimentally tested in our field trials, see Chapter 1 for methods and section 6.3 for results). This configuration represents a relatively simple fixed camera mounting option that avoids

extremely vertical imaging angles. The final camera angle configuration we tested in simulations is the most complex. It assumes that the camera is mounted on an adjustable mount, such that the camera azimuth can be alternated during flight between two positions: 0° azimuth (forward directed) and 180° azimuth (rear directed), always with a camera elevation of 45°.

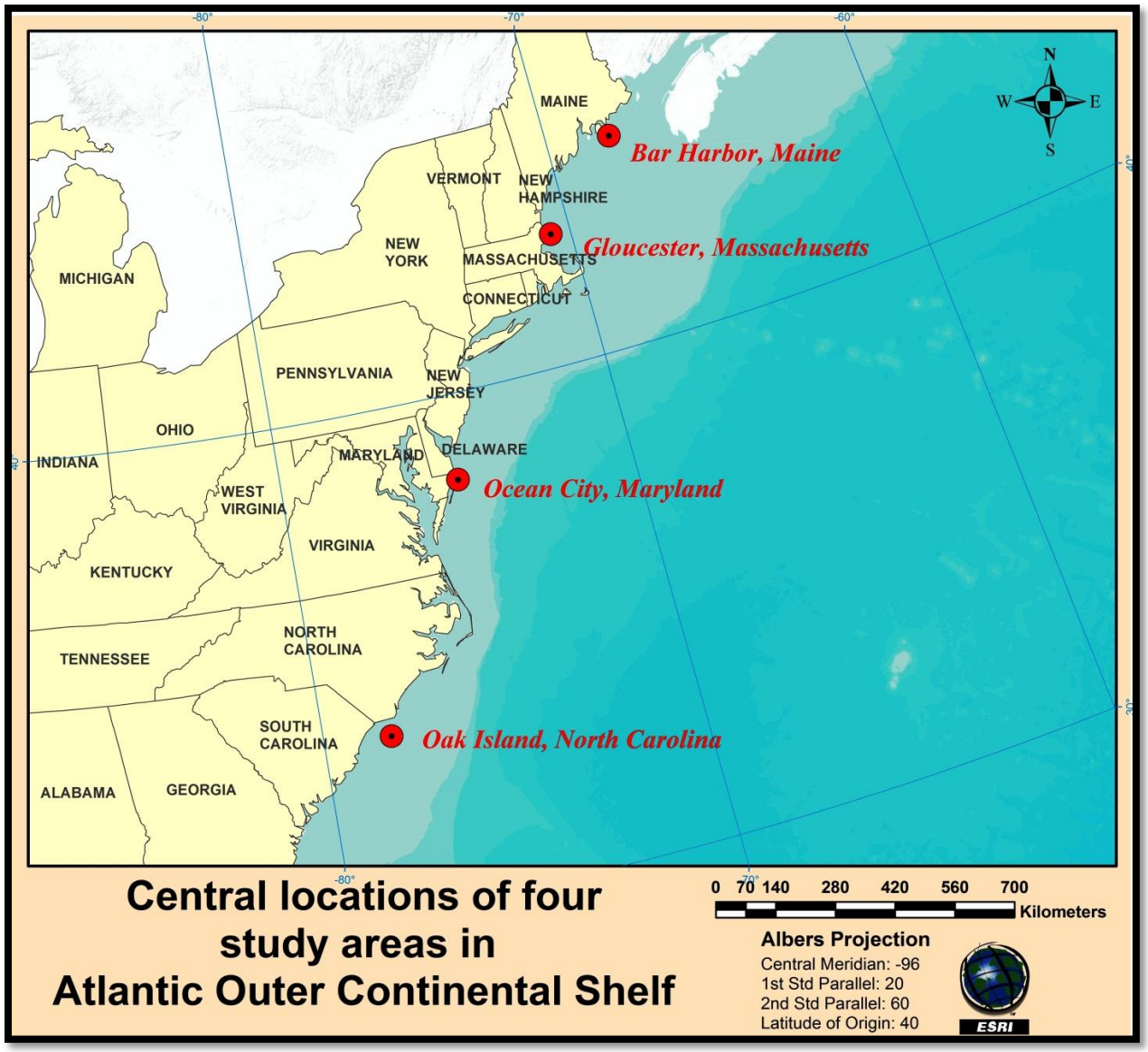

Figure 4–8. Central location of four study areas in the Atlantic Outer Continental Shelf (AOCS).

Simulation Results

Vertically Directed Camera

Our simulations revealed that with a camera directed straight vertically downward (tilt = 0° camera elevation = 90°), a very large fraction of available daylight survey hours will produce images with excessive glare, over the glare threshold of 67° ADGS. This is illustrated for all four tested AOCS localities, at all four dates over the course of the year, over the complete span of daylight hours in Table 4–4. When the camera is directed straight down, camera azimuth, and hence ADGS, are not affected by flight direction. Hence, flight direction is not presented for this set of simulations.

Table 4–4.

Angular Deviation from the Glint Spot (ADGS) Values (in Degrees) for Simulated Offshore Aerial Imaging Surveys with the Imaging Camera Directed Straight Down (Tilt = 0° Camera Elevation = 90°), for Four Atlantic Outer Continental Shelf Locations, for Four Calendar Dates Spanning the Extremes of Solar Angle Variation over the Course of a Year, for All Daylight Hours (See Text)

Date	Time	Maine	Maryland	Massachusetts	North Carolina
Winter solstice	9:00:00	82.78	83.03	83.13	82.36
	10:00:00	75.75	74.45	75.6	72.8
	11:00:00	70.62	67.62	69.92	64.9
	12:00:00	67.89	63.19	66.64	59.4
	13:00:00	67.88	61.72	66.14	57.02
	14:00:00	70.59	63.4	68.49	58.15
	15:00:00	75.71	68.01	73.39	62.6
	16:00:00	82.74	74.98	80.35	69.72
	17:00:00	Dark	83.66	88.63	78.76
	18:00:00	Dark	Dark	Dark	88.86
Spring equinox	8:00:00	85.66	Dark	87.38	Dark
	9:00:00	75.14	79.16	76.61	81.19
	10:00:00	65.04	67.72	66.09	68.92
	11:00:00	55.97	56.96	56.49	57.12
	12:00:00	48.72	47.56	48.55	46.39
	13:00:00	44.32	40.63	43.34	37.81
	14:00:00	43.69	37.64	41.96	33.18
	15:00:00	47	39.52	44.77	34.18
	16:00:00	53.48	45.66	51.07	40.38
	17:00:00	62.08	54.6	59.69	49.84
	18:00:00	71.92	65.1	69.68	61.02
	19:00:00	82.37	76.42	80.36	73.02
	20:00:00	Dark	87.89	Dark	85.31

Date	Time	Maine	Maryland	Massachusetts	North Carolina
Summer solstice	6:00:00	88.77	Dark	Dark	Dark
	7:00:00	79.54	86.61	81.84	Dark
	8:00:00	69.35	75.97	71.53	80.03
	9:00:00	58.73	64.63	60.71	68.2
	10:00:00	48	52.97	49.69	55.96
	11:00:00	37.57	41.23	38.84	43.5
	12:00:00	28.24	29.83	28.81	31.07
	13:00:00	21.83	19.84	21.22	19.2
	14:00:00	21.38	14.87	19.43	10.6
	15:00:00	27.18	19.37	24.76	14.19
	16:00:00	36.27	29.21	33.95	25.18
	17:00:00	46.61	40.57	44.53	37.45
	18:00:00	57.33	52.3	55.52	49.93
	19:00:00	67.99	63.98	66.47	62.3
	20:00:00	78.25	75.34	77.07	74.37
	21:00:00	87.68	86.04	86.91	85.83
Fall equinox	8:00:00	83.15	87.9	84.85	Dark
	9:00:00	72.68	76.43	74.06	78.3
	10:00:00	62.78	65.12	63.72	66.1
	11:00:00	54.07	54.62	54.44	54.5
	12:00:00	47.4	45.69	47.05	44.16
	13:00:00	43.83	39.56	42.66	36.33
	14:00:00	44.16	37.68	42.28	32.93
	15:00:00	48.31	40.67	46.02	35.27
	16:00:00	55.39	47.61	52.97	42.42
	17:00:00	64.36	57	62	52.39
	18:00:00	74.41	67.76	72.21	63.82
	19:00:00	84.92	79.2	82.98	75.95
	20:00:00	Dark	Dark	Dark	88.16

Note: Red cells indicate ADGS values below the 67° threshold. In the red range, animal detectability in the images will be significantly degraded because of sun glare effects (see text).

Table 4–4. illustrates that although there is some seasonal variation, a very large proportion of available daylight hours are lost because of low ADGS values throughout the year at all four localities in this set of simulated protocols. Interestingly, glare effects, which are more acute at lower latitudes, counterbalance and outweigh the loss of available daylight survey hours due to short day length at high latitudes during winter, rendering Maine the location with the greatest amount of available suitable survey time at all seasons under this camera configuration, as shown in Table 4–5.

Table 4–5.

Total Number of Daylight Hours with Angular Deviation from the Glint Spot (ADGS) above 67° for Simulated Offshore Aerial Imaging Surveys with the Imaging Camera Directed Straight Down (Tilt = 0°, Camera Elevation = 90°), for Four Atlantic Outer Contintental Shelf Locations, for Four Calendar Dates Spanning the Extremes of Solar Angle Variation Over the Course of a Year (See Text).

	Winter Solstice	Spring Equinox	Summer Solstice	Fall Equinox
Maine	8	4	6	4
Massachusetts	7	4	4	4
Maryland	6	4	4	4
North Carolina	5	4	4	3

Camera Fixed at 45° Elevation, 180° Azimuth

One way to potentially mitigate high glare imaging due to low ADGS is to mount the camera at a tilt to create camera elevation angles off of straight vertical. For daylight hours when the solar elevation is very high, this will often increase ADGS, depending on camera and solar azimuths, resulting in imagery with less glare. This was, in effect, a solution that was shown to be effective in the field during the Op House imaging experiments, in which the best imagery during the hours closest to midday was often obtained with the camera tilt at 44° (camera elevation of 46°) (see Chapter 1 and section 6.3). In our second set of simulations, we assumed that the camera was fixed at 45° elevation (45° tilt) and 180° azimuth (directed toward rear of aircraft). In such a configuration, the camera azimuth varies with flight direction of the aircraft. Specifically, the camera azimuth is 180° opposite the flight direction. Because of this variation, we incorporated specific flight directions into this set of simulations, with straight east–west outbound transects alternating with straight west–east transects. The same four localities and calendar dates were simulated across the complete span of daylight hours, and the resulting ADGS values are presented in Table 4–6.

Table 4–6.

Angular Deviation from the Glint Spot (ADGS) Values (in Degrees) for Simulated Offshore Aerial Imaging Surveys with the Imaging Camera Always at 45° Tilt (45° Camera Elevation) and 180° Azimuth Relative the Aircraft Flight Direction for Four AOCS Locations, for Four Calendar Dates Spanning the Extremes of Solar Angle Variation Over the Course of a Year, for All Daylight Hours (See Text)

Date	Time	Flight Direction	Maine	Maryland	Massachusetts	North Carolina
Winter Solstice	9:00:00	East	115.21	118.22	116.57	118.84
	10:00:00	West	55.30	49.91	53.59	46.47
	11:00:00	East	90.80	92.87	91.85	92.89
	12:00:00	West	69.43	61.24	66.79	56.14

Date	Time	Flight Direction	Maine	Maryland	Massachusetts	North Carolina
	13:00:00	East	69.49	70.08	70.04	69.25
	14:00:00	West	90.73	81.76	87.79	76.40
	15:00:00	East	55.33	53.57	55.04	51.48
	16:00:00	West	115.14	106.22	107.27	101.03
	17:00:00	East	Dark	50.02	52.82	46.88
	18:00:00	West	Dark	Dark	Dark	127.14
Spring Equinox	8:00:00	East	130.58	Dark	132.36	Dark
	9:00:00	West	32.37	34.82	33.14	36.46
	10:00:00	East	106.20	110.76	107.97	112.70
	11:00:00	West	32.02	25.83	29.96	22.36
	12:00:00	East	80.19	83.94	81.74	85.24
	13:00:00	West	51.26	42.27	48.31	36.91
	14:00:00	East	54.84	57.40	56.02	57.91
	15:00:00	West	76.25	67.48	73.30	62.53
	16:00:00	East	34.04	33.98	34.31	33.03
	17:00:00	West	102.26	94.31	99.55	89.95
	18:00:00	East	30.53	25.96	29.11	22.74
	19:00:00	West	127.07	120.73	124.90	117.27
	20:00:00	East	Dark	42.89	Dark	40.35
Summer Solstice	6:00:00	East	125.45	Dark	Dark	Dark
	7:00:00	West	39.65	48.15	42.52	Dark
	8:00:00	East	113.27	118.50	115.03	121.66
	9:00:00	West	13.99	21.47	16.41	26.05
	10:00:00	East	92.75	97.94	94.61	100.68
	11:00:00	West	15.43	6.41	12.44	1.52
	12:00:00	East	68.62	73.44	70.43	75.73
	13:00:00	West	41.24	33.11	38.08	28.95
	14:00:00	East	42.93	47.26	44.63	49.16
	15:00:00	West	66.98	59.74	64.44	56.10
	16:00:00	East	17.04	20.41	18.40	21.88
	17:00:00	West	91.26	85.30	89.15	82.37
	18:00:00	East	12.44	7.42	10.57	5.66
	19:00:00	West	112.12	108.36	110.75	106.61

Date	Time	Flight Direction	Maine	Maryland	Massachusetts	North Carolina
	20:00:00	East	37.96	34.15	36.36	33.09
	21:00:00	West	125.09	125.38	125.13	125.77
Fall Equinox	8:00:00	East	127.91	132.90	129.75	Dark
	9:00:00	West	30.91	32.55	31.39	33.83
	10:00:00	East	103.21	107.69	104.95	109.55
	11:00:00	West	33.51	26.61	31.24	22.58
	12:00:00	East	77.20	80.85	78.72	82.06
	13:00:00	West	53.99	44.97	51.01	39.62
	14:00:00	East	52.13	54.48	53.24	54.89
	15:00:00	West	79.26	70.56	76.33	65.67
	16:00:00	East	32.49	31.94	32.59	30.73
	17:00:00	West	105.29	97.45	102.62	93.17
	18:00:00	East	31.94	27.10	30.40	23.81
	19:00:00	West	129.79	123.75	127.74	120.41
	20:00:00	East	Dark	Dark	Dark	43.16

Note: Flight directions are either straight eastbound, in which case the camera azimuth is straight west (270°), or straight westbound, in which case the camera azimuth is straight east (90°). Red cells indicate ADGS values below the 67° threshold. In The red range, animal detectability in the images will be significantly degraded because of sun glare effects (see text).

This set of simulations resulted in a very different pattern of image loss due to ADGS values below 67° than the first set, but did not represent a significant overall improvement in most cases (Table 4–7). Improvements in morning eastbound flights were offset by losses in morning westbound flights, and improvements in afternoon westbound flights were offset by losses in afternoon eastbound flights, as very good ADGS alternated with very bad ADGS as a function of flight direction. This simulation illustrates an inherent difficulty with using fixed camera mounts to mitigate glare impacts in imaging survey design. If the camera azimuth is fixed, then only a small range of flight directions will produce high ADGS values at any particular time and place. This effectively precludes implementing any sort of zigzagging or alternating flight transect pattern, as such patterns necessarily entail flying in alternating directions that are opposed to one another, thus introducing azimuths that vary by close to 180°. If such directional opposition is not included, then the aircraft will wind up flying a long distance, rather than staying within a small, defined area. The area of interest on the AOCS is a long, striplike area with a north–south orientation, hence for very large scale surveys, it would theoretically be possible to maintain relatively constant flight direction and plan a fixed camera mount with an azimuth that keeps ADGS values within the suitability threshold for many, if not all of the surveys. However, such surveys would always have to be primarily either north–south or south–north, which would introduce a number of serious methodological complexities and disadvantages, including increased air travel costs for return trips, survey movement directions correlated with animal migratory movement directions, and inefficiencies related to variation in AOCS width across its length.

Table 4–7.

Total Number of Daylight Hours with Angular Deviation from the Glint Spot (ADGS) Values (in Degrees) for Simulated Offshore Aerial Imaging Surveys with the Imaging Camera Always at 45° Tilt (45° Camera Elevation) and 180° Azimuth Relative the Aircraft Flight Direction for Four AOCS Locations, for Four Calendar Dates Spanning the Extremes Of Solar Angle Variation Over the Course of a Year, for All Daylight Hours (See Text)

	Winter Solstice	Spring Equinox	Summer Solstice	Fall Equinox
Maine	6	6	7	6
Massachusetts	5	6	6	6
Maryland	5	5	6	6
North Carolina	6	4	6	4

Note: Flight directions are either straight eastbound, in which case the camera azimuth is straight west (270°), or straight westbound, in which case the camera azimuth is straight east (90°). Red cells indicate ADGS values below the 67° threshold. In the red range, animal detectability in the images will be significantly degraded because of sun glare effects (see text). Above 67° for simulated offshore aerial imaging surveys with the imaging camera always at 45° tilt (45° camera elevation) and 180° azimuth relative the aircraft flight direction, for four AOCS Locations, for four calendar dates spanning the extremes of solar angle variation over the course of a year (see text). Flight directions are either straight eastbound, in which case the camera azimuth is straight west (270°), or straight westbound, in which case the camera azimuth is straight east (90°).

Camera Angle Adjustable in Flight, Alternating between 180° and 0° Azimuth, Always 45° Tilt

To explore more effective glare mitigation solutions, we tested a final set of simulated survey protocols in which the camera angle could be adjusted in flight, to accommodate alternating flight directions while maintaining high ADGS values. Although many such systems are theoretically possible, we tested a simple scenario where the camera angle is able to be alternated in flight between two possible positions: rear directed (180° azimuth) and fore directed (0° azimuth), with a camera tilt of 45° (camera elevation 45°) in both positions. We used the same flight pattern as in the previous set of simulations with east–west flights alternating with west–east flights, but we assume that during morning hours when the sun is in the east, the camera is always oriented to the west. This entails placing it in its rear-directed position during eastbound flights, and in its fore-directed position during westbound flights. In the afternoon, the positions are reversed again, in order for the camera to be pointing as far away from the glint spot as possible, with the camera in its fore-directed position during eastbound flights, and its rear-directed position during westbound flights. These positional adjustments are illustrated (for morning flights only) in Figure 4–9 and Figure 4–10.

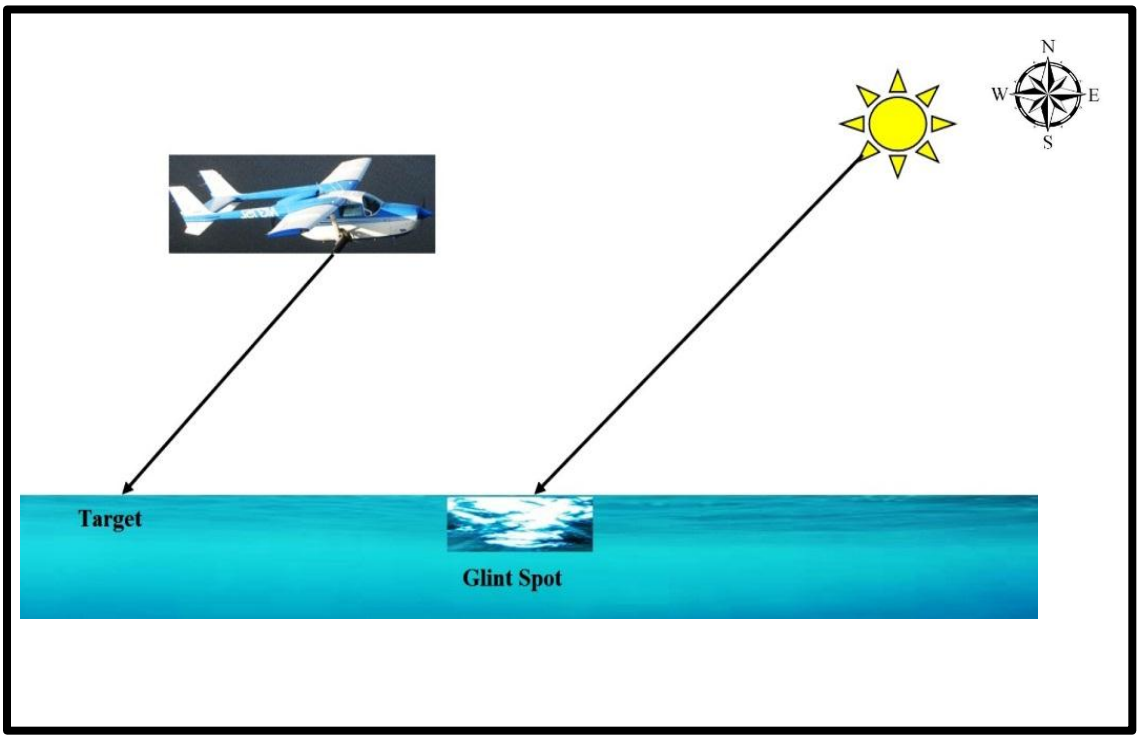

Figure 4–9. Illustration of camera angle relative to sun for survey protocol simulations with adjustable camera mount for maximum glare mitigation. This graphic represents an eastbound flight in morning with the camera in one of its two positions: 45° tilt (45° elevation) and 180° azimuth relative to aircraft orientation (rear-directed). For an eastbound flight, this results in a camera azimuth of 270° (west-looking).

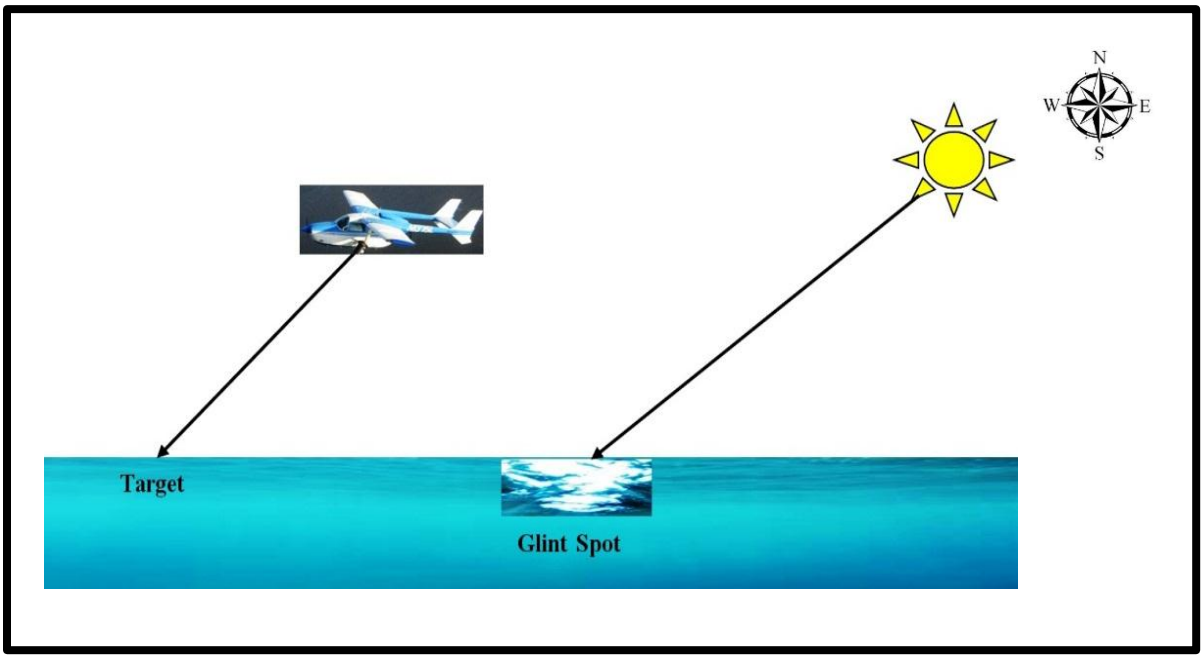

Figure 4–10. Illustration of camera angle relative to sun for survey protocol simulations with adjustable camera mount for maximum glare mitigation. This graphic represents a westbound flight in morning with the camera in the other of its two positions (first position illustrated in Figure 4–9) as follows: 45° tilt (45° elevation) and 0° azimuth relative to aircraft orientation (fore-directed). For a westbound flight, this results in a camera azimuth of 270° (west-looking).

Simulating survey protocols over the same set of localities and dates using this imaging configuration resulted in radical improvements in ADGS (Table 4–8), and radical gains in available suitable survey time (Table 4–9.) across the entire AOCS and throughout the year.

Table 4–8.

Angular Deviation from the Glint Spot (ADGS) Values (in Degrees) for Simulated Offshore Aerial Imaging Surveys with the Imaging Camera on an Adjustable Mount with Two Positions as Follows: Position 1: 45° Tilt (45° Camera Elevation) And 180° Azimuth Relative the Aircraft (Rear-directed); Position 2: 45° Tilt (45° Camera Elevation) and 0° Azimuth Relative The Aircraft (Fore-directed) for Four AOCS Locations, for Four Calendar Dates Spanning the Extremes of Solar Angle Variation over the Course of a Year, for All Daylight Hours (See Text)

Date	Time	Flight Direction	Maine	Maryland	Massachusetts	North Carolina
Winter Solstice	9:00:00	East	115.21	118.22	116.57	118.84
	10:00:00	West	102.77	105.36	104.00	105.70

Date	Time	Flight Direction	Maine	Maryland	Massachusetts	North Carolina
	11:00:00	East	90.80	92.87	91.85	92.89
	12:00:00	West	79.57	80.99	80.41	80.63
	13:00:00	East	79.51	70.08	76.66	69.25
	14:00:00	West	90.73	81.76	87.79	76.40
	15:00:00	East	102.70	93.69	99.72	88.39
	16:00:00	West	115.14	106.22	107.28	101.03
	17:00:00	East	Dark	119.10	124.78	114.07
	18:00:00	West	Dark	Dark	Dark	127.15
	8:00:00	East	130.58	Dark	132.36	Dark
	9:00:00	West	118.81	123.71	120.65	125.99
	10:00:00	East	106.20	110.76	107.97	112.70
	11:00:00	West	93.24	97.41	94.91	99.04
	12:00:00	East	80.19	83.94	81.74	85.24
	13:00:00	West	67.30	70.53	68.69	71.47
Spring Equinox	14:00:00	East	63.46	57.40	60.48	57.91
	15:00:00	West	76.25	67.48	73.30	62.53
	16:00:00	East	89.26	80.84	86.41	76.18
	17:00:00	West	102.26	94.31	99.55	89.95
	18:00:00	East	114.99	107.68	112.49	103.72
	19:00:00	West	127.07	120.73	124.90	117.27
	20:00:00	East	Dark	88.20	Dark	130.28
	6:00:00	East	125.45	Dark	Dark	Dark
	7:00:00	West	120.87	125.70	122.43	Dark
	8:00:00	East	113.27	118.50	115.03	121.66
	9:00:00	West	103.67	108.95	105.51	111.91
	10:00:00	East	92.75	97.94	94.61	100.68
	11:00:00	West	80.97	86.00	82.82	88.50
	12:00:00	East	68.62	73.44	70.43	75.73
Summer Solstice	13:00:00	West	55.89	60.48	57.91	62.58
	14:00:00	East	54.21	47.26	51.54	49.16
	15:00:00	West	66.98	59.74	64.44	56.10
	16:00:00	East	79.39	72.71	77.04	69.40
	17:00:00	West	91.26	85.30	89.15	82.37
	18:00:00	East	102.31	97.29	100.51	94.86
	19:00:00	West	112.12	108.36	110.75	106.61
	20:00:00	East	120.03	118.01	119.26	117.18
	21:00:00	West	125.09	125.38	125.13	125.77

Date	Time	Flight Direction	Maine	Maryland	Massachusetts	North Carolina
Fall Equinox	8:00:00	East	127.91	132.90	129.75	Dark
	9:00:00	West	115.91	120.74	117.73	122.95
	10:00:00	East	103.21	107.69	104.95	109.55
	11:00:00	West	90.22	94.32	91.87	95.86
	12:00:00	East	77.20	80.85	78.72	82.06
	13:00:00	West	64.39	67.49	65.74	68.34
	14:00:00	East	66.38	54.48	63.39	54.89
	15:00:00	West	79.26	70.56	76.33	65.67
	16:00:00	East	92.30	83.98	89.48	79.37
	17:00:00	West	105.29	97.45	102.62	93.17
	18:00:00	East	117.94	110.79	115.49	106.91
	19:00:00	West	129.79	123.75	127.74	120.41
	20:00:00	East	Dark	Dark	Dark	133.16

Note: ADGS below threshold value are shaded. NAs are before and after daylight time. Flight directions are either straight eastbound or straight westbound. The camera is alternated between the two mount positions in between individual flight segments such that the camera is always pointing westward in morning and eastward in the afternoon (see text). Red cells indicate ADGS values below the 67° threshold. In the red range, animal detectability in the images will be significantly degraded because of sun glare effects (see text).

Table 4–8 illustrates that very little of the available daylight time for surveys will produce images with unacceptable levels of glare under this camera mount scenario. The exception is near midday during the portions of the year when the sun is at or north of the equator. Table 4–9. illustrates the significantly larger number of available survey hours under this scenario.

Table 4–9.

Total Available Suitable Survey Hours for Simulated Offshore Aerial Imaging Surveys with the Imaging Camera on an Adjustable Mount with Two Positions as Follows: Position 1: 45° tilt (45° Camera Elevation) and 180° Azimuth Relative the Aircraft (Rear-directed); Position 2: 45° tilt (45° Camera Elevation) and 0° Azimuth Relative the Aircraft (Fore-directed) for Four AOCS Locations, for Four Calendar Dates Spanning the Extremes of Solar Angle Variation over the Course of a Year, for All Daylight Hours (See Text).

	Winter Solstice	Spring Equinox	Summer Solstice	Fall Equinox
Maine	8	11	13	10
Massachusetts	9	11	12	10
Maryland	9	11	12	11
North Carolina	10	10	11	10

Note: Flight directions are either straight eastbound or straight westbound. The camera is alternated between the two mount positions in between individual flight segments such that the camera is always pointing westward in morning and eastward in the afternoon.

A comparative summary of our simulated imaging survey protocols results is presented in Figure 4–11.

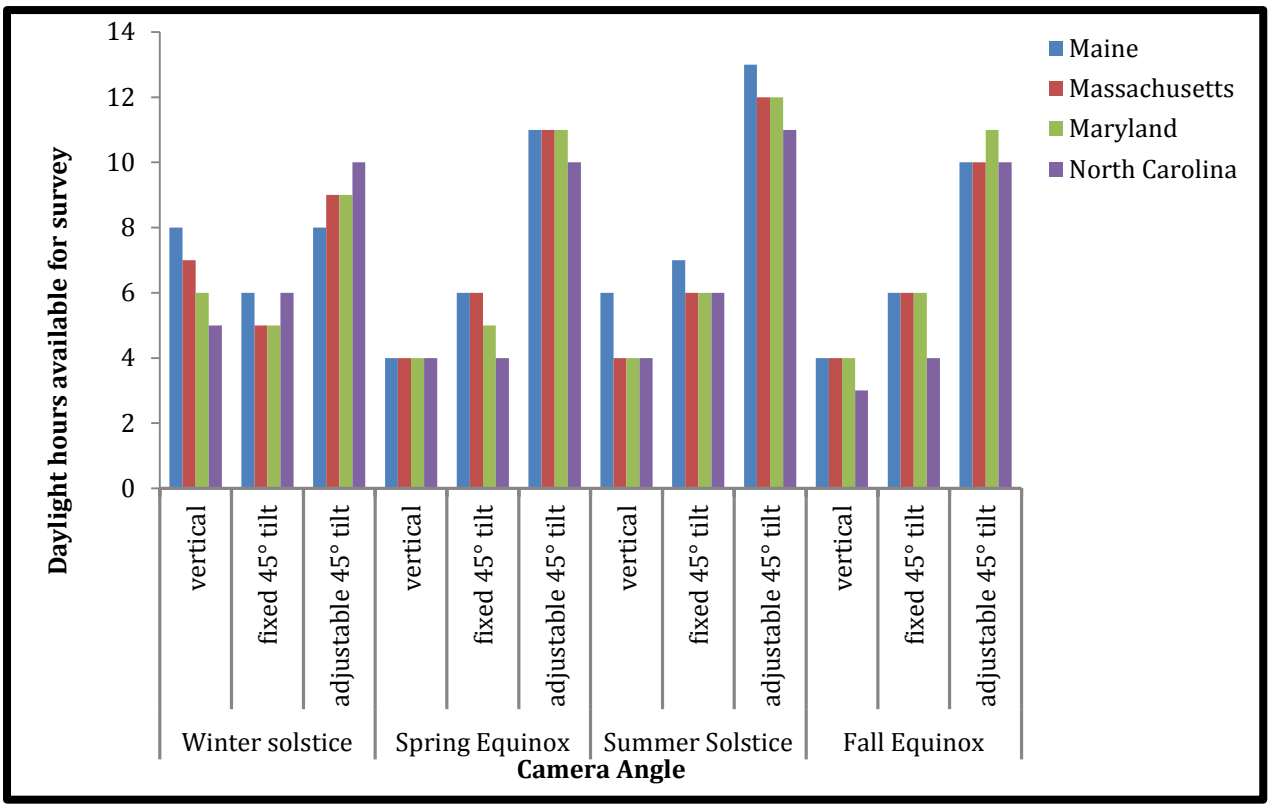

Figure 4–11. Comparison of total suitable imaging hours available for aerial surveys at four locations on the Atlantic Outer Continental Shelf (ME, MA, MD, and NC) on four calendar dates that span the annual variation in solar angles, under three different simulated camera mounting scenarios (see text). In all cases, the third camera mounting scenario (adjustable 45° tilt) results in substantial gains in available survey time. In this scenario, the mount can be alternated in flight between fore-directed and rear-directed orientations, both with 45° tilt, to point the camera away from the sun's reflection. Gains are most significant during non-winter months.

4.2.8 Summary and Conclusion

Our analysis revealed that sun glare can cause substantial data losses in offshore aerial high-resolution wildlife imaging survey protocols if care is not taken to avoid the conditions that produce unacceptable glare levels. Specifically, we used manual review of imagery collected during experimental imaging trials to determine the glare level above which animal detection in imagery was degraded beyond levels that would be generally deemed scientifically acceptable. We characterized this glare threshold in terms of green pixel exposure levels, and it corresponded to a value of 2 on the glare scale used in our experiments. We then characterized the combinations of camera and sun angles that result in crossing this glare threshold. The angular components are combined into a single variable—angular deviation from the glint spot (ADGS). We present a

formula for calculating ADGS for any given point in time and space as a function of four input variables for which data is easily attainable, and that collectively incorporate the three-dimensional angular components of sun and camera orientation in relation to each other. Empirical analysis of experimental data revealed that ADGS below 67° may result in exceeding the glare threshold, except during overcast conditions. Aerial imaging survey simulations revealed that when fixed angle camera mounts are used (either vertical or 45° tilt), more than half of available daylight hours will produce images with unacceptable levels of glare (over the glare threshold) because of ADGS lower than 67° over much of the AOCS for much of the year, with the worst losses occurring at low latitudes and during the warmer months. Using a camera mount whose angle is adjustable in flight represents an effective solution to the sun glare problem. Simulated surveys assuming a simple adjustable mount with two possible camera positions resulted in roughly doubling the amount of daylight hours during which images of acceptable quality (low glare levels) would be produced, with benefits occurring throughout the year and across the entire AOCS, but with the most pronounced benefits occurring in any season other than winter.

4.3 Analysis and Study Design Considerations based on European Experience

4.3.1 Introduction

The design of offshore high-resolution aerial wildlife imaging survey protocols is a multifaceted challenge, entailing myriad statistical and biological considerations in addition to technology choices and imaging parameters. In this section, we present a discussion of several selected issues in survey design that have emerged as essential considerations in European applications of such surveys for offshore wind energy development environmental risk/impact studies. This discussion is contributed by Dr. Chris Thaxter of the BTO, one of the leading scientific experts in offshore high-resolution wildlife imaging survey methodology in the UK, where such surveys have become widely applied to the offshore wind energy sector in recent years.

4.3.2 Survey Design Issues

Traditional Methods

With high-resolution imagery methods, the analytical protocol differs from conventional visual survey methodology, because the survey uses strip transect methodology that assumes all animals in the strip are counted. This is in contrast to design-based visual methods where line transect methodology is used and a detection function is applied to estimate the number of animals missed (Buckland et al. 2001), implemented in Program Distance (Thomas et al. 2009; Thomas et al. 2010). Design-based visual line transect methodology can be used to estimate abundance (N) in each sample section block (b) as:

$$N_b = A_b \frac{n_b}{2L_b\mu} E[s]$$

(after Buckland et al. 2001; Burt et al. 2010)

Where: Ab is size of the block, nb the number of detected groups, Lb the length of transect, μ the estimate of the effective search half-width (effective survey swath width, obtained from the detection function, is the distance from the transect line beyond which as many birds are detected as are missed at distances smaller than effective survey swath width), and E[s] is the estimate of the mean group size, obtained from a regression of probability of detection and the logarithm of group size, allowing for greater difficulty in seeing single birds and small groups farther away (Burt et al. 2010).

Model-based Estimation

Model-based density estimation is an alternative way of estimating abundance of animals in a survey region (e.g., Petersen 2007 and Petersen et al. 2011). These methods may require transects to be subdivided into smaller segments accounting for probability of detection. Here, the number of birds in each segment can then be modelled in a general additive model (GAM), with an offset term for the area of the segment, and a logarithmic link function. Particular clumped distributions of birds (Transect versus Grid Sampling Designs section below), however, may require over-dispersed Poisson or quasi-Poisson, or even more extreme exponential tweedie models. Density may then be estimated for the region using bootstrap simulations sampling segments with replacement to calculate the variance of the abundance estimate (Burt et al. 2009, 2010).

Digital Surveys

For digital surveys, all birds in the strip are detected; hence a single estimator can be used in calculating an estimated abundance in each block as:

$$N_b = A_b \frac{n_b}{2wL_b}$$

(after Burt et al. 2010)

Transect versus Grid Sampling Designs

Within the UK and Europe, several trials of methodologies have taken place for digital methods, including testing of different survey designs (e.g., Burt et al. 2009, 2010).

In estimating the population size within an area, a crucial element centers around the variance. In particular, a design-based approach must control for variance in the survey design. This applies for both visual and digital survey methods, and can be achieved by using a systematic survey design, with each line covering the full range in density, aiming for similar encounter rates between lines (the greater the encounter rate difference, the greater the variance), and a higher number of lines to increases sample sizes or survey coverage.

A simple line visual transect design is shown in Figure 4–12.

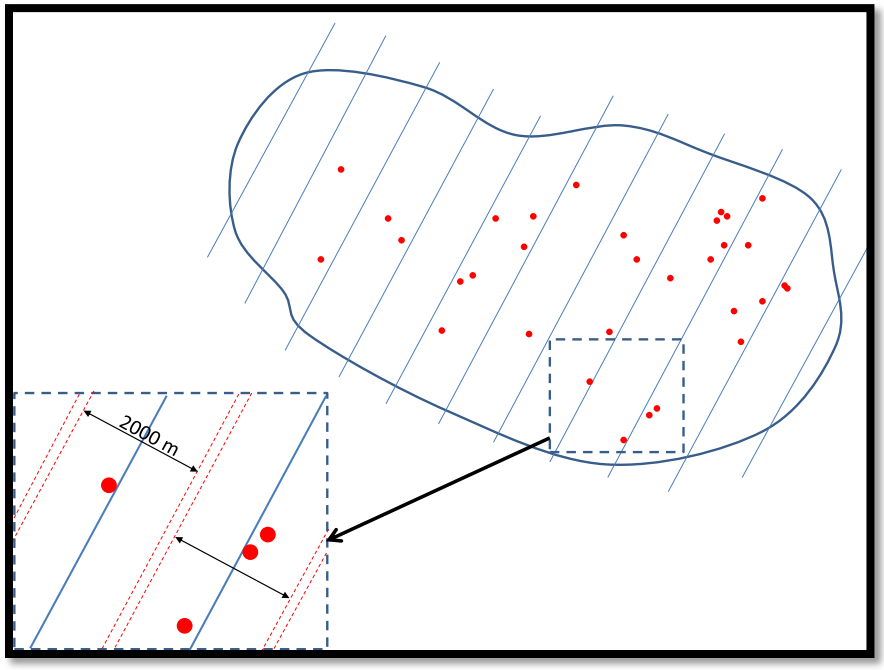

Figure 4–12. Hypothetical survey using visual-based aerial methods (1,000 m either side of aircraft).

Line visual transect survey design as illustrated above (Figure 4–12) is translated into a digital survey design with the same number of transects in Figure 4–13. This digital example assumes no digital protocol; however, one could survey as illustrated in Figure with 11 transects, or sub-sample to create smaller segment transects. This approach increases sample size. This can be done for both digital video and still image methods.

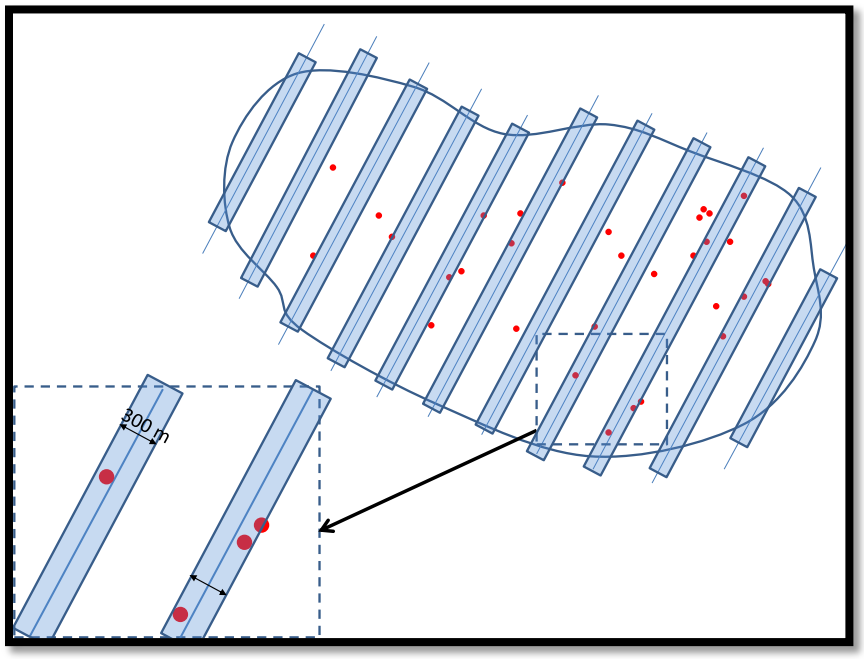

Figure 4–13. Digital survey swathes along same transects as in Figure 4–12. In this example, a value of 300 m is used as an example based on UK and European experiences.

The subsampling approaches (e.g., Figure 4–14 and Figure 4–15) are designed to increase sample size and precision in final population estimates. In the UK Round 3 aerial surveys, both video-based and still image-based approaches are being used, the latter using the gridded approach illustrated in Figure 4–15. There is great flexibility built into these designs, and all techniques are considered robust if surveys are conducted and data analysed in the correct manner (Buckland et al. 2012).

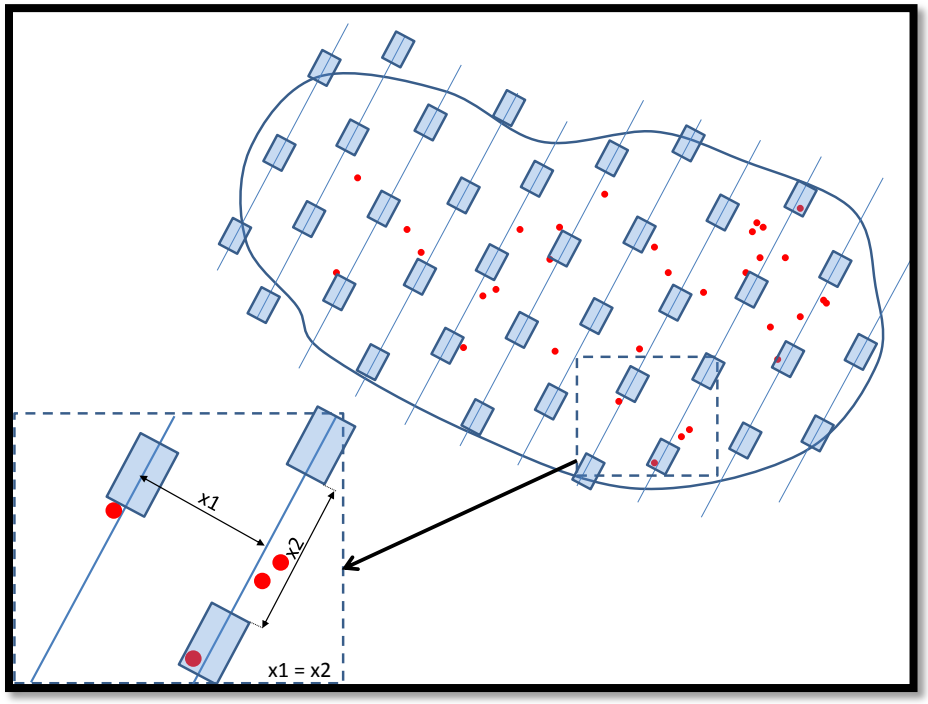

Figure 4–14. Hypothetical example of video subsampling.

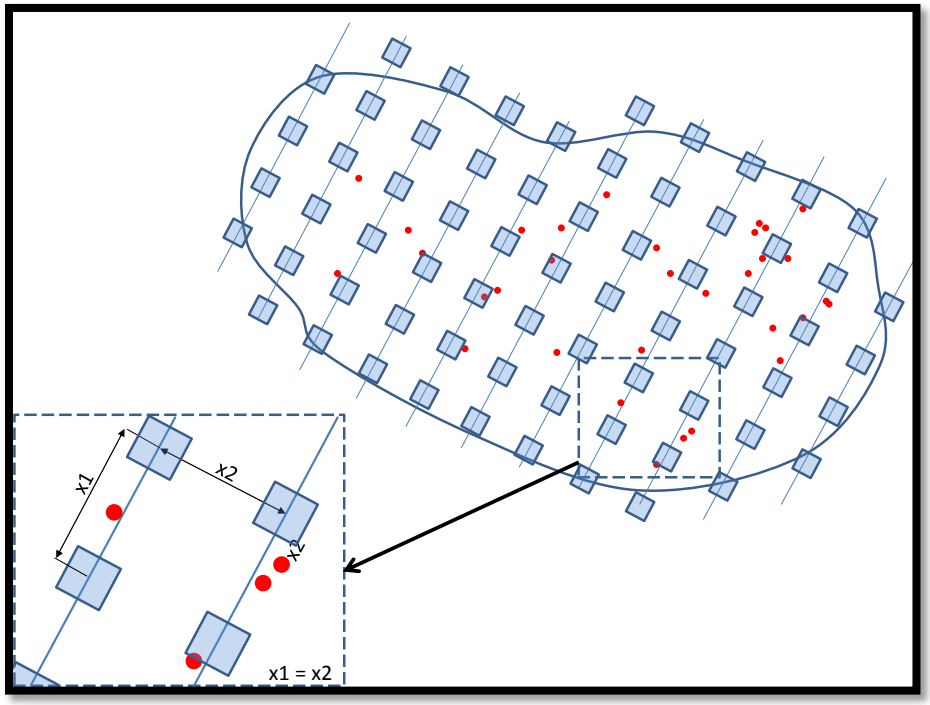

Figure 4–15. Hypothetical example of still image grid-based approach.

Spatial Aggregation of Species

Where there are clumped or aggregated species, these present difficulties when conducting strip surveys in particular. The chance of hitting an aggregation is determined by how many lines and the percentage coverage of the region, which would reveal more precise population estimates. In their comparison of Carmarthen Bay, Burt et al. (2010) set out to test a clumped species (Common Scoter, *Melanitta nigra*) in comparison to a more ubiquitous one (all gulls) with the belief that for Common Scoter their clumped distributions would make population estimation problematic and variance in estimates elevated. Digital surveys that covered a 300-m effective sample width failed to successfully estimate populations of species with clumped distributions. To improve estimates, the recommendation was to increase the number of flight lines to increase the chances of hitting aggregations, lowering the coefficient of variation (Thaxter and Burton 2009). Subsampling may also help in this regard.

Likewise, a similar issue arises for numbers of diving species, which may spend a considerable amount of time underwater and may be missed by digital methods. There is little information on how this may affect final estimates and is not something that has been included in estimates of divers, for example, in recent UK (London Array) and European (Danish: Nysted / Hors Rev) projects. However, it may be possible to use information on the daily time spent underwater per day using information from the literature (e.g., for diving alcids, Thaxter et al. 2009, 2010), which is something that UK regulators accept may be a useful correction factor to population estimates.

Spatial Sample Coverage

A 10% subsampling was discussed in Thaxter and Burton (2009) to achieve appropriate coverage of the area to be surveyed. However, as also noted in Thaxter and Burton (2009) the level at which the survey is targeted will also come into play, as well as the need for population estimates, and the species types that are noted in the region. If population estimates for species (e.g., in EIAs) are required from the survey, it is increasingly important to conduct pilot surveys to allow bespoke survey designs (Burt et al. 2010). These surveys will also require rigorous power assessment with a view to adjusting protocols if need be to allow appropriate power of population change to be met and to give defensible population estimates. Such bespoke or adjusted designs would therefore permit greater coverage, or more flight lines, to meet the desired level of precision. As such, caution should be placed on using blanket percentages and proscriptive transect spacing for ultimate surveys. However, model-based and combined visual and digital approaches are also very attractive for estimating population size in the survey region. For instance, they can be less sensitive to unequal survey coverage in the region.

Caution should also be placed on carrying out extensive post-hoc subsampling of areas for comparisons over different periods of time due to the influx and outflux of populations (Burt et al. 2009). Careful surveys need to be set up to detect reliable changes in such areas over time, for example, using rigorous date-specific surveys in design-based estimates also controlling for influx in the area through completed surveys in a single day, or prediction for equivalent dates from modelled surfaces and smooth date-trendsin general additive models.

Temporal Sampling Coverage of Survey

A recent review of high-resolution methods (Thaxter and Burton 2009) highlighted that a survey cannot cover different subsections of an area on different days due to the mobile nature of birds and

mammals, which would therefore risk double counting the same birds in a different area on another day. At very least it was recommended that where a survey cannot cover an area in one, consecutive days are preferable, and if possible surveying the same area again on another day can reduce coefficients of variation in final population estimates. However, recent developments in this protocol have allowed for alternating transect lines to be covered on different days; therefore, still covering the same target area, but not precisely the same lines as before. This enables increased coverage of the whole area as well. This situation is highlighted in Figure 4–16, whereby alternating A and B lines are conducted on different surveys. This approach is currently being undertaken in some Round 3 surveys.

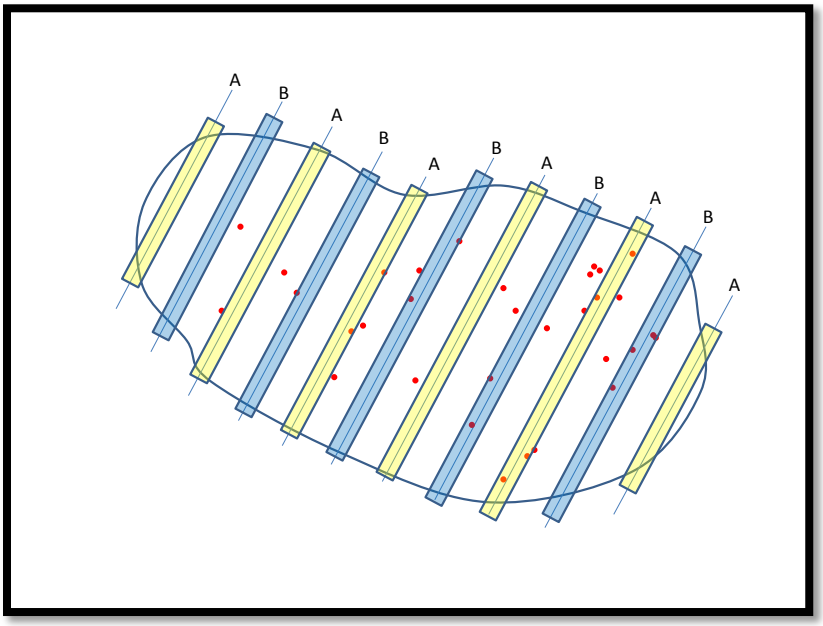

Figure 4–16. Alternating transects pattern with A transects covered on day 1 and B transects covered on day 2 to enable full target coverage of the zone.

Seasonal variation is something to be considered as well in survey design. For current Round 3 digital surveys in the UK, surveys are being conducted at least once a month. This approach allows population estimates to be produced for target species for the area on a month by month basis, and seasonal patterns (e.g., passage movements, summer, and winter) can be investigated in more detail. Such seasonal approaches can be highly informative to EIAs where different species grouping may be present at different times of the year. In particular, foraging areas connected with particular breeding colonies may be captured during surveys, therefore picking up a large breeding seabird component from those colonies. However, it is highly unlikely that the same species will remain present throughout the year. Different species will pass through the area, including waterbirds and other migrants, and potentially species not recorded during summer months. Therefore, surveys should be conducted at least once a month to capture such seasonal variation. Further consideration would also need to be given to whether those populations occur in nationally or internationally

important numbers, with reference to the appropriate citations giving populations throughout the biogeographic range. The only way to get a handle on whether these thresholds are met is through repeated monthly surveys. Likewise, annual variation in monthly abundance is often very variable, hence monitoring over longer periods has been desirable in UK digital surveys.

4.4 Aerial High-resolution Wildlife Imaging Survey Protocols

4.4.1 Introduction

In this section, we provide protocols for conducting digital aerial high-resolution wildlife imaging surveys covering the US AOCS for the purpose of providing the necessary ecological data to support a commercial offshore wind leasing program. These protocols were developed based on the research, information synthesis, and experimental results of this study, drawing on the expertise of the entire project team. The specific geographic area covered is defined by BOEM regulatory jurisdiction and by developability for offshore wind, and extends from the northern end of the Maine coast to Miami, Florida, from the states' seaward boundaries (3 nautical miles from shore) outward to the 30 m isobaths (Figure 4–17). For each protocol, we have identified a complete set of vehicle, hardware, and methodological recommendations for obtaining the desired data with optimal safety and cost effectiveness based on the detailed evaluations of technology, methodology, scientific requirements, and various other considerations contained in other chapters of this report. For each protocol, we have identified approximate levels of effort and other costs necessary to execute the protocols, under costing assumptions explained in the sections below. Our intent was to make these protocols as operational and feasible as possible, and to provide all of the information necessary for consideration and execution of these protocols within this chapter.

Our protocols include recommended survey frequencies or intervals over the course of a single year, but they do not include recommended study durations in terms of numbers of years. All protocols in this chapter are presented as 1-year studies, which we regard as a minimum recommendation for any of the protocols to encompass the complete spectrum of possible seasonal variations over the complete annual cycle.

Our choice to present the protocols in 1-year formats was made for convenience and is not a recommendation of the 1-year duration. We anticipate that our annualized descriptions of tasks, effort, and costs can easily be converted into multiyear protocols. To further facilitate this, we have included information on how all of the various labor components scale with survey effort. For example, some tasks and associated labor components are one time only components, such as survey design/planning and imaging hardware/mount design and development. Other tasks and associated labor components scale directly with the extent of flight time (e.g., onboard personnel labor), data gathered (target identification and data QA/QC), or the number of continuous survey segments or bouts (equipment mobilization/demobilization). The number of years over which survey protocols should be conducted depends on the extent of interannual variation in the phenomena of interest. Currently, this is not well-known for marine wildlife populations and communities of the US AOCS. However, it is important to note that interannual variation is only one of many important scientific phenomena that can be illuminated with offshore high-resolution imaging survey data; hence, the second year of survey data is likely to have significantly lower marginal scientific value than the first, and the marginal value will continue to diminish with each additional year of data gathering thereafter.

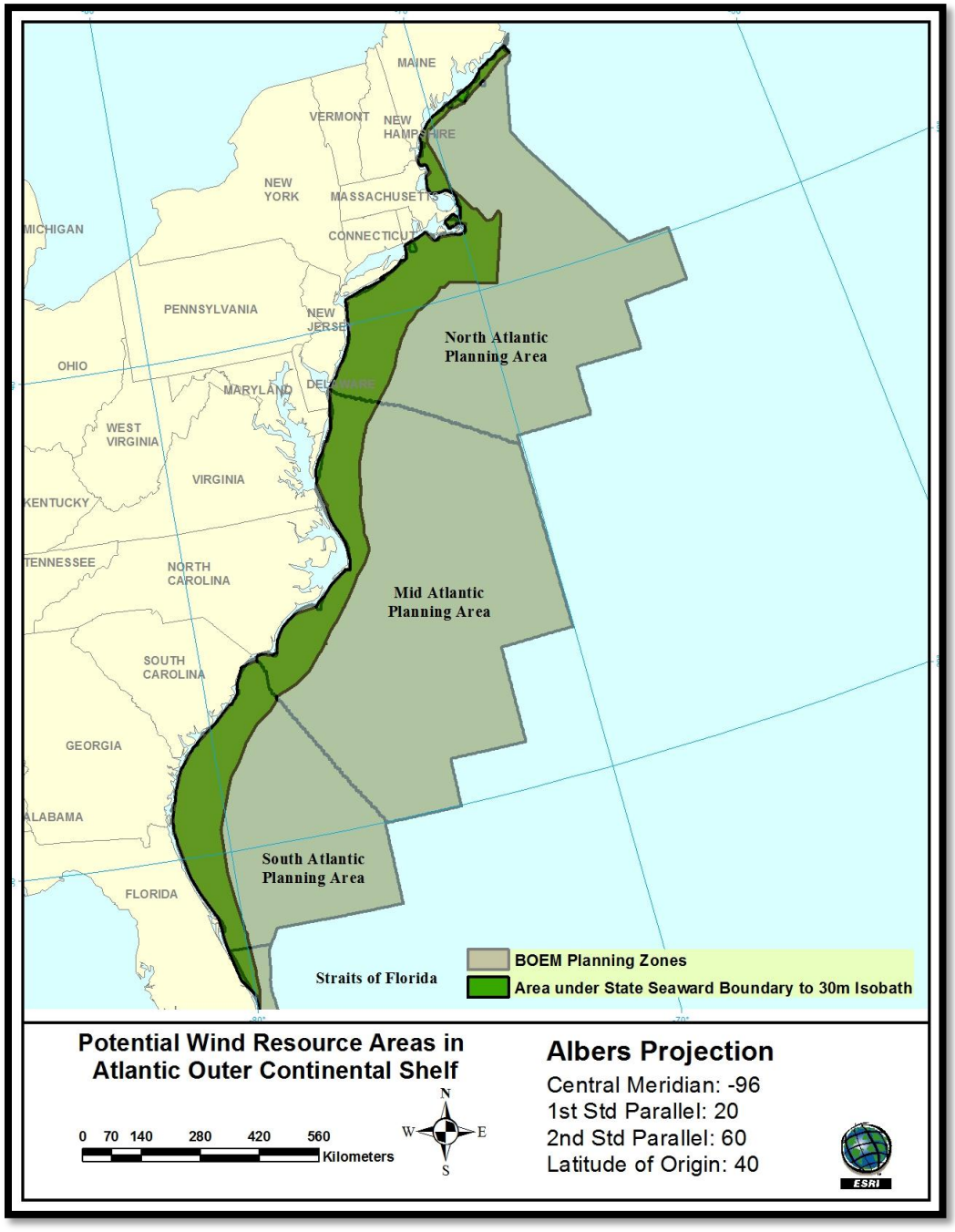

Figure 4–17. Potential wind resource areas in Atlantic Outer Continental Shelf (AOCS). The green area is the total area of interest for the protocols presented in this section, defined by BOEM regulatory jurisdiction and developability for offshore wind using current technology.

4.4.2 Taxonomic Scope

Because of the comprehensiveness of the required environmental risk analyses, we define the biological scope of these protocols to include all taxa for which high-resolution diurnal aerial imaging surveys are expected to provide high quality data suitable for addressing the relevant ecological risk/impact issues. This includes all species of marine turtles and mammals that regularly occur within the AOCS, as well as 84 species of birds that regularly occur within the AOCS for more than ephemeral, transitory passage. A guide to the nature, extent, and quality of data that can be expected for each of these taxa from high-resolution aerial imaging surveys is presented in section 6.4 of this report.

4.4.3 Target Detection Software

One key assumption for all of the protocols outlined in this chapter is the availability of image processing software that automates the process of initially detecting animals in the recorded imagery. This is an essential step for cost-effective analysis, as under normal circumstances, data volumes will be extremely large, and the overall densities of animals will be extremely low. A preliminary version of such software was developed for this project using the experimental images gathered under this project on the AOCS of North Carolina in May 2011, as an adaptation of pre-existing target detection software owned by the imaging and image processing specialized subcontractor on this project, Boulder Imaging (see Chapter 0). It is important to note that the version of target detection software developed for this project is preliminary, and would require significant additional development before it effectively serves the purpose of automated animal detection in offshore aerial high-resolution wildlife survey imagery, as is assumed in the protocols presented in this chapter.

In Europe, where high-resolution aerial imaging surveys have become widely used for offshore wind environmental studies, automated animal detection software has been developed and refined over a number of years by several private firms each possessing highly specialized internal image processing expertise, and each of whom regards such software as valuable intellectual property. In addition to a robust, pre-existing automated target detection algorithm, effective functioning of automated target detection software for offshore aerial high-resolution wildlife imaging surveys in any particular region requires adaptation of pre-existing software to the visual appearance of the specific wildlife, potential confusion objects (e.g., *Sargassum* algae), and water appearance present in the specific region being surveyed. It is essential that the application of effective automated animal detection software be incorporated into any consideration of performing offshore aerial high-resolution wildlife imaging surveys in US waters. Furthermore, it is also essential to include a provision for quality assurance and control of automated target detection algorithms within any high-resolution imaging project. This entails manual review of subsets of imagery to assess false positive and false negative rates for specific types of animals in the automated target detection process, essential for assessing and reporting animal detection success rates. Such quality assurance and control review processes are a standard component of the application of high-resolution imaging surveys to offshore wind environmental studies in the UK, and should be regarded as an integral part of any survey protocol.

4.4.4 Three-scale Approach

We developed a three-scale approach to high-resolution AOCS marine wildlife imaging survey protocols. This approach arose from the recognition that biological objectives, biological dynamics,

and costs are not identical at different spatiotemporal scales, hence optimal survey methodologies vary across scales. Relatively crude information is often satisfactory for larger area surveys, while small area surveys typically require higher levels of biological precision. For this reason, we have created three distinct protocols for high-resolution digital marine wildlife imaging surveys, corresponding to three distinct spatial scales, with higher levels of biological precision at smaller scales. Definitions of the three scales and general descriptions of the differing protocol considerations at these scales follow.

AOCS Scale

The entire US portion of the AOCS encompasses 1,090,000 km^2. Of this, about 210,000 km^2 can be regarded as potentially developable for offshore wind using current technology and under US federal jurisdiction, and is located between the states' seaward boundaries and the 30m isobaths (green area in Figure 4–17). At the largest spatial scales, broad baseline information is needed to characterize the distributions of general types of animals within the area of interest. This corresponds roughly to a baseline characterization (Thaxter and Burton 2009), in which somewhat crude scales of taxonomic, spatial, and temporal resolution can effectively serve the purpose of the survey, and allow an entity who may be interested in such a large area, such as a federal agency, to cost effectively gather data at this scale.

Regional Scale

We defined the regional scale as 25,000 km^2 based on the general size of the area that would need to be surveyed for offshore wind leasing studies within individual BOEM planning regions. This general scale of protocol should also be applicable to state-by-state subdivision of the federally regulated, developable AOCS (e.g., baseline studies of single state portions of the AOCS). At this scale, federal entities, states, or multistate consortia may be interested in gathering information at intermediate taxonomic and spatiotemporal scales for studies with more specific biological objectives and data gathering requirements than an AOCS-wide baseline study, but less detailed data gathering needs than a project-specific study. This generally corresponds to Environmental/Biological Assessment or Stock Assessment scale described by Thaxter and Burton (2009), and may include NEPA analyses of the AOCS at the state or planning region scale.

Project Scale

We defined the project scale as 150 km^2 based on the general size of the area that might be proposed for a typical, commercial-scale offshore wind project. This corresponds to roughly twice the size of the original Cape Wind project area, and would likely accommodate 200 to 250 commercial marine wind turbines at typical turbine spacing. At this scale, private developers would be required to gather information at fine taxonomic and spatiotemporal scales required for their permitting studies, corresponding to the Project-specific Assessment described by Thaxter and Burton (2009).

Many of the protocol elements are the same for all three scales; however, some elements are specific to particular survey scales. We discuss the protocol elements common to all scales and scale-specific protocol elements separately in the next sections of this chapter. All of the protocols presented in this report have been developed using manned, fixed wing aircraft as the survey platform. We expect that much of the information contained within these protocols regarding optimum imaging parameters and flight patterns would apply equally well to protocols using UAS survey platforms. However,

many aspects of such protocols would be different. Further research into feasible UAS-based solutions, as well as changes to current FAA UAS permitting guidelines would be required to develop realistic, practical, and cost-effective protocols for using UASs in offshore aerial high-resolution wildlife imaging surveys.

4.4.5 Protocol Elements Common to All Three Scales

Flight Altitude

To avoid turbine rotor collision and wildlife disturbance, aerial imaging surveys should be carried out from a minimum altitude of 450 m. In the protocols outlined in this chapter, we recommend a flight altitude of 600 m above sea level, although adaptations of this protocol for flight altitudes ranging from 450 to 1,200 m may be optimal in some circumstances (e.g., higher altitude to accommodate extremely wide survey swaths)

Flight Direction

The protocols developed in this section assume that all flights are strictly east–west, alternating with west–east, with 180° turns interspersed. Although successful protocols could be developed for many different flight directions, we used strictly easterly and westerly flight directions as a convenient solution for mitigating sun glare effects (see section 4.2)

Flight Speed

Our protocols are designed for an aerial survey speed of 277.8 km/hr (150 kts). Slower speed can give clearer pictures and may prove useful in assisting identification of species, but current speeds in the range of ca. 220 to 350 km/hr are appropriate as images at these speeds are suitable in many instances for identification of birds to the species level. Furthermore, higher speed can increase cost effectiveness as long as image quality degradation is minimal, particularly for large-scale surveys.

Environmental Conditions

A detailed study of region- and season-specific weather patterns should be carried out before planning the survey to take into account the days expected to be unsuitable for surveying due to adverse weather conditions. Thaxter and Burton (2009) recommended avoiding surveying through low clouds and in conditions in excess of Beaufort Scale 4 (excessive waviness) to ensure that birds are not missed and that they are correctly identified. In addition, low elevation fog will create unsuitable conditions for aerial imagining surveys.

Color

Color images should be used in all surveys.

Cameras

Our protocols are designed for an imaging setup that includes two 29 MP Imperx ICL/IGV-B6620C-KF0 cameras, mounted in a unique arrangement that would need to be custom built for these surveys (see below for mount details). The camera model we selected for these protocols is the new generation of 29 MP sensor that has gained ascendancy in the market in the time since our experiments were originally designed and conducted. This is essentially a refinement of the camera that proved most successful in our flight trials with the manned aircraft-based imaging system in our study, the Imperx Bobcat ICL-B4822C-KFO 16 MP area-scan camera (see section 3.3). The new

camera is smaller, has a shutter speed that is twice as fast as its predecessor, and draws less power. Most importantly, its image resolution is 81% larger than the 16 MP sensors, meaning that a larger image can be obtained at a higher altitude and the same or higher resolution image can be gathered at the same altitude. This new camera is shown in Figure 4–18, and its current market price is $16,995. We recognize that camera technology is changing rapidly, and we expect that as newer cameras with larger megapixel capacity become available, they will be substituted into the protocols presented in this chapter. Such advances will reduce the overall costs of executing the protocols, as they will enable wider survey swaths, and hence larger areas to be imaged per kilometer of flight distance, reducing the extent of flights necessary to conduct the surveys.

Figure 4–18. ICL/IGV-B6620C-KF0 29 megapixel camera recommended for use in the high-resolution aerial wildlife imaging survey protocols presented in this chapter.

Each camera is fitted with Sigma APO 120-300mm F2.8 EX DG OS HSM lens (Figure 4–19). This lens was selected based on its ability to achieve image resolution of 1 cm on the ocean's surface at flight altitudes up to 600 m, image resolution of 2 cm on the ocean's surface at flight altitudes up to 1,200 m, and contains the following characteristics:

- Adjustable focal length from 100 to 600 mm
- Aperture of f/2.8 @ 300 mm, f/5.6 @ 600 mm
- Manually adjustable aperture
- Length of assembly at 600mm < 15 inches
- Maximum diameter of assembly < 4.5 inches
- 35 mm sensor coverage
- Depth of field at 1,200 m altitude, 2 cm image resolution of at least 200 m

Under some circumstances, the addition of a Sigma 2×Tele-converter (Figure 4–19) may be desirable to double focal length while maintaining mount capability. However, even though it doubles the attainable resolution, is also introduces a point that transmits vibrations that can significantly degrade image quality. Therefore, it is likely that better images will be obtained without the teleconverter in most cases. The current market prices of lens and converter are US $3,200 and US $300, respectively.

Figure 4–19. Sigma APO 120-300 mm F2.8 EX DG OS HSM lens and tele-converter recommended for use in the high-resolution aerial wildlife imaging survey protocols presented in this chapter. The use of the teleconverter may not be optimal in many cases because of the potential to exacerbate vibrational effects (see text).

Imaging Rate

We have incorporated an imaging rate of three frames per second into the protocols presented in this chapter, which produces overlapping sets of images at the indicated flight speed, equivalent to video data gathering methods that have been described in previous studies (Thaxter and Burton 2009). During the experimentation conducted for this study, the area-scan camera was run consistently at three frames per second. Depending on resolution/flight altitude and the position of the animal within the imaging swath, this provided one to six images of each animal. Our analysis revealed that multiple pictures of each animal enhanced the ability of image analysts to identify the taxonomic identity of animals (see section 6.3). However, we recognize that high frame capture rates add costs by increasing the volume of data collection. An alternative method is to use slower frame capture rates, producing nonoverlapping series of stills (Thaxter and Burton 2009). Video and stills methods are more or less equivalent in their effectiveness for producing statistically robust density estimates of animals (Buckland et al. 2012); hence, we regard both stills and video methods as viable solutions (Thaxter and Burton 2009; Buckland et al. 2012).

Camera Tilt and Gyrostabilization

Camera tilt and gyrostabilization are two of the most important issues for successful imaging. Our protocols assume that the cameras are mounted so that they can be tilted up to 45° forward or 45° backward (front-back axis of aircraft), and are adjustable in flight by the operator, so that they can be pointed westward in the morning and eastward in the afternoon, regardless of flight direction. This is a crucially important equipment parameter for mitigating glare effects, and is equivalent to the adjustable mount that was envisioned in the third set of simulations in the glare mitigation section of

this chapter (see section 4.2). Furthermore, we recommend that all cameras be gyrostabilized, as the gyrostabilizer resulted in a significant improvement in image quality in our experiments (see section 3.3).

Internal Camera Mount

Our protocols have been developed for a unique mount that accommodates the camera tilt, adjustability, and gyrostabilization requirements described in the previous paragraph. Such a mount would need to be custom designed and built for these surveys. The design of such a mount was conceived by the project's aviation and imaging experts based on pre-existing expertise, a review of current practices in aerial high-resolution imaging surveys by other practitioners, the experience gathered over the course of our imaging flight experiments, and the unique needs of the surveys envisioned in the protocols. The specific design elements and rough costs of developing the mount are described herein.

The protocols presented in this report require the following parameters be met in the camera mounting system:

- The cameras are mounted inside the plane, viewing water below through a belly hatch. This is preferable to external mounts because of increased operator access, reduced vibration, and increased protection of imaging equipment from precipitation.
- Two cameras are mounted, each with a lens that is 7 inches long and 4 inches wide, to achieve the desired image resolution of 1 cm at 600 m flight altitude or 2 cm at 1,200 m altitude.
- The cameras need to be able to be tilted up to 12.5° to the side to produce juxtaposed images on the water's surface, effectively doubling the survey swath width over that of a single camera.
- The cameras need to be able to be tilted up to 45° forward and 45° backward, adjustable in flight by the operator, so that they may always be oriented westward in the morning and eastward in the afternoon, regardless of whether the aircraft is flying to the east or to the west.
- The cameras are mounted with gyrostabilizers in order to enhance image quality (reduce blur).

Although internal camera mounts are used extensively today in aerial photography, the aerial camera systems typically used in such applications are not suitable for the purpose of conducting high-resolution aerial wildlife imaging surveys. Typically aerial cameras are used to cover larger target areas, and do not possess the high-resolution needed for high altitude marine wildlife surveys. However, the mounting method used by traditional aerial photography operators is generally suitable for high-resolution wildlife surveys, as long as the camera port is large enough to accommodate the stabilization and camera angle adjustability required. In such systems, cameras are mounted above a viewing window in the belly of the fuselage with access through the floor of the cabin.

Our protocols have been developed for three specific aircraft, two of which already possess sufficient camera ports (or hatches) in the belly, and one of which does not (see below). If a sufficient camera port does not already exist in an aircraft that has been selected for an imaging survey, the aircraft must be modified to create such a port, ideally in the belly of the plane, through which imaging will occur. One point that must be considered if such modifications are undertaken is the fact that the fuselage belly skin is separated by some distance from the cabin floor. In larger aircraft this distance may be significant enough to limit the camera's field of view, similar to looking through a cardboard box with the bottom cut out. The image below is an example of a camera port on a smaller, single engine Cessna aircraft and illustrates this point (Figure 4–20).

Figure 4–20. Example of a typical camera port in the belly of a small aircraft. The yellow area, internal to the camera hatch, represents the distance between the internal floor of the cabin and the external skin of the aircraft, which can constrain available camera angles (see text).

In Figure 4–20, the painted (white) fuselage skin has been cut and fairings added to streamline the installation. Additionally, the reader can see yellow painted structural members visible inside the opening. Above these structural members is the cabin floor. In this installation, the distance from the belly to the cabin floor is a few inches. However, in a large aircraft this distance may be as large as several feet. This gap between the skin and floor is utilized not only for structural elements of the aircraft, but also to route electrical wiring, flight controls cables, hydraulic lines, or even fuel lines. Often, when installing a camera hatch, structural modifications must be made in addition to rerouting electrical wiring or hydraulic lines.

Installing a camera port in an aircraft requires careful planning and skilled technicians to accomplish the work. In addition, FAA approval is required to certify that the aircraft remains in an airworthy

and safe condition after the installation is completed. This approval may be in the form of a one time, field approval accomplished via a FAA Form 337 (Major Repair and Alteration form). However, if the installation is to be used extensively on a certain make and model of aircraft, the designer may seek a Supplemental Type Certificate (STC) from the FAA. An STC is essentially FAA approval to modify an aircraft from its original design. This process results in a blanket approval to make the alteration to the aircraft make and model listed on the STC. This is historically a time-consuming and expensive process depending on the complexity of the design modification and requires engineering, flight testing, careful documentation, and certification. STCs are also used for installing updated avionics, skis, speed enhancements, or electrical improvements to aircraft.

To accommodate the camera and mounting requirements recommended in our protocols, mounting the high-definition camera system will require a large camera port. Port size must be sufficient to allow two cameras to view their respective, adjacent target areas through the hole and also permit the two cameras to be mounted at various angles without obstruction (see above). For example, NOAA's fleet of De Havilland Twin Otter marine aerial survey aircraft are reported to have 18 × 16-inch camera ports in the belly (T. Cole, pers. comm. 2011). This is fully sufficient to satisfy the requirements stated above. By contrast, a 6-inch camera port, as illustrated in Figure 4–21, would be too small to allow more than one camera to be mounted in the port, or to allow sufficient camera angle flexibility.

Figure 4–21. Cabin view of a 6-inch diameter tubular type camera port (indicated by the yellow arrow). This type of camera port would not be sufficient for conducting the aerial imaging survey protocols described in this report (see text).

Once the sufficiency of the camera port has been established, the mount must be developed and installed. Various commercial systems are available to mount commercially available aerial photography cameras such as the popular Zeiss series (Figure 4–22). This large format camera system is used extensively in commercial aerial photography. A secure mount is provided to mate the camera system to the opening in the aircraft floor.

Figure 4–22. Zeiss Jena LMK 2000 mapping camera mounted in a Cessna 206.

Although the commercial mounts shown in Figure 4–21 and Figure 4–22 are perfectly suitable for some types of commercial photography, they are not suitable for the unique mounting requirements of marine high-resolution aerial wildlife imaging surveys. Most mounts, including the mount shown in Figure 4–22, are designed to mate a large format commercial camera to the camera port. Some, such as the T-AS mount, also incorporate gyrostabilization to further reduce the effects of vibration on the image quality (Figure 4–23). As discussed in section 3.3, gyrostabilization is essential in any mounting system for the extremely high-resolution imaging systems discussed in this report. Therefore, gyrostabilization must be incorporated into the proposed belly port camera mounting system.

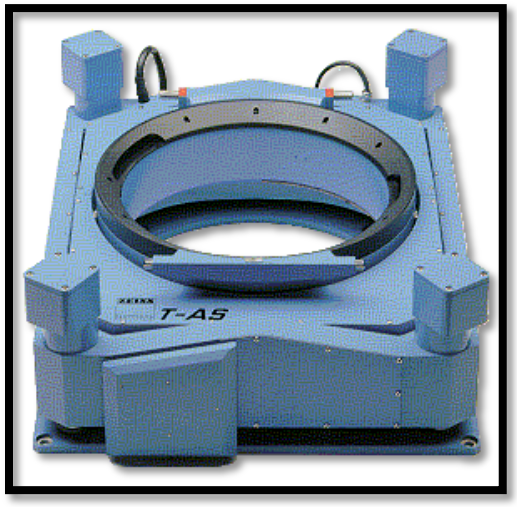

Figure 4–23. T-AS gyrostabilized suspension mount.

Given the specific mounting requirements of the protocols presented in this chapter, a custom engineered and fabricated camera mounting system will be required, as no suitable commercial mounts are available. In addition, the entire camera/mount assembly must be gyrostabilized, requiring isolation mounts between the camera mount and the aircraft structure. These isolation mounts will allow the gyrostabilizers to stabilize the mount and not attempt to stabilize the entire aircraft. In other words, the mount assembly must float to some degree for the gyrostabilizer to work effectively.

Specialized mounts are not uncommon as new technology is applied to aerial sensing and imaging. For the purpose of the protocols presented in this chapter, the custom mount must accommodate two separate cameras. Each individual camera mounting bracket must be adjustable both side to side, and fore and aft as specified above. Additionally, each individual camera mounting bracket must accommodate precise angle measurements by the operator. This mount will require extensive engineering, design, and testing prior to installation in the aircraft.

We have incorporated a rough description and approximate costs into the protocols presented in this report to enable effective planning, scoping, and provisioning of future high-resolution aerial marine wildlife survey efforts using these protocols. An example of a specialized, custom designed and fabricated camera mount similar to the one that would need to be constructed for this protocol is illustrated in Figure 4–24. In this example, the designer, Gyromounts.com, created a gyrostabilized table which allows various sensors, antennas, or cameras to be mounted to a rolling or banking vehicle. This example uses a KS-8 electric gyrostabilizer similar to the one used in the imaging experiments that were conducted for this project on the Skymaster (manned aircraft, see section 2.2). The overall structure of the mount illustrated in Figure 2–3 provided a suitable, gyrostabilized framework for mounting cameras at the angles and positions that were required for that specific application.

Once such a mount has been constructed and integrated into the survey aircraft, electrical power will need to be supplied either via the aircraft power system or from carry-on battery packs. Once fully installed, the entire system and mount will require ground and flight testing and FAA airworthiness determination, as was accomplished with the Skymaster camera system for the experimental imaging system used for this project during the Op House imaging experiments (section 2.2).

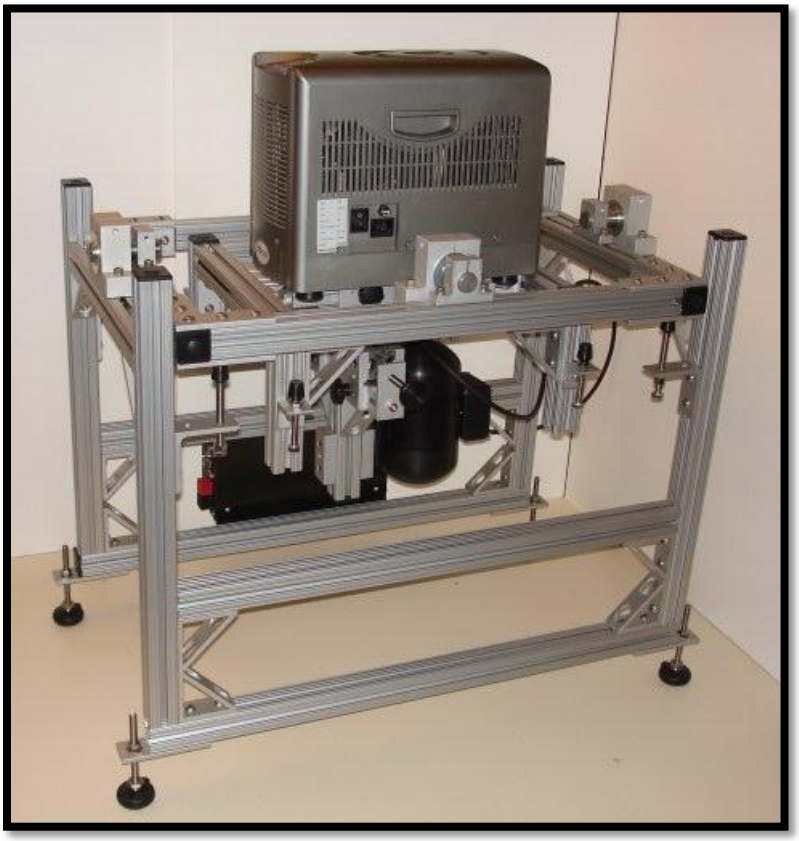

Figure 4–24. An example of a custom designed and fabricated by Gyromounts.com, gyro-stabilized camera mount similar to one that is envisioned for the high-resolution offshore wildlife imaging protocols presented in this chapter.

Rough Order of Magnitude Costs

Gyrostabilized Camera Mount:

- Engineering, design, fabrication, and testing: $80,000
- Each additional mount: $25,000

Camera Port

The camera port is completely dependent on aircraft model and whether a suitable camera port STC is available or a previous Form 337 installation was approved for the same model aircraft. Starting from scratch, installing a large camera port in a large twin engine or turbine aircraft could cost more than $100,000 per installation, depending on how much structural work needs to be done. In the protocols presented in this report, we assume that new camera ports would need to be created in the Kodiak 100 aerial survey aircraft (USFWS), but not in the De Havilland Twin Otter (NOAA) or Partenavia-Vulcanair P68 aircraft recommended for chartering for regional and project scale protocols, as the latter two aircraft already possess suitable camera hatches.

On-board Data Recording and Storage Devices

The data recording system required for onboard acquisition and storage of image data would be similar to the one utilized in the imaging experiments with the manned aircraft system undertaken for this study, Boulder Imaging's Quazar VR400R, which costs approximately $30,000 per system (one system per aircraft) (see sections 2.2 and 3.5). The specifications for a system sufficient to serve the purposes of data recording and storage onboard the aircraft for the protocols described in this report are as follows:

- Support high-resolution imaging
- Recording from multiple inputs
- No loss of data recording
- GPS input
- Long recording duration with high rates
- Fast data transfer
- Resistant to aircraft vibrations and shock
- Appropriate size, weight, and power

Land-based Data Transfer and Storage Devices

After each day of imaging flight survey, image data and metadata would need to be transferred to backed up, land-based data storage systems at the field sites. This would be accomplished using portable hard drives. At the end of each survey bout, data would be transferred to permanent servers for subsequent processing, analysis, and archival. This transfer would be accomplished by shipping one set of drives containing one copy of the data to the home office of the entity where manual image review and data analysis would occur.

Labor Effort

At all three scales, the aerial survey protocol consists of seven general tasks, with each task containing a set of subtasks, and would be conducted by a project team requiring a certain set of personnel with specific areas of expertise to perform specific roles on the project. The tasks of the protocols and the composition of the project team required to conduct them are described in this section. Although the basic nature of the project tasks and the personnel required to perform them is generally constant across the three scales of survey protocols, the amount of labor effort needed for the different tasks may vary across the scales depending on the nature of the tasks, as described below.

Project Team Composition

Project Manager: The role of the project manager is to coordinate and direct the entire project team through all phases of the project to ensure the successful completion of the protocol. The project manager should be an experienced senior staffer with a high level of scientific expertise (e.g., an advanced degree in biological sciences) and also excellent skills and experience with managing staffers, subcontractors, and complex projects.

Project Coordinator: The project coordinator is primarily responsible for assisting and supporting the project manager by carrying out administrative tasks associated with executing the project that do not require technical expertise. Such tasks include subcontracting, invoices and payments to subcontractors and service/equipment providers, and making logistical arrangements for field surveys.

Pilot: Skilled and appropriately licensed pilots are required for operation of the aircraft. While one pilot per aircraft is a minimum requirement, having two pilots aboard each flight is preferable for added safety, in the event that one pilot becomes incapacitated during flight for any reason. For the cost calculations, we have incorporated pilot labor into the aircraft hourly charter fees, as is normally done for commercial chartering, for the regional and project scale protocols. For the AOCS-scale protocols, we assume that government staff pilots are used; hence, we use lower hourly rates for aircraft utilization that were provided by the agencies of interest (USFWS and NOAA-NMFS for Kodiak 100 and De Havilland Twin Otter fleets, respectively), corresponding to the estimates of hourly flight cost that they have estimated.

Aviation Engineer: One or more aviation engineer(s) are required to design, fabricate, install, and test the camera mounts, as well as any modifications that need to be made to the camera ports in the aircraft to conduct the survey. The aviation engineers must possess the specialized technical knowledge and experience necessary to perform these roles, as well as knowledge of FAA procedures and requirements for the types of aircraft modifications and airworthiness determinations that are entailed in adapting or otherwise preparing aircraft for imaging surveys as described in this report.

Principal Scientist: One or more biologists with advanced degrees are required to assist the project manager in researching and designing an optimized survey design for the unique marine fauna of the region to be surveyed, and also to conduct the scientific analysis, interpretation, and write-up of the data that results from the survey. Normally, some advanced expertise in the areas of marine birds, marine mammals, and sea turtles will be required; therefore, this role will often be filled by multiple scientists. Depending on the type of analysis to be conducted, expertise in conducting GIS-based spatial ecological analyses may be required, as well as advanced statistical expertise, and familiarity with the concepts and technical literature of marine ecology.

Biological Technician: One or more biological technicians are required to support the extraction of biological data from the gathered images. Although automation of animal recognition in the imagery is required and assumed to allow for efficient and cost-effective processing of extremely large volumes of image data, taxonomic identification of imaged animals is expected to be performed by biological technicians who are familiar with visual recognition of the marine fauna of the imaged region, based on their manual examination of the images of the detected animals. This process will

normally entail multiple biological technicians to be able to include some control of observer effects through double review processes, and also to ensure that technical expertise of the observers includes all of the taxa (e.g., birds, mammals, turtles). Furthermore, the biological technicians will also support quality assurance and control of the automated animal recognition algorithm function by manually examining subsets of the imagery to be able to calculate false positive and false negative rates for the algorithm. Biological technicians will also support the work of the principal scientists, performing scientific tasks associated with data entry, organization, and analysis as they are capable.

Imaging Engineer: The imaging engineer has primary responsibility for image acquisition, as well as early image processing (automated animal detection). One component of this role is the design and development of the onboard imaging system, including cameras, optics, data recording equipment, camera calibration and control mechanisms. The imaging engineer is also responsible for developing, applying, and quality assuring and controlling the function of the automated animal recognition algorithm that is essential as a first step for cost-effective processing of extremely large volumes of image data. As such, two distinct but overlapping areas of high level engineering expertise are required within the image engineer category—imaging and image processing. The imaging engineer(s) must possess advanced engineering degrees with significant experience in these areas.

Imaging Technician: Because of the highly specialized nature of the imaging equipment, an imaging technician is expected to be aboard all imaging flights to calibrate the equipment at the beginning of the flight, and to ensure successful operation of the equipment during all imaging flights. This technician does not need to possess the level of training, experience, and expertise of the imaging engineer, but must be able to operate and troubleshoot the imaging equipment in flight, and to work with the aviation team for successful mobilization and demobilization of the imaging equipment, as it is integrated into an aircraft, pretested, and subsequently removed from the aircraft.

Project Tasks

Study Design and Planning: This involves creating an appropriate study design based on the scientific objectives of the project. This includes mapping out the area to be surveyed, developing the transect pattern, survey frequency and imaging protocol, taking into consideration the sun glare, weather conditions, expected species present, and any other factors germane to the design of the surveys. During this task, the entire data gathering and analysis effort are anticipated and planned out to best meet the scientific objectives of the project. This is a one time task that occurs during the early part of the project, and is primarily undertaken by the project manager and principal scientists, with input from the imaging and aviation engineers, as well as the client, to optimize the feasibility, practicality, cost effectiveness, and scientific validity of the study within the constraints of the project budget and timeline, guided by the project's objectives. Larger scale protocols will require larger study design and planning efforts, but not in proportion to survey size, as some economy of scale is expected.

Project Management: This task includes all personnel and/or subcontractor management for the assembly, coordination, supervision, and administration of the project team required for the implementation of all stages of the survey project; hence, this task lasts throughout the life of the project, and is the primary responsibility of the project manager with support from the project

coordinator. Some project management subtasks will be one time only, while others are expected to scale with the number of survey bouts or the total imaging transect length flown.

Imaging System Development, Integration, and Pretesting: During this task, imaging engineers develop and assemble the complete imaging system, including cameras, optics, and onboard data recording and storage system. Imaging engineers then coordinate with aviation engineers, who perform any engineering work necessary to integrate the imaging equipment into the aircraft. This includes any necessary modifications to the aircraft in cases where a sufficient camera hatch does not already exist on the aircraft, as well as the design, fabrication and installation of the camera mount. This imaging equipment is then integrated into the aircraft and pretested, including flight tests, to obtain FAA airworthiness approval and certification, and to ensure that the entire imaging system is functioning properly within the aircraft. This task is coordinated and overseen by the project manager with assistance from the project coordinator, but most of the labor effort is on the part of the imaging and aviation engineers and technicians. This is a one time effort at the beginning of a project, and does not include routine mobilization and demobilization of the imaging system for each survey (included in survey execution, below). This task will be less intensive for projects using imaging aircraft and equipment that have been previously developed and used for high-resolution aerial imaging surveys. For the protocols presented in this chapter, we assume that a new system must be developed. The effort required for this task is expected to be similar between regional and project scale surveys, both of which are expected to utilize a single aircraft and set of onboard imaging equipment. For AOCS-scale surveys where four aircraft equipped with onboard imaging equipment are expected to to utilized simultaneously, the effort required for this task is expected to be approximately four times as great as for either of the other two scales.

Survey Execution: The execution of surveys is primarily performed by two pilots flying the aircraft, as well as an onboard imaging technician as a strict function of flight time, as these three personnel are assumed to be onboard all survey flights. This task also includes a variety of labor effort expenditures that are assumed to be a function of the number of continuous survey segments or bouts, defined as periods within which a particular survey aircraft conducts surveys on consecutive, or nearly consecutive, days (e.g., includes brief weather or logistical delays). Survey execution labor components that are per segment include logistical coordination, undertaken primarily by the project coordinator as directed by the project manager, as well as routine mobilization and demobilization of the imaging equipment by the aviation engineer and imaging technician, assuming that the imaging equipment would need to be removed from the aircraft in between survey segments, as would normally be the case for charter or other multipurpose aircraft. To ensure that field surveys are completed smoothly and successfully, with the entire team working in coordination, we have assumed that a project coordinator visits the field site once for each survey bout. We have also assumed that the project manager occasionally visits the field sites to support the project coordinator, and that the imaging and aviation engineers occasionally visit field sites to assist the imaging technician with ensuring that imaging equipment and mounts are functioning properly. We note that for the AOCS scale, where we assume that a dedicated fleet of government aircraft are used for surveys, mobilization and demobilization effort and cost associated with survey execution can be eliminated if there is no need to remove and reinstall imaging equipment in between survey segments.

Data Extraction and Automated Image Processing: Our protocols assume that the previously developed automated target (animal) detection process occurs in real time during the survey flights, such that potentially huge image data volumes are reduced, containing primarily of frames in which potential animals have been detected by the automated animal detection algorithm. In addition to this filtered image data, the onboard data recorder should record and retain periodic subsamplings of complete, raw (unfiltered) image data, which will subsequently be used to determine false negative rates of the target detection algorithm. After the execution of each day of survey effort, all of the retained image data, as well as complete survey metadata, must be transferred from the onboard data storage system to a secure, backed up, land-based data storage system. After the completion of each survey segment, all recorded data will be transferred to permanent, backed up servers for subsequent data processing steps. This task primarily entails effort on the part of the imaging technician who manages the early stages of image data capture, automated processing, storage, and transfer in the field, as well as the project coordinator, who coordinates the transfer of all data to the permanent storage system and data analysis team. Although we assume that an adequate automated target detection algorithm already exists prior to the project, we also assume that in the application of most, if not all high-resolution imaging survey protocols, some ongoing review and adjustment of the automated target detection algorithm's performance and function will be necessary on the part of the imaging team. We include such efforts in this task of the project, as a function of the extent of time and space covered by the protocol, as such development work will be a function of the breadth and variety of different animals and environments in which imaging is conducted, though significant economies of scale are achieved with larger survey areas.

***Target Identification, Quality Control, and Initial Manual Data Processing*:** This task entails identifying all of the imaged targets (animals) using identification manuals, measurements, and other literature resources, performed by biological technicians who are experienced and capable at the identification of the full range of animals expected to occur within the imagery, based on visual examination of the imagery. This task also entails verifying and organizing the geoposition, time stamps, and other metadata so that data files can be produced into formats suitable for GIS-based, statistical, and other scientific analysis processes. In addition, this task includes all manually performed QA/QC checks, such as review of raw image segments for false negative rate measurement, multiple observer review of data subsets for observer effect control and identification confidence assessment, and general review and verification of data and metadata validity and accuracy. Effort during this task will primarily be undertaken by the biological technicians, and will scale directly with the quantity of data gathered as a function of total transect length imaged, although we expect that some efficiencies will be gained for larger projects.

***Data Analysis and Reporting*:** Once the imaged animals have all been identified, and the data have all been sufficiently QA/QC checked, reviewed, organized, and assembled, scientific analysis of the data will be undertaken primarily by the principal scientists and project manager. The nature and extent of this analysis will be driven by the project's objectives, and is likely to include spatiotemporal analysis of animal distribution and abundance, as well as risk characterization, entailing the application of GIS, statistics, modeling, and/or other scientific analytical techniques. This task will also include the interpretation of observed results in the context of previously published studies and other ideas synthesized by the principal scientists (including the project manager) from technical literature, and based on their own scientific judgment and expertise.

Additionally, this task includes the preparation of presentations and reports from the final data analysis and interpretation. Labor in this phase is assumed to scale with total data volume, with substantial economies of scale achieved for larger projects. Additional effort that would be entailed in subsequent agency consultation, permitting processes, or the preparation of NEPA documents is not included in our protocols.

Labor Effort Scaling Factors

As discussed in the previous section, different elements and subtasks within each of the different general project tasks scale differently with project size for a variety of reasons. In this subsection, we provide two tables that serve as a general guide to some of this variation. Table 4–10 illustrates how some of the most important scaling factors vary across the three spatial scales of protocols we have developed. Table 4–11 illustrates roughly how the labor effort required for each of the seven general project tasks is expected to vary across the three different scales of protocols. These factors are discussed in the text above, and are incorporated into our cost estimates for each of the three protocols at the end of this section.

Table 4–10.

Scaling Factors Associated with Three Scales of Aerial Offshore High-resolution Imaging Survey Protocols—Values in Parentheses Represent the Size of the Given Value Relative to the Size of the Corresponding Value for the Project scale Protocol (x)

Scaling Factor (unit)	AOCS Scale	Regional Scale	Project Scale (x)
Survey area (km^2)	210,000 (1,400x)	25,000 (167x)	150
Segments (bouts)	8 (x)	4 (0.5x)	8
Total transect length (km)[1]	154,864 (72x)	78,528 (36x)	2,160
Aircraft	4 (4x)	1 (x)	1
Aircraft survey days	100 (13x)	39 (5x)	8

[1]including all repeat surveys, i.e., 1 km surveyed 4x/year = 4 km of transect

Table 4–11.

Labor Effort Scaling by Task, Associated with Three Scales of Aerial Offshore High-resolution Imaging Survey Protocols

Task	AOCS Scale	Regional Scale	Project Scale (x)
Design/planning	4x	2x	x
Project management	8x	4x	x
Develop, integrate, pretest imaging equipment	4x	x	x
Execute surveys	15x	15x	x
Data extraction/automated image processing	10x	5x	x
Target identification, manual data processing	50x	30x	x
Data analysis, interpretation, reporting	6x	3x	x

Note: Values reported for the larger scale protocols represent the amount of overall labor effort relative to the project scale protocol (x). These values represent composites of the different personnel, and the different subtasks that compose each general project task (see text for rationale and assumptions).

4.4.6 Scale-specific Protocol Elements

Atlantic Outer Continental Shelf (AOCS) Scale

The AOCS scale survey protocol covers the broadest possible spatial scale, encompassing the entire 210,000 km^2 extent of the US AOCS from the states' seaward boundaries out to the 30 m isobaths (Figure 4–25). At this scale, the primary scientific objective is likely to be correspondingly broad in scope, for example to provide a baseline of background information on marine wildlife distribution and abundance over the entire US AOCS to serve as a foundation for understanding the potential environmental impacts of offshore wind energy development within this region. The broad and general nature of the most likely scientific objectives of such a survey enable a somewhat coarser approach to data gathering than is recommended for the smaller scale surveys. This coarseness is essential for practicality and affordability because of the inherent cost and operational challenges entailed with conducting surveys of such a large area. Because of the unique and very large spatial extent of this survey, we have developed this protocol with a number of features, as follows:

Spatial Extent

The entire US AOCS encompasses 1,090,000 km^2. Of this, about 210,000 km^2 can be regarded as potentially developable for offshore wind using current turbine and foundation technology, and under US federal jurisdiction, located between the states' seaward boundaries and the 30 m isobaths (Figure 4–25). This entire area is selected as the survey area in the AOCS-scale protocol.

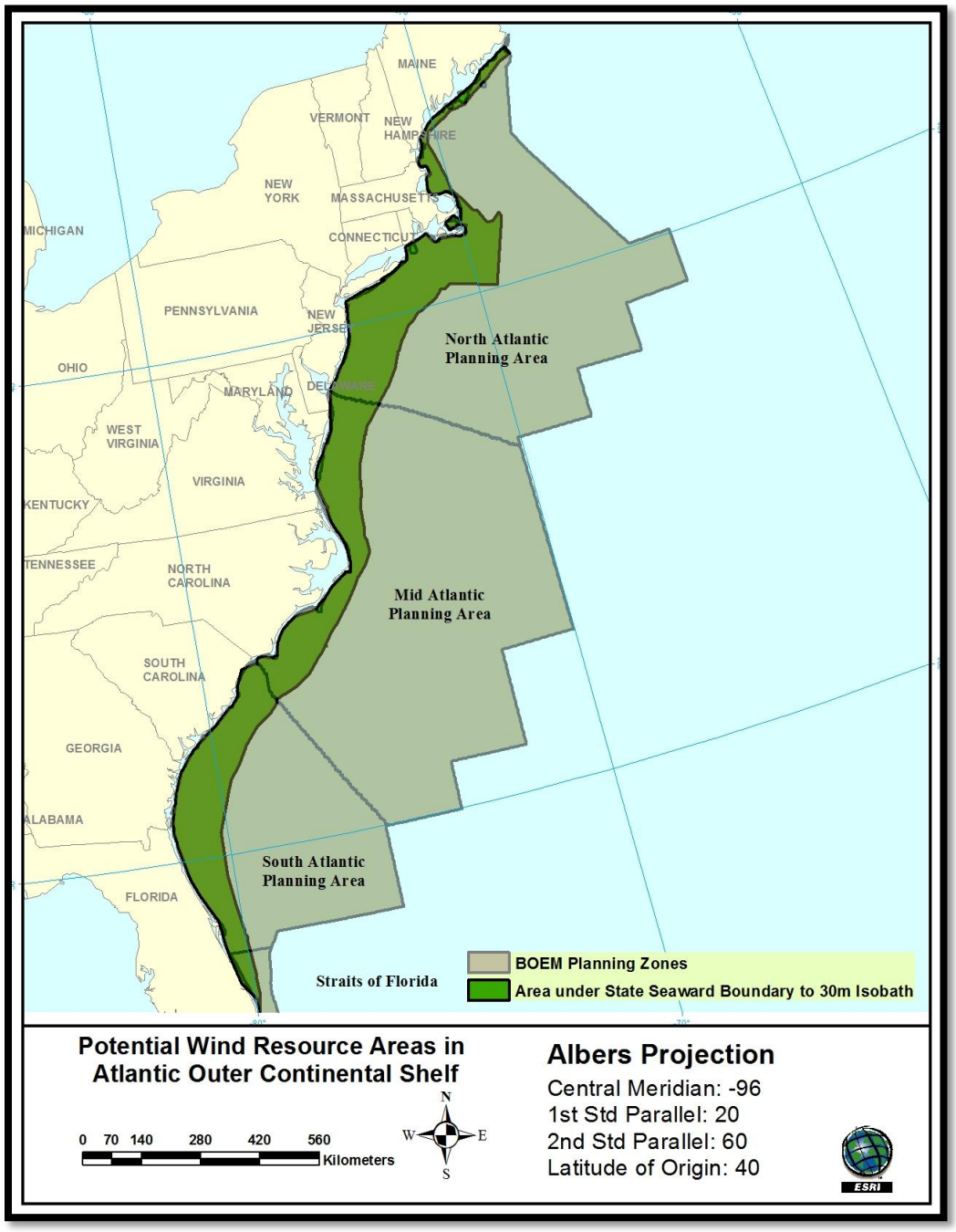

Figure 4–25. Potential wind resource areas in Atlantic Outer Continental Shelf (AOCS).

Sampling Frequency and Timing

We recommend that this entire region be surveyed twice per year: once during the middle of the warm season (between late May and early August), and once during the middle of the cold season (between late November and the end of February). This timing is selected to satisfy the objective of

characterizing marine wildlife distribution during the two relatively sedentary (i.e., nonmigratory) periods of the year. While characterization of migration patterns is important, it would require relatively rapid sampling of the entire study region, so that animals on the move are not double counted or missed by survey efforts that move at equal or slower rates. Such rapid sampling is not practical for such a large area with current technology. The omission of migratory periods is justifiable in the context of the broader, coarser scientific objectives that are likely to shape the design of an AOCS-wide baseline study, as this protocol would still produce a robust and extensive characterization of all animals' nonephemeral occupancy of any and all portions of the region of interest. We note that migratory movements can occur throughout the year, particularly for such a broad spectrum of animals, and that the particular dates and timing may be adjusted based on taxonomic priorities. The dates listed above were selected to exclude the bulk of the migratory periods for the majority of bird species that spend either the warm season or the cold season within the study region.

Aircraft

After considering all factors, we determined that using multiple aircraft, each conducting simultaneous surveys in different portions of the study area, was the optimal solution for the AOCS-scale protocol. Using fewer aircraft would entail subsampling less than 10% of the total area, individual survey durations longer than the entire warm or cold seasons, image resolutions too coarse for sufficient taxonomic identification of imaged animals, or survey swaths larger than can be obtained with current imaging technology. The principal challenge of conducting a survey of such a large area, and of using multiple planes simultaneously, is cost. For this reason, we developed this survey protocol for two aircraft fleets currently owned by US federal government entities, and intended for the purpose of conducting large scale aerial wildlife surveys. In both cases, four aircraft are potentially available for conducting simultaneous surveys. Furthermore, assuming that these fleets would be utilized and that the protocol would be conducted by the government agency that owns and operates these fleets allows the reasonable assumption that the aircraft acquisition costs, as well as the labor costs of the aviation engineers and pilots, do not need to be incorporated into the overall project costs.

The two fleets for which we developed this protocol are the USFWS fleet of Kodiak 100 aircraft and the NOAA-NMFS fleet of De Havilland Twin Otters (Figure 4–26a and Figure 4–26b, respectively). Both types of aircraft were included in our review and evaluation of candidate aircraft, and both are generally suitable for the purpose of conducting this protocol (see section 3.2 for complete evaluations and comparisons of these aircraft with other candidates). The Kodiak 100 is a single engine turbine plane designed for bush-type travel. The USFWS currently uses its fleet of Kodiak 100s for continental scale surveys of North American waterfowl breeding populations, breeding habitat, and wintering sea duck distributions on the AOCS. One unique consideration of using the USFWS Kodiak 100 fleet for conducting AOCS-scale offshore high-resolution wildlife imaging surveys is that sufficient camera hatches would need to be installed in each plane (see section 4.4.5). The NOAA fleet of De Havilland Twin Otter (DHC-6) aircraft have been used for offshore surveys from Alaska to the Caribbean for many years, and are currently used for visual observer based marine wildlife surveys under the auspices of the AMAPPS project. Each of these aircraft has a large fuselage with a 16″ × 18″ belly hatch that is capable of fitting the mounts and cameras intended for this protocol described earlier (Figure 4–26c). The endurance of the Kodiak 100 is 6 hours while that

of the Twin Otter is 7 hours; hence, the specific transect flight plans we have developed for each of these fleets are slightly different, assuming 5 and 6-hour maximum flight durations for the Kodiak 100s and Twin Otters, respectively (see below). The cost of operation for the Twin Otters is also slightly higher than is that of the Kodiaks, primarily because of fuel consumption rates.

a. b. c.

Figure 4–26. Aircraft selected for AOCS-scale high-resolution offshore aerial wildlife imaging survey protocols: a) Kodiak 100, the survey aircraft owned by the USFWS and currently used for continental-scale, visual observer-based waterfowl surveys, b) De Havilland Twin Otter, the survey aircraft owned by NOAA-NMFS and currently used for large-scale, visual observer-based marine wildlife surveys, and c) the belly hatch on a De Havilland Twin Otter aircraft where cameras could be mounted for high-resolution imaging surveys. Kodiak 100s do not have a camera hatch, and would need to be modified and camera hatches installed for the aircraft to be suitable for conducting offshore wildlife imaging surveys.

Image Resolution

The recommended image resolution for this large scale survey is 2 cm, meaning that 1 pixel of the image corresponds roughly to 2 cm^2 of the water's surface, given the flight altitude and optical magnification of the image (see section 3.3 and Chapter 1 for complete discussions of image resolution technique and effectiveness). This image resolution is coarser than the 1 cm resolution recommended for the smaller scale survey protocols, which will result in less refined taxonomic identity discrimination in the imaged animals. However, it is still within an acceptable range for the purposes of a broad ecological baseline characterization study (see Chapter 1), and it enables twice as much area to be imaged per unit of flight time, which is essential for cost-effective coverage of such a large area. This difference in image resolution between AOCS scale and both of the smaller scale survey protocols results in corresponding differences in shutter speed, camera orientation and survey swath, and flight transect spacing.

Shutter Speed (Exposure Time)

The exposure time is the time that the shutter remains open when taking a photograph. Exposure time must be carefully chosen to prevent motion blur across pixels during exposure of each individual frame. Exposure time can be calculated based on ground speed of the imaging platform and imaging resolution (see below). When the speed of the aircraft is 277 km per hour, the amount of time the imaging platform takes to move 1 pixel (2cm) is ~260 µs. Therefore maximum exposure

time for each frame is 260 µs. If exposure time is set to 260 µs or less, each pixel in the image will contain data for exactly 1 pixel on the ground, with no motion blur present across pixels.

The fundamental calculation is:

277 km / hr = 2 cm / Exposure time (hr)

*Exposure time (µs) = 2 cm * 1*60*60*1,000,000 µs / 277 *1,000*100 cm*

=~260 µs

Camera Orientation and Imaging Swath Width

Two cameras would be mounted side by side, each tilted 12.5° to the side. This would result in the cameras taking adjacent, side by side images on the water's surface. At 2 cm resolution for the 29 MP images taken by these cameras, the result would be a total survey swath of 264 m (see also earlier camera description).

Extent of Spatial Subsampling

We recommend subsampling 10% of the entire study area in the AOCS-scale survey protocol, following the recommendation of Thaxter and Burton (2009).

Number of Transects and Spacing

Given the imaging swath width of 264 m and the 10% recommended subsampling level, the recommended spacing between the transects in the AOCS-scale protocol is 2.64 km. This spacing was used in the analysis below to develop the specific survey transect patterns for this protocol.

General Survey Pattern

The protocol we have developed entails flying four imaging aircraft simultaneously to conduct semiannual imaging surveys that collectively encompass the entire region of interest. Each of these four aircraft would cover roughly one quarter of the north–south extent of the area of interest, and each survey would entail each aircraft conducting a single pass through its assigned portion of the region, requiring from 10 to 16 days of surveying (see detailed breakdown below). Allowing for weekend days off and roughly 1 day of weather-related delay per week, we expect that each survey of the entire region would last for roughly 4 weeks. This would be conducted twice per year, hence in summary, eight total 4-week surveying bouts would be conducted each year: four simultaneous bouts with four aircraft each assigned to one quarter of the total region in summer, and four simultaneous bouts with the same four aircraft in winter. Specific survey patterns for each of these four aircraft are provided below.

Available Low Glare Daylight Survey Hours:

The amount of available survey time varies as a function of two factors. The first is day length, which varies with both latitude and calendar date. The second is suitability for capturing low glare images, which is a function of the ability of the mount to achieve ADGS values below the 67° suitability threshold (see section 4.2 for explanation of terms and discussion of glare impacts and mitigation). We calculated available daylight hours for low glare surveying for each locality at each time of year as follows: We assume that camera mounts are adjusted in flight between two available

camera angles (see mount description) to maximize ADGS on each flight transect, assuming alternating east–west and west–east flight directions. This essentially entails always pointing the camera westward in the morning and always pointing the camera eastward in the afternoon regardless of flight direction (see section 4.2). We then used the formula for calculating ADGS presented in section 4.2 to determine the total number of daylight hours during which ADGS under 67° could be achieved for each imaging location in each survey season.

Specific Flight Patterns

Specific transect flight patterns were developed for each of the four aircraft as follows: the number of available daylight hours in which low glare imaging could be achieved was calculated for each region and time of year (see above) and was regarded as the maximum flight time in a day; and specific transect paths were mapped using the specific boundaries of the portion of the AOCS of interest in each quarter region, and applying strictly east–west, and west–east flights in an alternating pattern, spaced at 2.64-km intervals. Using the endurance of the aircraft minus 1 hour as a maximum flight duration, and assuming that the nearest available airport for refueling was 40 km away from the last transect completed before the need to refuel, the total transect paths in each quarter region were divided into individual flight bouts as they would fit into the available low glare survey time per day, assuming airspeed of 278 km/hour.

The resulting transect patterns, along with accompanying descriptive data on the survey parameters, are detailed below for each of the four aircraft in each season, and for each of the two different types of aircraft envisioned.

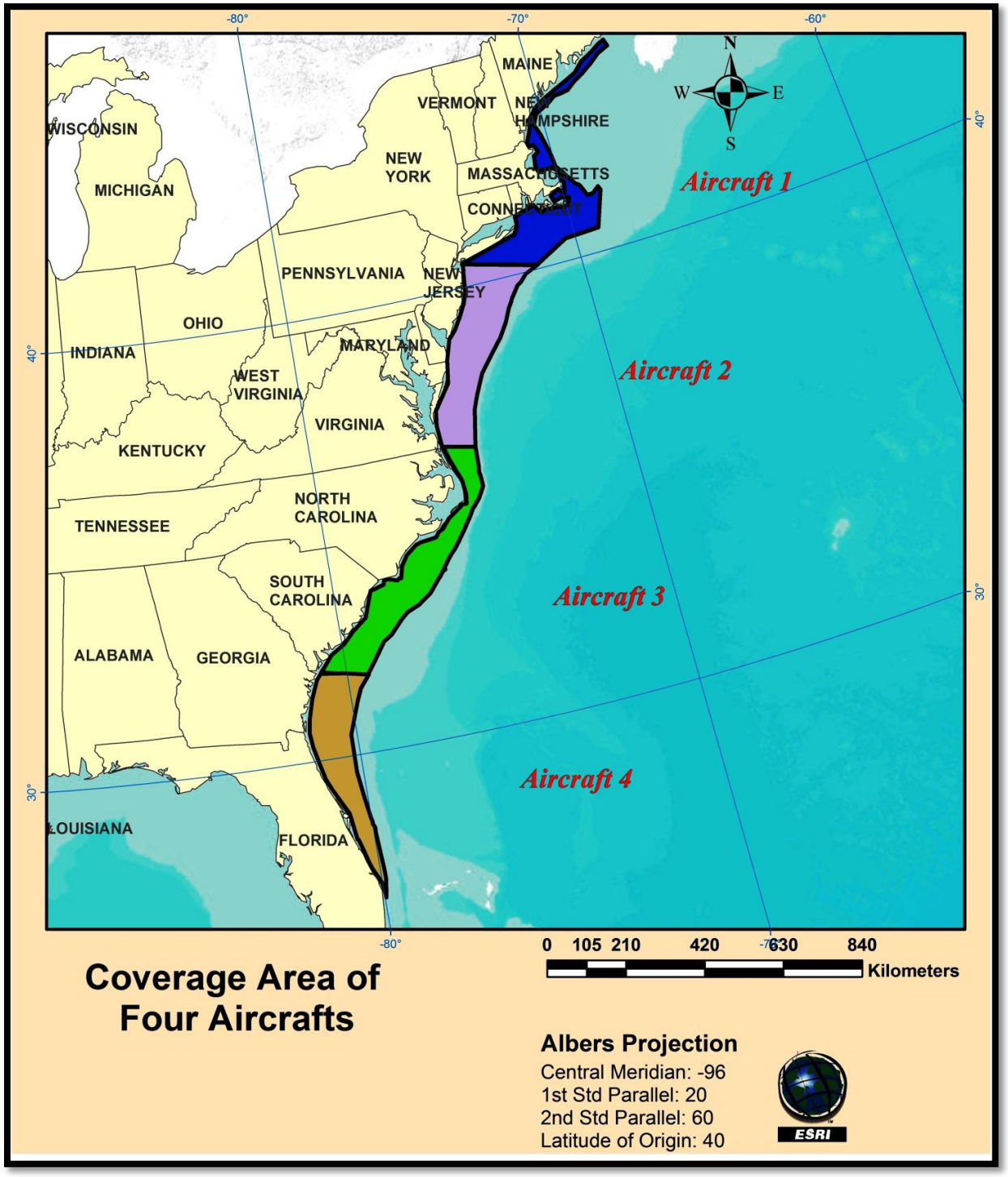

Figure 4–27. Total area surveyed in the AOCS-scale high-resolution wildlife imaging survey protocol, divided into four differently colored regions corresponding to the portions of the total region covered by each of the four imaging aircraft envisioned in this protocol.

Flight Patterns of the Individual Aircraft in the Atlantic Outer Continental Shelf-scale Protocol

Aircraft 1. The first aircraft will cover the northernmost quarter of the study region, extending from Maine southward through New York (Figure 4–28). The north–south coastal length of this segment is approximately 600 km, and the area is approximately 45,000 km^2. With the assumptions described above and presented in Table 4–12, the total flight distance to complete one pass through this survey area is estimated at 18,168 km or 18,079 km for Kodiak 100 and Twin Otter aircraft, respectively, including refueling trips and flights between transects (Table 4–12). The cost for the aircraft operation per season is $15,619 for the Kodiak 100, and $21,760 for the De Havilland Twin Otter (Table 4–12), which only includes the fuel and other basic operating costs of these aircraft, because we assume that government-owned aircraft are utilized in this protocol.

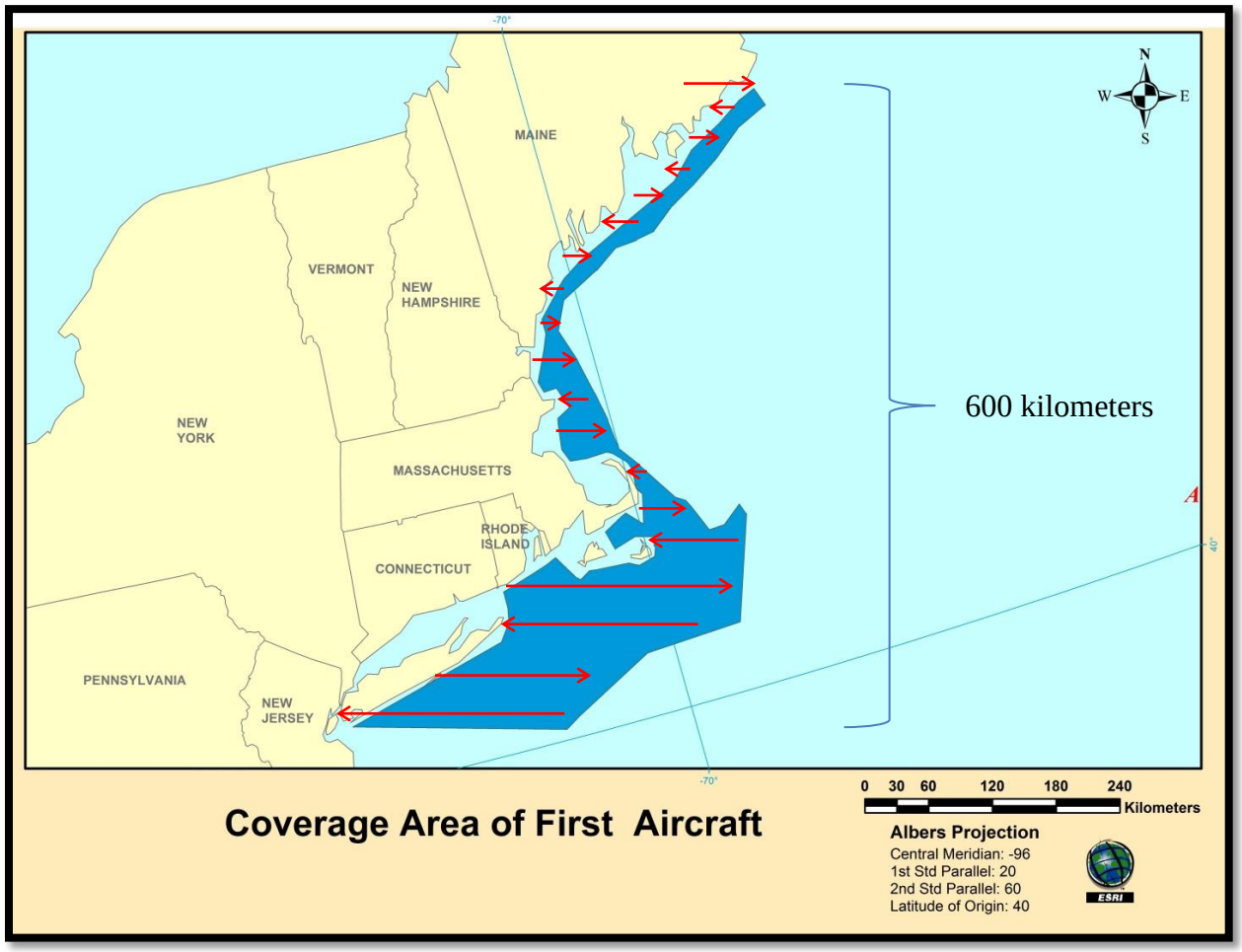

Figure 4–28. Survey area (dark blue) and general survey pattern of the northernmost of four aircraft engaged in the Atlantic Outer Continental Shelf (AOCS)-scale high-resolution wildlife imaging survey protocol. The red arrows indicate the general structure of individual flight transects; however, they do not illustrate the actual transect pattern, which entails 227 individual flight segments spaced at even, 2.64 km increments along this 600 km span of the total AOCS survey area (Table 4–12).

Winter Survey

On the winter solstice (21 December), there are 9 hours of daylight during which images of acceptable glare levels could be collected given the imaging equipment and solar position, calculated for the central location of this segment, Gloucester MA (section 4.2). To accommodate some loss of available time due to adverse environmental conditions such as cloud cover and excessively rough seas, we assume that 6 hours are available each day for aerial surveys. This results in a total of 11 days required to complete a single pass through this area. To accommodate some loss of available survey days due to adverse weather, we assume that 13 survey days will be required to complete this portion of the survey during the winter season (Table 4–12).

Summer Survey

On the summer solstice (21 June), there are 12 hours of daylight during which images of acceptable glare levels could be collected given the imaging equipment and solar position, calculated for the central location of this segment, Gloucester MA (section 4.2). To accommodate some loss of available time due to adverse environmental conditions such as cloud cover and excessively rough seas, we assume that 8 hours are available each day for aerial surveys. This results in a total of 8 days required to complete a single pass through this area. To accommodate some loss of available survey days due to adverse weather, we assume that 10 survey days will be required to complete this portion of the survey during the summer season (Table 4–12).

Table 4–12.

Aerial Survey Flight Details for the Northernmost of Four Aircraft in the Atlantic Outer Continental Shelf (AOCS)-scale High-resolution Imaging Survey Protocol

Item	Kodiak 100		Twin Otter	
	Amount	Unit	Amount	Unit
Total area	45,000	km^2	45,000	km^2
Area to be surveyed	4,500	km^2	45,00	km^2
Swath width	264	m	264	m
Total transect length	17,045	km	17,045	km
North–south coastal length	600	km	600	km
Total flight distance between transects	600	km	600	km
Number of Transects	227	times	227	times
Aircraft speed	278	km/hr	278	km/hr
Aircraft endurance	6	hrs	7	hrs
Survey time in one flight	5	hrs	6	hrs
Number of refuel trips	13	times	11	times
Refueling distance	40	km	40	km
Total refuel trip distance	523	km	434	km

Item	Kodiak 100		Twin Otter	
	Amount	Unit	Amount	Unit
Total flight length	18,168	km	18,079	km
Flight cost per hour	239	$	335	$
Flight hours required for survey	65	hrs	65	hrs
Total cost of flight per season	15,619	$	21,760	$
Low-glare imaging light/day (winter)	6	hrs	6	hrs
Low-glare imaging light/day (summer)	8	hrs	8	hrs
Number of days required (winter)	13	days	13	days
Number of days required (summer)	10	days	10	days
Total annual survey hours	131	hrs	130	hrs
Total annual survey days	23	days	23	days

Aircraft 2. The second aircraft will cover the quarter of the AOCS immediately south of the area covered by the first aircraft, including offshore of New Jersey, Delaware, Maryland, and Virginia (Figure 4–29). The north–south coastal length of this segment is approximately 490 km, and the area is approximately 56,870 km^2. With the assumptions described above and presented in Table 4–12, the total flight distance to complete one pass through this survey area is estimated at 22,684 km or 22,573 km for Kodiak 100 and Twin Otter aircraft, respectively, including refueling trips and flights between transects (Table 4–12). The cost for the aircraft operation per season is $19,502 for the Kodiak 100, and $27,201 for the De Havilland Twin Otter (Table 4–12), which only includes the fuel and other basic operating costs of these aircraft, as we assume that government-owned aircraft are used in this protocol.

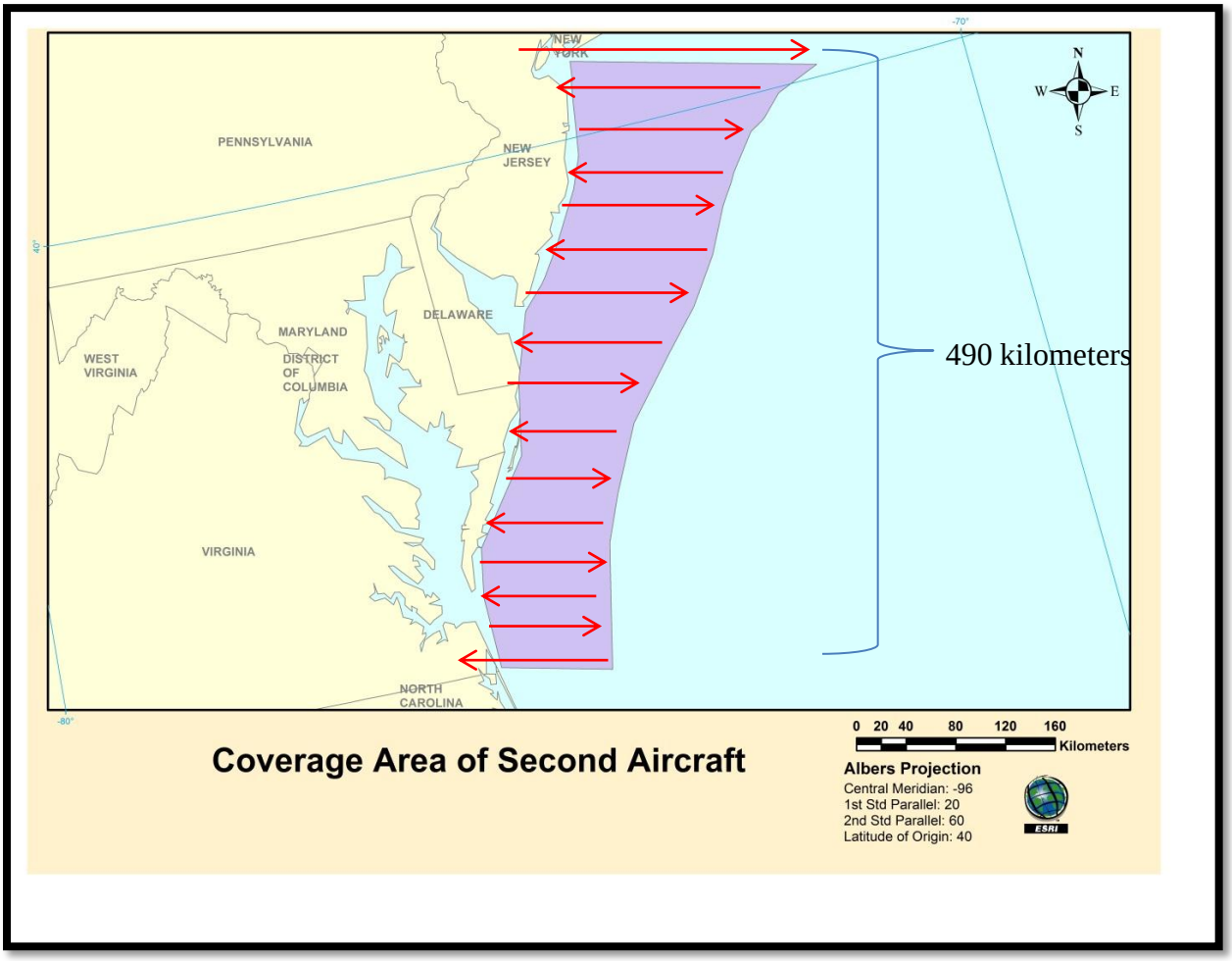

Figure 4–29. Survey area (purple) and general survey pattern of the second of four aircraft engaged in the Atlantic Outer Continental Shelf (AOCS)-scale high-resolution wildlife imaging survey protocol. The red arrows indicate the general structure of individual flight transects; however, they do not illustrate the actual transect pattern, which entails 186 individual flight segments spaced at even, 2.64 km increments along this 490 km span of the total AOCS survey area (Table 4–13).

Winter Survey

On the winter solstice (21 December), there are 9 hours of daylight during which images of acceptable glare levels could be collected given the imaging equipment and solar position, calculated for a central location of this segment, Ocean City MD (section 4.2). To accommodate some loss of available time due to adverse environmental conditions such as cloud cover and excessively rough seas, we assume that 6 hours are available each day for aerial surveys. This results in a total of 14 days required to complete a single pass through this area. To accommodate some loss of available survey days due to adverse weather, we assume that 16 survey days will be required to complete this portion of the survey during the winter season (Table 4–13).

Summer Survey

On the summer solstice (21 June), there are 12 hours of daylight during which images of acceptable glare levels could be collected given the imaging equipment and solar position, calculated for a central location of this segment, Ocean City MD (section 4.2). To accommodate some loss of available time due to adverse environmental conditions such as cloud cover and excessively rough seas, we assume that 8 hours are available each day for aerial surveys. This results in a total of 10 days required to complete a single pass through this area. To accommodate some loss of available survey days due to adverse weather, we assume that 12 survey days will be required to complete this portion of the survey during the summer season (Table 4–13).

Table 4–13.

Aerial Survey Flight Details for the Second of Four Aircraft in the Atlantic Outer Continental Shelf (AOCS)-scale High-resolution Imaging Survey Protocol

Item	Kodiak 100		Twin Otter	
	Amount	Unit	Amount	Unit
Total area	56,870	km^2	56,870	km^2
Area to be surveyed	5,687	km^2	5,687	km^2
Swath width	264	m	264	m
Total transect length	21,542	km	21,542	km
North–south coastal length	490	km	490	km
Total flight distance between transects	490	km	490	km
Number of Transects	186	times	186	times
Aircraft speed	278	km/hr	278	km/hr
Aircraft endurance	6	hrs	7	hrs
Survey time in one flight	5	hrs	6	hrs
Number of refuel trips	16	times	14	times
Refueling distance	40	km	40	km
Total refuel trip distance	653	km	541	km
Total flight length	22,684	km	22,573	km
Flight cost per hour	239	$	335	$
Flight hours required for survey	82	hrs	81	hrs
Total cost of flight per season	19,502	$	27,201	$
Low-glare imaging light/day (winter)	6	hrs	6	hrs
Low-glare imaging light/day (summer)	8	hrs	8	hrs
Number of days required (winter)	16	days	16	days
Number of days required (summer)	12	days	12	days
Total annual survey hours	163	hrs	162	hrs
Total annual survey days	28	days	28	days

Aircraft 3. The third aircraft will cover the quarter of the AOCS immediately south of the area covered by the second aircraft, including offshore of North Carolina and South Carolina (Figure 4–30). The north–south coastal length of this segment is approximately 610 km, and the area is approximately 56,384 km^2. With the assumptions described above and presented in Table 4–14, the total flight distance to complete one pass through this survey area is estimated at 22,618 km or 22,507 km for Kodiak 100 and Twin Otter aircraft, respectively, including refueling trips and flights between transects (Table 4–14). The cost for the aircraft operation per season is $19,445 for the Kodiak 100 and $27,122 for the De Havilland Twin Otter (Table 4–14), which only includes the fuel and other basic operating costs of these aircraft, as we assume that government-owned aircraft are used in this protocol.

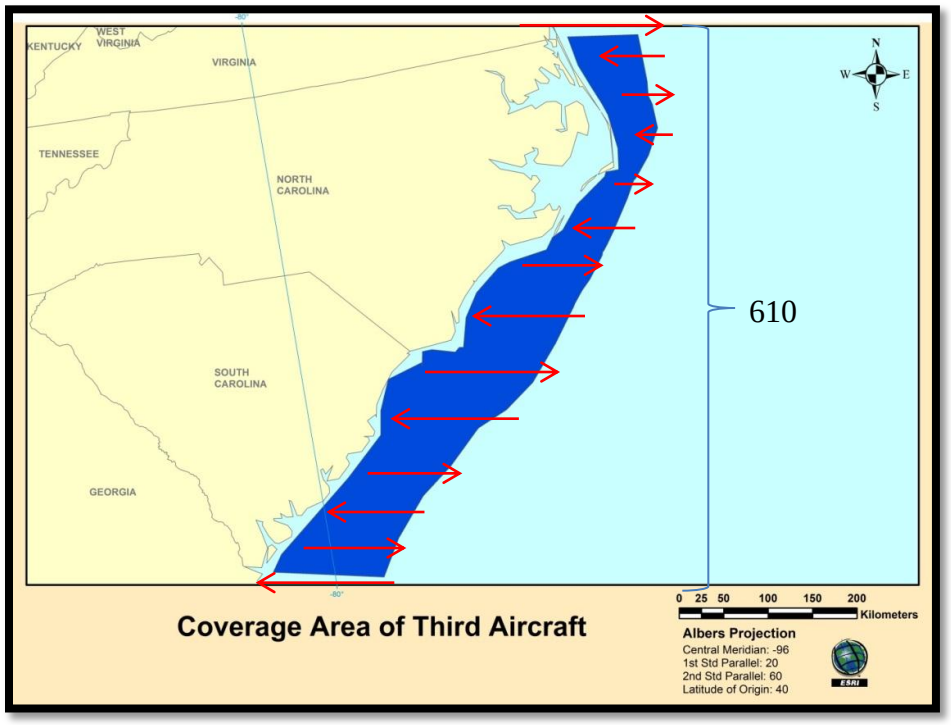

Figure 4–30. Survey area (dark blue) and general survey pattern of the third of four aircraft engaged in the Atlantic Outer Continental Shelf (AOCS)-scale high-resolution wildlife imaging survey protocol. The red arrows indicate the general structure of individual flight transects; however, they do not illustrate the actual transect pattern, which entails 231 individual flight segments spaced at even, 2.64 km increments along this 610 km span of the total AOCS survey area (Table 4–14).

Winter Survey

On the winter solstice (21 December), there are 10 hours of daylight during which images of acceptable glare levels could be collected given the imaging equipment and solar position, calculated for a central location of this segment, Oak Island NC (section 4.2). To accommodate some loss of available time due to adverse environmental conditions such as cloud cover and excessively rough seas, we assume that 7 hours are available each day for aerial surveys. This results in a total of 12 days required to complete a single pass through this area. To accommodate some loss of available survey days due to adverse weather, we assume that 14 survey days will be required to complete this portion of the survey during the winter season (Table 4–14).

Summer Survey

On the summer solstice (21 June), there are 11 hours of daylight during which images of acceptable glare levels could be collected given the imaging equipment and solar position, calculated for a central location of this segment, Oak Island NC (section 4.2). To accommodate some loss of available time due to adverse environmental conditions such as cloud cover and excessively rough seas, we assume that 8 hours are available each day for aerial surveys. This results in a total of 10 days required to complete a single pass through this area. To accommodate some loss of available survey days due to adverse weather, we assume that 12 survey days will be required to complete this portion of the survey during the summer season (Table 4–14).

Table 4–14.

Aerial Survey Flight Details for the Third of Four Aircraft in the Atlantic Outer Continental Shelf (AOCS)-scale High-resolution Imaging Survey Protocol

Item	Kodiak 100		Twin Otter	
	Amount	Unit	Amount	Unit
Total area	56,384	km^2	56,384	km^2
Area to be surveyed	5,638	km^2	5,638	km^2
Swath width	264	m	264	m
Total transect length	21,358	km	21,358	km
North–south coastal length	610	km	610	km
Total flight distance between transects	610	km	610	km
Number of Transects	231	times	231	times
Aircraft speed	278	km/hr	278	km/hr
Aircraft endurance	6	hrs	7	hrs
Survey time in one flight	5	hrs	6	hrs
Number of refuel trips	16	times	13	times
Refueling distance	40	km	40	km
Total refuel trip distance	651	km	540	km

Item	Kodiak 100		Twin Otter	
	Amount	**Unit**	**Amount**	**Unit**
Total flight length	22,618	km	22,507	km
Flight cost per hour	239	$	335	$
Flight hours required for survey	81	hrs	81	hrs
Total cost of flight per season	19,445	$	27,122	$
Low-glare imaging light/day (winter)	7	hrs	7	hrs
Low-glare imaging light/day (summer)	8	hrs	8	hrs
Number of days required (winter)	14	days	14	days
Number of days required (summer)	12	days	12	days
Total annual survey hours	163	hrs	162	hrs
Total annual survey days	26	days	26	days

Aircraft 4. The fourth aircraft will cover the southernmost quarter of the AOCS, including offshore of Georgia and Florida (Figure 4–31). The north–south coastal length of this segment is approximately 600 km, and the area is approximately 46,166 km^2. With the assumptions described above and presented in Table 4–15, the total flight distance to complete one pass through this survey area is estimated at 18,623 km or 18,531 km for Kodiak 100 and Twin Otter aircraft, respectively, including refueling trips and flights between transects (Table 4–15). The cost for the aircraft operation per season is $16,010 for the Kodiak 100 and $22,331 for the De Havilland Twin Otter (Table 4–15), which only includes the fuel and other basic operating costs of these aircraft, because we assume that government-owned aircraft are used in this protocol.

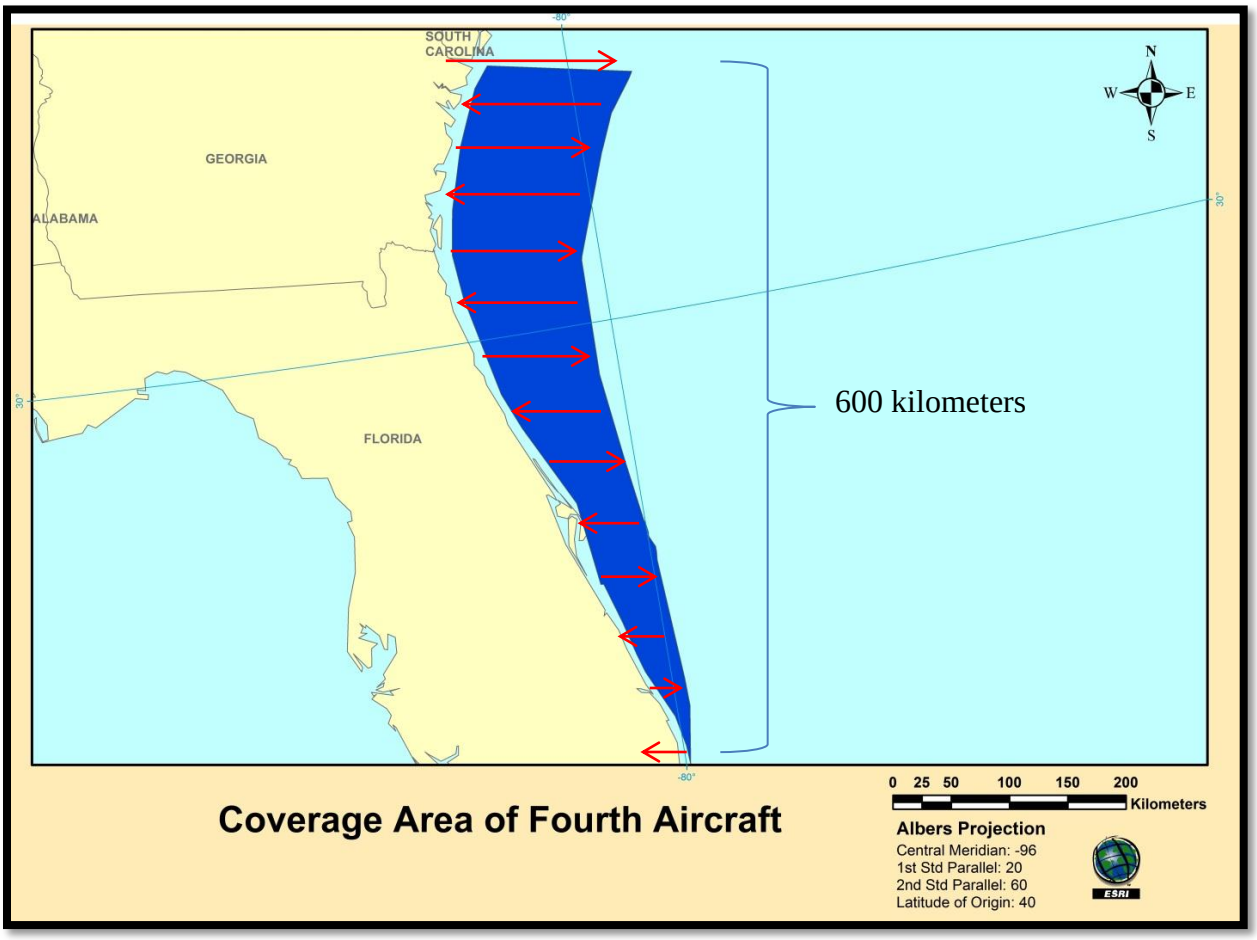

Figure 4–31. Survey area (dark blue) and general survey pattern of the fourth of four aircraft engaged in the AOCS-scale high-resolution wildlife imaging survey protocol. The red arrows indicate the general structure of individual flight transects; however, they do not illustrate the actual transect pattern, which entails 227 individual flight segments spaced at even, 2.64 km increments along this 600 km span of the total AOCS survey area (Table 4–15).

Winter Survey

On the winter solstice (21 December), there are 10 hours of daylight during which images of acceptable glare levels could be collected given the imaging equipment and solar position calculated for a central location of this segment, Palm Coast FL. To accommodate some loss of available time due to adverse environmental conditions such as cloud cover and excessively rough seas, we assume that 7 hours are available each day for aerial surveys. This results in a total of 10 days required to complete a single pass through this area. To accommodate some loss of available survey days due to adverse weather, we assume that 12 survey days will be required to complete this portion of the survey during the winter season (Table 4–15).

Summer Survey:

On the summer solstice (21 June), there are 10 hours of daylight during which images of acceptable glare levels could be collected given the imaging equipment and solar position, calculated for a central location of this segment, Palm Coast FL. To accommodate some loss of available time due to adverse environmental conditions such as cloud cover and excessively rough sea states, we assume that 7 hours are available each day for aerial surveys. This results in a total of 10 days required to complete a single pass through this area. To accommodate some loss of available survey days due to adverse weather, we assume that 12 survey days will be required to complete this portion of the survey during the summer season (Table 4–15).

Table 4–15.

Aerial Survey Flight Details for the Fourth of Four Aircraft in the Atlantic Outer Continental Shelf (AOCS)-scale High-resolution Imaging Survey Protocol

Item	Kodiak 100		Twin Otter	
	Amount	Unit	Amount	Unit
Total area	46,166	km^2	46,166	km^2
Area to be surveyed	4,617	km^2	4,617	km^2
Swath width	264	m	264	m
Total transect length	17,487	km	17,487	km
North–south coastal length	600	km	600	km
Total flight distance between transects	600	km	600	km
Number of Transects	227	times	227	times
Aircraft speed	278	km/hr	278	km/hr
Aircraft endurance	6	hrs	7	hrs
Survey time in one flight	5	hrs	6	hrs
Number of refuel trips	13	times	11	times
Refueling distance	40	km	40	km
Total refuel trip distance	536	km	444	km
Total flight length	18,623	km	18,532	km
Flight cost per hour	239	$	335	$
Flight hours required for survey	67	hrs	67	hrs
Total cost of flight per season	16,010	$	22,331	$
Low-glare imaging light/day (winter)	7	hrs	7	hrs
Low-glare imaging light/day (summer)	7	hrs	7	hrs
Number of days required (winter)	12	days	12	days
Number of days required (summer)	12	days	12	days
Total annual survey hours	134	hrs	133	hrs
Total annual survey days	23	days	23	days

Estimated Total Project Cost per Annum

The expected annual cost of the AOCS-scale high-resolution offshore aerial wildlife imaging survey is $2,215,738 if using four of the Kodiak 100 aircraft from the USFWS survey fleet, or $1,872,378 if using four De Havilland Twin Otters fom the NOAA-NMFS survey fleet. It is important to note that once the Kodiak 100 aircraft have been modified with suitable belly hatches for camera mounting, the annual cost of using that fleet will be slightly lower than that of the NOAA-NMFS Twin Otter fleet, as the per hour flight cost of the latter is higher. Complete breakdowns of all costs are presented in Table 4–16 and Table 4–17 for labor and nonlabor costs, respectively. To supplement the earlier descriptions of the labor and nonlabor elements of this protocol, and to maximize adjustability and flexibility of these cost estimates for protocol planning purposes, we provide a list of additional costing assumptions below.

Table 4–16.

Breakdown of Labor Effort and Costs by Task and Personnel Type for Atlantic Outer Continental Shelf (AOCS)-scale Offshore High-resolution Aerial Wildlife Imaging Survey Protocol (See Text for Complete Explanation of Tasks, Personnel Roles, and Costing Assumptions)

Task	Project Manager	Project Coordinator	Aviation Engineer	Principal Scientist	Biological Technician	Imaging Engineer	Imaging Technician	Total Labor Cost (US$)
Daily rate (US$)	1,000	520	1,250	800	520	1,600	520	
Survey design, planning	16	16	2	16		2		42,820
Project management	95.9	89.9						145,768
Develop/integrate/pretest imaging equip.	3	3	45			10	30	92,410
Survey execution	6	24	31		16	19	125	160,950
Data extraction, automated data processing					15	15	30	47,400
Target identification and manual image review, quality assurance/quality control				80	400	2	10	280,400
Data analysis and reporting	12	6	1	24	48	2	2	64,770
Total labor cost (US$)	**132,900**	**75,348**	**98,750**	**96,000**	**249,080**	**80,000**	**102,440**	**$834,518**

Note: Labor rates and cost totals are presented in US dollars while effort values are provided in numbers of days.

Table 4–17.

Breakdown of Nonlabor Costs by Item for Atlantic Outer Continental Shelf (AOCS)-scale Offshore High-resolution Aerial Wildlife Imaging Survey Protocol (See Text for Complete Explanations of Items and Costing Assumptions)

	USFWS Kodiak 100		NOAA-NMFS Twin Otter	
Item	**Unit Price**	**Number of Units**	**Unit Price**	**Number of Units**
Aircraft use fee	$239/hr	590	$335/hr	590
Belly hatch installation	$100,000	4	n/a	
Commercial transport (per person per round trip to field sites)	$600	40	$600	40
Travel expenses (per person per day on field sites)	$350	435	$350	435
Camera	$16,995	8	$16,995	8
Lens	$3,500	8	$3,500	8
Onboard data storage system	$30,000	4	$30,000	4
Mount design/fabrication	$45,000	4	$45,000	4
Data storage/transfer equipment	$10,000	20	$10,000	20
Total nonlabor annual cost		**$1,381,220**		**$1,037,860**

Note: All price and cost values are given in US dollars.

Additional Costing Assumptions and Notes (See Also Earlier Text Sections)

- Daily travel expenses include lodging, food, rental car (daily fee), and are incurred as a function of person x days in the field, including travel days. Two travel days are required for each person x field visit in addition to the number of estimated flight survey days.
- Commercial transport expenses are based on commercial airline tickets for traveling between home and field sites, and are incurred as a function of person x trips to the field.
- Belly hatch installation fee includes all labor as well as nonlabor costs for aviation personnel required to perform and certify the airworthiness of modifications to the aircraft. This is a one time cost for a project (i.e., not required in year 2 or subsequently).
- Camera mount design and installation fee includes all labor as well as nonlabor costs for aviation personnel required to design, fabricate, and install the mounts. This is a one time project cost (i.e., not required in year 2 or subsequently).
- Pilot hourly rates are not included, as protocols assume governmental agency staff pilots are used. However, daily travel expenses and commercial transport expenses (per survey bout) are included for two pilots for the entire survey effort.
- Hourly billing rates for all listed personnel are derived from normal commercial billing rates for the corresponding types of technical expertise. Additional overhead or profit fees have not been included in these cost estimates.

- Labor allocation for data extraction and automated target detection assumes that a pre-existing target detection algorithm capable of real time, onboard animal detection is used. A limited allocation is built in for the imaging engineer and technician to allow for site- and taxon-specific adaptation and refinement of the pre-existing algorithm (see earlier text).
- Number of survey flight hours is based on the specific transect flight pattern breakdowns of the four survey aircraft in the AOCS-scale survey protocol described in the previous section.
- Labor allocation for project management task is calculated for both the project manager and the project coordinator as 10% of the total labor effort of all personnel on tasks 3 through 7.

Regional Scale

The regional scale survey protocol covers a spatial scale intermediate between the AOCS scale (entire region) and the single project scale. Examples of regional scale surveys would include surveys of the portions of the developable AOCS within single BOEM planning regions, or offshore of single states, or several state consortia. At this scale, the scientific objectives are somewhat more refined than they are at the whole AOCS scale, but they are still broader and more general in nature than they would be at the scale of a single proposed offshore wind facility. We expect that surveys undertaken at the regional scale would be designed as ecological baseline studies, intended to provide a foundation of information on marine wildlife distribution and abundance over the region of interest for the purposes of siting offshore wind energy areas and individual offshore wind facilities within the areas of least possible conflict. The intermediate nature of the anticipated scientific objectives of such a survey suggests an intermediate precision approach to data gathering, as follows.

Spatial Extent

We defined the regional scale as approximately 25,000 km^2 based on the general size of a state- or region-specific area that would need to be surveyed for an offshore wind baseline study within the overall portion of interest of the AOCS (Maine to Florida, from states' seaward boundaries to the 30 m isobath). For the purpose of protocol development, we arbitrarily selected a 25,914 km^2 area off the coasts of North and South Carolina, depicted in Figure 4–32.

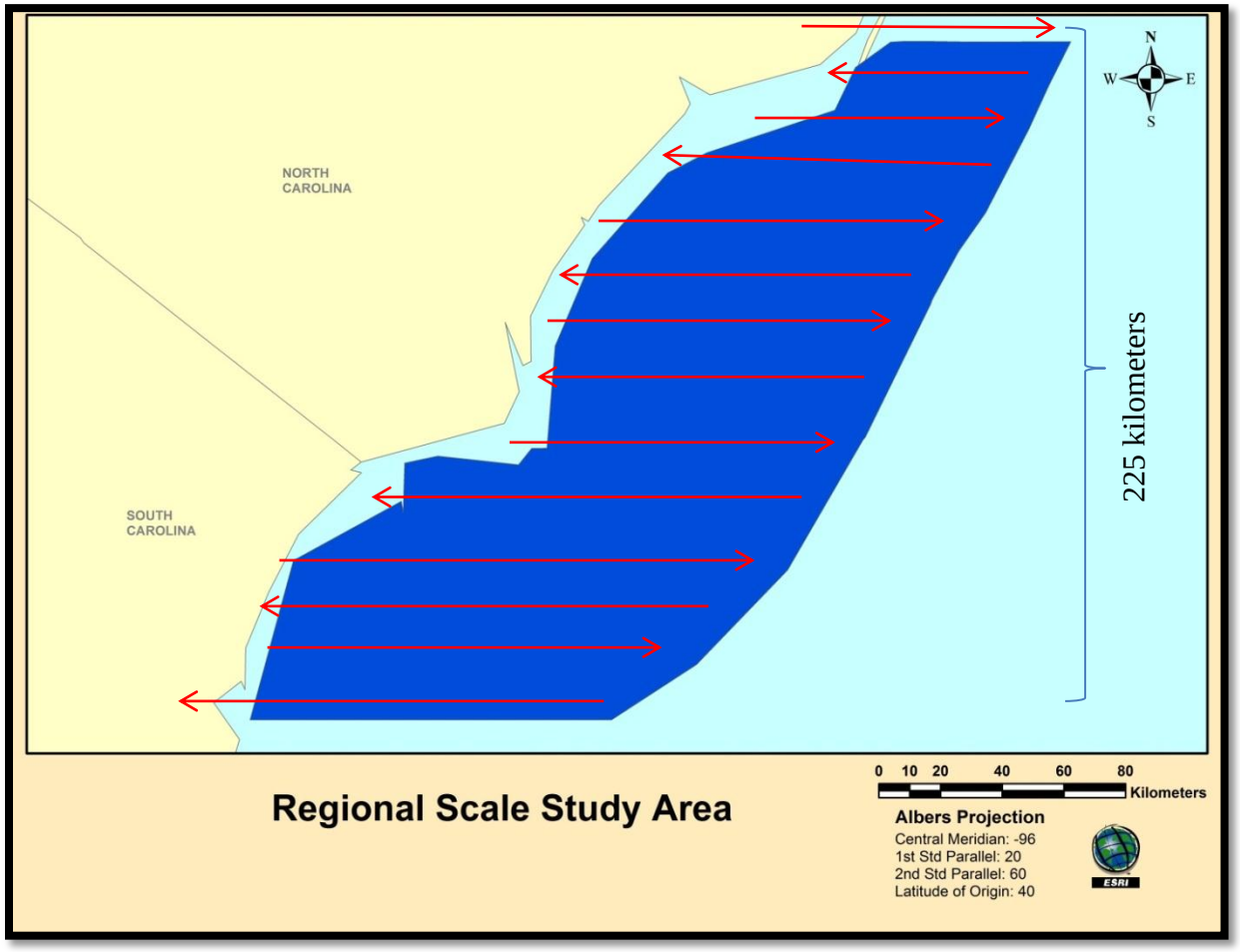

Figure 4–32. Survey area (dark blue) and general survey pattern used to develop the regional scale high-resolution wildlife imaging survey protocol. This area was arbitrarily selected as a subsection of the entire Atlantic Outer Continental Shelf (AOCS) study region of interest (Maine to Florida, from states' seaward boundaries to the 30 m isobath, see previous section) representing the general size of area that might be surveyed for state- or region-specific environmental baseline studies to support offshore wind energy development. The red arrows indicate the general structure of individual flight transects; however, they do not illustrate the actual transect pattern, which entails 170 individual flight segments spaced at even 1.32 km increments along this 225 km span of the total AOCS survey area (see Table 4–12).

Sampling Frequency and Timing

We recommend that this entire region be surveyed four times per year: once during the middle of the warm season (between late May and early August), and once during the middle of the cold season (between late November and the end of February), and once each during spring and fall migration seasons (spring: March to mid-May; fall: mid-August to mid-November). This timing is selected to

satisfy the objective of characterizing marine wildlife distribution during the two relatively sedentary (i.e., nonmigratory) periods of the year, and also to provide a snapshot of activity during each of the primary migration seasons. For the relatively sedentary periods (summer and winter), single snapshots may be regarded as relatively comprehensive for documenting animal distribution and abundance, although as noted previously, we recognize that some animal movement does take place during each of those time periods. However, because different animals migrate at different times of year, no single snapshot of an entire migratory period could capture a complete spectrum of migratory activity. Therefore, the single survey conducted during each migratory season, while adding substantial depth to the overall survey in terms of capturing a relatively complete annual cycle, would still, nonetheless be fairly crude with respect to documenting migratory routes and timing of marine birds, mammals, and turtles within the selected region. The particular dates and timing of the spring and fall surveys should be adjusted to the specific region based on the expected dates of passage of a majority of taxonomically prioritized species (e.g., listed species) through the region of interest.

Aircraft

We have developed our regional scale protocol assuming that a single chartered aircraft would be used as the platform for the entire survey effort. Based on our evaluation of candidate aircraft (see section 3.2), we have selected the Vulcanair P68 Observer 2 as a representative aircraft that would be highly suitable for this purpose, although we note that other aircraft are also suitable and could be selected for regional scale survey protocols. Among the attractive features of the Vulcanair P68 Observer 2 are its 10-hour endurance and its 63 cm × 46 cm belly hatch, which would accommodate the two-camera, gyrostabilized, adjustable-angle mount envisioned and described earlier. For the purposes of developing a cost estimate for this proposal, we assume that this aircraft would need to be chartered from a private company, who would also provide two trained pilots for all survey flights. In our cost estimate, we use a current market rate for chartering this aircraft of US $580 per flight hour, which includes pilot labor as well as all fuel and aircraft operating costs. This price does not include travel fees for the pilots; therefore, we have added daily and per-survey bout travel expenses for both pilots within our cost estimate (see below).

Figure 4–33. Aircraft selected for development of the regional scale protocol for offshore high-resolution aerial wildlife imaging surveys: the Vulcanair P68 Observer 2 (left) and its belly hatch (right).

Image Resolution

The recommended image resolution for the regional scale survey is 1 cm, meaning that 1 pixel of the image corresponds roughly to 1 cm^2 of the water's surface, given the flight altitude and optical magnification of the image (see section 3.3 and Chapter 1 for complete discussions of image resolution technique and effectiveness). This image resolution is finer than the 2 cm resolution recommended for the AOCS scale survey protocol, and equal to the resolution recommended for the project scale survey protocol. This level of resolution is finer than what was recommended by Thaxter and Burton (2009) based on their review of high-resolution survey methodology in Europe at the time. However, it is consistent with more recent practice in Europe, and with the results of our own experimentation and analysis which suggest that for consistent and reliable species-level identification of most imaged animals, 1 cm resolution is desirable (section 6.4). This increase in image resolution relative to the AOCS-scale protocol results in corresponding differences in shutter speed, camera orientation and survey swath, and flight transect spacing, discussed below.

Shutter Speed (Exposure Time)

The exposure time is the time that the shutter remains open when taking a photograph. Exposure time must be carefully chosen to prevent motion blur across pixels during exposure of each individual frame. Exposure time can be calculated based on ground speed of the imaging platform and imaging resolution (see below). When the speed of the aircraft is 277 km per hour, the amount of time the imaging platform takes to move 1 pixel (1cm) is ~130 µs. Therefore, maximum exposure time for each frame is 130 µs. If exposure time is set to 130 µs or less, each pixel in the image will contain data for exactly 1 pixel on the ground, with no motion blur present across pixels.

The fundamental calculation is:

277 km / hr = *1cm / Exposure time (hr)*

*Exposure time (*µs*)* = *1cm * 1*60*60*1,000,000* µs */ 277 *1,000*100 cm*

= *~130* µs

Camera Orientation and Imaging Swath Width

Two cameras would be mounted side by side, each tilted 6.3° to the side. This would result in the cameras taking adjacent, side by side images on the water's surface. At 1 cm resolution for the 29 MP images taken by these cameras, the result would be a total survey swath of 132 m (see also camera description earlier).

Extent of Spatial Subsampling

We recommend subsampling 10% of the entire study area in the regional scale survey protocol, following the recommendation of Thaxter and Burton (2009).

Number of Transects and Spacing

Given the imaging swath width of 132 m and the 10% recommended subsampling level, the recommended spacing between the transects in the AOCS-scale protocol is 1.32 km. This spacing was used in the analysis below to develop the specific survey transect patterns for this protocol.

General Survey Pattern

The protocol we have developed entails flying a single imaging aircraft to conduct quarterly imaging surveys, each providing imagery of 10% of the entire region of interest. The region, as depicted in Figure 4–32, encompasses a 25,914 km^2 area regarded as potentially developable for offshore wind using current technology and under US federal jurisdiction, located between the states' seaward boundaries and the 30 m isobaths. The north–south coastal length of this segment is approximately 225 km. Since the swath width of each transect survey is 132 m and the extent of subsampling is 10%, each of the four seasonal surveys will consist of flying 170 transects of varying length, alternating between east–west and west–east in direction, with 1.32 km spacing between transects. The total flight distance to complete one seasonal survey is approximately 20,179 km, including refueling trips and flights between the transects (Table 4–18). Each of these four passes through the region would require from 11 to 12 days of surveying depending on available daylight for low glare image gathering (see below). Allowing for weekend days off and roughly one day of weather-related delay per week, we expect that each survey of the entire region would last for roughly 4 weeks. This would be conducted four times per year, hence in summary, four total 4-week surveying bouts would be conducted each year. The specific survey pattern and season-specific flight pattern detail is provided below.

Available Low Glare Daylight Survey Hours

The amount of available survey time varies as a function of two factors. The first is day length, which varies with both latitude and calendar date. The second is suitability for capturing low glare images, which is a function of the ability of the mount to achieve ADGS values below the 67° suitability threshold (see section 4.2 for an explanation of terms and discussion of glare impacts and mitigation). We calculated available daylight hours for low glare surveying for a representative central locality within the region, Oak Island NC, for each time of year. We assume that camera mounts are adjusted in flight between two available camera angles (see mount description) to maximize ADGS on each flight transect, assuming alternating east–west and west–east flight directions. This essentially entails always pointing the camera westward in the morning and always pointing the camera eastward in the afternoon regardless of flight direction (see section 4.2). We then used the formula for calculating ADGS presented in section 4.2 to determine the total number of daylight hours during which ADGS under 67° could be achieved for each survey season. Our results were as follows: 10 suitable survey hours per day for winter solstice, spring equinox, and fall equinox; 11 suitable survey hours per day for summer solstice (Table 4–18). Allowing for some loss of suitable survey time for adverse weather or visibility conditions, we assume 7 suitable survey hours per day during winter, spring and fall, and 8 suitable survey hours per day during summer. Under these assumptions, the survey would require 9 days of flight surveys in summer and 10 days during the other seasons. We adjust this to 11 (summer) or 12 days (other season) to provide a buffer of 2 days per season lost to adverse weather or other unforeseen circumstances.

Table 4–18.

Aerial Survey Flight Details for the Regional Scale High-resolution Imaging Survey Protocol

Item	Vulcanair P68 Observer 2	
	Amount	**Unit**
Total area	25,914	km^2
Area to be surveyed	2,591	km^2
Swath width	132	m
Total transect length	19,632	km
North–south coastal length	225	km
Total flight distance between transects	225	km
Number of transects	170	times
Aircraft speed	278	km/hr
Aircraft endurance	10	hr
Survey time in one flight	9	hr
Number of refuel trips in one season	8	times
Refueling distance	40	km
Total refuel trip distance	323	km
Total flight distance for one season survey	20,179	km
Flight cost per hour	580	$
Flight hours required for one season survey	73	hr
Total cost of flight per season	42,101	$
Low-glare imaging light/day (winter)	7	hr
Low-glare imaging light/day (spring)	7	hr
Low-glare imaging light/day (summer)	8	hr
Low-glare imaging light/day (fall)	7	hr
Number of days required (winter)	12	days
Number of days required(spring)	12	days
Number of days required (summer)	11	days
Number of days required (fall)	12	days
Total annual survey hours	292	hrs
Total annual flight cost	168,404	$
Total annual survey days	47	days

Estimated Total Project Cost Per Annum

The expected annual cost of the regional scale high-resolution offshore aerial wildlife imaging survey is $879,600. Complete breakdowns of all costs are presented in Table 4–19 and Table 4–20 for labor and nonlabor costs, respectively. To supplement the earlier descriptions of the labor and nonlabor elements of this protocol, and to provide for maximum adjustability and flexibility for planning purposes, we provide a list of additional costing assumptions below.

Table 4–19.

Breakdown of Labor Effort and Costs by Task and Personnel Type for Regional scale Offshore High-resolution Aerial Wildlife Imaging Survey Protocol (See Text for Complete Explanation of Tasks, Personnel Roles, and Costing Assumptions)

Task	Project Manager	Project Coordinator	Aviation Engineer	Principal Scientist	Biological Technician	Imaging Engineer	Imaging Technician	Total Labor Cost (US$)
Daily rate (US$)	1,000	520	1,250	800	520	1,600	520	
Survey design, planning	8	8	1	8		1		**21,410**
Project management	46.5	46.5						**70,680**
Develop/integrate/pretest imaging equipment	2	2	15			5	10	**34,990**
Survey execution	6	12	14		1	8	64	**76,340**
Data extraction, automated data processing					6	10	15	**26,920**
Target identification and manual image review, quality assurance/quality control				40	200	2	5	**141,800**
Data analysis and reporting	6	3	1	12	24	1	1	**33,010**
Total labor cost (US$)	**$68,500**	**$37,180**	**$38,750**	**$48,000**	**$120,120**	**$43,200**	**$49,400**	**$405,150**

Note: Labor rates and cost totals are presented in US dollars, while effort values are provided in numbers of days.

Table 4–20.

Breakdown of Nonlabor Costs by Item for Regional scale Offshore High-resolution Aerial Wildlife Imaging Survey Protocol (See Text for Complete Explanation of Items and Costing Assumptions)

Nonlabor Items	Unit Price	Number of Units
Aircraft use fee	$580/hr	292
Commercial transport (per person per round trip to field sites)	$600	19
Travel expenses (per person per day on field sites)	$350	222
Camera	$16,995	2
Lens	$3,500	2
Onboard data storage system	$30,000	1
Mount design/fabrication	$45,000	1
Data storage/transfer equipment	$10,000	10
Total nonlabor annual cost		**$474,450**

Note: All price and cost values are given in US dollars.

Additional Costing Assumptions and Notes (See Also Earlier Text Sections)

- Daily travel expenses include lodging, food, rental car (daily fee), and are incurred as a function of person x days in the field, including travel days. Two travel days are required for each person x field visit.
- Commercial transport expenses include commercial airline tickets for traveling between home and field sites, and are incurred as a function of person x trips to the field.
- Camera mount design and installation fee includes all labor as well as nonlabor costs for aviation personnel required to design, fabricate, and install the mounts. This is a one time project cost (i.e., not required in year 2 or subsequently).
- Pilot hourly rates are not included, as their rates are incorporated into charter aircraft hourly usage fees. However, per day and per trip travel costs are factored into the costs for two pilots assumed to be present for all survey days, as such costs are not included in hourly charter aircraft fees.
- Hourly billing rates for all listed personnel are derived from normal commercial billing rates for the corresponding types of technical expertise. Additional overhead or profit fees have not been included in these cost estimates.
- Labor allocation for data extraction and automated target detection assumes that a pre-existing target detection algorithm capable of real time, onboard animal detection is used. A limited allocation is built in for the imaging engineer and technician to allow for site- and taxon-specific adaptation and refinement of the pre-existing algorithm (see earlier text).

- Labor allocation for project management task is calculated for both the project manager and the project coordinator as 10% of the total labor effort of all personnel on tasks 3 through 7.

Project Scale

The project scale survey protocol covers the smallest spatial scale, equivalent to the rough order of magnitude of the size of a single, commercial scale offshore wind energy facility. At this scale, the scientific objectives are likely to be finer toothed than they are at the larger scales, requiring a higher degree of biological precision. We expect that surveys undertaken at the scale of single offshore wind energy facilities would be designed specifically to satisfy the requirements for permitting single facilities, e.g., as required in the BOEM site assessment plan (SAP) prior to construction, or during the operational phase of the facility, as specified in the construction and operations plan (COP). In accord with this set of anticipated objectives, we have structured this protocol as follows.

Spatial Extent

We defined the project scale as approximately 150 km^2 based on the anticipated size of a typical commercial scale offshore wind energy project. This corresponds to roughly twice the size of the original Cape Wind Project footprint, and is expected to accommodate roughly 200 to 250 marine wind energy turbines spaced at standard intervals in a grid-like configuration. For the purpose of protocol development, we arbitrarily selected a 178 km^2 area off the coast of North Carolina, depicted in Figure 4–34.

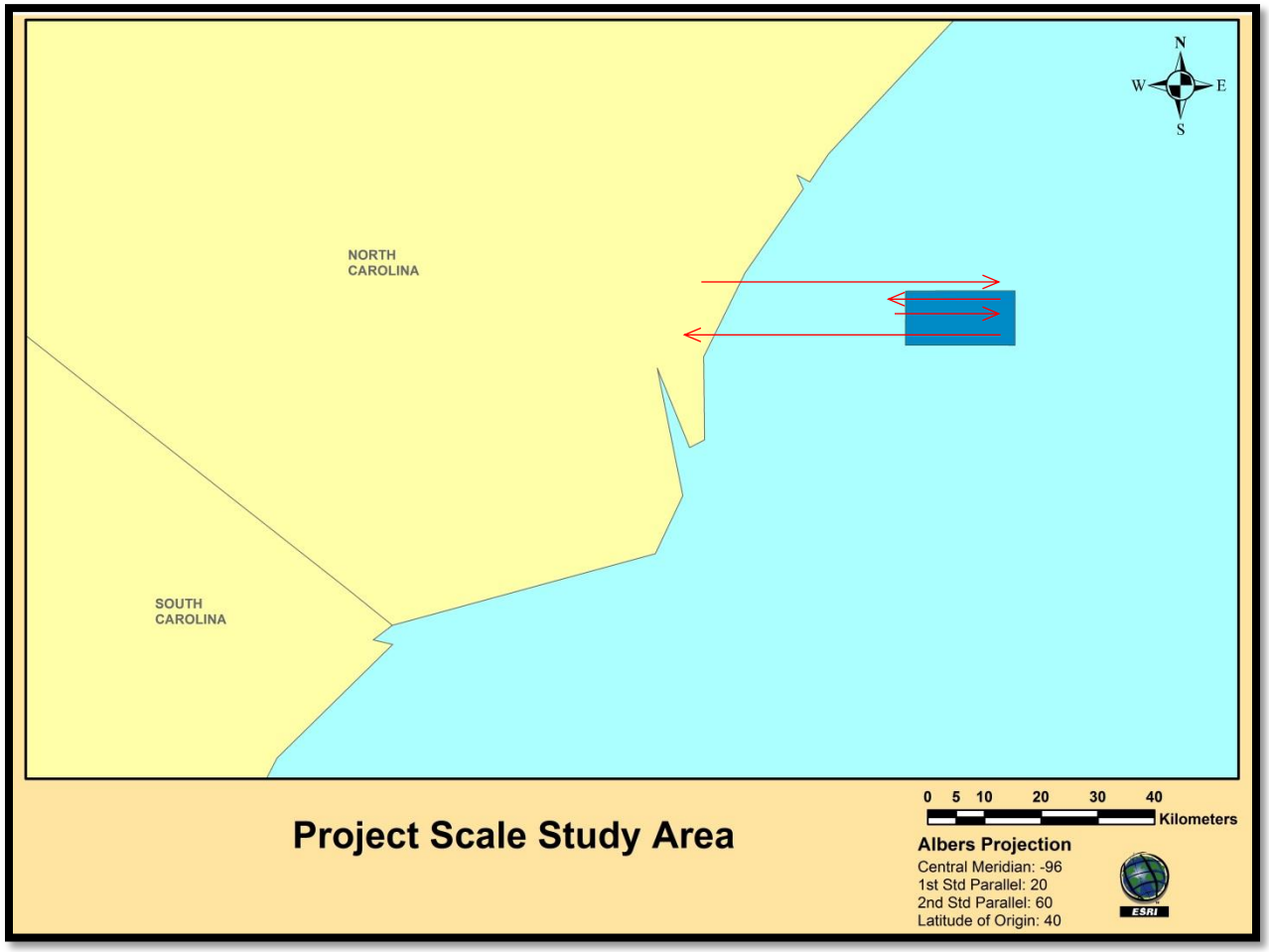

Figure 4–34. Survey area (dark blue) and general survey pattern used to develop the project scale high-resolution wildlife imaging survey protocol. This area was arbitrarily selected within the Atlantic Outer Continental Shelf (AOCS) study region of interest (Maine to Florida, from states' seaward boundaries to the 30 m isobath, see previous sections) representing the general size of the footprint of a single, commercial scale offshore wind energy project. The red arrows indicate the general structure of individual flight transects; however, they do not illustrate the actual transect pattern, which entails 15 individual flight segments spaced at even 0.66 km increments along the 10 km north–south span of the total proposed area for the project (Table 4–21).

Sampling Frequency and Timing

We recommend that this entire region be surveyed eight times per year, spaced at roughly even (6 to 7-week) intervals over the course of the year. This timing is selected to satisfy the objective of producing a relatively complete characterization of the distribution and abundance patterns of marine birds, sea turtles, and marine mammals through the entire spectrum of seasonal variation over the

annual cycle. Although this level of sampling would render a more comprehensive characterization of annual variation than would either of the two larger scale protocols described earlier, it is important to note that with 6 to 7-week intervals in between surveys, gaps would still remain in the seasonal activity patterns produced by this survey, as migratory, or other local movement of animals are expected to occur throughout the year at this time scale. Even a daily survey of an area (e.g., 365 times per year) could not possibly capture all migratory animal passage through any proposed project area, as migrating marine wildlife may cover hundreds of kilometers of distance within a single day. It is possible to provide continuous monitoring of small areas with stationary monitoring devices (e.g., underwater hydrophones for continuous, stationary, passive acoustic monitoring of marine mammals). However, survey methods, including high-resolution aerial imaging surveys, are intended to provide comprehensive coverage of large spatial extents (e.g., an entire project area in this case), at the expense of temporally continuous monitoring. We note that in recent years, monthly sampling has become a standard practice for offshore high-resolution aerial wildlife imaging surveys in the UK (R. Langston, S. Clough, pers. comm.). The sampling frequency of any survey effort is inevitably a balance between scientific rigor and cost, driven by the pace of biological dynamism in the phenomenon of interest, the biological objectives and requirements of the study, and budgetary constraints. While there is no single correct answer for how many surveys should be conducted per year, we recommend eight per year as a representative level intended to satisfy reasonable requirements for seasonal comprehensiveness for characterizing marine wildlife distribution and abundance patterns for single commercial-scale offshore wind energy projects.

Aircraft

We have developed our project scale protocol assuming that a single chartered aircraft would be used as the platform for the entire survey effort. Based on our evaluation of candidate aircraft (see section 3.2), we have selected the Vulcanair P68 Observer 2 as an aircraft that would be highly suitable for this purpose, although we note that other aircraft are also suitable and could be selected for project scale surveys. Among the attractive features of the Vulcanair P68 is its 63 cm × 46 cm belly hatch that would accommodate the two-camera, gyrostabilized, adjustable-angle mount envisioned for this protocol. For the purposes of developing a cost estimate for this proposal, we assume that this aircraft would need to be chartered from a private company, who would also provide two trained pilots for all survey flights. In our cost estimate, we use a current market rate for chartering this aircraft of US $580 per flight hour, which includes pilot labor as well as all fuel and aircraft operating costs. This price does not include travel fees for the pilots, so we have added daily and per-survey bout travel expenses for two pilots in our cost estimate. Each survey bout is expected to last approximately 1 hour, yet we have built in a possible 1-day weather-related delay into each of the eight surveys over the course of the year. Therefore, some overnight expense allocations are expected to be necessary for the pilots.

Figure 4–35. Aircraft selected for development of the project scale protocol for offshore high-resolution aerial wildlife imaging surveys: the Vulcanair P68 Observer2 (left) and its belly hatch (right).

Image Resolution

The recommended image resolution for the project scale survey is 1 cm, meaning that 1 pixel of the image corresponds roughly to 1 cm^2 of the water's surface, given the flight altitude and optical magnification of the image (see section 3.3 and Chapter 1 for complete discussions of image resolution technique and effectiveness). This image resolution is finer than the 2 cm resolution recommended for the AOCS scale survey protocol, and equal to the resolution recommended for the regional scale survey protocol. This level of resolution is finer than what was recommended by Thaxter and Burton (2009) based on their review of high-resolution survey methodology in Europe at the time. However, it is consistent with more recent practice in Europe, and with the results of our own experimentation and analysis, which suggest that for consistent and reliable species-level identification of most imaged animals, 1 cm resolution is desirable (section 6.4). This increase in image resolution relative to the AOCS scale protocol results in corresponding differences in shutter speed, camera orientation and survey swath, and flight transect spacing, discussed below.

Shutter Speed (Exposure Time):

The exposure time is the time that the shutter remains open when taking a photograph. Exposure time must be carefully chosen to prevent motion blur across pixels during exposure of each individual frame. Exposure time can be calculated based on ground speed of the imaging platform and imaging resolution (see below). When the speed of the aircraft is 277 km per hour, the amount of time the imaging platform takes to move 1 pixel (1cm) is ~130 µs. Therefore, maximum exposure time for each frame is 130 µs. If exposure time is set to 130 µs or less, each pixel in the image will contain data for exactly 1 pixel on the ground, with no motion blur present across pixels.

The fundamental calculation is:

277 km / hr = *1cm / Exposure time (hr)*
Exposure time (µs) = *1cm * 1*60*60*1,000,000* µs */ 277 *1,000*100 cm*
= *~130 µs*

Camera Orientation and Imaging Swath Width

Two cameras would be mounted side by side, each tilted 6.3° to the side. This would result in the cameras taking adjacent, side by side images on the water's surface. At 1 cm resolution for the 29 MP images taken by these cameras, the result would be a total survey swath of 132 m (see also camera description).

Extent of Spatial Subsampling

We recommend subsampling 20% of the entire study area in the project scale survey protocol. This is twice as thorough sampling as was recommended by Thaxter and Burton (2009), and provides a more precise characterization of animal density and occurrence within the survey area than the other scales, in accordance with the more fine toothed scientific data gathering objectives that would normally be associated with project scale survey efforts. Lowering the level of subsampling is intended to ensure that more accurate animal density estimates are obtained, even for animals with more spatially clumped distributions (see section 4.3).

Number of Transects and Spacing

Given the imaging swath width of 132 m and the 20% recommended subsampling level, the recommended spacing between the transects in the AOCS scale protocol is 0.66 km. This spacing was used in the analysis below to develop the specific survey transect patterns for this protocol.

General Survey Pattern:

The protocol we have developed entails flying a single imaging aircraft to conduct imaging surveys eight times over the course of a year, each providing imagery of 20% of the entire wind energy project area. The area, as depicted in Figure 4–34, encompasses a 178 km^2 area as could be proposed for a single, commercial scale offshore wind energy project, and is located within the area regarded as potentially developable for offshore wind using current technology, and under US federal jurisdiction, located between the states' seaward boundaries and the 30 m isobaths. The north–south length of this area is 10 km. Because the swath width of each transect survey is 132 m, and the extent of subsampling is 20%, each of the eight surveys over the course of a year will consist of flying 15 transects of 10 km each, alternating between east–west and west–east in direction, with 0.66 km north–south spacing between transects. The total flight distance to complete one survey of the entire area is approximately 280 km, including a single trip to and from the mainland, and flights between the transects (Table 4–21). Each of the eight surveys over the course of a year would require 1 hour of survey flight time; hence, it could easily be conducted in a single day in any season, at any locality along the US AOCS. Allowing for 1 day of weather-related delay per survey, we have allotted 2 days for each of the eight surveys over the course of the year. In summary, eight total 2-day surveying bouts would be conducted each year. The specific survey pattern, and season-specific flight pattern detail is provided below.

Available Low Glare Daylight Survey Hours

Because only a single hour of survey flight time is required to complete a survey of the entire area, the amount of available daylight is not a significant protocol constraint, either in terms of overall day length of the particular latitude and time of year of the survey, or in terms of hours suitable for low glare image gathering as a function of ADGS given particular solar angles. Nonetheless, in the planning of this protocol, care should be taken to avoid conducting imaging surveys at times when

the 67° ADGS suitability threshold would be crossed (see section 4.2 for explanation of terms and discussion of glare impacts and mitigation).

Table 4–21.

Aerial Survey Flight Details for the Project Scale High-resolution Imaging Survey Protocol

Item	Vulcanair P68 Observer 2	
	Amount	**Unit**
Total area	178	km^2
Area to be surveyed	36	km^2
Swath width	132	m
Total transect length	150	km
North–south coastal length	10	km
Total flight distance between transects	10	km
Number of transects	15	times
Aircraft speed	278	km/hr
Aircraft endurance	10	hr
Maximum survey time in one flight	9	hr
Number of refuel trips in one survey (transit between airport and project area)	2	times
Refueling (transit) distance	40	km
Total transit trip distance	80	km
Total flight distance for one season survey	280	km
Flight cost per hour	580	$
Flight hours required for one season survey	1.01	hr
Total cost of flight per season	586	$
Number of days required per survey (all seasons, assumes weather delay)	2	days
Total annual survey hours	8.08	hrs
Total annual flight cost	4,687	$
Total annual survey days	16	days

Estimated Total Project Cost per Annum

The expected annual cost of the project scale high-resolution offshore aerial wildlife imaging survey is $368,884. Complete breakdowns of all costs are presented in Table 4–22and Table 4–23 for labor and nonlabor costs, respectively. To supplement the earlier descriptions of the labor and nonlabor elements of this protocol, and to provide for maximum adjustability and flexibility for planning purposes, we provide a list of additional costing assumptions below.

Table 4–22.

Breakdown of Labor Effort and Costs by Task and Personnel Type for Project scale Offshore High-resolution Aerial Wildlife Imaging Survey Protocol (See text for Complete Explanation of Tasks, Personnel Roles, and Costing Assumptions)

Task	Project Manager	Project Coordinator	Aviation Engineer	Principal Scientist	Biological Technician	Imaging Engineer	Imaging Technician	Total Labor Cost (US$)
Daily rate (US$)	1,000	520	1,250	800	520	1,600	520	
Survey design, planning	4	4	1	4		1		12,130
Project management	16.7	16.7						25,384
Develop/integrate/pretest imaging equipment	2	2	15			5	10	34,990
Survey execution	6	24	16		2	7	24	63,200
Data extraction, automated data processing					4	5	10	15,280
Target identification and manual image review, quality assurance/quality control				5	10	1	1	11,320
Data analysis and reporting	2	1	1	4	8	1	1	13,250
Total labor cost (US$)	**$30,700**	**$24,804**	**$41,250**	**$10,400**	**$12,480**	**$32,000**	**$23,920**	**$175,554**

Note: Labor rates and cost totals are presented in US dollars, while effort values are provided in numbers of days.

Table 4–23.

Breakdown of Nonlabor Costs by Item for Project Scale Offshore High-resolution Aerial Wildlife Imaging Survey Protocol (See Text for Complete Explanation of Items and Costing Assumptions)

Nonlabor Items	Unit Price	Number of Units
Aircraft use fee	$580/hr	8
Commercial transport (per person per round trip to field sites)	$600	38
Travel expenses (per person per day on field sites)	$350	114
Camera	$16,995	2
Lens	$3,500	2
Onboard data storage system	$30,000	1
Mount design/fabrication	$45,000	1
Data storage/transfer equipment	$10,000	1
Total nonlabor annual cost		**$193,330**

Note: All price and cost values are given in US dollars.

Additional Costing Assumptions and Notes (See Also Earlier Text Sections)

- Daily travel expenses include lodging, food, rental car (daily fee), and are incurred as a function of person x days in the field, including travel days. Two travel days are required for each person x field visit.
- Commercial transport expenses include commercial airline tickets for traveling between home and field sites, and are incurred as a function of person x trips to the field.
- Camera mount design and installation fee includes all labor as well as nonlabor costs for aviation personnel required to design, fabricate, and install the mounts. This is a one time project cost (i.e., not required in year 2 or subsequently).
- Pilot hourly rates are not included, as their rates are incorporated into charter aircraft hourly usage fees. However, per day and per trip travel costs are factored into the costs for two pilots assumed to be present for all survey days, as such costs are not included in hourly charter aircraft fees.
- Hourly billing rates for all listed personnel are derived from normal commercial billing rates for the corresponding types of technical expertise. Additional overhead or profit fees have not been included in these cost estimates.
- Labor allocation for data extraction and automated target detection assumes that a pre-existing target detection algorithm capable of real time, onboard animal detection is used. A limited allocation is built in for the imaging engineer and technician to allow for site- and taxon-specific adaptation and refinement of the pre-existing algorithm (see earlier text).
- Labor allocation for project management task is calculated for both the project manager and the project coordinator as 10% of the total labor effort of all personnel on tasks 3 through 7.

5 Target Detection Algorithm

5.1 Introduction

Marine wildlife surveys using high-resolution imaging entail the collection of image data in quantities so large that manual review of all such data is cost prohibitive, particularly for larger scale survey efforts. The need to automate at least a portion of the extraction of biological data from the collected imagery was anticipated by BOEM on the basis of early European experience with this methodology, and built into task 7 of this contract, "Develop software to automate data analysis." In this section, we describe the process by which this software was developed. The software is appended to this report (Supplemental Volume II), as is a user's manual for the software (Supplemental Volume III).

The focus of our animal detection software development effort was on automating the process of detection, but not identification of animals captured in the imagery. It was anticipated that taxonomic identification of animals would be more efficiently performed by the expert human eye than by an algorithm, as the appearance of the animals would be highly variable in the image as function of the animal's position relative to the camera, body posture and behavior, and ambient light characteristics. Such factors can be integrated and considered relatively easily by a human observer, hence developing algorithms capable of equally accurate automated taxonomic identification of animals across the entire spectrum of possible variations in appearance for individual species would be extremely difficult. By contrast, animal detection was anticipated to be a simpler process to automate accurately. Furthermore, because of expected low animal densities in many marine environments, automating the animal detection process was expected to produce the most significant gains in overall image processing efficiency, solving the fundamental data volume challenge described earlier. In effect, if 10 terabytes of imagery contain only 100 images of animals, there is much more overall effort to be saved by automating the animal detection process than by automating the animal identification process.

The animal detection software development process depended on two key resources as follows:

1) High-resolution images gathered during the Op House experimental imaging flights conducted by the project team using a fixed wing manned aircraft off of Oak Island NC, between 10 and 20 May 2011. These experiments are described in detail in Chapter 1 of this report, and provided all of the raw material for developing algorithms to detect marine birds, turtles, and mammals *in situ* in a marine environment.
2) Quazar image processing software, developed by Boulder Imaging, Inc. This software served as the platform for the development of the target detection algorithm(s) for this project. In essence, the target detection algorithm(s) we produced for this project are specific routines, built on Boulder Imaging's pre-existing image analysis and target detection software platform, which have been specially adapted for detecting birds, marine mammals, and sea turtles in aerial high-resolution imagery of the marine environment off of North Carolina.

The animal detection software development process occurred in two overlapping and interrelated phases, as follows:

1) Manual review of experimental images. Following the collection of high-resolution aerial images in the marine environment off of Oak Island NC during Op House, all imagery was reviewed manually by Normandeau biological technicians to identify the image frames, positions, and taxonomic identity of all animals captured in the images. This manual review effort provided a complete inventory of animal image data, which served as the basis for all false positive/false negative tests and evaluations of target detection algorithm performance during its development, as well as a set of reference targets of known identity used by Boulder Imaging's image processing team to develop and refine the target detection algorithm(s). The manual image review process is described in section 5.2 of this chapter.
2) Creation, testing, and assessment of animal detection algorithms. Working in coordination with Normandeau's manual image review team, image processing specialists at Boulder Imaging used their pre-existing Quazar software system as a platform on which to develop target detection algorithms tuned to detect birds, marine mammals, and sea turtles in the marine environment, based on the Op House imagery. Multiple project-specific algorithms were developed and tested, each tuned to different types of animals based on different appearance characteristics, and these algorithms were then tested and refined over the course of roughly 12 months following the Op House experiments. The development, refinement, testing, and evaluation of the algorithm(s) developed for this project by the Boulder Imaging team are described in section 5.2.2 of this chapter.

5.2 Algorithm Development, Testing, and Evaluation Narrative

5.2.1 Introduction

Op House imaging flights conducted by the project team between 10 and 20 May 2011 off of Oak Island NC (see Chapter 1) yielded more than 9 terabytes of image data. Manual review of this data served as the basis for the development of the target detection software (section 5.2.2), and also as the basis for the evaluation of the impact of different imaging parameters on survey effectiveness from a biological standpoint (see Chapter 1).

The first step in image review was to organize the flight segments according to their metadata, and to create an inventory of the different imaging flight segments, so that all segments and images could be compared with respect to any of the imaging variables of interest (see complete description and segment inventory in Chapter 1).

Next, an initial manual review was conducted of all gathered imagery. This resulted in a decision not to conduct comprehensive manual review of the imagery gathered with the line-scan camera either for target detection algorithm development or for detailed analysis of survey effectiveness, due to excessive vibrational effects present in the imagery (see section 3.3). A relatively small amount of data was gathered with the line-scan camera during the Op House experiments, as the extreme vibrational effects were noticed early on during the experiments, hence a decision was made to emphasize use of the area-scan camera, maximizing the amount of experimental imaging that could be done with this more effective camera.

Within the images gathered with the area-scan camera, the reference object sequences were the only ones not systematically searched frame by frame for animals. The reference object sequences were short flight segments included in every imaging flight during which the aircraft imaged a preselected set of docks and boats along the coast. These reference sequences were gathered to provide direct comparisons of images of the same set of objects across all imaging flights, for qualitative comparative analysis of image quality variation associated with variation in imaging parameters such as flight altitude, resolution, and angle. Selected images from the reference sequences are included and discussed in Chapter 1.

The remaining 7 terabytes of imagery were manually reviewed by biological technicians in Normandeau's image analysis laboratory between September 2011 and February 2012 to search for all images of marine animals contained within the images. A total of 236,349 individual frames were manually searched, resulting in the discovery of 4,465 total animal images, including 3,163 images of birds, 77 of sea turtles, 37 of marine mammals, and 1,188 of other aquatic wildlife (e.g., rays, sharks, and fish). Because of the high frame capture rates used during the imaging flights (equivalent to video methods), an average of roughly three separate images were obtained for each presumed individual animal captured in the imagery (i.e., several images of each individual animal were obtained for most animals).

Images were examined in Normandeau's image analysis laboratory by one of a team of five analysts using Quazar, a custom software program created by Boulder Imaging, Inc., enabling review of film segments by individual frame. Analysts viewed images using 30-inch, high-definition LCD computer monitors. The review process was standardized and supervised to minimize differences among reviewers, with analysts given specific instructions on magnification levels for viewing, and the amount of time to spend per frame, allowing some flexibility for variation in image analysis rates due to glare effects and other factors. Effort was taken to avoid reviewer fatigue by implementation of frequent rests and change of focal distance. Subsets of images reviewed by each of the image analysts were periodically double reviewed by a project coordinator to monitor and subsequently minimize variations among observers in animal detection rates.

All certain or probable animals detected in the images by reviewers were assigned a unique identification number and recorded in an Excel spreadsheet, along with all relevant metadata—including date, resolution, swath width, flight altitude, image frame number, time stamp, animal type, image glare level (quantitative scale based on green pixel exposure level, described in section 4.2), x and y pixel location of the animal within the frame, and various measurements of the animal, depending on animal type, that were calculated using the known resolution of the image.

For all images of birds, marine mammals, or sea turtles of decent or better quality, a high quality JPEG file was created of just the cropped portion of the image containing the animal. These images were then measured and reviewed subsequently by biological experts in each taxonomic group to render best professional judgments of the taxonomic identity of each imaged animal. All JPEGs were named according to their data set number, taxonomic identity, image resolution, flight altitude, and camera tilt level and housed in an image gallery, which was made available to project personnel on the project's Sharepoint site. This gallery was organized and structured to facilitate highly accessible browsing by taxon or image resolution, as follows: the gallery contained two copies of all images, one in a folder containing subfolders organized by taxon, and one in a folder containing subfolders

organized by image resolution. A copy of the complete image gallery is included with this report as Supplemental Volume I.

Additional review of the JPEGs of the detected animals was conducted for the purposes of assessing observer variability and identification effectiveness. This review is described in Chapter 1 as it was used exclusively for the purpose of examining taxonomic identification success and consistency. This additional review was not incorporated into the development of the animal detection algorithm.

5.2.2 Software Development, Testing, and Final Performance Evaluation

The development of target (animal) detection algorithms, as well as the testing, evaluation, and refinement of these algorithms was conducted by image processing engineers at Boulder Imaging, using their Quazar software as a platform. As described earlier, the primary focus was to eliminate as much of the animal-free imagery as possible. A trained biologist would then review this reduced set of video frames—ideally with the location of the animals highlighted within the frame—and make a determination as to whether or not the detected object was, indeed, an animal, and also to discern the taxonomic identity of the animal to the finest level possible.

Identifying Test Data (Alpha and Beta Data Sets)

To develop an algorithm that could effectively identify the marine animals present in the video, we needed a system that would allow us to measure how well our algorithm was performing. To this end, we selected several sets of video segments that represented the various flight conditions (altitude, camera angle, time of day, ocean conditions, etc.). These sets were prioritized for Normandeau's manual image review (see above), and the resulting data on the locations of each animal within these sequences provided the gold standard, which was then used to determine how many of the animals the algorithm had detected and how many had been missed, as well as the false positive rate.

Alpha Data Set

The first subset of image data identified for algorithm development was termed the alpha data set. This set of imagery was used for initial testing of the target detection software. The alpha data set imagery was selected to be relatively clean of glare, and to contain mostly imagery of the highest quality, to allow us to focus on tuning the detection algorithm to differentiate between animals and the water's surface under relatively calm ocean conditions. Some imagery containing mild glare and mild to severe ocean conditions was also included in this data set for early evaluation of the effectiveness of the algorithm under these conditions. This data set included about 2.5 hours of video of the following types of imagery.

Imagery Captured During Flights Over Bird Island (~1.5 hour).

In addition to the transect imaging sequences gathered during the Op House experiments, a number of imaging sequences were performed by flying directly over certain targets intended to produce higher densities of animal images (see Chapter 1). One of these targets was a small island located near the outlet to the Atlantic Ocean just west of Bald Head, termed Bird Island. This island contained a high density of colonially nesting coastal birds, including Brown Pelicans (*Pelecanus occidentalis*) and Laughing Gulls (*Leucophaeus atricilla)*. Flyover sequences of the water surrounding this island produced large numbers of images of birds against a water background, and

contained the highest bird densities of all imagery gathered during experimentation. The alpha data set included the following variations in Bird Island flyover sequences:

- Flights at 600 m and 1,000 m altitudes
- Flights with both 15° and 44° camera tilt
- Flights at 1.5 cm and 2.5 cm image resolutions
- Flights with low to medium glare
- Flights performed at all times of the day (including early morning and late evening)
- Flights with, and without, the gyrostabilizer installed
- All imagery was taken without a polarizer installed
- Only imagery over water was selected

Imagery Captured During an Outgoing Offshore Transect Survey Segment (~20 minutes). This imagery was taken over relatively deep ocean water and was chosen because it is very clean imagery over the ocean, which contains a relatively high number of animals for an offshore transect (although such sequences normally contained low animal densities). The imagery had the following characteristics:

- 1,000 m flight altitude
- 15° camera tilt
- 2.5 cm image resolution
- Strong, midday light
- Little to no glare
- Calm ocean conditions

Imagery Captured During an Incoming Transect Along the Coastline (~30 minutes). The imagery had the following characteristics:

- Presence of mild clouds during imaging (entering field of view, then leaving fairly quickly)
- Presence of shadows from clouds overhead (entering field of view, then leaving fairly quickly)
- Mildly choppy ocean conditions
- Low to mild glare
- 1,000 m flight altitude
- 44° camera tilt
- 2.5 cm image resolution
- Strong, mid-morning light
- Mild to highly choppy ocean conditions (white caps)

Imagery Captured During a Different Outgoing Offshore Transect Survey Segment with Rougher Ocean Conditions (~15 minutes). This imagery contains low to mild glare, but contains somewhat severe ocean conditions (white caps). The imagery had the following characteristics:

- Very choppy ocean conditions
- Continual presence of white caps
- 1,000 m flight altitude
- 44° camera tilt
- 2.5 cm image resolution
- Strong, mid-afternoon light

Beta Data Set

In the later stages of development, to measure the performance of the animal detection algorithm over a larger and more diverse set of imagery, we selected a second set of image sequences, defining it as the beta data set. This data set contained a significantly higher percentage of flights over the ocean (transects) and was composed of approximately 3 hours of video from the following recordings:

Coastal Transect 1

- 1.5 cm image resolution, 425 m flight altitude
- Low to medium glare
- Presence of clouds above plane (in and out)
- Mild ocean conditions

Coastal Transect 2

- 2.5 cm image resolution, 1,000 m flight altitude
- Low to medium glare
- Abundance of white caps
- Presence of clouds above plane (in and out)

Coastal Transect 3

- 1.5 cm image resolution, 600 m flight altitude
- Low glare
- Low light (clouds overhead)

Coastal Transect 4

- 2.5 cm and 3 cm image resolutions
- 1,000 m and 1,200 m flight altitudes
- Low glare

- Rough ocean

Coastal Transect 5

- 2.5 cm image resolution, 1,000 m flight altitude
- Medium ocean conditions, low glare

Coastal Transect 6

- 2.5 cm image resolution, 1,000 m flight altitude
- Calm ocean conditions
- Low glare
- Clouds come in and out of the field of view below camera

Bird Island Flyover Sequence

- 332 m flight altitude, 1 cm image resolution

Creating Testing Tools

With the alpha and beta data sets defined, and all the animals that appeared each video segment identified, together with their location within the video frame in which they appeared, we created a system for measuring how well the target detection algorithm performed. The general approach for testing was as follows:

1) Automatically choose parameters affecting animal detection (e.g., resolution) based on the type of imagery being processed.
2) Process a video using the animal detection algorithm, generating results including frame numbers and positions of animals within those frames.
3) Compare results from an automated test run against the gold standard of locations provided by Normandeau analysts' manual review of the video.

The specific algorithm performance metrics tested and analyzed are listed and described in Table 5–1.

Table 5–1.

Performance Metrics Used to Test and Evaluate the Performance of the Automated Animal Detection Algorithm

Metric	Description
Percent animals detected	Percentage of total animal occurrences that were detected
Percent birds detected	Percentage of total bird occurrences that were detected
Percent non-birds detected	Percentage of total non-bird animal occurrences that were detected
Percent frames with animals	Percentage of frames that were detected which contain animals
Ratio false positive frames over all frames	The percentage of false positive frames over the total number of original frames.
Ratio false positive frames over positive frames	The number of false positive frames that were found for every real frame found that contained an animal.
Ratio false positive animals over positive animals	The number of false positive animals that were found for every real animal that was found.
Percent data reduction	The total percentage that the data set was reduced by after detection

The testing tools were critical during the development of the detection algorithm, as they allowed us to easily test the algorithm, evaluate the results, modify the algorithm, and then retest. This iterative approach facilitated experimentation and allowed us to identify the most promising avenues for algorithm improvement.

Adapting and Testing the Blob Detector

Boulder Imaging had previously developed code that could automatically process video and identify anomalies in the frames. This code is referred to as the blob detector, and it served as a starting point for developing a modified algorithm to detect the marine animals that had been identified in the alpha data set. Through a process of experimentation, optimization, and tuning of the initial blob detector based on the attributes of the animal images contained in the alpha data set, we developed a configuration of the blob detector specifically adapted to detect marine animals against the background of the ocean's surface in the Op House images. Table 5–2 summarizes the best results that were obtained from the adapted blob detector after roughly six months of optimization and tuning to project-specific imagery.

Table 5–2.

Performance of the Final Blob Detector Algorithm on the Alpha Data Set of High-resolution Offshore Aerial Images from the Operations House Experiments

Metric	Value
Percent animals detected	75%
Percent birds detected	91%
Percent non-birds detected	5%
Percent frames with animals detected	79%
Percent frames with animals missed	20%
Ratio false positive frames over all frames	27
Ratio false positive frames over positive frames	5
Ratio false positive animals over positive animals	38
Percent data reduction	68%

Development of Hue-Saturation-Value (HSV) Detection Algorithm

While the blob detector algorithm worked fairly well for detecting light colored birds, it wasn't as successful at detecting darker animals, such as turtles and rays, that didn't have a lot of contrast with the ocean background. One of the reasons it failed to detect these darker animals is because the original blob detector was only able to process grayscale images. It essentially converted the color image that was recorded by the camera into a black and white image. This eliminated all of the color information that the human eye uses to easily identify these animals, even when the contrast between the animal and the ocean is low.

To address this issue, we developed another detection algorithm that used color information to aid in the detection of the darker animals. This algorithm uses what is known as the hue-saturation-value (HSV) color space as a basis for distinguishing marine animals from the ocean background and, therefore, is called the HSV algorithm**,** as. This HSV color space more closely models the way the human eye perceives a scene. A description of this color space, together with the details of the HSV algorithm, is given in the next section.

Hue-Saturation-Value (HSV) Algorithm Details

There were three main steps incorporated into the HSV algorithm. They were:

1) Convert the red-green-blue (RGB) image to the HSV color space.
2) Threshold the HSV image to separate foreground objects from the background.
3) Filter the thresholded images to eliminate noise.

In the first step of the algorithm, the native images that were recorded by the camera were converted into a format that made it easier to identify objects with a different color than the background ocean, even if the brightness or intensity of the objects did not differ significantly from the ocean's

intensity. The camera records images in RGB format, using an array of pixels to detect how much light is striking the sensor at three different wavelengths—red, green, and blue. For a given pixel, the overall color of the pixel cannot be determined by just looking at one of these three values. Rather, a combination of the three values is needed to reproduce the correct color.

When the images were converted to the HSV color space, the hue, saturation, and value data were converted into three separate channels. As mentioned earlier, the hue is the color of the light hitting the pixel sensor. The saturation can be thought of as the purity of the color, or how close to black the color is. Value is the intensity of the light hitting the pixel sensor, and when viewed separately from the other two channels, the value appears as a grayscale version of the image.

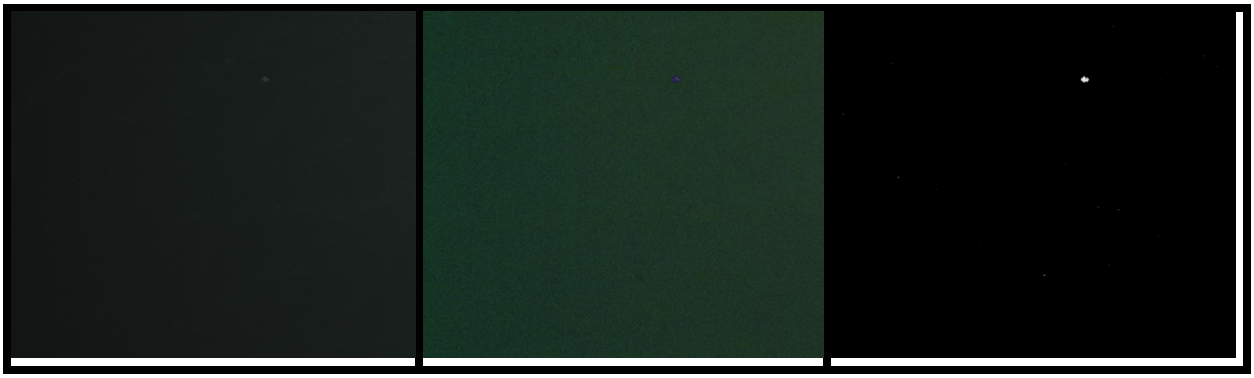

Original Red-Green-Blue (RGB) Image | Converted to HSV | Thresholded Image

Figure 5–1. Examples of image color transformation steps used in the hue-saturation-value (HSV) animal detection algorithm (see text for details).

With the images separated into hue, saturation, and value, we then applied a threshold algorithm to isolate the foreground objects or animals from the background ocean. This part of the algorithm was tuned by empirically measuring the HSV values from numerous examples of animals and ocean patches, and then plotting these values to identify boundaries that would separate the animals from the ocean. Figure 5–2 through Figure 5–4 show the results of these plots.

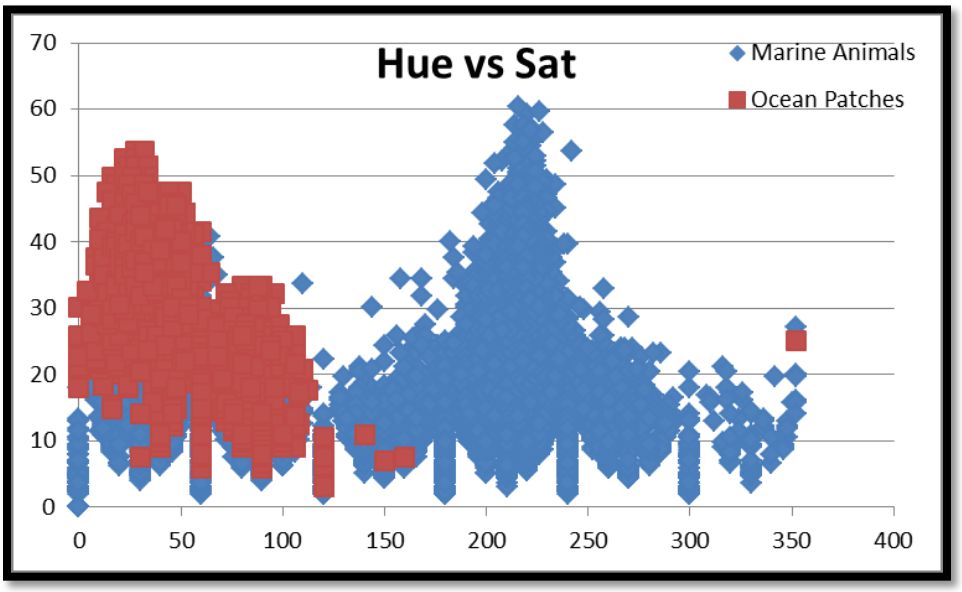

Figure 5–2. Hue (x axis) plotted versus the saturation values (y axis) for marine animals compared with ocean patches. A boundary between animals and ocean can be seen in the vicinity of hue = 120, and was incorporated into the HSV-based animal detection algorithm.

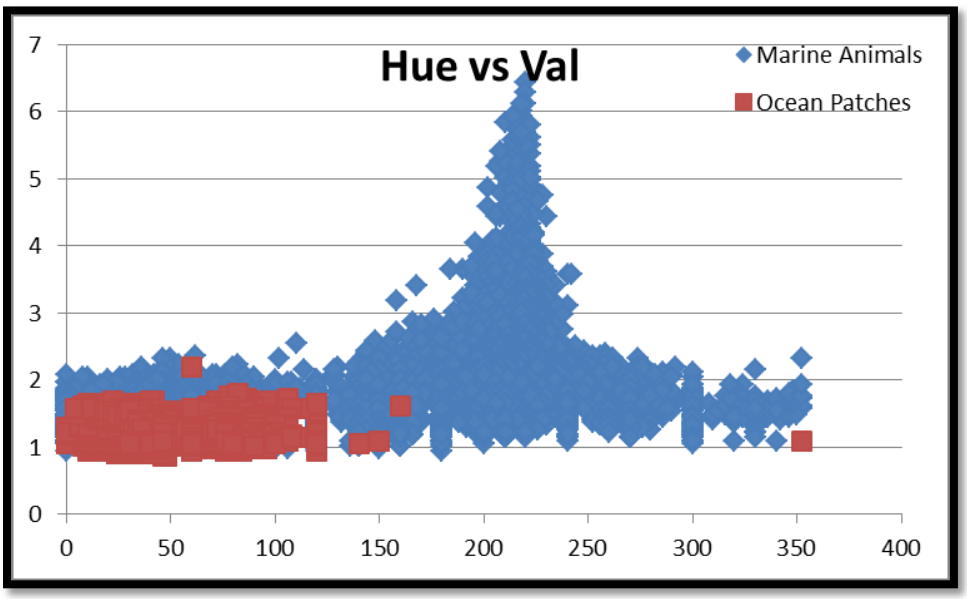

Figure 5–3. Hue (x axis) plotted versus the value (y axis) for marine animals compared with ocean patches. A boundary between animals and ocean can be seen in the vicinity of hue = 120, up to value ≈ 1.8, and was incorporated into the HSV-based animal detection algorithm.

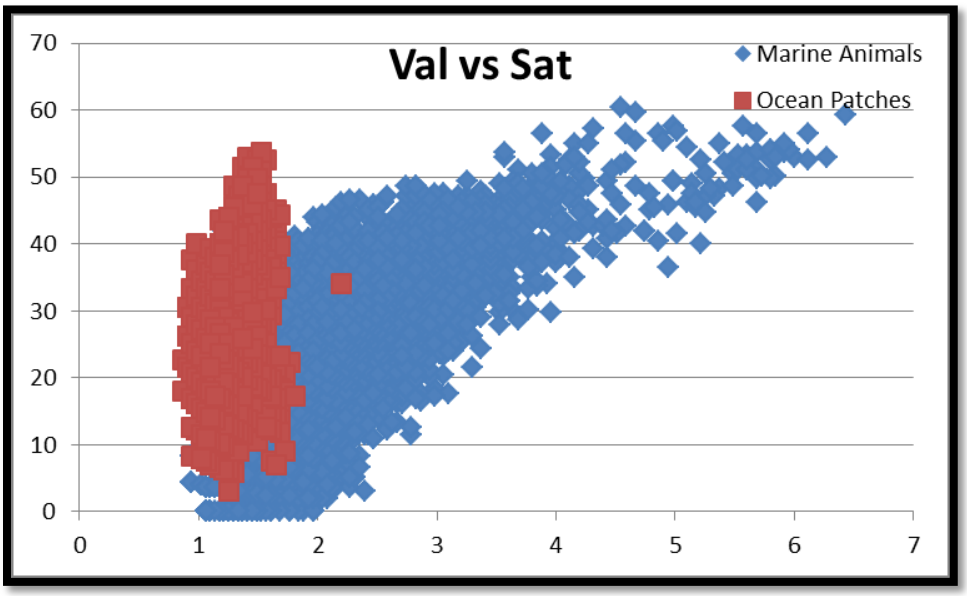

Figure 5–4. Value (x axis) plotted versus the saturation (y axis) for marine animals compared with ocean patches. A boundary between animals and ocean can be seen in the vicinity of value ≈ 1.8, for saturation levels above 5, and was incorporated into the HSV-based animal detection algorithm.

While there is no perfectly clean boundary that separates the animals from the background ocean in any one of the three variables (hue, saturation, and value), plots of two-variable combinations produced clearer separation of animals from ocean background. Both ocean pixels and marine animal pixels had similar ranges of saturation, so that channel wasn't used to for thresholding. A pixel was considered to be part of a marine animal if its hue was between 120 and 360, and its value was greater than 20% (equivalent to 2 on the scales in Figure 5–3 and Figure 5–4). Otherwise, it was considered to be part of the background ocean.

The final step of the animal detection algorithm was to filter the foreground objects to try and eliminate as many false positives as possible. The individual foreground pixels were first grouped together into blobs, and then several characteristics were measured for each blob, including size, aspect ratio, and fill density. Depending on the resolution of the video, we filtered out any blobs under a certain size, as well as any blobs that we considered too elongated or not filled in enough to be an animal.

Assessment of Hue-Saturation-Value (HSV) Algorithm Performance

We tested the final HSV animal detection algorithm with the same automated testing tools that were previously described for the blob detector performance tests. Table 5–3 illustrates the performance of both of these algorithms with respect to the different metrics.

Table 5–3.

Performance of the Final Blob Detector and Hue-Saturation-Value (HSV) Algorithms on the Alpha Data Set of High-resolution Offshore Aerial Images from the Op House Experiments.

Metric	Blob Detector	HSV Algorithm
Percent animals detected	75%	90%
Percent birds detected	91%	98%
Percent non-birds detected	5%	88%
Percent frames with animals detected	79%	99%
Percent frames with animals missed	20%	1%
Ratio false positive frames over all frames	27	95
Ratio false positive frames over positive frames	5	19
Ratio false positive animals over positive animals	38	1,338
Percent data reduction	68%	0%

The final HSV algorithm detected more birds than did the final blob detector (98% versus 91%), and it achieved a much higher detection rate for non-birds (88% versus 5%). Although this is a very substantial improvement in the detection rate (or reduction of the false negative rate), it comes at the expense of a much higher false positive rate. This can be seen in the ratio of false positive frames over all frames—the HSV algorithm marked almost 100 frames as having an animal when none was present for every one frame that it correctly identified as having an animal. Also, the data reduction rate dropped from 68% for the blob detector to 0% for the HSV algorithm. This is due to the HSV algorithm detecting an animal in nearly every frame, when in reality there were animals in only about 5% of the frames.

We conclude that while there is a promise of potential with the HSV algorithm, there is a need for additional research to tune the filtering stage so that the number of false positives can be reduced to a reasonable level. The blob detector, while missing quite a few non-birds, did a better job at eliminating a great majority of the video frames and delivering a smaller subset of frames for a biologist to analyze. However, the blob detector was not generally successful at detecting sea turtles or marine mammals.

Discussion of Automated Target Detection Challenges

The two automated animal detection algorithms we developed for this project each achieved a measure of success with respect to the goal of automating the animal detection process in high-resolution offshore aerial survey imagery. However, significant limitations in both algorithms would need to be addressed through further research and development efforts in order to provide an effect tool, or set of tools for efficient and effective automated image processing.

One of the key areas in which improvement is most needed is the reduction in the false positive rate in the HSV-based algorithm. This is essential to significantly reduce the amount of imagery that needs to be reviewed manually by analysts. The number of false positives is affected by many factors, including the sea state in which the images are captured. When the wind is blowing strongly enough to create whitecaps on the surface, then both HSV-based and blob detection algorithms have a tendency to inappropriately identify the whitecaps as potential animals. Using the methods we were using, and with the data sets that we had, it was extremely difficult to eliminate the whitecaps from being detected while still detecting light colored birds. We opted to err on the side of identifying too many objects rather than being overly aggressive with our filtering and potentially missing an animal. With additional research, however, it should be possible to bring down the false positive rate, potentially by combining hue- and shape-based algorithms.

Another area in which significant improvement is needed for future viability is algorithm speed. As this was our first version of the animal detection algorithm, we concentrated our efforts on making the algorithm as accurate as possible. We didn't focus on optimizing the algorithm for speed, and as a result the video took about four times longer to process than it did to record. Although this was sufficiently fast for us to perform our tests in the lab while developing the algorithm, real time processing speed for onboard target detection would also require additional research and development effort.

6 Evaluation of Effectiveness of High-definition Aerial Image Gathering for Conducting Surveys of Marine Birds, Turtles, and Mammals

6.1 Introduction

This chapter presents a biological evaluation of the effectiveness of high-resolution aerial imaging for conducting offshore marine wildlife surveys. The nature and intent of this evaluation is defined more specifically as task 8 of the contract: to "evaluate the effectiveness of high-resolution aerial surveys for detecting and estimating abundance of birds, marine mammals, and sea turtles and compare its effectiveness to that of traditional survey methods, such as boat surveys and low-level aerial surveys using human observers."

One key element of our evaluation is a distinction between effectiveness for detection/quantification and effectiveness for taxonomic identification of animals. Although these two elements are somewhat interrelated in some cases, they are essentially distinct, and the performance of digitial relative to conventional methodologies is different with respect to each. In essence, our evaluation of the effectiveness of digital survey methods for marine wildlife detection/quantification involves asking the question: "How well can we count animals?" The answer to this question determines the effectiveness of digital methods for producing scientifically valid and robust population density estimates of animals in particular areas at particular times. Our evaluation of the effectiveness of digital survey methods for taxonomic identification of marine wildlife entails asking the question: "How well can we tell what they are?" The answer to this question determines the effectiveness of digital methods for accurately characterizing the spatiotemporal abundance patterns of particular marine animal taxa. Discussions of both elements of digital survey effectiveness are infused throughout this chapter.

We have taken a four-pronged approach to conducting our evaluation of the effectiveness of digital survey methods, corresponding to the four remaining subsections of this chapter, as follows:

1) **Evaluation based on European offshore wind experience.** In Europe, where marine high-resolution aerial wildlife imaging surveys have been used since 2007 and are now widely applied (see section 1.2), significant lessons have been learned about the effectiveness of this methodology for providing scientifically valid and robust data on marine wildlife abundance and distribution to support offshore wind energy development environmental studies. In section 6.2 of this chapter, we evaluate the effectiveness of high-resolution wildlife imaging surveys based on European experience with this technique. This discussion is contributed by Chris Thaxter of the BTO. Dr. Thaxter and his colleague Dr. Burton are leaders in this emerging field, having published the seminal evaluation of high-resolution imaging methodology for offshore wind environmental study purposes in 2009 based on a review and workshop sponsored by the COWRIE consortium. Drs. Thaxter and Burton continue to be engaged in research and QA/QC review of high-resolution imaging data collected for offshore wind energy developments in the UK, and their experience with the ever-changing

application of this new methodology to marine wildlife studies in Europe serves as the basis for this discussion.

2) **Evaluation based on a comparison between experimental aerial imaging surveys and synchronous control surveys conducted with conventional, visual observer-based methods.** The Op House high-resolution imaging flight trials conducted in May 2011 were all undertaken with synchronous control surveys by boat and low flying aircraft. These control surveys entailed wildlife data gathering using conventional methodology derived from the visual observations of taxonomic experts aboard the survey vehicles. The design and execution of both the imaging flight trials and the control surveys are described in Chapter 1 of this report. In section 6.3 of this chapter, we evaluate the effectiveness of digital survey methods compared with visual observer-based survey methods with respect to both detection/quantification and taxonomic identification of marine animals, based on an analysis of the data gathered in the course of these experimental surveys. This subsection is written in the format of a scientific technical manuscript.

3) **Evaluation of optimal high-resolution imaging methodology based on experimentation**. A core component of the Op House imaging flight trials (Chapter 1) was experimentation with different imaging methodological parameters for the purpose of evaluating which specific high-resolution imaging configurations work best. Imaging parameters with which we experimented to varying degrees include flight altitude, camera tilt, image resolution, image gyrostabilization, camera type, light polarization, and time of day. Some of the results of this imaging methodological experimentation have been discussed previously in section 3.3. In section 6.4 of the current chapter, we present a more in-depth discussion of the importance of image resolution and camera tilt on high-definition imaging survey effectiveness, particularly with respect to taxonomic identification of the imaged animals. In this section, we also examine the impact of an imaging variable that has emerged as one of the key methodological questions in European studies: video versus stills (Thaxter and Burton 2009; Buckland et al. 2012). While Buckland et al. (2012) recently compared these two methods with respect to effectiveness for population density estimation, we provide the first direct comparison of these methods with respect to effectiveness for taxonomic identification of imaged animals. This subsection of our evaluation is based on our analysis of over 9 terabytes of imagery gathered during the Op House experiments. Our procedures for manual review of, and animal image extraction from, this imagery were described in Chapter 0 of this report, and our procedures for quantitative and qualitative analysis of animal identification depth, agreement, and confidence in this imagery as affected by the imaging parameters of interest are described in the current subsection.

4) **Evaluation of the taxon-specific utility of high-resolution imaging on the US AOCS.** While high-resolution digital imaging surveying represents a promising and broad spectrum solution for offshore wildlife studies, it is not a magic bullet nor a one-stop shop for all offshore wildlife data gathering needs. The effectiveness of this new method for gathering scientific data on animals in marine environments, and the type of data that can be gathered varies across taxa as a function of taxon-specific appearance features, behavioral characteristics, and spatiotemporal distributions. In subsection 6.5 of this chapter, we present

a taxonomic guide to the utility of high-resolution imaging surveys on the US AOCS. This guide is intended to answer the following questions: "For which taxa will this technique work, and for which taxa won't it? What type of data can be gathered using this technique?" We developed this guide based on a comprehensive review of technical literature and visual identification resources for the bird, marine mammal, and sea turtle fauna of the entire region of interest for this study (US AOCS from Maine to Florida, from states' seaward boundaries to the 30 m isobaths, see Chapter 1), combined with our assessment of the capabilities afforded by this new technique, as constrained by its inherent limitations.

6.2 Review of European Experience

6.2.1 Effectiveness of High-resolution Imaging for Detection/Quantification of Marine Wildlife

An important question to ask is: "How reliable are the population estimates produced from digital surveys and given the different survey methodologies they require, and how rigorous are they compared to conventional visual-based estimates"? To address this concern in Europe, several recent studies have compared the use of traditional visual techniques for estimating abundance and distribution alongside digital methods of still images and video. Moreover, the studies go further by focusing on different methods for both visual and digital methods in estimating abundance using both design-based and model-based population estimates. Here, we draw primarily on two such studies comparing methods at two sites in the UK: Norfolk Round 3 region (Burt et al. 2009) and Carmarthen Bay (Burt et al. 2010).

Norfolk

Two aerial surveys were conducted in Spring 2009 in the Norfolk Round 3 (Zone 5). The area was subdivided into eight strata (the area could not be covered in a single day), and abundance estimates were derived using distance sampling and modelled density surfaces for visual methods and strip transects and modelled density surfaces for digital video methods. Note, still image digital methods were not compared in this study. To estimate trends in abundance, power calculations were also performed—this is an important step to understanding whether the power of a survey is sufficient to detect change with appropriate precision, and in this case helped assess whether enough information was available to assess whether slopes of trends differed significantly from zero. Also, due to subsampling areas within the survey region, the digital survey effort was also broken into smaller blocks than dictated by the original survey design.

Burt et al. (2009) did not produce abundance estimates at the species level, but rather grouped at the higher levels of seabird, gull, and diver—although divers could not be compared between the methods due to a lack of those recorded by digital methods. However, Burt et al. (2009) found that abundance estimates were comparable for gulls, but confidence estimates did not overlap for seabirds. Of more importance, however, is the issue of precision of those estimates. In understanding their precision by survey strata/analysis/species groups, Burt et al. (2009) conclude that: 1) conventional distance sampling of visual methods produced the most precise estimates (coefficient of variation [CV], ca. 0.10); 2) density surface visual model estimates for gulls and digital strip surveys of seabirds and strip transect digital estimates of seabirds produced less precise estimates (CV, ca. 0.30); and 3) all other combinations produced CVs 0.45 to 0.66. CVs of 0.30 are quite low

and require substantial annual changes in the population (ca. 11% over 10 years) to enable the survey to have enough power (at 0.8 level) to detect that trend. Thought, therefore, needs to be given as to how the survey is designed for the species of interest (Thaxter and Burton 2009) and the method of how final estimates are derived.

Carmarthen Bay

A separate study was conducted recently at Carmarthen Bay (over four dates in March 2009) to also compare the estimates produced from different survey methods of visual and digital surveys (Burt et al. 2010). This was a controlled study under which close attention was paid to minimizing potential biases, for example, by carrying out the surveys on the same days at approximately the same time of day to avoid temporal and influx issues. This analysis was also very useful to compare estimates of abundance for groups of species that show very different clumped and nonclumped distributions of individuals at sea—well aggregated species may be easily detected in numbers but may require differing survey protocols to actually estimate their abundance throughout a region, such as more flight lines, to increase the chances of hitting a clump of birds. Burt et al. (2010)therefore, focused on: scoter species that have large aggregations at sea and gulls that are less clumped as a species group. This study used both model-based and design-based estimates of abundance, following on from an initial investigation from Rexstad and Buckland (2009) comparing visual-based methods using distance sampling, and compared both digital still image methods, and digital video-based methods. Protocols for each method are described in detail in Burt et al. (2010).

The clumped distribution of scoters gave estimates with poor precision for most of the survey-type analysis combinations, on average with a CV of 0.50. Model-based digital video methods achieved a CV of 0.40 for scoter, which may have been due to more transects used thus increasing chances of hitting a clump of birds. For gulls, although the average CV was found to be similar (0.45) to scoters, the range of CVs was greater, between 0.25 and 0.80. Therefore, even under controlled conditions, estimates for the different methods in Burt et al. (2010) were very variable, and the authors conclude that no consistent differences between methods and survey analysis types emerged. Burt et al. (2010) suggest that bespoke survey designs are a necessity, informed by knowledge from pilot surveys, enabling sufficient effort to produce reliable estimates. Otherwise, a lack of effort for a species could result, and for a species as clumped as scoter could produce estimates that are not meaningful owing to poor precision. Scoter as a species group requires higher coverage of the study region than other species groups.

6.2.2 Effectiveness of High-resolution Imaging for Taxonomic Identification of Marine Wildlife

The information regarding animal identification in relation to resolution and image quality is not generally in the public domain, and the different methods used by different companies are subject to commercial confidentiality. The levels of identification recommended as minimal in Thaxter and Burton (2009) of 5 cm, are now surpassed in all current surveys and, in general, 3 cm could be considered as being coarse in Europe with many surveys reaching 2 cm or 1 cm in current surveys. Technology will also increase beyond this in the near future. In the UK, regulators have agreed that identifying to species level is desirable, but if digital methods cannot reach that level then the next appropriate species grouping should be selected for identification—groupings are based on those previously used from boat and aerial surveys from the JNCC in the UK (Thaxter and Burton 2009),

which oversees and regulates such surveys. For instance, alcid spp., large gull spp., small gull spp., and diver spp. are frequently used. Often separation of species under these categories is difficult in current digital survey methods. However, it is not currently clear whether 3 cm is less satisfactory than 2 cm or 1 cm in producing identified species or groups, because there is currently little to no information available publically to address this question. Nor is there any information on whether particular camera settings are more or less beneficial in this regard. However, Hexter (2009a) provides a discussion on camera and survey set up for video-based methods.

It is important, however, not to stretch to species-level identification when the image does not allow such certainty. Therefore, rigorous QA/QC is carried out in all current UK Round 3 surveys as a result of direct recommendations in Thaxter and Burton (2009). Where species-level identification is not achieved, the next grouping up is selected with alternative identifications also given as a second choice. A randomly chosen subsample of the images collected are passed on for external quality assurance and control in a double-blind assessment, and a 90% agreement level is sought. Where this is not met, post-QA/QC discussions take place between the external reviewer and the surveyor, and if quality assurance is then not agreed on, then a rerun of the QA/QC is carried out.

To fully understand the impact a development may have on a species, species-level identifications are required for all impact assessments. It should, therefore, be noted that traditional visual surveys are still required by regulators alongside all digital survey methods, as stated in section 4.3.1. Digital methods as a stand-alone product in Europe cannot currently be used in isolation for producing population estimates, but are a crucial component in overall abundance given their particular advantages they have over visual methods (see Thaxter and Burton 2009).

6.3 Comparison of Digital and Visual Observer-based Methods for Surveying Birds, Turtles, and Mammals in Marine Environments

6.3.1 Abstract

As demand increases to exploit natural resources in the offshore environment, there is a growing need to expand our knowledge of the density and distribution of animals inhabiting this environment to better predict and mitigate the impact of development. Three survey methods are commonly used to gather data on distribution and abundance of birds, sea turtles, and marine mammals—two traditional methods using visual observers on boat or aircraft, and a newer technique that uses aircraft equipped with digital imaging technology. However, the extent to which these methods produce comparable estimates of density, comparable taxonomic identification depth and accuracy, and the overall relative merits of each method for surveying different taxa, remain poorly understood.

We compared the effectiveness of these three methods for surveying marine birds, turtles, and cetaceans by performing a set of field surveys offshore of Oak Island NC during May 2011. Fourteen experimental transect survey trials were conducted for the purpose of comparing animal detection and density calculation/estimation between aerial high-resolution digital imaging surveys and synchronous conventional control surveys using expert visual observers aboard a boat and a low flying aircraft. Taxonomic identification patterns were compared across platforms using data from

additional surveys in animal-rich marine environments conducted with all three survey platforms in the vicinity of, and within the same general time frame, as the experimental transect surveys.

The rate at which observed birds were identified to the species level was slightly higher (77%) using digital survey data than it was for either of the visual observer survey platforms (71% and 45% for boat and aerial visual observer surveys, respectively). For turtles and mammals, visual observers achieved higher rates of species-level determination than did analysts using the digital survey data, although strong observational biases in animal detection rates for both of these taxa on visual observer platforms suggest that this apparent increase in taxonomic determination depth may not represent a real increase in data quality. Analysis of interobserver variation in species-level determination rate (all platforms) and multiobserver agreement on species-level determinations (digital data only) suggest that taxonomic identifications from digital survey data are likely to be more consistent, accurate, and less affected by observer biases than are identifications from visual observer based surveys.

Animal density estimates (visual observer methods) or calculations (digital) did not generally exhibit pronounced variation across methods, possibly reflecting the overall low density of marine birds, turtles, and mammals at the time and place where experimental transect surveys were conducted. The exception was sea turtles, for which density calculations from the digital surveys were significantly higher than were the density estimates from either visual observer platform (10 times higher than boat-based and four times higher than aircraft-based observer survey density estimates). This difference is likely to reflect greater accuracy of digital methods, and suggests that digital surveys offer a significant methodological improvement over visual observer based surveys for this group. For marine birds and mammals in low-density situations, digital and observer based survey methods may produce similar density calculations/estimations, although digital density calculations are likely to be more accurate and precise because of precise definition of areal coverage and reduced animal disturbance/attraction effects. However, we note that in areas with higher animal densities, animal density calculations from digital methods are likely to be significantly more accurate than are density estimates from visual observer based surveys, as the latter are known to be severely affected by observer swamping effects under such conditions.

6.3.2 Introduction

There is a growing interest in, and need to exploit, the energy resources of the offshore environment (USDOE 2008). A number of developments, especially for wind facilities and oil and gas exploration, require baseline surveys to assess potential impacts to fauna. Furthermore, assessing the impact on the environment caused by construction and the efficiency of mitigation measures requires periodic and sometimes long-term monitoring. The offshore environment is a very extensive area to survey that is difficult or dangerous and often very expensive to access. There is little pre-existing knowledge of species distribution and density, and for those species for which there are data, density is usually low and distribution more often than not heterogeneous. These limitations make the characterization of animals' spatiotemporal distributions and the prediction of environmental impacts especially challenging in the offshore environment, and create a need for scientifically rigorous and cost-effective survey methods.

Visual surveys by expert observers positioned on ships or other marine platforms have been used since the early twentieth century to assess the abundance and distribution of marine birds (Henkel et

al. 2007; Tasker et al. 1984), and have recently been applied extensively to offshore wind environmental baseline studies in the US (Paton et al. 2010; NJDEP 2010). These surveys have the advantage of potentially allowing observers sufficient time to identify the species, sex, and age class of marine animals based on appearance, and also to observe behavioral traits that may be useful in taxonomic identification. However, vessel-based visual observer surveys have well-known limitations that restrict the scientific accuracy and robustness, as well as the cost effectiveness of this survey method. Among the most important limitations of vessel-based surveys are slow survey speed, which makes coverage of large areas difficult and costly, a variety of biases that are introduced into the survey data both by animal attraction/repulsion effects from the vessel, and observer effects such as interobserver skill variability and distance estimation error.

Aerial visual observer based surveys, provide a faster alternative, and have now been in use for several decades (e.g., Rexstad and Buckland 2009; Camphuysen et al. 2004; Komdeur et al. 1992); and have also been used in US offshore wind baseline studies (Paton et al. 2010; NJDEP 2010). Such surveys entail flying an aircraft at altitudes sufficiently low for expert observers to identify animals at or near the water's surface, usually from 79 to 180 m flight altitudes (Hyrenbach et al. 2007; Henkel et al. 2007; Camphuysen et al. 2004; Shoop and Kenney 1992). Relative to vessel-based surveys, aerial observer surveys allow larger areas to be covered in a relatively short amount of time, and are less hampered by sea conditions. Additional advantages of aerial relative to vessel-based surveys include the ability to survey shallow water areas with subsurface reefs and sandbanks, lower animal attraction effects, and wider effective survey swath width (Camphuysen et al. 2004). However, the suitability of aerial visual observer-based surveys is also constrained by several well-known limitations. First, there are safety concerns with use of low flying aircraft in a marine environment. Second, the activity of low flying aircraft is known to disturb many marine animals (Thaxter and Burton 2009; Allison et al. 2008). This disturbance affects the quality of the resulting data by causing certain animals to dive or flee, which impacts not only the ability to generate accurate density or abundance estimates (Thaxter and Burton 2009; Burt et al. 2009), but also the accurate characterization of natural, *in situ* animal behavior and movement (Camphuysen et al. 2004). Finally, similar to vessel-based visual observer surveys, the accuracy of the data resulting from aerial, observer based surveys is affected by well-known observer biases including observer swamping, observer variability in identification ability, and false negatives (failure to observe animals) (Henkel et al. 2007; Hyrenbach et al. 2007; Burt et al. 2009). The lack of a pre-observer data archive in observer-based surveys makes observer biases difficult or impossible to quantify or eliminate from survey data.

A third survey method which has emerged recently with the advent of high-resolution imaging technology is aerial digital imaging. In these surveys, an aircraft with a mounted camera flies at higher elevations (typically 450 to 600 m) in a transect pattern over a specified marine area, gathering either overlapping (video) or nonoverlapping (stills) images of the water's surface, and storing them for subsequent extraction of animal data from the imagery, usually assisted by specially developed image recognition software. Such surveys were initially applied in western Europe in the mid-2000s, and have been widely applied since then for offshore wind environmental studies, particularly in the UK (Burt et al. 2009; Rextad and Buckland 2009; Thaxter and Burton 2009; Buckland et al. 2012). Compared with observer based aerial surveys, the higher flight altitude of digital imaging surveys increases operator safety, reduces or eliminates wildlife disturbance effects,

and enables the possibility of conducting postconstruction monitoring at offshore wind facilities, as survey flights are well above the rotor swept zone of commercial marine wind turbines. Furthermore, because a pre-observer archive of raw observational data is gathered, taxonomic identification of observed animals can be improved by applying quantitative measurements, and consulting identification manuals while reviewing images. In addition, imagery can be revisited and verified by multiple observers to reduce, measure, and control observer effects (Buckland et al. 2012; Burt et al. 2009; Thaxter and Burton 2009; Camphuysen et al. 2004).

With respect to obtaining accurate estimates of animal density or abundance in marine environments, digital survey methods represent a significant improvement over visual based methods, as they are not subject to several of the sources of error that severely constrain the accuracy of animal density estimates from visual based surveys. First, digital surveys produce precisely defined survey areas that are not subject to variation in observers' abilities to estimate distances, or variation in animal detectability at different distances. Second, digital survey data are not subject to observer swamping effects that distort the accuracy of visual observer based density estimates particularly in dense animal aggregations, such as commonly occur in many bird species in marine environments.

Several recent studies have begun to explore the efficacy of different survey methods by comparing the results of simultaneous bird surveys using different methods (Buckland et al. 2012; Burt et al. 2009, 2010; Rextad and Buckland 2009; Henkel et al. 2007). However, none of these previous studies compared simultaneous surveys by boat and aircraft based observers as well as aerial digital surveys. Also, none of these previous studies analyzed results for marine mammals and turtles in addition to birds.

We conducted a set of survey experiments intended to compare density estimates and taxonomic identification of animals between observer based methods (vessel and aerial based) and digital aerial imaging methods for surveys of birds, turtles, and mammals in marine environments.

6.3.3 Methods

Field Surveys

We performed a series of field surveys between 10 and 20 May 2011, off the coastline of Oak Island NC (-78.100700 33.911838 decimal degrees). Field surveys were conducted with three survey platforms.

Boat-based Visual Observer Surveys (Boat)

The observer vessel was the 13.4 m sport fishing boat Voyager. Two expert observers for mammals and turtles and two expert observers for birds were on board, one on each side of the vessel, following recommendations by Maclean et al. (2009) and Camphuysen et al. (2004). Each observer was equipped with binoculars, data sheets, range finders, time piece, and digital voice recorder. Observers surveyed the air and water from 0 to 1,000 m from the vessel. Before each survey, surveyors calibrated distance estimation using a laser rangefinder on objects (e.g., buoys) at a variety of distances. One observer scanned 90° starboard through 0° and the other observer scanned the same to port. Bowriding animals or animals or birds milling around the boat were counted only by the starboard observer with count and identification agreement from the port observer. All other sightings were independent of one another and care was taken to avoid observers' attention being drawn to any activity by another observer or crew member during surveys.

Animals or cues (e.g., flukes, blows) seen ahead of the perpendicular distance were recorded, and sighting data were recorded up until the point the animal or cue was perpendicular to the observer. Animals or cues beyond 1,000 m were recorded but were not included in any analyses. All observations were recorded along with timestamp (to the nearest second) to enable georeferencing through comparison with timestamps and coordinates recorded continuously by a GPS unit on board the vessel.

Aerial Visual Observer Surveys (V-plane)

During aircraft based visual surveys, two marine mammal and turtle observers, one covering each side of the aircraft, and two avian observers, one covering each side of the aircraft, were stationed within a Skymaster aircraft. The aircraft flew at 150 m altitude, within the scope of similar surveys (Hyrenbach et al. 2007; Henkel et al. 2007; Camphuysen et al. 2004; Shoop and Kenney 1992). Each observer was equipped with binoculars, data sheets, inclinometer, time piece, and digital voice recorder. Observers recorded all observations instantly on a digital voice recorder using timestamps of hours, minutes, and seconds to allow georeferencing by comparison with continuously recorded GPS data. Inclinometers were initially used to measure the angle of declination from the window, but given the cramped conditions within the aircraft it became more efficient to place hatch marks on the struts of the aircraft marking distances of 100 m (11°), 200 m (22°), 300 m (31°), 400 m (39°), and 500 m (45°) from the track line.

Aerial High-resolution Digital Imaging Surveys (C-plane)

Digital videos were recorded using an Imperx IGV-B4820 16 MP area-scan camera. The camera was mounted external to a Skymaster aircraft on the port side, using a custom fabricated steel mount with a windscreen. The aircraft had two pilots and one camera operator stationed inside. Following European protocols, the lowest altitude flown was 450 m (Thaxter and Burton 2009; Maclean et al. 2009). Altitudes as high as 1,000 m were flown, which exceeded the typical maximum altitude of European high-resolution imaging surveys by 400 m (Thaxter and Burton 2009). The camera was tilted to avoid glare at either 15° or 44°. These variations in altitude and tilt resulted in a range of image resolution from 1 cm to 3 cm, where image resolution is defined as the length of the side of a single, roughly square pixel on the surface of the water, produced as a result of a particular combination of optical magnification and flight altitude. Imaging swath widths ranged from 49 to 146 m, as a function of image resolution. GPS coordinates were recorded by the camera operator and timestamps correlated with video images.

Survey Design

Two types of surveys were conducted, as follows:

Experimental Offshore Transect Survey Trials were conducted with all three survey platforms in parallel, to compare animal detection and density estimation results across platforms. These surveys employed a line transect method as recommended by Camphuysen et al. (2004) and Thaxter and Burton (2009). For maximum comparability and experimental control, the C-Plane and V-plane always flew the same transects, displaced by approximately 5 minutes (with the V-plane 5 minutes behind the C-plane) with the two planes never coming closer than 1 km to each other, to allow for safe flight operation. The C-plane always flew ahead of the V-plane because its greater altitude was assumed to result in a lower probability of disturbing animals. The boat covered the same transect

several hours in advance (in the morning) or behind (in the afternoon), also to minimize effects of disturbance and interference between the surveys (Table 6–1 and Table 6–1). The camera plane and visual observer plane flew at roughly 200 km/hr (C-plane 153 km/hr to 232 km/hr, average 205 km/hr; V-plane 180 km/h to 258 km/hr, average 213 km/hr), in line with other documented survey methods (Burt et al. 2010; Burt et al. 2009; Thaxter and Burton 2009; Camphuysen et al. 2004). Plane surveys were conducted between 11:30 and 14:00. Typically, the boat departed the dock between 07:00 to 09:30, performed its outbound transect survey trial on one transect in the morning, and performed its inbound transect survey trial on the same transect in the afternoon, averaging 30 km/hr speed during surveys (range 27 km/hr to 34.5 km/hr). This is slightly faster than speeds reported by Camphuysen et al. (2004) and Henkel et al. (2007), but was preferable given the distance to travel and low density of fauna. Following standard recommendations, no survey trials were conducted in a sea state greater than Beaufort 3 (Camphuysen et al. 2004; Maclean et al. 2004). These surveys were conducted from 70 to 110 km offshore in water depths ranging from 10 m to 100 m. Table 6–1 illustrates the set of transect survey trials that was conducted, and Figure 6–1 illustrates the locations of the two transect routes that were used.

Table 6–1.

Experimental Transect Survey Trials Conducted 10 to 20 May 2011 Off Oak Island NC.

Platform	Trial	Start Time	End Time
C-plane	1	13:19:45	13:33:23
Boat	1	8:43:31	10:18:45
V-plane	1	13:19:45	13:35:27
C-plane	2	13:33:23	13:47:02
Boat	2	10:18:45	11:54:00
V-plane	2	13:35:27	13:51:10
C-plane	3	14:07:48	14:21:40
Boat	3	14:08:00	15:22:35
V-plane	3	13:55:33	14:06:22
C-plane	4	14:21:40	14:35:31
Boat	4	15:22:35	16:37:10
V-plane	4	14:06:22	14:17:10
C-plane	5	12:54:53	13:07:04
Boat	5	8:10:30	9:43:30
V-plane	5	12:54:53	13:08:47
C-plane	6	13:07:04	13:19:15
Boat	6	9:43:30	11:16:30
V-plane	6	13:08:47	13:22:41
C-plane	7	13:31:40	13:46:58

Platform	Trial	Start Time	End Time
Boat	7	13:32:50	14:55:25
V-plane	7	13:24:13	13:37:26
C-plane	8	13:46:58	14:02:17
Boat	8	14:55:25	16:18:00
V-plane	8	13:37:26	13:50:40
C-plane	9	12:53:21	13:07:30
Boat	9	9:14:50	10:13:25
V-plane	9	12:53:20	13:04:43
C-plane	10	13:07:30	13:21:38
Boat	10	10:13:25	11:12:00
V-plane	10	13:04:43	13:16:05
C-plane	11	12:47:09	13:00:44
Boat	11	7:23:00	8:54:00
V-plane	11	12:49:59	13:02:42
C-plane	12	13:00:44	13:14:19
Boat	12	8:54:00	10:25:00
V-plane	12	13:02:42	13:15:24
C-plane	13	11:39:57	11:55:02
Boat	13	7:02:00	8:45:13
V-plane	13	11:39:56	11:57:20
C-plane	14	11:55:02	12:10:06
Boat	14	8:45:13	10:28:26
V-plane	14	11:57:20	12:14:45

Note: C-plane is the Digital Imaging Survey Plane, V-plane is the Visual Observer Survey Plane, and Boat is the Visual Observer Survey Boat.

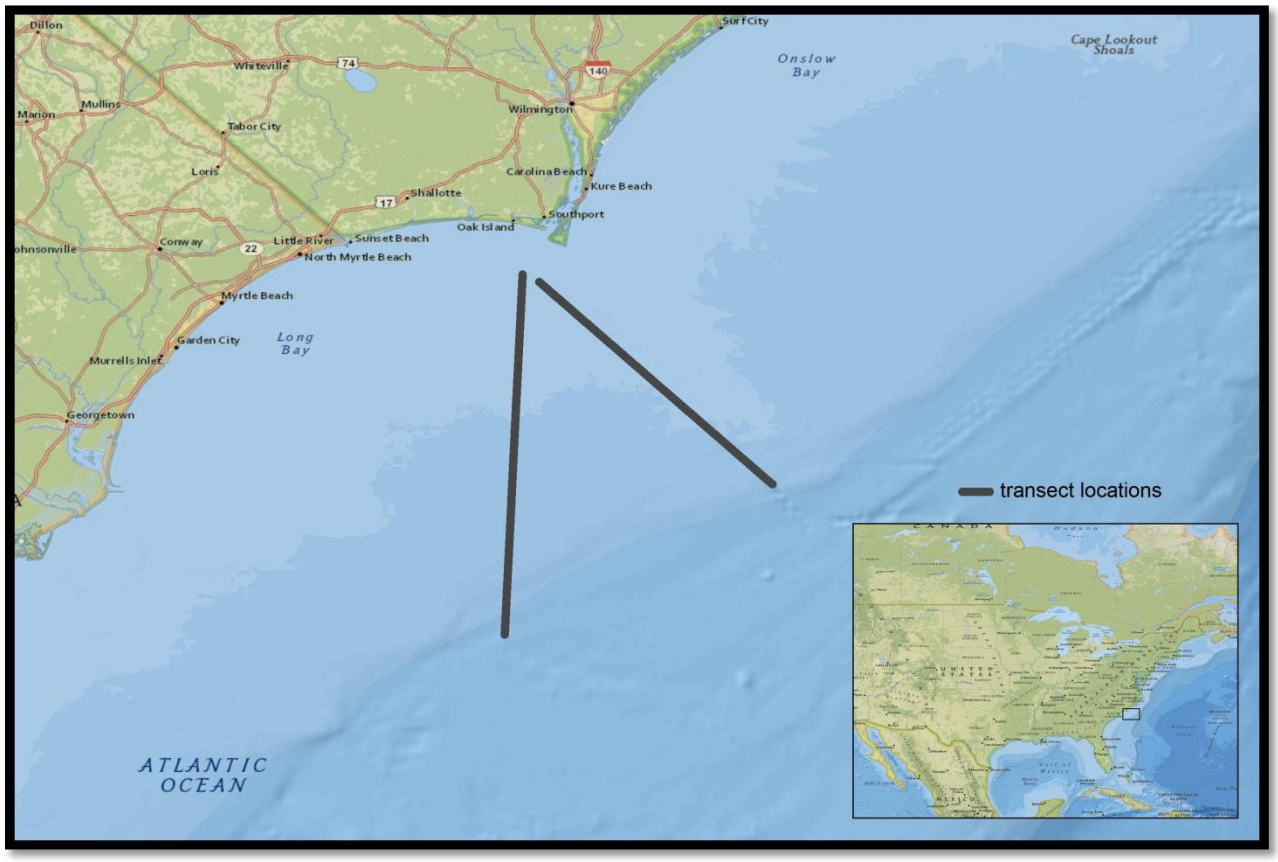

Figure 6–1. Location of experimental transect survey routes followed by all three survey platforms (boat with visual observers, aircraft with visual observers, aircraft with camera) during marine wildlife survey experiments conducted 10 to 20 May 2011 offshore of Oak Island NC.

Supplemental Surveys in Animal-rich Areas were also conducted with all three platforms. These surveys were conducted opportunistically within 20 miles of the transect survey locations depicted in Figure 6–1, in animal-rich areas including along the coast, over a boat located far offshore that was chumming to attract seabirds, and in the vicinity of a coastal seabird nesting colony. Data from these supplemental surveys were not used in the animal detection or density estimation comparisons, but were included in the comparisons of taxonomic identification patterns across platforms in order to bolster sample sizes.

Digital Video Image Analyses

Analyses of all image data gathered by the C-plane, both during the transect flights listed in Table 6–1 and during the supplemental flights for additional animal image gathering, were completed between September 2011 and February 2012 in the Normandeau Associates image analysis laboratory in Gainesville FL. Image analysts used Quazar, a custom-made software platform created by Boulder Imaging, Inc., to view each frame on a high-definition LCD screen. The viewing process was kept identical for each analyst, but with some variation in time taken over the same number of

screen scans for images with sections of wave or glare. For each potential animal detected in the imagery, a cropped image of the animal was saved for later identification, along with image metadata, for cross referencing and for record verification. Independent identifications from the extracted JPEG images were made by at least two people familiar with each taxonomic group to improve identification accuracy. Approximately 10% of the image data viewed by each analyst were reviewed by another analyst, to assess the extent of false negatives, and an independent review was made of all image metadata such as date, timestamp, camera configuration, survey information and analysis data.

Density Estimation

Animal densities were calculated or estimated from the data produced by all three survey platforms for the experimental transect surveys only. Although the three platforms covered the same total length of transect, the distance up to which animals were recorded perpendicular from each platform differed, resulting in differences in the total effective area surveyed. The image swath width for the digital surveys varied as a strict function of image resolution/magnification, and the total area surveyed was calculated as the transect length multiplied by the width of swath covered by the camera. For visual observations, however, the area being surveyed could not be defined as precisely, because detectability of individuals typically declines with distance from the observer. To account for this, we estimated total area surveyed for each of the visual observer platforms using standard methods that correct for variation in detectability as a function of the distance of the animal to the observer. We used distance software (Thomas et al. 2009) to estimate the effective survey swath width separately for each visual observer platform (boat, V-plane), and for each major taxonomic group (marine birds, mammals, turtles) by fitting a variety of potential curves to observed animal detection × distance data to model the decrease in detectability with increasing distance. We compared uniform, half-normal, and hazard-rate key functions for each effective survey swath width estimate, all with the default cosine series expansion, and chose the model with the best fit based on the lowest Akaike's information criterion (AIC) value. Cluster size was estimated using the program default options, under the assumption that larger clusters are more easily detected at greater distances than are smaller clusters. To account for such differences in detectability among clusters, we multiplied the density estimate by estimated cluster size divided by mean observed cluster size.

Inspection of the V-plane data showed a peak in observed animal abundance at approximately 150 to 250 m distance for all groups. This peak may have resulted from distance estimation errors by observers or observational biases in different distance zones. There have been similar problems encountered in other studies where observers appeared to concentrate on detecting animals in one more easily observed distance band (Burt et al. 2009). To examine the density of animals recorded by V-plane observers in this intermediate distance band, we created an alternative measure of density for V-plane data, consisting only of data from this distance band. We refer to this density measure as peak density. To examine whether there were distinct variations in recorded density within the peak band, we separated the data into four 25-m distance bins within the 150 to 250-m peak density band, deriving four separate estimates of density and its mean within the peak distance band. We did not observe any significant differences in abundance across these four bins. Because the sources of bias causing this abundance peak at intermediate distance from the plane are not known, it is not clear which measure of density from the V-plane data is more accurate—overall density (entire effective

swath width) or peak density (density within 150 to 250 m peak density band only), so we included both in our analyses.

We used a Kruskal-Wallis test implemented in the software PAST (Hammer et al. 2001) to assess the significance of differences in density recorded or estimated for each group and platform by treating each trial as an independent measure of density. Analysis of the density data showed no evidence of spatial autocorrelation or repeatable spatial patterns in density among trials, and they were thus treated as independent. The significance of differences in density measures between pairs of platforms was assessed by calculating p-values for each pairwise comparison using a Mann-Whitney U test, adjusted for multiple tests by Bonferroni's correction.

Taxonomic Identification

We compared the depth of taxonomic identification level achieved, and also the variation between, and agreement among, observers in taxonomic determinations of observed animals using data from all three platforms from both the experimental transect surveys and the supplemental, animal-rich flyover surveys.

For the visual observer surveys, taxonomic identifications were rendered by the expert observers during the surveys based on their observations of the animals, as per standard protocols. For the digital imaging surveys, a pre-observer archive of the image data served as the basis for taxonomic identification of the imaged animals. Identifications were made by comparing animal images with images and other information from taxon-specific identification manuals and a variety of additional reference materials. Identifications were aided by direct measurements of the animal dimensions (body length, wing chord, wingspan, bill length) in the images, and comparing them to known dimensions of animal species from various literature sources. Body dimensions were inferred from the imagery as a function of known image magnification levels, and assuming that imaged animals were near the surface of the water. The latter assumption was shown to be robust to relatively minor variations in bird flight altitude, given the relatively high altitude of the camera.

For three-platform comparisons, we examined the percentage of individuals identified to species as a metric of identification performance by platform. We also examined variation among visual observers in this variable. With C-plane data, because animal identifications were performed using a pre-observer data archive, we were also able to examine agreement in taxonomic determinations between separate experts reviewing the same images. Agreement was analyzed using taxonomic determinations from cross-observer bird identification trials, in which images of 220 individual birds chosen from representative experimental survey treatment factor combinations of altitude and resolution were examined, measured, and taxonomically identified independently by two separate taxonomic experts.

6.3.4 Results

Density Calculation/Estimation

Across the 14 comparable transect survey trials conducted by the three platforms, the C-plane recorded 47,580 frames of video data, containing 19 bird individuals, 11 turtle individuals, and two dolphin individuals over 3.25 survey hours. Observers on the V-plane recorded 57 birds, 20 turtles, and two dolphins over 3.25 survey hours, and observers on the boat recorded 101 birds, one turtle, and 34 dolphins over 20 survey hours. Animal density calculations or estimates for all three

platforms are presented in Table 6–2. For the visual observer based platforms, density estimates are based on the total estimated effective survey swath widths. For the V-plane, animal density estimates from the peak density band (150 to 250 m from the plane) are also given in Table 6–2. The only taxonomic group for which estimates of mean density were significantly different across all three platforms was turtles, with density estimates significantly higher from the C-plane than from the boat ($p = 0.018$) or from the V-plane, regardless of whether uncorrected density ($p = 0.032$) or peak density ($p = 0.047$) was used from the V-plane.

Table 6–2.

Density Estimates for the Three Surveyed Taxa from Three Survey Platforms (C-plane = Aerial Imaging Survey; V-plane = Aerial Visual Observer Survey; Boat = Boat-based Visual Observer Survey), as Recorded During Experimental Transect Surveys Conducted 10 to 20 May 2011 off of Oak Island NC

	Birds				Turtles				Cetaceans			
Trial	**C-plane**	**V-plane**	**V-plane (PD)**	**Boat**	**C-plane**	**V-plane**	**V-plane (PD)**	**Boat**	**C-plane**	**V-plane**	**V-plane (PD)**	**Boat**
1	0	0.032	0.092	1.235	0	0.03	0.092	0	0	0	0	0
2	0	0.664	1.935	0	0.376	0.03	0.092	0	0	0	0	0
3	0	0	0	0	0	0	0	0	0	0	0	0
4	3.426	0.072	0.210	0	0.428	0	0	0	0	0.026	0.105	0
5	0	0	0	0.516	0.327	0	0	0	0	0	0	0
6	0	0.041	0.119	0.142	0.327	0	0	0	0	0	0	0
7	0.253	0.032	0.092	0.142	0	0.09	0.276	0	0	0	0	0
8	0.253	0.285	0.829	4.826	0	0.06	0	0	0	0	0	0
9	0.231	0.431	0.698	1.06	0.231	0	0	0	0	0	0	0
10	0	0.096	0	0	0.231	0	0	0	0	0	0	2.032
11	0.692	0	0	2.536	0	0	0	0	0	0	0	0.405
12	0	0.36	0.105	0.127	0	0.034	0	0.272	0	0	0	0
13	0.504	0.252	0.643	1.69	0.504	0.33	0.368	0	0	0	0	0
14	0	0.063	0.184	0.998	0.126	0.03	0.092	0	0.252	0.023	0	10.62
Mean	**0.383**	**0.143**	**0.351**	**0.948**	**0.182***	**0.043***	**0.066***	**0.019***	**0.018**	**0.004**	**0.007**	**0.933**

*Statistically significant difference across platforms (pairwise Mann-Whitney U tests with Bonferroni correction)

Note: Animal Density Values Are Presented in Terms of Animals per km^2, and Were Calculated Differently for the Different Platforms, as Follows: C-plane—Animals Detected within Imaging Swath; Boat—Animals Estimated within Effective Survey Swath; V-plane—Animals Estimated within Effective Survey Swath (Unlabeled) or Animals Estimated within Peak Density Band Only (PD).

Taxonomic Identification of Animals

The addition of data from the supplemental surveys conducted in animal-rich areas resulted in larger sample sizes of observed and imaged animals for the evaluation of taxonomic identification patterns across platforms, presented along with percentage of animals identified to the species-level for each major taxon and each platform in Table 6–3.

Digital Aerial Surveys (C-Plane). Combining the transect surveys with the supplemental surveys in animal-rich areas resulted in a total of 238,489 images generated by the digital aerial survey plane, all of which were manually reviewed—resulting in the discovery of 3,185 images of birds, 77 turtles, and 37 marine mammals. Examinations of all discovered animal images by taxonomic experts resulted in 77% of birds being identified to species, 57% of turtles identified to species, and 60% of cetaceans identified to species (Table 6–3). In cross-observer taxonomic identification trials on bird images from all imaging configurations combined, observer 1 identified 83% to species level, and observer 2 identified 71% to species level (Table 6–4). Of 220 total bird images reviewed independently by both observers in these trials, 150 (68%) were identified by both observers to the species level, and the agreement between the two observers was 91% (136 of 150).

Aircraft-based Visual Observer Surveys (V-Plane) Transect and supplemental surveys combined resulted in a total of 2,474 observations of animals by seven different observers aboard the visual observer survey plane (2,185 birds, 131 turtles, 158 mammals). Overall, observers identified 45% of birds, 80% of turtles, and 72% of cetaceans to species (see Table 6–3). Interobserver variation in the percentage of animals identified to species level ranged from 0% to 66% for birds, from 83% to 84% for cetaceans, and from 67% to 89% for turtles (Table 6–4).

Boat-based Visual Observer Surveys (V-Plane) Transect and supplemental surveys combined resulted in a total of 1,160 observations of animals by seven different observers aboard the boat (1,071 birds, 13 turtles, 76 mammals). Observers identified 71% of birds, 91% of turtles, and 100% of cetaceans to species (Table 6–3). Interobserver variation in percent of animals identified to species level ranged from 33% to 100% for birds, was always 100% for cetaceans, and ranged from 82% to 100% for turtles (Table 6–4).

Table 6–3.

Total Animals Observed and Percent Identified to Species by Major Taxonomic Group for Three Survey Platforms (C-plane = Aerial Imaging Survey; V-plane = Aerial Visual Observer Survey; Boat = Boat-based Visual Observer Survey), Based on Transect and Supplemental Survey Data Combined, from Marine Wildlife Surveys Conducted Offshore of Oak Island NC, 10 to 20 May 2011.

Platform	Taxonomic Group	Number of Animals Observed	Percent Identified to Species (%)
C-plane	Birds	3,185	77
C-plane	Cetaceans	37	60
C-plane	Turtles	77	57
Boat	Birds	1,071	71
Boat	Cetaceans	76	100
Boat	Turtles	13	91
V-plane	Birds	2,185	45
V-plane	Cetaceans	158	72
V-plane	Turtles	131	80

Table 6–4.

Interobserver Variation in the Percentage of Animals Identified to Species by Major Taxonomic Group for Three Survey Platforms (C-plane = Aerial Imaging Survey; V-plane = Aerial Visual Observer Survey; Boat = Boat-based Visual Observer Survey), Based on Transect and Supplemental Survey Data Combined, from Marine Wildlife Surveys Conducted Offshore of Oak Island NC, 10 to 10 May 2011.

Observer	Platform	Taxonomic Group	Percent Identified to Species (%)
1	V-plane	Birds	55
2	V-plane	Birds	66
3	V-plane	Birds	66
4	V-plane	Birds	0
1	V-plane	Cetaceans	84
2	V-plane	Cetaceans	83
1	V-plane	Turtles	67
2	V-plane	Turtles	83
3	V-plane	Turtles	89
1	Boat	Birds	96
2	Boat	Birds	36
3	Boat	Birds	82
4	Boat	Birds	33
5	Boat	Birds	100
1	Boat	Cetaceans	100
2	Boat	Cetaceans	100
1	Boat	Turtles	100
2	Boat	Turtles	82
1	C-plane	Birds	83
2	C-plane	Birds	71

6.3.5 Discussion

Our comparisons of three different marine wildlife survey platforms revealed that aerial high-resolution digital imaging is likely to produce superior animal detection, density calculation, and taxonomic identification accuracy compared with conventional visual observer surveys from either boat or aircraft.

Animal Detection/Density Estimation

With respect to animal detection/density calculation, the increase in accuracy of digital versus visual observer based survey methods is likely to be very pronounced for a number of reasons. First, the total area surveyed (imaged) can be calculated with very high precision in digital surveys, whereas

large errors are introduced into density estimates from visual observer based surveys by estimations of effective survey swath width. Such estimations are known to include observer errors in distance estimation, as well as errors from variation among observers and among taxa in actual effective detectability distances (Buckland et al. 1993; Hyrenbach et al. 2007), neither of which is incorporated into density calculations using digital imaging survey data. The impact of detectability distance variation and effective survey swath width estimation is evidenced by the difference in density estimates between peak density (150 to 250 m from plane only) and uncorrected effective swath width in our data. Densities of all three major animal taxa were nearly double using the former estimation method rather than the latter. A peak in observed animal density at intermediate distances from aircraft has been previously noted in other aerial visual observer survey studies (Laake and Borchers 2004). Although it is unknown whether peak density or density estimates from uncorrected effective survey swath width are more accurate for aerial visual observer surveys, the large impact of swath width estimation assumptions stands as a case in point for the higher accuracy of animal densities produced from digital survey methods, as swath width is calculated precisely, eliminating an important source of error.

Second, animal attraction/repulsion effects are reduced or eliminated with high-resolution aerial imaging surveys relative to visual observer based surveys. This difference is more significant for boats than for aircraft. Boats are known to attract certain types of marine wildlife and repel others (Shoop and Kenney 1992; Hammond 1995). These effects may exert strong influences on density estimates. In our field study, dolphins were frequently observed riding the waves near the bow of the boat. This is the most likely explanation for cetacean density estimates two orders of magnitude higher for the boat based survey data than for the data from either of the aerial surveys. Although aerial visual observer surveys are not likely to attract animals, they are known to cause some marine animals to dive deep or fly away (Shoop and Kenney 1992; Henkel et al 2007; Buckland et al. 2012). High-resolution digital surveys reduce or eliminate this problem by flying at higher altitudes. Visual observer surveys must be flown at low altitudes (typically 50 to 200 m; Komdeur et al. 1992; Henkel et al. 2007; Paton et al. 2010; NJDEP 2010), so that expert human observers are able to discern the taxonomic identity of animals at high speed during the surveys. Using high-resolution cameras, digital imaging surveys can be flown at much higher altitudes (450 to 1,000 m) at which disturbance effects are reduced or eliminated (Thaxter and Burton 2009). We observed one clear illustration of this effect in our sea turtle data, where density estimates were roughly four times higher for the digital imaging survey data than for the aerial visual observer data. Although the observed difference in density estimates does not automatically suggest which density estimate is more accurate, the increased accuracy of the digitally derived density calculations is suggested by the behavioral states that were recorded along with the visual observations and in the images. For the aerial visual observer surveys, roughly half of the observed turtles were reported as diving, which is typical of aerial sea turtle surveys (M. J. Barkaszi, ECOES Consulting, Inc., pers. comm., 2011). By contrast, almost all of the imaged sea turtles were basking or resting at the water's surface, suggesting that animal disturbance effects are contributing to significant underestimation of true sea turtle density in aerial visual observer surveys.

The similar bird density calculations/estimates we observed across all three survey platforms suggest that in low bird density environments, such as were surveyed in this study, aerial or boat based visual observer surveys may perform nearly as well as digital surveys with respect to animal detection and density estimation. We did not observe a single aggregation of more than 20 birds during any of the

transect surveys conducted during this study. However, it is important to note that dense aggregations of birds are a normal and frequent element of seabird spatial ecology, often associated with dense food concentrations caused by ocean current upwellings, tidal rips, or other highly localized phenomena (Tasker et al. 1984). Under such circumstances, density estimations from visual observer based surveys are known to be strongly influenced by observer swamping effects, as well as search image effects (Laursen et al. 2008). Although clumped distributions of birds at sea hamper bird density calculations from digital survey data as well due to subsampling issues (Burt et al. 2009, 2010), such issues can be substantially ameliorated by adjustments in survey design and/or statistical correction factors (Buckland et al. 2012); whereas, no comparable solutions are available to correct for observer swamping effects in aerial visual observer survey data.

One set of marine animals for which digital surveys may have limited utility for obtaining population density estimates is rare animals that produce infrequent visual cues, which are visible at great distances. This set of animals includes most baleen whales. The rarity of these animals, combined with the large proportion of time they spend under water and therefore, invisible to aerial imaging cameras, means that under normal circumstances, very few images would be captured of such animals in systematic digital surveys. This is likely to result in surveys containing zero observations, which will result in density calculations of zero in areas where the animals are, indeed, present, albeit at low density. In such situations, visual observers may have an advantage, as they are able to home in on long distance visual cues given intermittently by baleen whales, such as blows, flukes, and breaches, essentially integrating large periods of time over large expanses of visible marine environments through continual visual scanning.

Discernment of the Taxonomic Identity of Animals

Overall, digital survey methods represent a significant improvement over visual observer based survey methods with respect to the discernment of the taxonomic identity of observed or imaged animals, although boat based visual observer surveys are likely to be necessary for obtaining robust species-level identifications of certain birds that are difficult to distinguish in photographs under any circumstances. We did not observe a notable difference in the depth of taxonomic identity discernment among any of the three survey types tested. The percentage of birds observed and identified to the species level was roughly equivalent on boat based surveys (71%) and digital imaging surveys (77%), with a somewhat lower rate (45%) for the aerial visual observer surveys. Visual observers aboard aircraft have such a small amount of time during which to observe animals and render judgments on taxonomic identity that lower identification rates are expected (Henkel et al. 2007). Boat based observers usually have more time to observe animals, and have access to additional cues that facilitate taxonomic identification for some animals that aerial observers or digital image analysts do not have, such as behaviors, flight style, vocalizations, and a broader range of viewing angles. For these reasons, boat based surveys are always likely to possess an advantage over other survey methods for rendering reliable species-level identifications of some birds that are difficult to identify from photographs. However, because of the slow speed of boats and the other limitations of boat based survey data, the utility of boat based surveys is expected to lie primarily in small scale, targeted species identification determinations, rather than in broad scale systematic surveys of large areas.

Boat based observers also identified turtles and cetaceans to the species level at higher rates than did aerial observers or analysts of digital survey imagery. However, these apparent advantages are artifacts of detectability biases, and do not represent real advantages of boat based surveys. In the case of turtles, it is well known that they are easily disturbed by boats, and very difficult to detect using boat based surveys, which is why aerial methods are generally preferred for sea turtle surveys (Shoop and Kenney 1992). Our boat based surveys yielded very few observations of sea turtles (13); hence, the high percentage of species-level identifications resulted from a very small sample size of individuals that boat based observers were able to observe at close range. For cetaceans, the 100% species-level identification rate resulted from the fact that all observed cetaceans were dolphins, and in all cases, the dolphins approached the boats, presumably because of attraction effects, enabling observers to view them at close range. The attraction of dolphins to boats is a useful feature for obtaining certain kinds of information about dolphins using boat based surveys. However, this advantage does not apply widely across marine animal taxa, the disadvantage is equally strong for animal species that are generally repelled by boats, and animal attraction and repulsion effects both hamper the utility of boat based survey data for obtaining accurate animal density estimates.

The principal advantage of digital methods over visual observer based methods with respect to the discernment of the taxonomic identity of animals stems from the fact that determinations are made subsequent to the surveys using a pre-observer archive of image data. By contrast, in visual observer surveys, taxonomic determinations must be rendered during the surveys by the observers, hence the data is not recorded and archived until after the taxonomic identity determinations have been made by the observers. The accuracy of such determinations cannot, therefore, be quality controlled or otherwise evaluated, and there are no reliable methods for reducing or removing observer effects. Strong observer effects in taxonomic identity determinations are known to be prevalent in visual observer survey data (Laursen et al. 2008; Maclean et al. 2009). In our data, such effects can be seen in the wide range of variation among observers in the percentage of birds that were identified to the species level (from 0% to 66% for aerial visual observer surveys, from 33% to 100% for boat based surveys).

One advantage of relying on a pre-observer archive of image data for making taxonomic identity determinations is the ability to use morphometric measurements of imaged animals to inform the determinations. This is particularly useful for discriminating among species with similar shapes and visual appearance features, but different sizes. In our survey data, this provided a significant benefit for identifying terns (family: Sternidae) to species and genus levels. A variety of tern species were commonly observed in our surveys, and the increased species-level discriminatory power afforded by the application of morphometric measurements is the principal reason that our species-level bird identification rates were higher for the digital survey data than for either of the visual observer surveys. An example is illustrated in Figure 6–2. The black cap, pale bill, whitish-gray upperparts, and general shape of the bird visible in the image clearly identify the bird as one of eight tern species that potentially co-occur offshore of North Carolina during mid-May. However, morphometric measurements of the bird in comparison with ranges reported in literature for the eight plausible tern species revealed that this bird is most likely a Common Tern, *Sterna hirundo* (Table 6–5).

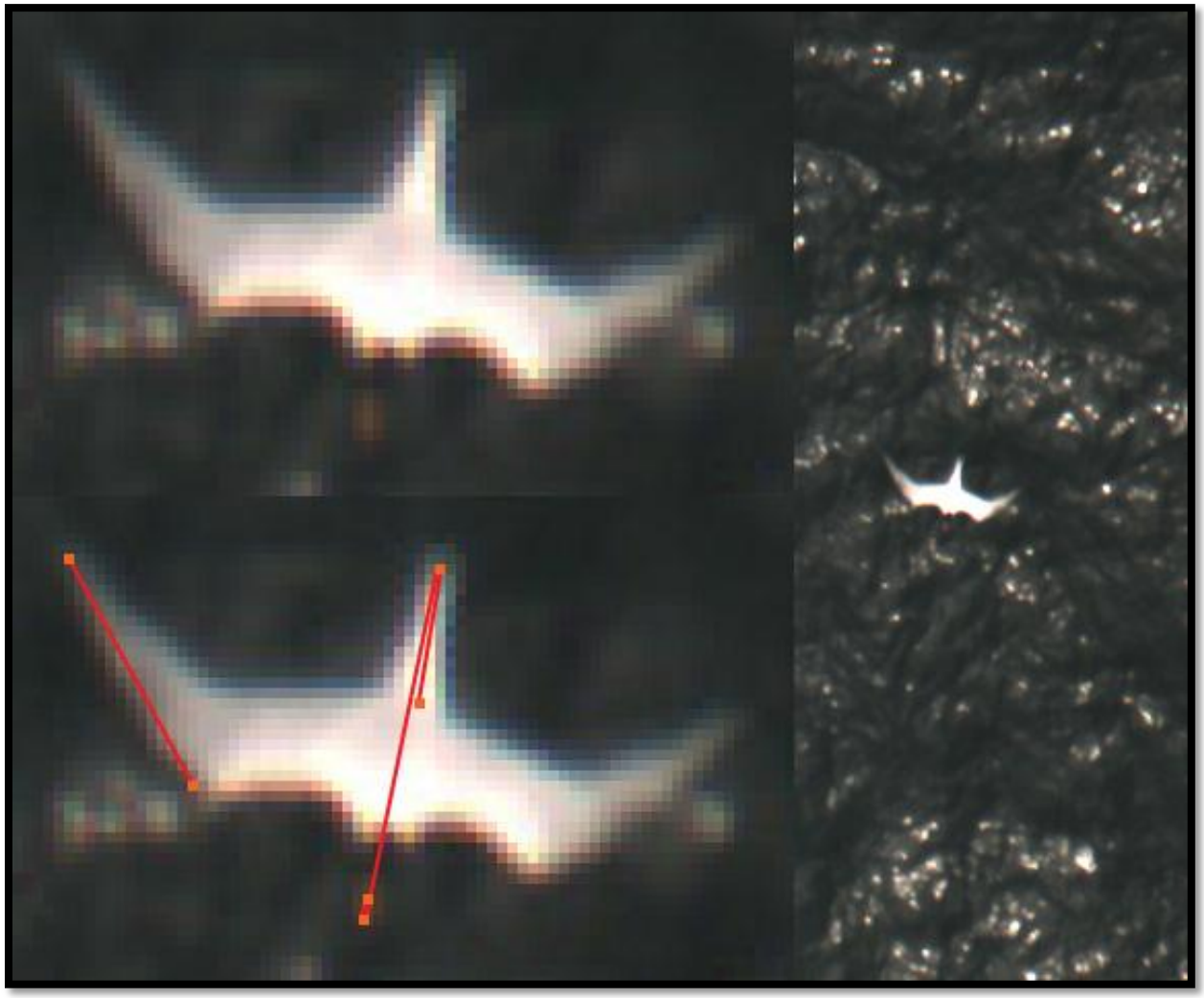

Figure 6–2. Three views of a single high-resolution image of a tern obtained during digital imaging surveys conducted 10 to 20 2011 offshore of Oak Island NC. The black cap, pale bill, whitish-gray upperparts, and general shape of the bird visible in the image are sufficient to identify it as one of eight co-occurring species of tern. However, the morphometric measurements illustrated with red lines in the image on the bottom left suggest that this bird is most likely a Common Tern, *Sterna hirundo*, although this determination is subject to some uncertainty based on the unknown flight altitude of the bird (see text and Table 6–5 and Table 6–6).

Table 6–5.

Mean Morphometric Measurement Ranges for Eight Tern Species that Potentially Co-occur Offshore of North Carolina in mid-May, and that Share the General Visual Appearance Features of the Bird Shown in Figure 6–2, Whose Measurements Are Also Shown, as derived from Measurements of the Image, Illustrated by the Red Lines on the Image of the Bird in the Lower Left of Figure 6–2

Species	Wing Chord (cm)	Body Length (cm)	Tail Length (cm)	Bill Length (cm)
Royal Tern	35.7–38.2	45–50	14–17	6.2–6.5
Caspian Tern	37.4–43.3	48–56	12–15.2	6–7
Sandwich Tern	28.0–31.1	34–45	11.7–13.7	4.7–5.7
Common Tern	**26.2–27.1**	**31–37**	**14.8–15**	**3.6–3.8**
Forster's Tern	25.8–27.2	33–36	16–19.3	3.5–4.2
Roseate Tern	22.8–23.2	33–41	17.5–18.5	3–3.9
Arctic Tern	25.4–28.5	33–39	7.2–12.6	2.8–3.8
Least Tern	15.3–18.0	22–24	6–8	2.4–3.2
Bird in Figure 6–2	***26***	***36***	***14.4***	***3.6***

Note: Measurement ranges reported for the eight species are the ranges of mean measurement values reported in Birds of North America accounts; hence, the ranges of values for these measurements on individual birds are somewhat wider. Dimensions of the bird from Figure 6–2 were generated by multiplying the measurements shown in the image by a factor corresponding to the image resolution, as a function of optical magnification and flight altitude. comparison of the imaged bird's dimensions to those reported in literature for the eight species suggest that the imaged bird is most likely a Common Tern, *Sterna hirundo*, although this determination is subject to some uncertainty resulting from the unknown flight altitude of the bird (see text).

Our calculations of animals' measurements were performed using image resolutions calculated for the water's surface, based on known optical magnification of the images, camera angles, and flight altitudes. These calculations, therefore, are based on the assumption that animals were observed near the water's surface. The water depth at which submerged animals can be successfully imaged is not precisely known, and will presumably vary across marine imaging surveys as a function of water clarity, ambient light characteristics, and animals' appearance characteristics. Flight altitudes of birds at sea are predominantly very low, almost always within 50 m of the water's surface, with most birds flying within 20 m of the surface (Paton et al. 2010; NJDEP 2010; Normandeau 2011). Still some seabirds have a tendency to fly higher, and infrequent high flying behavior is possible for virtually any bird species observed at sea. We analyzed the sensitivity of this assumption to expected variation in bird flight height using simple geometric calculations of apparent bird dimensions imaged from aircraft flying at either 450 or 600 m (Table 6–6). Although the sensitivity of morphometric calculations is relatively low for normal seabird flight altitudes, particularly at higher imaging flight altitudes, the extent of possible deviations of apparent morphometric dimensions from

actual dimensions based on birds' flight altitude underscores the importance of developing robust flight altitude determinations on imaged animals for applying measurement-based taxonomic discrimination criteria.

Table 6–6.

Sensitivity of Morphometric Calculations to Variation in Birds' Flight Altitude. Percent Deviation of Measurements and Quantitative Deviations for an Actual 50 cm Morphometric Measurement are Shown Based on 450 and 600 m Imaging Flight Altitudes

Flight Altitude of Bird ↓	Percent (%) Measurement Deviation Relative to Bird on Water's Surface		Apparent Length of an Actual 50 cm Morphometric Dimension	
Imaging altitudes→	600 m	450 m	600 m	450 m
20 m	3.44	8.44	51.72	54.22
50 m	9.10	12.5	54.55	56.25
100 m	20.0	28.6	60.0	64.3

The reliance on a pre-observer archive of image data for rendering determinations of the taxonomic identity of animals imaged during high-resolution aerial imaging surveys does not remove all observer effects from such determinations. Determinations must still be based on observations of the images and the application of qualitative and quantitative criteria to discriminate among possible animal taxa. Even if the observer is an identification algorithm, such as are being developed by several European digital imaging survey practitioners, observer effects are still present in the taxonomic identity determinations made using digital imaging survey data. However, unlike with visual observer based survey data, observer effects in taxonomic identity determinations from digital survey data can be quantified and controlled through multiobserver reviews of identical sets of images, thereby greatly reducing observer effects and augmenting inferential power. Multiple observer reviews of subsets of digital imagery data have become a standard quality assurance and control practice in the application of marine aerial high-resolution digital wildlife imaging surveys to the offshore wind energy industry in the UK (C. Thaxter, BTO, pers. comm., 2011), where a standard of 90% between-observer agreement on taxonomic identity determinations has emerged as a general recommended minimum acceptable level of identification consistency (Thaxter and Burton 2009). The 91% between-observer agreement in species-level bird identifications we obtained from the multiobserver identification reviews we conducted on 220 bird images from our high-resolution surveys is generally consistent with this standard. In practice, the application of this standard is complex, as between-observer agreement levels may vary among observers, as a function of how multi-taxon confusion groups are defined, and also as a function of the similarity of appearance characteristics of particular sets of co-occurring animal taxa in particular marine environments. Nonetheless, the ability to perform multiple observer imagery reviews enables the taxonomic identity of animals to be analyzed with greater accuracy from digital survey data in comparison with visual observer survey data, where no subsequent evaluation of the accuracy of taxonomic identifications rendered by observers is possible.

6.4 Impacts of Selected High-resolution Imaging Parameters on Image Quality and Animal Identification Capability

6.4.1 Introduction

One of the core objectives of this study, and the rationale for the application of an experimentalist paradigm to the field surveys, was to optimize methodological parameters for high-resolution imaging for the purpose of conducting marine wildlife surveys in support of an offshore wind energy leasing program in US waters. A large number of methodological parameters were varied during our imaging experiments, to provide a basis for assessing which specific imaging configurations performed best for the intended scientific purpose. The complete spectrum of methodological experimentation was described in Chapter 1. In the current chapter, we focus on three methodological parameters that were selected for more intensive experimentation and analysis based on the previously known or anticipated importance of these parameters for optimizing high-resolution wildlife imaging survey methodology. These parameters are image resolution, camera angle (or tilt), and single versus multiple images. Over the course of our experiments, multiple trials were conducted with each possible combination of image resolution and camera angle treatments, and the impact of single versus multiple images of birds was assessed for all of these trials using subsampling of the multiple images gathered for most animals, resulting from frame capture rates of three frames per second. Our analysis of image resolution, camera angle, and single versus multiple pictures is restricted entirely to the impacts of variation in these imaging parameters on the ability of image analysts to accurately and consistently discern the taxonomic identity of the animals from the images we gathered during the Op House imaging flight surveys.

Image Resolution

This parameter refers to the fineness of spatial resolution of the image, and is expressed in terms of centimeters, where an image resolution of 1 cm refers to the resolution at which the length of one side of a roughly square pixel in the image is equivalent to a length of 1 cm on the surface of the water below the imaging aircraft. Image resolution is, therefore, a function of a particular combination of optical magnification and the distance from the camera to the water it is imaging. The latter distance is most strongly affected by the altitude of the survey aircraft, but it is also affected by camera angle. For example, the distance from the camera to the water's surface being imaged is slightly longer for a tilted camera than for a camera directed vertically downward, because the latter case represents the shortest possible distance between the camera and the water's surface. Image resolutions for all imaged animals were calculated based on distance of the camera to the water's surface, yet many of the imaged animals were either flying above, or swimming below, the water's surface; hence, actual image resolutions on the imaged animals may deviate slightly from those reported (see discussion of sensitivity of resolutions to bird flight heights in section 6.2.2). In our experiments, image resolution varied between 1 and 3 cm. This is finer than the minimum image resolution of 5 cm recommended in Thaxter and Burton (2009) and was selected based on contemporary practice in Europe, which had evolved toward finer resolutions than were used in the earliest European offshore high-resolution wildlife imaging studies.

Camera Angle

This parameter refers to the angle at which the camera is oriented. In this discussion, we refer to camera angle, or tilt, as it is described in Chapter 1, and as it was implemented in our imaging

experiments, where a tilt of 0° refers to a camera directed straight downward, a tilt of 15° refers to a camera directed 15° away from a straight downward position, angled slightly toward the back of the aircraft, and a tilt of 44° refers to a camera directed 44° away from the 0° position, also directed rearwards along the anterior-posterior axis of the aircraft. Our analysis focuses on 15° and 44° camera angle treatments. This is primarily because a large proportion of our images would have been rendered unusable with 0° camera angle because of high sun glare levels, given the high angles of insolation that occurred during much of our survey period (see section 4.2). We hypothesized that camera angle could impact the ability of the taxonomic identity of imaged animals to be correctly discerned because of pixel distortion. Pixel distortion occurs when there is variation among the pixels in an image in the way they correspond to the size and dimensions of the objects being imaged. When the imaging camera is oriented straight downward (0° tilt), each pixel in the image corresponds to a virtually identically sized and shaped portion of the water's surface. By contrast, when the camera angle is tilted away from straight downward, pixel distortion is introduced, as there is variation among the pixels in the image with respect to the size and shape of the portion of the water's surface they contain.

Single versus Multiple Images

This parameter refers to whether determinations of the taxonomic identity of imaged animals were made using a single image or multiple images of the animal. This distinction corresponds roughly to what has emerged as a keystone methodological dichotomy in European high-resolution wildlife imaging surveys—the difference between video and stills methods (Thaxter and Burton 2009; Buckland et al. 2012). Video methods usually produce multiple images of imaged animals because frames are captured at high frame rates, producing overlapping image areas. Stills methods capture images at slower rates, producing a set of images of nonoverlapping areas; hence, only a single image is produced for each imaged animal. Much of the discussion of this dichotomy in Europe has focused on the statistical methods and accuracy of animal density estimation based on the different spatial subsampling in these two different imaging systems (Thaxter and Burton 2009; Buckland et al. 2012), but we do not address that difference in this chapter, focusing only on the impact of this methodological choice on the accuracy and consistency with which the taxonomic identity of the imaged animals can be discerned from the images, as a function of image clarity and quality. Although our single versus multiple images analysis corresponds roughly to the video versus stills dichotomy in discussions of European methodology, it is important to note that it is not exactly equivalent. In particular, subsampling of images from video sequences, such as we present in our analysis, while capable of exactly replicating the spatiotemporal subsampling patterns of stills methods, may not reproduce the image quality of stills methods that permit the use of additional image quality enhancing techniques, such as airplane motion correctors, by virtue of their slower image capture rates. In general, image clarity and quality is a function of many technological and methodological characteristics of the imaging equipment, and imaging technology is rapidly changing; therefore, any characterization of image quality in relation to a particular imaging parameter is equipment specific, and subject to change as technology improves.

6.4.2 Qualitative Comparisons

We have segmented our analysis into qualitative and quantitative sections, as each applies a very different methodology to gain insights into the impacts of the three factors (resolution, angle, single

versus multiple images) on image quality, and the accuracy and consistency of determinations of animals' taxonomic identity. The qualitative analysis section is based on direct visual comparisons of imagery gathered with different methods.

Image Resolution

Qualitative analysis of images across a spectrum of image resolution values confirms the intuitive conclusion that finer image resolutions produce clearer images of objects, enabling more confident determination of the taxonomic identity of imaged objects, including animals. More specifically, we believe that image resolutions of 3 cm or cruder are not likely to result in acceptable levels of confidence and accuracy in determining the taxonomic identity of imaged marine birds, mammals, and sea turtles under most circumstances, and for most scientific or environmental risk/impact study purposes. The importance of image resolution is illustrated in Figure 6–3 and Figure 6–4, which show a series of different imaging configurations, including a complete spectrum of the image resolutions we tested. Figure 6–3 shows the same dock imaged 8 different times, from the reference object sequences that we captured at the beginning of each of our offshore imaging survey flights (Chapter 1). Image resolutions of 1 to 1.5 cm are shown in the top row, and image resolutions in the 2 to 2.5 cm range and 3 cm are shown in the middle and bottom rows, respectively. Figure 6–4 shows 10 images of adult Laughing Gulls under the same sets of image resolutions and other imaging configurations as in Figure 6–3. Both figures illustrate an overall degradation in image quality as resolution gets coarser. The impact of image resolution on taxonomic identity determinations is evident from the specific appearance characteristics of Laughing Gulls that are visible in the images of Figure 6–4. In the 1 to 1.5 cm resolution images, many of the key diagnostic features of Laughing Gulls can be discerned, including black hood, white posterior stripe on the wing, and reddish bill. In the 2 to 2.5 cm resolution images, the reddish bill cannot be discerned, and the black hood and posterior wing stripe are difficult to discern. In the 3 cm resolution images, the black hood and posterior wing stripe cannot be discerned.

Figure 6–3 and Figure 6–4 also illustrate that image quality and clarity is not a simple function of image resolution. Some variation in image clarity is apparent among different images taken with the same, or very similar, image resolution levels. There are many factors that may contribute to variation in image quality in addition to resolution, including ambient light level, exposure time, optical magnification level, vibrational effects, and other factors discussed in detail in section 3.3. Image gyrostabilization is among these factors, and at first glance, the images in Figure 6–3 and Figure 6–4 do not appear to support our assessment that the benefit of gyrostabilization was substantial enough to warrant its inclusion as a standard component of high-resolution aerial imaging systems (section 3.3). Figure 6–3 and Figure 6–4 show that it is also possible to obtain high quality images without gyrostabilization. However, unstabilized imaging trials typically resulted in a mix of high quality and lower quality (more blurry) images, whereas gyrostabilized trials produced consistently high quality images. The nonstabilized images shown in Figure 6–3 and Figure 6–4 were selected to illustrate the impacts of resolution, and include only high quality unstabilized images; hence the impact of gyrostabilization is not readily apparent in these figures.

Another key factor is survey flight altitude. Flight altitude is intertwined with image resolution and optical image magnification. It is possible to hold image resolution constant across different flight altitudes by adjusting optical magnification correspondingly. For example, 1-cm image resolution can be achieved at different altitudes by using different lenses, with higher optical magnification at

higher altitude rendering identical image resolution. Although the image resolution levels would be the same in that case, the image quality might not be, particularly as vibrational effects would be increasingly magnified with the higher zoom levels needed at the higher altitudes. We conducted trials over a range of image resolutions at each of the survey flight altitudes with which we experimented. However, we did not try all image resolutions at all flight altitudes; therefore, we cannot be fully separate the impacts of image resolution from the impacts of flight altitude in our experiment. Our experimental imagery demonstrates that 2.5-cm resolution images can be obtained at flight elevations well above those typically implemented in European surveys, by using higher optical magnification levels. With gyrostabilization, such images are generally of comparable quality to images with identical resolution levels taken at more typical survey flight altitudes (Figure 6–3 and Figure 6–4). Further research is necessary to ascertain whether significant image quality degradation is introduced by the very high optical magnification levels necessary to achieve the finest resolutions (e.g., 1 cm) at the highest survey flight altitudes (e.g., 1,000 to 1,200 m).

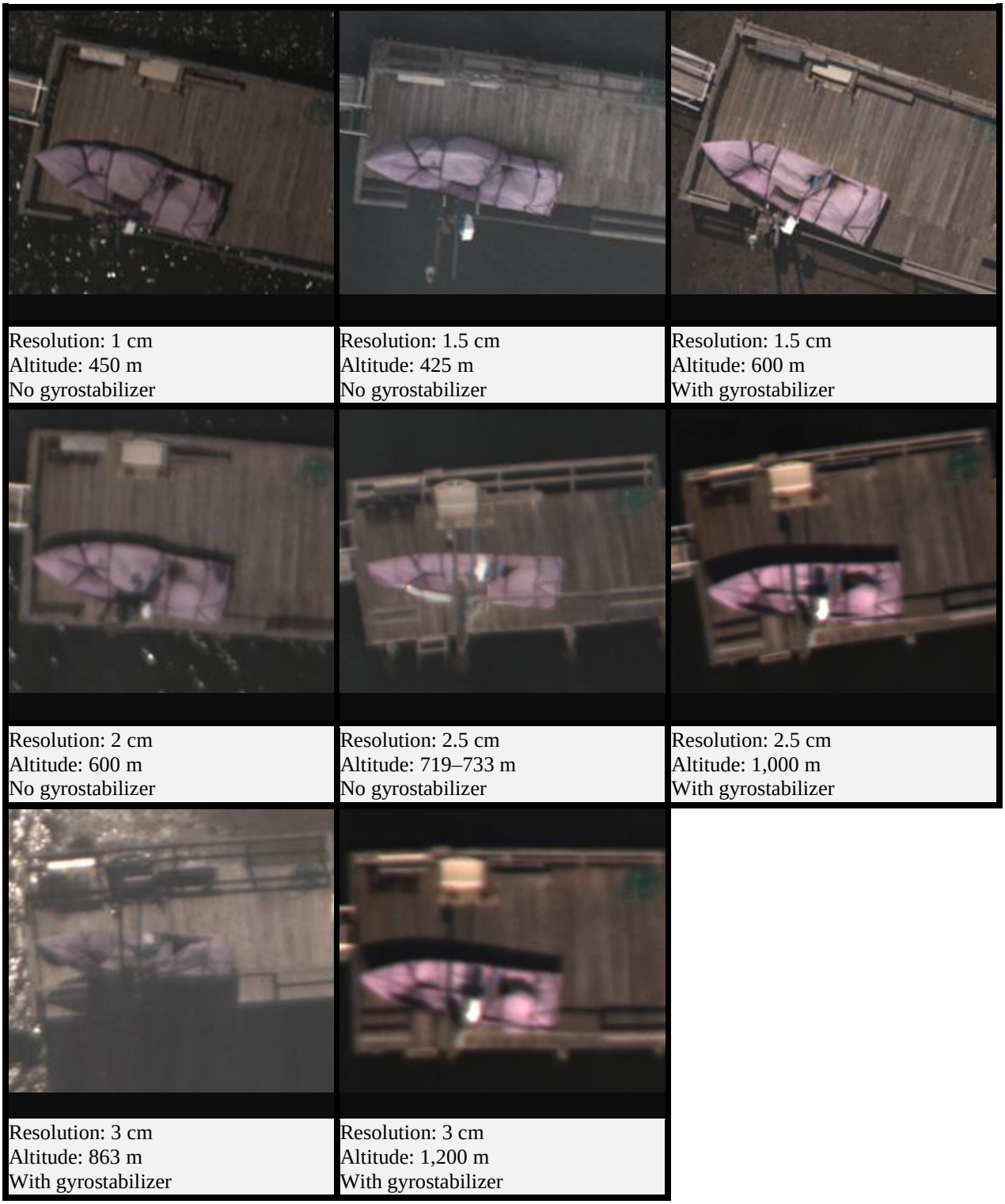

Figure 6–3. Comparison of reference object images illustrating the importance of image resolution for image clarity.

Eight views of the same dock are shown from the reference-run segments of experimental high-resolution imaging flights conducted 10 to 20 May 2011 near Oak Island NC. The images in the top row were taken with the finest image resolutions (1 to 1.5 cm). The images in the middle row were taken with intermediate image resolutions (2 to 2.5 cm), and the images in the bottom row were taken with the coarsest image resolutions (3 cm). Survey flight altitudes and the inclusion of an image gyrostabilizer are also indicated below each individual image. A general degradation of image quality with increasingly coarse image resolution can be seen, but it also apparent that image resolution is not the only factor influencing image clarity. These pictures do not accurately reflect the impact of gyrostabilization, as only high quality unstabilized images were selected for the resolution comparisons.

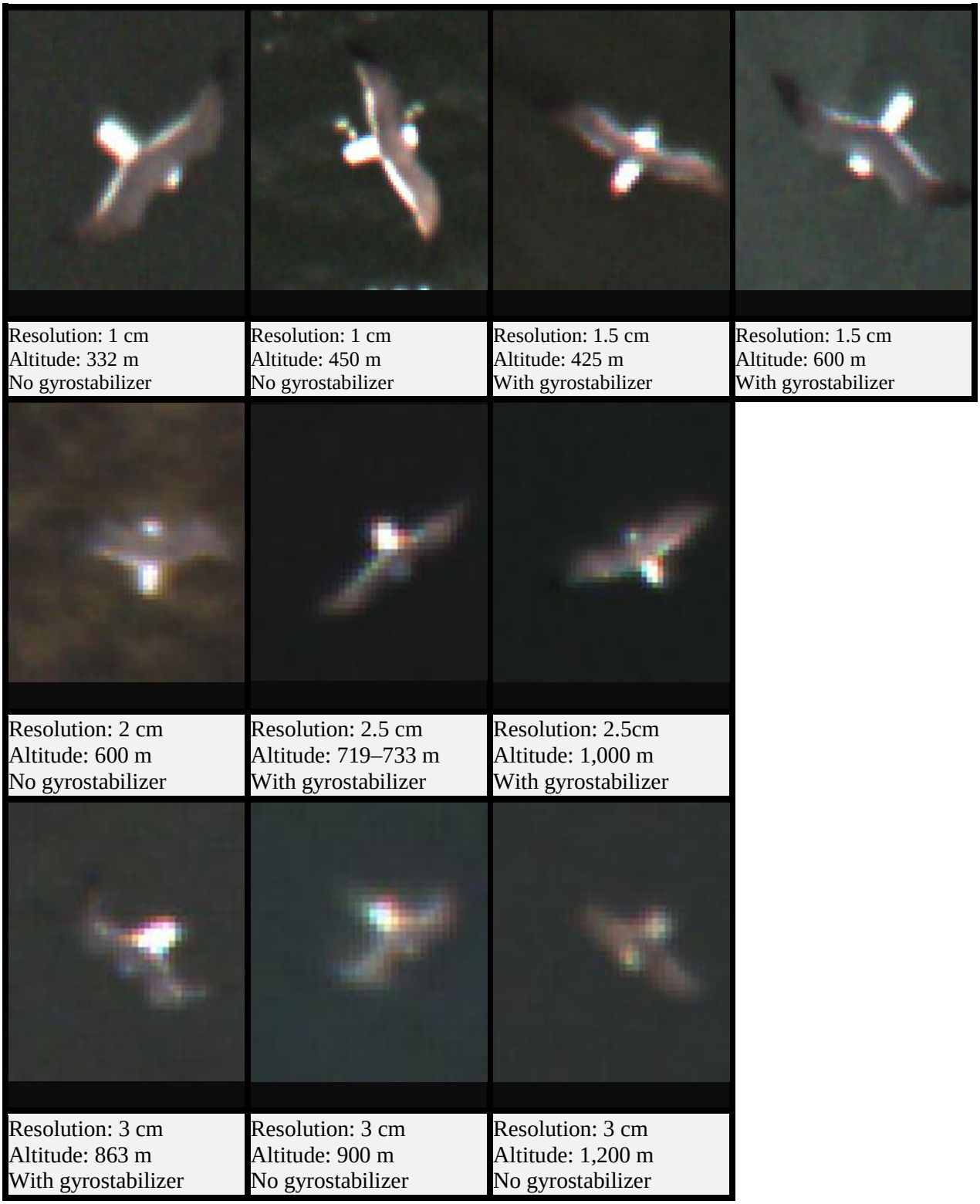

Figure 6–4. Comparison of bird images illustrating the importance of image resolution for image clarity.

Ten views of adult Laughing Gulls are shown from the offshore segments of experimental high-resolution imaging flights conducted 10 to 20 May 2011 near Oak Island NC. The images in the top row were taken with the finest image resolutions (1 to 1.5 cm). The images in the middle row were taken with intermediate image resolutions (2 to 2.5 cm), and the images in the bottom row were taken with the coarsest image resolutions (3 cm). Survey flight altitudes and the inclusion of an image gyrostabilizer are also indicated below each individual image. A general degradation of image quality with increasingly coarse image resolution can be seen, but it also apparent that image resolution is not the only factor influencing image clarity. These pictures do not accurately reflect the impact of gyrostabilization, as only high quality unstabilized images were selected for the resolution comparisons.

Camera Angle

Qualitative analysis of images across a spectrum of camera angle (tilt) values revealed that pixel distortion exerts a negligible impact on image quality and clarity for angles up to 44°. Our assessment is that camera angles within this range can be used in high-resolution aerial wildlife imaging surveys without significantly impacting the confidence and accuracy with which the taxonomic identity of imaged marine birds, mammals, and sea turtles can be determined under most circumstances. This result is illustrated in Figure 6–5, which shows three images of Laughing Gulls taken at camera angles of 44°, where pixel distortion effects are potentially at their most acute. If pixel distortion effects were acute, there would be a notable degradation of image quality moving from the lower portion of the frame to the upper portion of the frame, as animals imaged in the upper parts of the frame are slightly farther from the camera than are animals in the lower parts of the frame, and the size and shape of the image pixels that capture animals in the different portions of the frame are different, with fewer, and more distorted pixels covering animals in the upper portion of the frame than in the lower portion. We qualitatively reviewed a large number of animal images from these different portions of frames for images taken with 44° camera angles and could not discern a degradation in image quality, as evidenced by the visibility of the reddish bill, black hood, and white posterior stripe on the wing of the adult Laughing Gull from the upper portion of the frame in Figure 6–5. The viability of camera angles up to 44° is a very significant finding for high-resolution imaging survey design, as acute camera angles are necessary to avoid capturing images with excessive sun glare during a large portion of available daylight hours over most of the year and over most of the AOCS (see section 4.2).

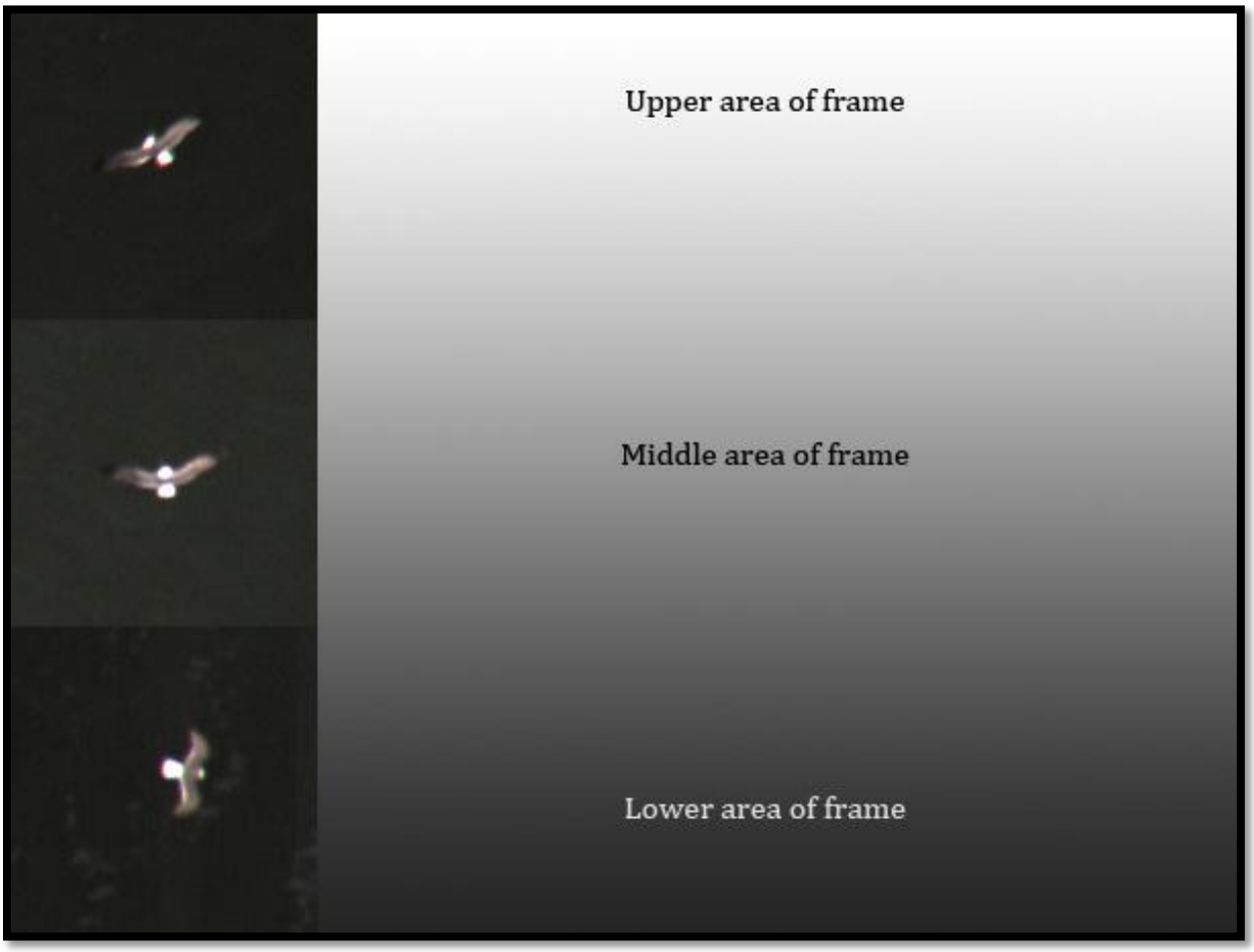

Figure 6–5. Comparison of bird images illustrating the importance of camera angle for image clarity. Three views of adult Laughing Gulls are shown from the offshore segments of experimental high-resolution imaging flights conducted 10 to 20 May 2011 near Oak Island NC, from three different portions of individual image frames (upper, middle, and lower portions of frames). All of these images were taken with a camera angle of 44°, with otherwise equivalent imaging parameters. The adverse impacts of pixel distortion on image quality are expected to be worst for the most acute camera angles (e.g., 44°), and in the upper portions of images, where fewer and more distorted pixels capture the image of individual animals. No such degradation is readily apparent in the images in this figure, suggesting that pixel distortion effects are not severe enough to preclude the use of camera angles up to 44° in high-resolution wildlife imaging surveys.

Single versus Multiple Images

Qualitative analysis of image series obtained for individual animals revealed that the accuracy and consistency of determinations of imaged animals' taxonomic identities is likely to be significantly

improved if multiple images are used to render such determinations, as opposed to single images. Multiple images are only produced using high frame capture rates, as is the case with video imaging methods (Thaxter and Burton 2009; Buckland et al. 2012). Two important caveats to this conclusion must be noted. First, part of the added value we observed from multi-image analysis was likely due to the intermittency of vibrational distortion effects in nongyrostabilized imagery (Figure 6–6). With image gyrostabilization, intermittent vibrational effects are removed, and this added value would disappear. Second, our analysis of single image identification was restricted to subsampling of images captured at high frame rates (video imaging). Therefore, our analysis is based on the assumption that single versus multiple images are exactly equivalent to one another with respect to all other factors that may influence image quality. We note that this assumption may be violated in cases where stills imaging methods permit image enhancing technologies (e.g., forward and horizontal motion correctors) that are unavailable for video imaging methodologies.

Even accounting for these caveats, we believe that using multiple images of individual animals to render taxonomic identity determinations adds significant value. This is primarily because having multiple views increases the likelihood that key diagnostic visual appearance features of imaged animals will be visible. For example, the visibility of various diagnostic marks on the wings of many marine birds will only be visible when the wings are held in certain positions, and wing position changes rapidly during flight with respect to video frame capture rates under most circumstances. Figure 6–6 illustrates the significance of this positional variation, even as it also illustrates significant variation in image quality due to intermittent vibrational effects, as noted above.

We note that increased numbers of images obtained for individual animals represents a potential advantage of lower resolution video imaging. The number of images that are captured for individual animals from an aircraft traveling at a given speed and capturing images at a given frame rate depends on the size of the area on the surface of the water being imaged. For any given number of image pixels, finer resolution images cover smaller areas than do coarser resolution images. Therefore, all else being equal, the lower quality of coarser resolution video images is partly counterbalanced by the increased number of images that will be captured for each imaged animal. In considering this potential benefit of coarse-resolution video imaging, it is important to note that it only applies to video imaging, and also that there is still expected to be a significant net loss in the accuracy and consistency of taxonomic identity determinations, as there is likely to be more value added through improvements in image resolution than there is through the capture of additional lower resolution images.

Figure 6–6. Comparison of a series of successive images of the same adult Laughing Gull from an experimental high-resolution imaging flight conducted between 10 and 20 May 2011 near Oak Island NC, illustrating the importance of multiple pictures for determination of the taxonomic identity of animals from high-resolution imagery. This series illustrates an extreme case in which image quality varied substantially across successive images, most likely due to variations in vibrational effects, as no gyrostabilizer was mounted on the camera when this sequence was captured. Variation in the bird's position can also be seen across the frames, which represents a more general advantage for the use of multiple pictures to render taxonomic identity determinations on imaged animals, as multiple views increase the likelihood that key diagnostic visual appearance characteristics will be visible.

6.4.3 Quantitative Comparisons

In addition to the qualitative analyses reviewed above, we also performed a set of quantitative analyses to gain insights into the importance of image resolution, camera angle, and single versus multiple images for obtaining accurate and consistent determinations of the taxonomic identity of animals imaged during our aerial high-resolution digital imaging surveys. The experimental and analytical methods of these analyses are described below, followed by description and interpretation of our results.

Methods

Multiple Observer Identification Trials

Our quantitative analysis of the impacts of image resolution, camera angle, and single versus multiple images on taxonomic identity determinations of imaged animals was based on a set of multiple observer identification trials we performed using the imagery we gathered during the Op House imaging surveys (Chapter 1), based on the recommendation of multiple observer image review in Thaxter and Burton (2009). As earlier image reviews had revealed the importance of image gyrostabilization, only gyrostabilized images were used in the multiobserver review trials. We selected a set of 916 images of 220 individual birds for the multiobserver review, consisting of all of the gyrostabilized bird images in our data set. These birds were distributed across camera angle and image resolution treatments in a roughly factorial design (Table 6–7), although we note that the distribution of birds across treatment combinations was not completely uniform.

Table 6–7.

Distribution of the 220 Birds Used in Multiobserver Identification Trials Across Image Resolution and Camera Angle Experimental Treatments

Image Resolution	Camera Angle (Tilt)	
	15°	44°
1.5 cm	50	10
2.5 cm	50	49
3 cm	16	45

Note: All of the images of these birds were from gyrostabilized experimental imaging flights conducted 10 to 20 May 2011 offshore of Oak Island NC. A total of 916 images of these 220 birds were used in the trials.

Two identification trials were conducted, with one trial conducted independently for each of two expert observers, as follows: identification trials were set up with all of the images for each bird contained within a single folder (220 separate folders). The order in which folders were numbered and viewed by the observers was randomized with respect to the treatment combinations. Each folder included the first image obtained for the individual bird from the experimental video sequence, as well as a subfolder containing the remainder of the images that had been obtained for that individual bird. Observers were instructed to examine the single (first) image in the folder first, and render and record a complete determination (see below) based on his or her analysis of that image alone, and then open the subfolder containing the remaining images of the same bird, and render and record a second determination for the same bird based on his or her analysis of all of the images for that bird. This process was repeated for all 220 individual birds during each trial. For each determination, observers recorded the taxonomic identity of the bird at the finest level possible, based on their application of the same identification resources, morphometric measurements, and image visualization procedures described earlier for the complete manual image review (Chapter 6.3.3).

Regression Analysis of Parameter Effects

We used linear, mixed effect binomial regression modeling of the data from the multiple observer identification trials to examine the impacts of image resolution, camera angle, and single versus multiple images on the effectiveness of taxonomic identity determinations of the imaged animals.

We derived two quantitative measures of effectiveness from the multiple observer trial data that served as the dependent, or response variables, in our regression analyses. Both were binomial variables (only two possible values). The first was the level of taxonomic depth achieved by the observer, which varied between 1 (species-level determination reached) and 0 (species-level determination not reached). For this variable, there were 880 samples, corresponding to each determination (single versus multiple images) by each observer (two observers) for each of the 220 individual birds. The second was agreement in species-level determination between observers, which

varied between 1 (two observers agree on which species) and 0 (two observers disagree). For this variable, there were only 150 samples, comprised of the 150 individual birds for which both observers had reached a species-level determination.

We used three independent, or potentially causal variables, corresponding to the three factors of interest (image resolution, camera angle, number of images), plus all possible factorial combinations of these variables as potential effects. Since all of the independent variables were at different scales, we standardized them by using sample mean and sample standard deviations.

All data were analyzed using R (R Development Core Team 2011) and R package lme4 (Bates and Maechler 2009) using a linear mixed effect binomial regression model. To avoid the language-as-a-fixed effect fallacy (Clark 1973), we used both bird number and observer as random effects (see Baayen et al. 2008) to account for the repeated sampling of same bird by two different observers. Number of images, image resolution, and camera angle were included in the models as fixed effects. Akaike's information criterion corrected for small sample size (AICc) was used to rank models relative to each other (Burnham and Anderson 2002). Using this approach, models with a difference in AICc (ΔAICc) of < 2 are considered to be similar; $2 \leq \Delta\text{AICc} \leq 4$ suggests evidence for considerable difference, $4 \leq \Delta\text{AICc} \leq 7$ suggests substantial evidence for difference, and $\Delta\text{AICc} > 7$ is generally indicative of overwhelming evidence for substantial difference in support (Burnham and Anderson 2002). In addition to AICc, we also used Akaike weights for model comparisons as they provide an effective way to scale and interpret differences in AICc values (Burnham and Anderson 2002). To evaluate the influences of individual independent variables on the response variables, and to address the issue of model selection uncertainty in the estimate and precision of model parameters, we calculated the model-averaged parameter estimates based on the Akaike weights of each model.

Results

Comparisons of Identification Effectiveness Measures Across Treatments

Results of the multiple observer identification trials according to the two metrics of identification effectiveness (species-level identification rate, between-observer agreement on species identity) were compiled for all possible combinations of the three effects variables (image resolution, camera angle, single versus multiple images), and are presented in Table 6–8 through Table 6–11 and Figure 6–7 through Figure 6–10 below.

Table 6–8.

Variation in Taxonomic Identity Determination Effectiveness Measures Across Image Resolution Treatments, for Determinations Using Multiple Images for Each Bird in the Multiple Observer Identification Trials (See Text)

Multiple Image Determinations	Image Resolution Treatment			
	All	1.5 cm	2.5 cm	3 cm
Total number of birds	220	60	99	61
Identified to species by both observers	150	52	71	27
Observers agree on species	136	48	65	23
Observers disagree on species	14	4	6	4
Agreement rate (of 150)	90.67%	92.31%	91.55%	85.19%
Species-level identification rate (of 440)	77.27%	92.50%	80.80%	56.56%

Table 6–9.

Variation in Taxonomic Identity Determination Effectiveness Measures Across Image Resolution Treatments, for Determinations Using Single Images for Each Bird in the Multiple Observer Identification Trials (See Text).

Single Image Determinations	Image Resolution Treatment			
	All	1.5 cm	2.5 cm	3 cm
Total number of birds	220	60	99	61
Identified to species by both observers	95	46	37	12
Observers agree on species	89	42	37	10
Observers disagree on species	6	4	0	2
Agreement Rate (of 150)	93.68%	91.30%	100.0%	83.33%
Species-level identification rate (of 440)	56.14%	85.00%	52.02%	34.43%

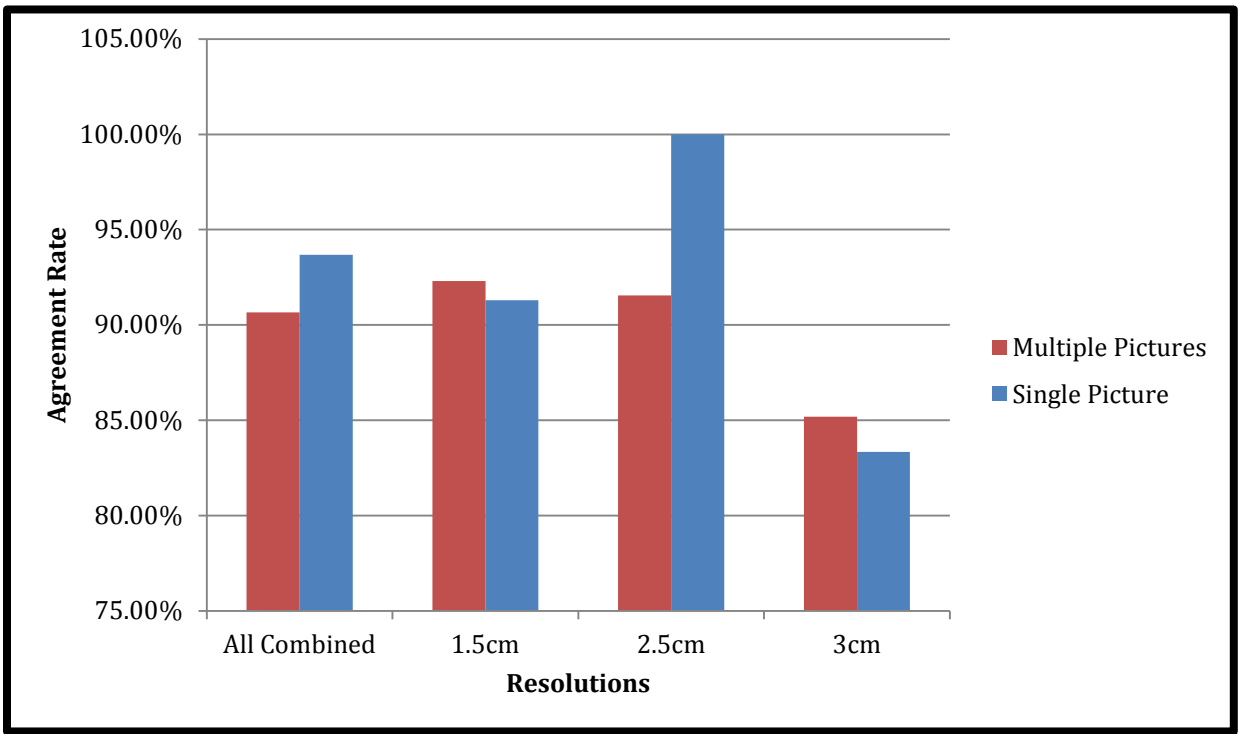

Figure 6–7. Variation in between-observer agreement rate on species-level taxonomic determinations from the multiple observer identification trials, across image resolution treatments, and for both single-image and multiple-image determinations (see text).

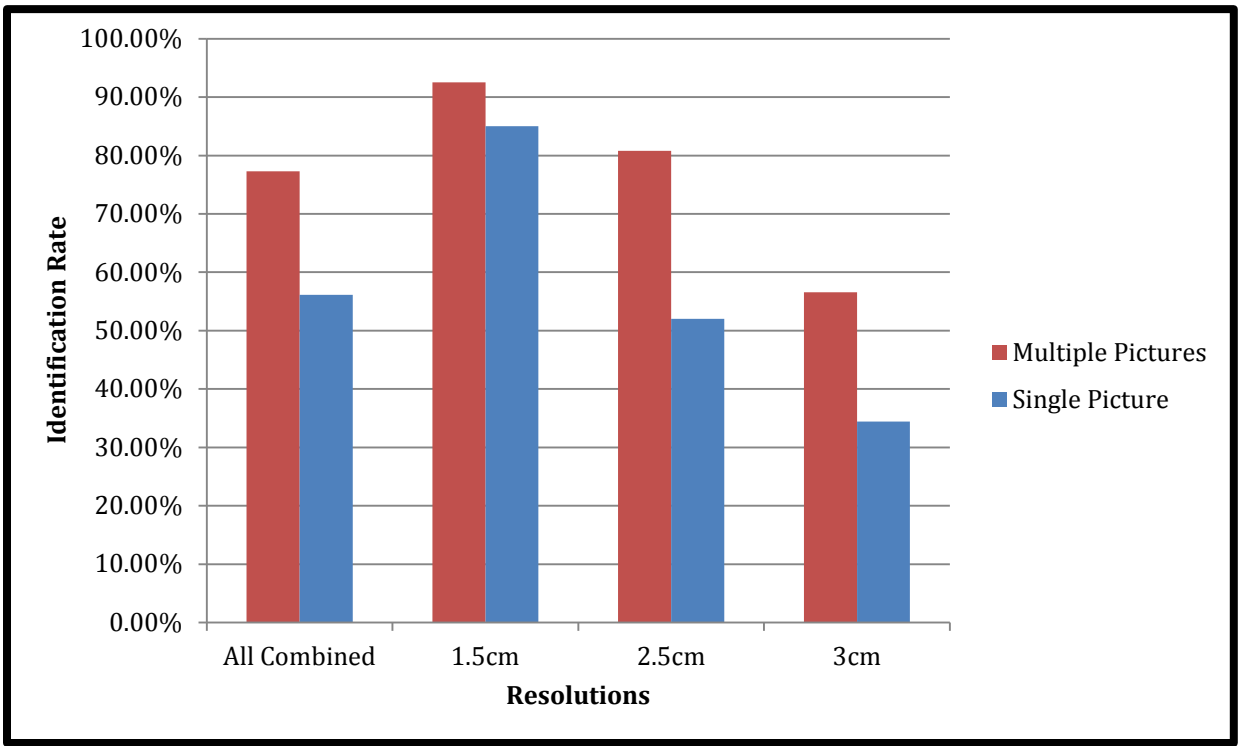

Figure 6–8. Variation in species-level identification rate from the multiple observer identification trials, across image resolution treatments, and for both single-image and multiple-image determinations (see text).

Table 6–10.

Variation in Taxonomic Identity Determination Effectiveness Measures Across Camera Angle Treatments, for Determinations Using Multiple Images for Each Bird in the Multiple Observer Identification Trials.

For Multiple Pictures	Camera Angle (Tilt) Treatment		
	All	15°	44°
Total number of birds	220	116	104
Identified to species by both observers	150	89	61
Observers agree on species	136	78	58
Observers disagree on species	14	11	3
Agreement rate (of 150)	90.67%	87.64%	95.08%
Species-level identification Rate (of 440)	77.27%	82.76%	71.15%

Table 6–11.

Variation in Taxonomic Identity Determination Effectiveness Measures Across Camera Angle Treatments, for Determinations Using Single Images for each Bird in the Multiple Observer Identification Trials.

For Single Pictures	Camera Angle (Tilt) Treatment		
	All	15°	44°
Total number of birds	220	116	104
Identified to species by both observers	95	61	34
Observers agree on species	89	55	34
Observers disagree on species	6	6	0
Agreement rate (of 150)	93.68%	90.16%	100%
Species-level identification Rate (of 440)	56.14%	63.36%	48.08%

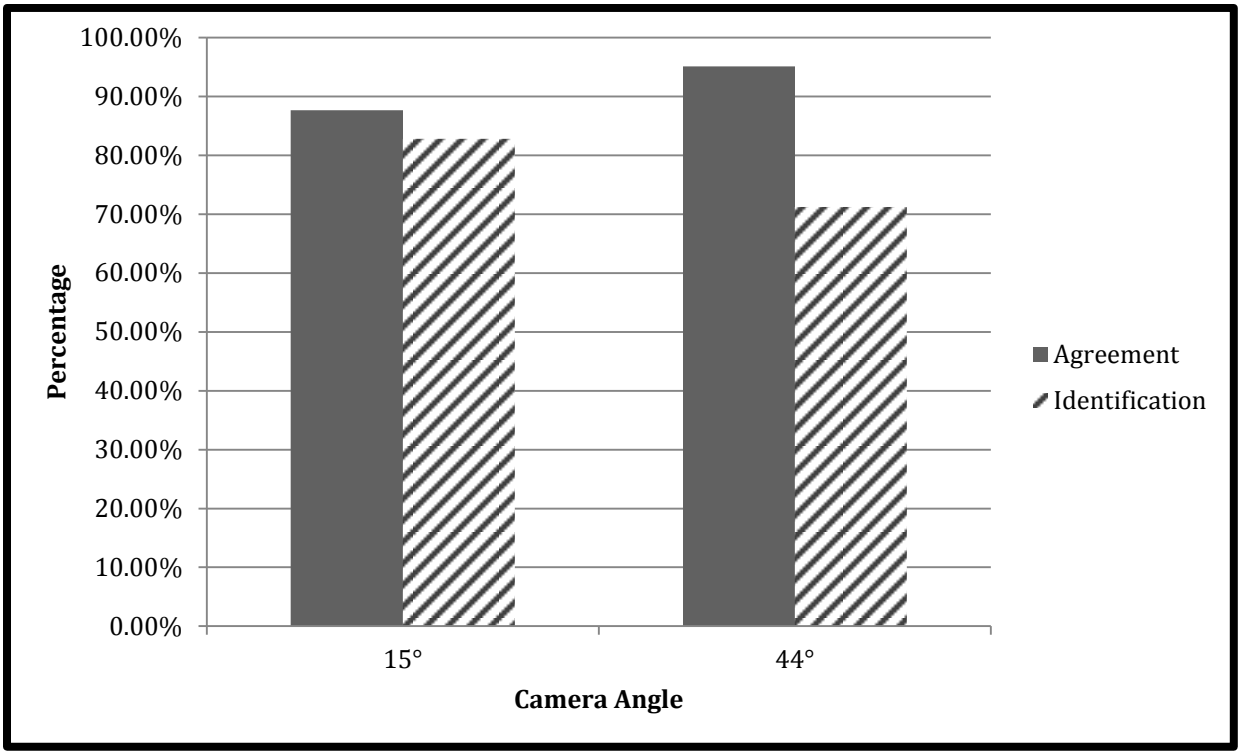

Figure 6–9. Variation in species-level identification rate (hashed bars) and between-observer agreement rate (gray bars) from the multiple observer identification trials, across camera angle treatments, for multiple-image determinations only (see text).

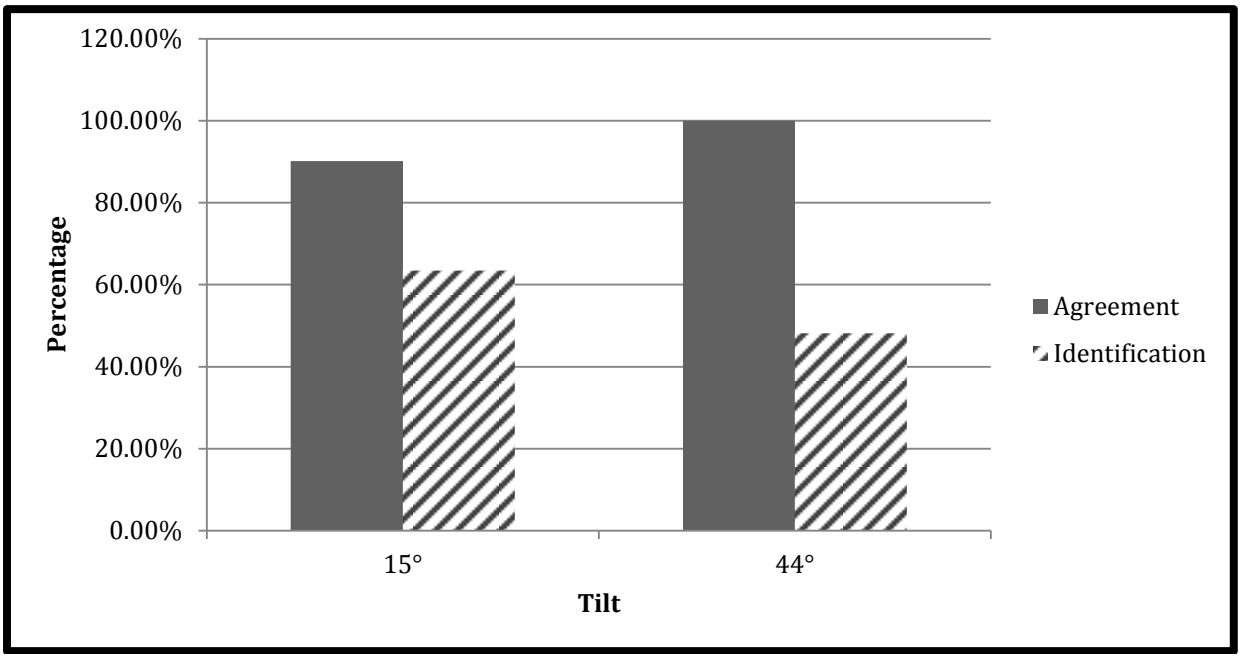

Figure 6–10. Variation in species-level identification rate (hashed bars) and between-observer agreement rate (gray bars) from the multiple observer identification trials, across camera angle treatments, for single-image determinations only (see text).

Modeling analysis

We developed and evaluated two sets of regression models, one corresponding to each of the response variables (or identification effectiveness measures), presented separately below.

Species-level Identification Rate: In our analysis of models using species-level identification rate as the response variable, or measure of identification effectiveness, both image resolution and number of pictures were shown to be important explanatory variables, but camera angle exerted almost no influence. The most parsimonious model included both the number of images and the image resolution (Table 6–12). Including camera angle to this model raised the AIC score, indicating that camera angle exerts little or no influence on species-level identification rate. Removing either image resolution or number of images resulted in significantly lower quality models, suggesting that both of these factors exert important influences on species-level identification rate. Analysis of model-averaged parameter estimates further confirmed that both image resolution and number of images reviewed exerted strong influences on species-level identification rates, as the 95% confidence intervals for the parameter values for both of these effects did not include zero (Table 6–13). By contrast, the 95% confidence interval did include zero for the camera angle parameter value, further confirming that camera angle does not exert a strong influence on species-level identification rate (Table 6–13).

Table 6–12.

Comparison Table for Models Explaining Species-level Identification Rate as a Function of Combinations of Image Resolution, Number of Images, and Camera Angle Effects.

Model	K	AICc	Δ AICc	Model Weight
No of Images + Resolution	5	730.578	0.000	0.611
No of Images + Resolution + Tilt	6	731.479	0.901	0.389
No of Images + Tilt	5	788.409	57.831	0.000
No of Images	4	806.872	76.295	0.000
Resolution	4	855.621	125.043	0.000
Resolution + Tilt	5	857.527	126.949	0.000
Tilt	4	902.754	172.176	0.000
Null	3	912.820	182.243	0.000

Note: For each of these models, observer and bird number were modeled as random effects. Table includes the number of parameters (K), Akaike's Information Criterion corrected for small sample size (AICc), Difference in AICc (ΔAICc) and model weight (relative likelihood of models in the set). The model with the lowest AIC value is listed first, and is regarded as best model. Models with ΔAICc values greater than 2 are regarded as significantly poorer than the best model.

Table 6–13.

Mean Parameter Estimates Averaged Over All of the Models Reported in Table 6–12, Reflecting the Relative Impacts of Different Potential Explanatory Variables on Species-level Identification Rate.

Variables	Mean	SE	LCL	UCL
Number of Images	1.795	0.181	1.441	2.149
Resolution	-3.116	0.434	-3.966	-2.266
Tilt	-0.392	0.364	-1.106	0.322

Note: Mean parameter values are reported, along with standard error (SE), 95% lower confidence interval (LCL) and 95% upper confidence interval (UCL) for each parameter value. If the interval between the upper and lower 95% confidence intervals for a parameter value does not include zero, the explanatory variable is considered to exert a statistically significant impact on the response variable.

Interobserver Agreement on Species-level Determinations: In our analysis of models using the rate of agreement between observers on species-level determinations as the response variable, or measure of identification effectiveness, both image resolution and number of pictures were again shown to be important explanatory variables, with camera angle exerting almost no influence. The most parsimonious model included both the number of images and the image resolution (Table 6–

14). Including camera angle (tilt) in this model raised the AIC score, indicating that camera angle exerted little or no influence on the rate of agreement between observers on species-level determinations. Removing either image resolution or number of images resulted in significantly lower quality models, suggesting that both of these factors exert important influences on the rate of agreement between observers on species-level determinations. Analysis of model-averaged parameter estimates further confirmed that both image resolution and number of images reviewed exerted strong influences on the rate of agreement between observers on species-level determinations, as the 95% confidence intervals for the parameter values for both of these effects did not include zero (Table 6–15). By contrast, the 95% confidence interval did include zero for the camera angle parameter value, further confirming that camera angle does not exert a strong influence on the rate of agreement between observers on species-level determinations (Table 6–15).

Table 6–14.

Comparison Table for Models Explaining the Rate of Agreement Between Observers on Species-level Determinations as a Function of Combinations of Image Resolution, Number of Images, and Camera Angle Effects.

Model	K	AICc	Δ AICc	Model Weight
No of Images + Resolution	4	418.483	0.000	0.702
No of Images + Resolution + Tilt	5	420.194	1.711	0.298
No of Images + Tilt	4	511.146	92.663	0.000
Resolution	3	518.446	99.963	0.000
Resolution + Tilt	4	520.419	101.936	0.000
No of Images	3	522.534	104.051	0.000
Tilt	3	557.102	138.619	0.000
Null	2	561.137	142.655	0.000

Note: For each of these models, observer and bird number were modeled as random effects. Table includes the number of parameters (K), Akaike's Information Criterion corrected for small sample size (AICc), difference in AICc (ΔAICc) and model weight (relative likelihood of models in the set). The model with the lowest AIC value is listed first, and is regarded as best model. Models with ΔAICc values greater than 2 are regarded as significantly poorer than the best model.

Table 6–15.

Mean Parameter Estimates Averaged Over All of the Models Reported in Table 6–14, Reflecting the Relative Impacts of Different Potential Explanatory Variables On The Rate Of Agreement Between Observers on Species-level Determinations

Variables	Mean	SE	LCL	UCL
Number of Images	7.009	1.564	3.943	10.074
Resolution	-11.780	2.859	-17.384	-6.176
Tilt	0.821	2.234	-3.558	5.199

Note: Mean parameter values are reported, along with standard error (SE), 95% lower confidence interval (LCL) and 95% upper confidence interval (UCL) for each parameter value. If the interval between the upper and lower 95% confidence intervals for a parameter value does not include zero, the explanatory variable is considered to exert a statistically significant impact on the response variable.

Discussion

Image Resolution

Qualitative and quantitative analyses suggest that image resolution is a critically important factor for effective determination of the species-level identity of marine birds, more important than any other factor examined in our study. The importance of image resolution was evidenced both in terms of the rate at which image analysts achieved species-level depth in their taxonomic determinations, and also in terms of the rate of agreement between independent observers in the species identity of imaged birds. The increase in performance for both measures of identification effectiveness was larger between 3 cm and 2.5 cm resolutions than between 2.5 cm and 1.5 cm resolutions, suggesting that image resolutions as coarse as 2.5 cm may be acceptable under some circumstances, depending on the level of taxonomic precision required for particular surveys. In general, we do not recommend using image resolutions of 3 cm or coarser for offshore wildlife risk, impact, or other scientific studies, unless species-level identification of animals is not required. We note that image quality is also affected by factors other than image resolution, and that it may be possible to achieve acceptable species-level identification effectiveness under some imaging circumstances, depending on the purpose of the study, and also on the visual appearance characteristics of the animals of interest.

Camera Angle

Our analyses revealed that camera angles up to 44° may be used in high-resolution offshore wildlife imaging surveys with no appreciable degradation in image quality or animal identification success relative to more vertical camera angles. This conclusion was supported by qualitative review of images, and also by quantitative analysis of the impacts of camera angle on both species-level identification rate, and also interobserver agreement in species-level determinations. Our conclusion based on these analyses is that pixel distortion effects are not severe enough under the range of camera angles with which we experimented to exert a significant impact on the ability of image analysts to render accurate and consistent determinations of the taxonomic identity of imaged animals. This finding is very significant within the context of high-resolution offshore wildlife

imaging survey design, as deviation of camera angles away from straight downward is an effective technique for mitigating the adverse impacts of excessive sun glare in aerial imagery, which is particularly important for offshore wildlife imaging surveys on the US AOCS, where lower latitudes result in higher insolation angles relative to northern Europe, where high-resolution offshore wildlife studies have been pioneered.

Single versus Multiple Images

Our quantitative and qualitative analyses revealed that the use of multiple images for individual birds enables image analysts to render higher rates of species-level determination, and produces higher levels of interobserver agreement in species-level taxonomic determinations of imaged birds. This result is likely due to two distinct differences between single and multiple image analyses in our study, only one of which is of general relevance for future applications. The first of these, and the one of limited or no relevance for future applications, is the intermittent vibrational blur that was incorporated into the experimental imagery we gathered using a camera mount with no gyrostabilization. Because of this impact, many of our image sequences for individual birds contained some extremely blurry images, and some notably clearer ones. With the recommended application of gyrostabilization in future high-resolution imaging studies, this effect would not likely be relevant, as there would be less variation in blurriness across images.

The other difference between single-image and multiple-image determinations, and the one of greater relevance for future high-resolution wildlife imaging applications, is the ability for analysts to see multiple views and multiple positions of individual animals when multiple images of the same animal are available. Although our qualitative analysis included imagery taken with an unstabilized camera mount, and hence may include both of these two differences as compounding factors contributing to the advantage of multiple image taxonomic identity determinations, our quantitative analysis of taxonomic determinations from multiple observer identification trials included only gyrostabilized images. Therefore, the improvements we observed in the rate at which birds were identified to species, and in the agreement between observers in specific identity of imaged animals, were likely due only to the latter, and more generally important difference between single-image and multiple-image determinations.

Although our quantitative analysis suggests that adding multiple images of individual animals does improve the accuracy and consistency of taxonomic identity determinations, we note that this difference was more important for coarse image resolutions than for fine resolutions. For image resolutions of 1.5 cm, the rate at which image analysts got to the species level was only 7.5% higher for multiple than for single-image determinations; whereas, for 3 cm image resolution, the multiple-image review rendered a 22.13% higher level of species-level determination than did single-image review. The rate of agreement between observers on the specific identity of imaged animals did not vary as widely between single-image and multiple-image reviews, although our logistic regression model analysis also suggested that adding multiple pictures does increase between observer agreement levels compared with single-image determinations. Because the value added from multiple images is reduced at fine image resolutions, we conclude that stills methods may be preferable to video methods when using image resolutions of 1.5 cm or finer, particularly in light of the additional image quality improvements, and the reduced data volumes and corresponding costs that are possible to achieve with stills methods.

6.5 Taxonomic Guide to the Utility of High-resolution Aerial Imaging Surveys on the Atlantic Outer Continental Shelf (AOCS)

6.5.1 Introduction

The final portion of our evaluation of the effectiveness of high-resolution aerial imaging for conducting offshore marine wildlife surveys on the US AOCS is not as much about the technique but about the taxa. It is intended as a guide to help prospective users of high-resolution wildlife imaging surveys on the AOCS better understand the species of birds, marine mammals, and sea turtles for which they can expect to gather useful data using high-resolution aerial imaging surveys, and what types of data they can expect this methodology to produce for each of these taxa in this region.

The centerpiece of this taxonomic guide is Table 6–16. This table consists of a complete matrix of AOCS bird, mammal, and turtle species for which AOCS high-resolution imaging surveys represent a potentially appropriate, useful, and applicable data gathering method. For each of these species, the matrix presents a series of descriptive information regarding its distribution on the AOCS, conservation/listing status, and a variety of behavioral and visual appearance characteristics that influence the expected effectiveness of high-resolution survey data and the expected types of data that such surveys are able to generate for each species.

One of the most essential elements of this taxonomic guide for AOCS wildlife imaging survey utility is the inclusion or exclusion of species from the matrix. Our intent was to include all, and only, those species of birds, marine mammals, and sea turtles for which diurnal high-resolution aerial imaging surveys should be regarded as a potentially appropriate, useful, and applicable data gathering method. We do not recommend relying solely on diurnal high-resolution aerial imaging surveys as a data gathering method for any species of bird, marine mammal, or sea turtle within the AOCS region.

Our criteria for the inclusion of species in the matrix were as follows:

- Occurs regularly within the US AOCS region of interest for this study (Maine to Florida, states seaward boundaries to 30 m isobaths, see Chapter 1)
    - Occurrence may be limited to a highly restricted portion of the year, but must be more frequent than accidental, vagrant, or occasional.

- Occurrence within study region is more than ephemeral migratory passage
    - Some passage migrants are included if they forage and feed in marine habitats during migratory transit (e.g., Arctic Tern). Songbirds and most shorebirds that merely fly through the region without stopping are excluded by this criterion because high-resolution aerial imaging surveys are not likely to generate useful data for such species.

- Regularly uses marine habitats, including nearshore waters

    - Species that do not regularly occur in marine habitats, including nearshore waters are excluded. By this criterion, species such as ardeids, and most shorebirds, who use

coastal terrestrial habitats such as marshes and beaches, but that do not use actual marine aquatic habitats, are excluded. Species whose typical habitat includes any type of marine habitat, including species with strong coastal affinity (e.g., Osprey, Bald Eagle, cormorants) are generally included, even though their occurrence within the strictly defined region of interest (Maine to Florida, from states' seaward boundaries outward) may be significantly lower than it is in coastal waters.

Table 6–16.

Taxonomic Guide to the Utility of High-resolution Aerial Imaging Surveys on the Atlantic Outer Continental Shelf (AOCS)

	Genus	Species	Common	Occurrence A = abundant, R = rare												Listing Status				Diving behavior affecting aerial detectability				Taxonomic depth of High resolution identification			Other features exhibiting diagnostic appearance variation (yes, no)		
				NORTHEAST				MIDATLANTIC				SOUTHEAST																	
				Winter	Spring	Summer	Fall	Winter	Spring	Summer	Fall	Winter	Spring	Summer	Fall	IUCN	Federal	State	Global	Dive Times	Dive-pause Times	Visibility Scale (1 = always visible, 10 = never visible)	Relative sensitivity to survey platforms (planes/boats)	Taxonomic Group (e.g. black-backed gulls, medium terns, large terns)	Species	Individual	Sexes Distinct	Age Class is Distinct	Seasonal Variation
SEA DUCKS																													
	Branta	*bernicla*	Brant	A	A	R	A	A	A	R	A	R	R	R	R	LC	NL	NL	G5	Surface Feeder	Surface Feeder	1	unknown	Mostly	Mostly	Never	No	No	No
	Anas	*rubripes*	American Black Duck	A	A	A	A	A	A	A	A	A	A	R	A	LC	NL	NL	G5	9.7 sec	unknown	2	moderate	Mostly	Mostly	Never	No	No	No
	Aythya	*valisineria*	Canvasback	A	A	R	A	A	A	R	A	A	A	R	A	LC	NL	NL	G5	15 sec	13.5 sec	2	unknown	Mostly	Rarely	Never	Yes	Yes	No
	Aythya	*americana*	Redhead	A	A	R	A	A	A	R	A	A	A	R	A	LC	NL	NL	G5	14.8 sec	9.6 sec	2	unknown	Mostly	Rarely	Never	Yes	Yes	No
	Aythya	*marila*	Greater Scaup	A	A	R	A	A	A	R	A	A	A	R	A	LC	NL	NL	G5	20.4 sec	unknown	2	unknown	Mostly	Rarely	Never	Yes	Yes	No
	Aythya	*affinis*	Lesser Scaup	A	A	R	A	A	A	R	A	A	A	R	A	LC	NL	NL	G5	11.8 sec	13.5 sec	2	unknown	Mostly	Rarely	Never	Yes	Yes	No
	Somateria	*spectabilis*	King Eider	A	A	R	A	A	A	R	R	R	R	R	R	LC	NL	NL	G5	68.5 sec	unknown	4	high	Mostly	Sometimes	Never	Yes	Yes	No
	Somateria	*mollissima*	Common Eider	A	A	A	A	A	A	R	A	R	R	R	R	LC	NL	NL	G5	38 sec	unknown	2	high	Mostly	Sometimes	Never	Yes	Yes	No
	Histrionicus	*histrionicus*	Harlequin Duck	A	A	R	A	R	R	R	R	R	R	R	R	LC	NL	NL	G4	25.9 sec	13.1 sec	2	moderate	Mostly	Sometimes	Never	Yes	Yes	No
	Melanitta	*perspicillata*	Surf Scoter	A	A	A	A	A	R	R	A	R	R	R	R	LC	NL	NL	G5	46 sec	25.7 sec	3	high	Mostly	Sometimes	Never	Yes	Yes	No
	Melanitta	*fusca*	White-winged Scoter	A	A	A	A	A	A	R	A	A	R	R	R	LC	NL	NL	G5	79.5 sec	unknown	4	high	Mostly	Sometimes	Never	Yes	Yes	No
	Melanitta	*nigra*	Black Scoter	A	A	A	A	A	A	R	A	A	A	R	A	LC	NL	NL	G5	17 sec	unknown	2	high	Mostly	Sometimes	Never	Yes	Yes	No
	Clangula	*hyemalis*	Long-tailed Duck	A	A	R	A	A	R	R	R	R	R	R	R	LC	NL	NL	G5	43.9 sec	16.6 sec	3	high	Mostly	Mostly	Never	Yes	Yes	Yes
	Bucephala	*albeola*	Bufflehead	A	A	A	A	A	A	R	A	A	A	R	A	LC	NL	NL	G5	12.5 sec	unknown	2	unknown	Mostly	Sometimes	Never	Yes	Yes	No
	Bucephala	*clangula*	Common Goldeneye	A	A	R	A	A	A	R	A	A	R	R	R	LC	NL	NL	G5	25 sec	16.05 sec	2	moderate	Mostly	Rarely	Never	Yes	Yes	No
	Bucephala	*islandica*	Barrow's Goldeneye	A	A	R	R	R	R	R	R	R	R	R	R	LC	NL	NL	G5	42.5 sec	unknown	3	moderate	Mostly	Rarely	Never	Yes	Yes	No
	Mergus	*serrator*	Red-breasted Merganser	A	A	A	A	A	A	R	A	A	A	R	A	LC	NL	NL	G5	31.4 sec	24.25 sec	3	unknown	Mostly	Mostly	Never	Yes	Yes	No
LOONS & GREBES																													
	Gavia	*immer*	Common loon	A	A	A	A	A	A	R	A	A	A	R	A	LC	NL	T_NH; SSC_MA, NY, CT	G5	34.2 sec	14.3 sec	3	unknown	Mostly	Sometimes	Never	No	No	Yes
	Gavia	*stellata*	Red-throated loon	A	A	A	A	A	A	R	A	A	R	R	R	LC	NL	NL	G5	65 sec	unknown	4	high	Mostly	Sometimes	Never	No	Yes	Yes
	Podiceps	*auritus*	Horned Grebe	A	A	R	A	A	R	R	R	A	R	R	R	LC	NL	NL	G5	26.45 sec	12.5 sec	2	unknown	Mostly	Mostly	Never	No	No	Yes
	Podiceps	*grisegena*	Red-necked Grebe	A	A	R	A	A	R	R	R	R	R	R	R	LC	NL	NL	G5	24.8 sec	unknown	2	moderate	Mostly	Mostly	Never	No	No	Yes
SHEARWATERS & PETRELS																													
	Fulmarus	*glacialis*	Northern Fulmar	A	A	A	A	R	R	R	R	R	R	R	R	LC	NL	NL	G5	Surface Feeder	Surface Feeder	1	low	Mostly	Sometimes	Never	No	No	No

	Genus	Species	Common	Occurrence A = abundant, R = rare												Listing Status				Diving behavior affecting aerial detectability				Taxonomic depth of High resolution identification			Other features exhibiting diagnostic appearance variation (yes, no)		
				NORTHEAST				MIDATLANTIC				SOUTHEAST																	
				Winter	Spring	Summer	Fall	Winter	Spring	Summer	Fall	Winter	Spring	Summer	Fall	IUCN	Federal	State	Global	Dive Times	Dive-pause Times	Visibility Scale (1 = always visible, 10 = never visible)	Relative sensitivity to survey platforms (planes/boats)	Taxonomic Group (e.g. black-backed gulls, medium terns, large terns)	Species	Individual	Sexes Distinct	Age Class is Distinct	Seasonal Variation
	Pterodroma	*arminojoniana*	Herald Petrel	R	R	R	R	R	R	R	R	R	R	R	R	VU	NL	NL	G4	Surface Feeder	Surface Feeder	1	unknown	Mostly	Rarely	Never	No	No	No
	Pterodroma	*cahow*	Bermuda Petrel	R	R	R	R	R	R	R	R	R	R	R	R	EN	NL	NL	G1	Surface Feeder	Surface Feeder	1	unknown	Mostly	Rarely	Never	No	No	No
	Pterodroma	*hasitata*	Black-capped Petrel	R	R	R	R	R	A	A	A	R	A	A	A	EN	NL	NL	G1	Surface Feeder	Surface Feeder	1	unknown	Mostly	Rarely	Never	No	No	No
	Pterodroma	*feae*	Fea's Petrel	R	R	R	R	R	R	R	R	R	R	R	R	NT	NL	NL	G1G2	Surface Feeder	Surface Feeder	1	unknown	Mostly	Rarely	Never	No	No	No
	Calonectris	*diomedea*	Cory's Shearwater	R	R	A	A	R	R	A	A	R	R	A	A	LC	NL	NL	G5	unknown	unknown	2	unknown	Mostly	Sometimes	Never	No	No	No
	Puffinus	*gravis*	Greater Shearwater	R	R	R	R	R	R	R	R	R	R	R	R	LC	NL	NL	G5	unknown	unknown	2	unknown	Mostly	Sometimes	Never	No	No	No
	Puffinus	*griseus*	Sooty Shearwater	R	A	A	A	R	A	A	R	R	R	R	R	NT	NL	NL	G5	unknown	unknown	2	unknown	Mostly	Sometimes	Never	No	No	No
	Puffinus	*puffinus*	Manx Shearwater	R	A	A	A	R	A	A	R	R	R	R	R	LC	NL	NL	G5	17.5 sec	unknown	2	unknown	Mostly	Sometimes	Never	No	No	No
	Puffinus	*lherminieri*	Audubon's Shearwater	R	R	R	A	R	R	A	A	R	A	A	A	LC	NL	NL	G4G5	unknown	unknown	2	unknown	Mostly	Sometimes	Never	No	No	No
	Oceanites	*oceanicus*	Wilson's Storm-Petrel	R	A	A	A	R	A	A	A	R	A	A	A	LC	NL	NL	G5	Surface Feeder	Surface Feeder	1	unknown	Mostly	Rarely	Never	No	No	No
	Pelagodrama	*marina*	White-faced Storm-Petrel	R	R	R	A	R	R	R	A	R	R	R	R	LC	NL	NL	G5	Surface Feeder	Surface Feeder	1	unknown	Mostly	Rarely	Never	No	No	No
	Oceanodroma	*leucorhoa*	Leach's Storm-Petrel	R	A	A	A	R	A	A	A	R	A	A	R	LC	NL	E_MA	G5	Surface Feeder	Surface Feeder	1	unknown	Mostly	Rarely	Never	No	No	No
	Oceanodroma	*castro*	Band-rumped Storm-Petrel	R	R	A	A	R	A	A	A	R	A	A	A	LC	NL	NL	G3	Surface Feeder	Surface Feeder	1	unknown	Mostly	Rarely	Never	No	No	No
TROPICBIRDS																													
	Phaethon	*lepturus*	White-tailed Tropicbird	R	R	R	A	R	R	A	A	R	A	A	A	LC	NL	NL	G5	Surface Feeder	Surface Feeder	1	unknown	Mostly	Mostly	Never	No	Yes	No
	Phaethon	*aethereus*	Red-billed Tropicbird	R	R	R	R	R	R	R	R	R	R	R	R	LC	NL	NL	G5	Surface Feeder	Surface Feeder	1	unknown	Mostly	Mostly	Never	No	Yes	No
SULIDS																													
	Fregata	*magnificens*	Magnificent Frigatebird	R	R	R	R	R	R	R	R	A	A	A	A	LC	NL	NL	G5	Surface Feeder	Surface Feeder	1	unknown	Mostly	Mostly	Never	Yes	Yes	No
	Sula	*dactylatra*	Masked Booby	R	R	R	R	R	R	R	R	R	R	R	R	LC	NL	NL	G5	Surface Feeder	Surface Feeder	1	unknown	Mostly	Sometimes	Never	No	Yes	No
	Sula	*leucogaster*	Brown Booby	R	R	R	R	R	R	R	R	A	A	A	A	LC	NL	NL	G5	Surface Feeder	Surface Feeder	1	unknown	Mostly	Sometimes	Never	No	Yes	No
	Morus	*bassanus*	Northern Gannet	A	A	A	A	A	A	A	A	A	A	A	A	LC	NL	NL	G5	Surface Feeder	Surface Feeder	1	low	Mostly	Mostly	Never	No	Yes	No
	Phalacrocorax	*auritus*	Double-crested Cormorant	A	A	A	A	A	A	A	A	A	A	A	A	LC	NL	NL	G5	23.5 sec	21.8 sec	2	unknown	Mostly	Sometimes	Never	No	Yes	No
	Phalacrocorax	*carbo*	Great Cormorant	A	A	A	A	A	A	R	A	R	R	R	R	LC	NL	NL	G5	20.5 sec	unknown	2	high	Mostly	Sometimes	Never	No	Yes	No
PELICANS																													
	Pelecanus	*occidentalis*	Brown Pelican	R	R	A	A	A	A	A	A	A	A	A	A	LC	NL	SSC_FL	G4	Surface Feeder	Surface Feeder	1	unknown	Mostly	Mostly	Never	No	Yes	Yes
ACCIPITRIFORMES																													
	Pandion	*haliaetus*	Osprey	A	A	A	A	A	A	A	A	A	A	A	A	LC	NL	NL	G5	Surface Feeder	Surface Feeder	1	unknown	Mostly	Mostly	Never	No	No	No
	Haliaeetus	*leucocephalus*	Bald Eagle	A	A	A	A	A	A	A	A	A	A	A	A	LC	NL	E_VT; T_NH, MA, CT	G4	Surface Feeder	Surface Feeder	1	unknown	Mostly	Mostly	Never	No	Yes	No

	Genus	Species	Common	Occurrence A = abundant, R = rare												Listing Status				Diving behavior affecting aerial detectability				Taxonomic depth of High resolution identification			Other features exhibiting diagnostic appearance variation (yes, no)		
				NORTHEAST				MIDATLANTIC				SOUTHEAST																	
				Winter	Spring	Summer	Fall	Winter	Spring	Summer	Fall	Winter	Spring	Summer	Fall	IUCN	Federal	State	Global	Dive Times	Dive-pause Times	Visibility Scale (1 = always visible, 10 = never visible)	Relative sensitivity to survey platforms (planes/boats)	Taxonomic Group (e.g. black-backed gulls, medium terns, large terns)	Species	Individual	Sexes Distinct	Age Class is Distinct	Seasonal Variation
SHOREBIRDS																													
	Phalaropus	*fulicaria*	Red Phalarope	A	A	A	A	A	R	R	R	A	R	R	R	LC	NL	NL	G5	Surface Feeder	Surface Feeder	1	unknown	Mostly	Mostly	Never	Yes	Yes	Yes
	Phalaropus	*lobatus*	Red-necked Phalarope	R	A	R	A	R	R	R	A	R	R	R	A	LC	NL	NL	G4G5	Surface Feeder	Surface Feeder	1	unknown	Mostly	Mostly	Never	Yes	Yes	Yes
GULLS & TERNS																													
	Rissa	*tridactyla*	Black-legged Kittiwake	A	A	A	A	A	R	R	R	R	R	R	R	LC	NL	NL	G5	Surface Feeder	Surface Feeder	1	low	Mostly	Sometimes	Never	No	Yes	No
	Xema	*sabini*	Sabine's Gull	R	R	R	A	R	R	R	A	R	R	R	A	LC	NL	NL	G5	Surface Feeder	Surface Feeder	1	unknown	Mostly	Sometimes	Never	No	Yes	Yes
	Larus	*philadelphia*	Bonaparte's Gull	A	A	A	A	A	A	R	A	A	A	R	A	LC	NL	NL	G5	Surface Feeder	Surface Feeder	1	unknown	Mostly	Sometimes	Never	No	Yes	Yes
	Chroicocephalus	*ridibundus*	Black-headed Gull	A	A	R	A	R	R	R	R	R	R	R	R	LC	NL	NL	G5	Surface Feeder	Surface Feeder	1	low	Mostly	Sometimes	Never	No	Yes	Yes
	Hydrocoloeus	*minutus*	Little Gull	A	A	R	A	R	R	R	R	R	R	R	R	LC	NL	NL	G5	Surface Feeder	Surface Feeder	1	low	Mostly	Sometimes	Never	No	Yes	Yes
	Leucophaeus	*atricilla*	Laughing Gull	R	A	A	A	A	A	A	A	A	A	A	A	LC	NL	NL	G5	Surface Feeder	Surface Feeder	1	unknown	Mostly	Sometimes	Never	No	Yes	Yes
	Leucophaeus	*pipixcan*	Franklin's Gull	R	R	R	R	R	R	R	R	R	R	R	R	LC	NL	NL	G4G5	Surface Feeder	Surface Feeder	1	unknown	Mostly	Sometimes	Never	No	Yes	Yes
	Larus	*delawarensis*	Ring-billed gull	A	A	A	A	A	A	A	A	A	A	A	A	LC	NL	NL	G5	Surface Feeder	Surface Feeder	1	unknown	Mostly	Sometimes	Never	No	Yes	No
	Larus	*argentatus*	Herring Gull	A	A	A	A	A	A	A	A	A	A	A	A	LC	NL	NL	G5	Surface Feeder	Surface Feeder	1	low	Mostly	Sometimes	Never	No	Yes	No
	Larus	*thayeri*	Thayer's Gull	R	R	R	R	R	R	R	R	R	R	R	R	LC	NL	NL	G5	Surface Feeder	Surface Feeder	1	unknown	Mostly	Sometimes	Never	No	Yes	Yes
	Larus	*glaucoides*	Iceland Gull	A	A	R	A	A	R	R	R	R	R	R	R	LC	NL	NL	G5	Surface Feeder	Surface Feeder	1	unknown	Mostly	Sometimes	Never	No	Yes	No
	Larus	*fuscus*	Lesser black-backed gull	A	A	R	A	A	A	R	A	A	A	R	A	LC	NL	NL	G5	Surface Feeder	Surface Feeder	1	low	Mostly	Sometimes	Never	No	Yes	Yes
	Larus	*hyperboreaus*	Glaucous Gull	A	A	R	A	R	R	R	R	R	R	R	R	LC	NL	NL	G5	Surface Feeder	Surface Feeder	1	unknown	Mostly	Sometimes	Never	No	Yes	No
	Anous	*stolidus*	Brown Noddy	R	R	R	R	R	R	R	R	R	R	A	A	LC	NL	NL	G5	Surface Feeder	Surface Feeder	1	unknown	Mostly	Sometimes	Never	No	No	Yes
	Onychoprion	*fuscatus*	Sooty Tern	R	R	R	A	R	A	A	A	R	A	A	A	LC	NL	NL	G5	Surface Feeder	Surface Feeder	1	unknown	Mostly	Sometimes	Never	No	Yes	Yes
	Onychoprion	*anaethetus*	Bridled Tern	R	R	A	A	R	A	A	A	R	A	A	A	LC	NL	NL	G5	Surface Feeder	Surface Feeder	1	unknown	Mostly	Sometimes	Never	No	Yes	Yes
	Sternula	*antillarum*	Least Tern	R	A	A	A	R	A	A	A	R	A	A	A	LC	E	E_ME, NH, NJ; T_CT, RI, NY, MD, FL; SSC_MA, GA	G4	Surface Feeder	Surface Feeder	1	unknown	Mostly	Sometimes	Never	No	Yes	Yes
	Sterna	*caspia*	Caspian Tern	R	A	A	A	A	A	A	A	A	A	A	A	LC	NL	NL	G5	Surface Feeder	Surface Feeder	1	unknown	Mostly	Sometimes	Never	No	Yes	Yes
	Chlidonias	*niger*	Black Tern	R	A	A	A	R	A	A	A	R	A	A	A	LC	NL	E_ME, VT	G4	Surface Feeder	Surface Feeder	1	low	Mostly	Sometimes	Never	No	No	Yes
	Sterna	*dougalli*	Roseate Tern	R	A	A	A	R	R	R	R	R	A	A	R	LC	E	E_ME, NH, MA, NY, CT,	G4	Surface Feeder	Surface Feeder	1	unknown	Mostly	Sometimes	Never	No	Yes	Yes

	Genus	Species	Common	Occurrence A = abundant, R = rare												Listing Status				Diving behavior affecting aerial detectability				Taxonomic depth of High resolution identification			Other features exhibiting diagnostic appearance variation (yes, no)		
				NORTHEAST				MIDATLANTIC				SOUTHEAST																	
				Winter	Spring	Summer	Fall	Winter	Spring	Summer	Fall	Winter	Spring	Summer	Fall	IUCN	Federal	State	Global	Dive Times	Dive-pause Times	Visibility Scale (1 = always visible, 10 = never visible)	Relative sensitivity to survey platforms (planes/boats)	Taxonomic Group (e.g. black-backed gulls, medium terns, large terns)	Species	Individual	Sexes Distinct	Age Class is Distinct	Seasonal Variation
																		NJ, DE, VT; T_FL											
	Sterna	*hirundo*	Common Tern	R	A	A	A	R	A	A	A	A	A	A	A	LC	NL	E_VT; T_NH, NY; SSC_MA, CT	G5	Surface Feeder	Surface Feeder	1	low	Mostly	Sometimes	Never	No	Yes	Yes
	Sterna	*paradisae*	Arctic Tern	R	A	A	A	R	A	R	R	R	A	R	R	LC	NL	T_ME; SSC_MA	G5	Surface Feeder	Surface Feeder	1	low	Mostly	Sometimes	Never	No	Yes	Yes
	Sterna	*forsteri*	Forster's Tern	R	R	A	A	A	A	A	A	A	A	A	A	LC	NL	NL	G5	Surface Feeder	Surface Feeder	1	unknown	Mostly	Sometimes	Never	No	Yes	Yes
	Sterna	*maxima*	Royal Tern	R	R	A	A	A	A	A	A	A	A	A	A	LC	NL	E_MD	G5	Surface Feeder	Surface Feeder	1	unknown	Mostly	Sometimes	Never	No	Yes	Yes
	Sterna	*sandivicensis*	Sandwich Tern	R	R	A	A	R	A	A	A	A	A	A	A	LC	NL	NL	G5	Surface Feeder	Surface Feeder	1	low	Mostly	Sometimes	Never	No	Yes	Yes
SKUAS & JAEGERS																													
	Catharacta	*skua*	Great Skua	A	R	R	A	A	R	R	R	R	R	R	R	LC	NL	NL	G4G5	Surface Feeder	Surface Feeder	1	low	Mostly	Sometimes	Never	No	No	No
	Catharacta	*maccormicki*	South Polar Skua	R	R	A	A	R	R	A	A	R	R	R	R	LC	NL	NL	G5	Surface Feeder	Surface Feeder	1	unknown	Mostly	Sometimes	Never	No	No	No
	Sterocarius	*pomarinus*	Pomarine Jaeger	A	A	A	A	A	A	A	A	A	A	A	A	LC	NL	NL	G5	Surface Feeder	Surface Feeder	1	unknown	Mostly	Sometimes	Never	No	No	No
	Sterocarius	*parasiticus*	Parasitic Jaeger	A	A	A	A	A	A	A	A	A	A	R	A	LC	NL	NL	G5	Surface Feeder	Surface Feeder	1	unknown	Mostly	Sometimes	Never	No	No	No
	Stercorarius	*longicaudus*	Long-tailed Jaeger	R	R	R	A	R	R	R	A	R	R	R	R	LC	NL	NL	G5	Surface Feeder	Surface Feeder	1	unknown	Mostly	Sometimes	Never	No	No	No
ALCIDS																													
	Alle	*alle*	Dovekie	A	A	A	A	A	A	R	R	R	R	R	R	LC	NL	NL	G5	52 sec	unknown	3	unknown	Mostly	Sometimes	Never	No	No	Yes
	Uria	*aalge*	Common Murre	A	A	A	A	R	R	R	R	R	R	R	R	LC	NL	NL	G5	38 sec	unknown	3	unknown	Mostly	Sometimes	Never	No	No	Yes
	Uria	*lomvia*	Thick-billed Murre	A	A	A	A	R	R	R	R	R	R	R	R	LC	NL	NL	G5	55 sec	unknown	3	unknown	Mostly	Sometimes	Never	No	No	Yes
	Alca	*torda*	Razorbill	A	A	A	A	A	R	R	R	R	R	R	R	LC	NL	T_ME	G5	35 sec	unknown	3	moderate	Mostly	Sometimes	Never	No	No	Yes
	Cepphus	*grylle*	Black Guillemot	A	A	A	A	R	R	R	R	R	R	R	R	LC	NL	NL	G5	73 sec	27.5 sec	4	moderate	Mostly	Sometimes	Never	No	Yes	Yes
	Fratercula	*artica*	Atlantic Puffin	A	A	A	A	A	R	R	R	R	R	R	R	LC	NL	T_ME	G5	25 sec	unknown	3	low	Mostly	Sometimes	Never	No	No	Yes
BALAENIDAE																													
	Balaena	*glacialis*	Northern Right Whale	A	A	A	A	A	R	R	A	A	R	R	A	EN	E	NL	G1	10 min	unknown	6	low	Mostly	Mostly	Rarely	No	No	No
BALAENOPTERIDAE																													
	Balaenoptera	*musculus*	Blue Whale	A	A	A	A	A	R	R	R	A	R	R	R	EN	E	NL	G3	11.5 min	unknown	6	low	Mostly	Mostly	Rarely	No	No	No
	Balaenoptera	*physalus*	Fin Whale	A	A	A	A	R	A	A	A	A	R	R	R	EN	E	NL	G3	10 min	unknown	6	low	Mostly	Mostly	Rarely	No	No	No
	Balaenoptera	*borealis*	Sei Whale	A	A	A	A	A	R	R	R	A	R	R	R	EN	E	NL	G3	17.5 min	unknown	6	unknown	Mostly	Mostly	Rarely	No	No	No

	Genus	Species	Common	Occurrence A = abundant, R = rare												Listing Status				Diving behavior affecting aerial detectability				Taxonomic depth of High resolution identification			Other features exhibiting diagnostic appearance variation (yes, no)		
				NORTHEAST				MIDATLANTIC				SOUTHEAST																	
				Winter	Spring	Summer	Fall	Winter	Spring	Summer	Fall	Winter	Spring	Summer	Fall	IUCN	Federal	State	Global	Dive Times	Dive-pause Times	Visibility Scale (1 = always visible, 10 = never visible)	Relative sensitivity to survey platforms (planes/boats)	Taxonomic Group (e.g. black-backed gulls, medium terns, large terns)	Species	Individual	Sexes Distinct	Age Class is Distinct	Seasonal Variation
	Balaenoptera	*brydei*	Bryde's Whale	R	R	R	R	A	A	A	A	A	A	A	A	DD	NL	NL	G4	5 min	unknown	5	low	Mostly	Mostly	Rarely	No	No	No
	Balaenoptera	*acutorostrata*	Minke Whale	R	A	A	A	R	A	A	A	A	R	R	R	NT	NL	NL	G5	11.5 min	unknown	6	low	Mostly	Mostly	Rarely	No	No	No
	Megaptera	*novaeangliae*	Humpback Whale	A	A	A	A	A	A	A	A	A	A	A	A	VU	E	NL	G4	5 min	unknown	5	low	Mostly	Mostly	Sometimes	No	No	No
PHYSETERIDAE																													
	Physeter	*macrocephalus*	Sperm Whale	A	A	A	A	A	A	A	A	A	A	A	A	VU	E	NL	G3	45 min	unknown	9	low	Mostly	Mostly	Rarely	No	No	No
	Kogia	*breviceps*	Pygmy Sperm Whale	R	R	R	R	A	A	A	A	A	A	A	A	LC	NL	NL	G4	unknown	unknown	unknown	high	Mostly	Sometimes	Rarely	No	No	No
	Kogia	*sima*	Dwarf Sperm Whale	R	R	R	R	A	A	A	A	A	A	A	A	LC	NL	NL	G4	unknown	unknown	unknown	high	Mostly	Sometimes	Rarely	No	No	No
ZIPHIIDAE																													
	Hyperoodon	*ampullatus*	Northern Bottlenose Whale	A	A	A	A	R	R	R	R	R	R	R	R	DD	NL	NL	G4	90 min	unknown	9	high	Mostly	Mostly	Rarely	No	No	No
	Ziphius	*cavirostris*	Cuvier's Beaked Whale	R	A	A	R	R	R	R	R	R	R	R	R	DD	NL	NL	G4	30 min	unknown	8	high	Mostly	Sometimes	Rarely	No	No	No
	Mesoplodon	*europaeus*	Gervais' Beaked Whale	R	A	A	A	A	A	A	A	A	A	A	A	DD	NL	NL	G3	unknown	unknown	unknown	high	Mostly	Sometimes	Rarely	No	No	No
	Mesoplodon	*mirus*	True's Beaked Whale	R	R	R	R	A	A	A	A	A	A	A	A	DD	NL	NL	G3	unknown	unknown	unknown	high	Mostly	Sometimes	Rarely	No	No	No
	Mesoplodon	*biden*	Sowerby's Beaked Whale	A	A	A	A	R	R	R	R	R	R	R	R	DD	NL	NL	G3	17.5 min	unknown	6	high	Mostly	Sometimes	Rarely	No	No	No
	Mesoplodon	*densirostris*	Blainville's Beaked Whale	R	R	A	R	A	A	A	A	A	A	A	A	DD	NL	NL	G4	32.5 min	unknown	8	high	Mostly	Sometimes	Rarely	No	No	No
DELPHINIDAE																													
	Orcinus	*orca*	Killer Whale	A	A	A	A	R	R	R	R	R	R	R	R	DD	NL	NL	G4	7 min	unknown	5	low	Mostly	Mostly	Rarely	Yes	No	No
	Globicephera	*melas*	Longfinned Pilot Whale	A	A	A	A	A	A	R	A	R	R	R	R	LC	NL	NL	G5	5.5 min	unknown	5	unknown	Mostly	Sometimes	Rarely	No	No	No
	Globicephera	*macrorhynchus*	Short Finned Pilot Whale	R	A	A	R	A	A	A	A	A	R	R	A	DD	NL	NL	G5	5.5 min	unknown	5	low	Mostly	Sometimes	Rarely	No	No	No
	Pseudorca	*crassidens*	False Killer Whale	R	R	R	R	R	R	R	R	R	A	A	R	LC	C	NL	G4	unknown	unknown	unknown	low	Mostly	Sometimes	Rarely	No	No	No
	Grampus	*Grisseus*	Risso's Doldpin	R	A	A	A	A	A	A	A	A	A	A	A	DD	NL	NL	G5	1.5 min	unknown	4	low	Mostly	Sometimes	Rarely	No	No	No
	Tursiops	*truncatus*	Bottlenose Dolphin	R	R	R	A	A	A	A	A	A	A	A	A	DD	NL	NL	G5	3.5 min	unknown	4	low	Mostly	Sometimes	Rarely	No	No	No
	Lagenorhynchus	*albirostris*	White-Beaked Dolphin	A	A	A	A	R	R	R	R	R	R	R	R	LC	NL	NL	G4	unknown	unknown	unknown	unknown	Mostly	Sometimes	Rarely	No	No	No
	Lagenorhynchus	*actus*	Atlantic White-Sided Dolphin	A	A	A	A	R	A	A	R	R	R	R	R	LC	NL	NL	G4	unknown	unknown	unknown	unknown	Mostly	Sometimes	Rarely	No	No	No
	Feresa	*attenuata*	Pygmy Killer Whale	R	R	R	R	R	A	A	A	A	A	A	A	DD	NL	NL	G4	unknown	unknown	unknown	moderate	Mostly	Sometimes	Rarely	No	No	No
	Peponocephala	*electra*	Melonheaded Whale	R	R	R	R	R	R	R	R	A	A	A	A	LC	NL	NL	G4	unknown	unknown	unknown	moderate	Mostly	Sometimes	Rarely	No	No	No
	Steno	*bredanensis*	Rough-Tooth Dolphin	R	R	R	R	R	A	A	A	A	A	A	A	DD	NL	NL	G4	4.5 min	unknown	5	unknown	Mostly	Sometimes	Rarely	No	No	No
	Lagenodelphis	*hosei*	Fraser's Dolphin	R	R	R	R	R	R	R	R	A	A	A	A	LC	NL	NL	NA	unknown	unknown	unknown	moderate	Mostly	Sometimes	Rarely	No	No	No
	Delphinus	*delphis*	Common Dolphin	A	A	A	A	A	A	A	A	R	R	R	R	LC	NL	NL	G5	4.5 min	unknown	5	unknown	Mostly	Sometimes	Rarely	No	No	No
	Stenella	*coeruleoalba*	Striped Dolphin	A	A	A	A	A	R	R	A	A	R	R	A	LC	NL	NL	G5	7.5 min	unknown	5	low	Mostly	Sometimes	Rarely	No	No	No
	Stenella	*attenuata*	Pantropical Spotted Dolphin	R	R	R	R	R	A	A	R	A	A	A	A	LC	NL	NL	G5	3 min	unknown	4	low	Mostly	Sometimes	Rarely	No	No	No

	Genus	Species	Common	Occurrence A = abundant, R = rare												Listing Status				Diving behavior affecting aerial detectability				Taxonomic depth of High resolution identification			Other features exhibiting diagnostic appearance variation (yes, no)		
				NORTHEAST				MIDATLANTIC				SOUTHEAST																	
				Winter	Spring	Summer	Fall	Winter	Spring	Summer	Fall	Winter	Spring	Summer	Fall	IUCN	Federal	State	Global	Dive Times	Dive-pause Times	Visibility Scale (1 = always visible, 10 = never visible)	Relative sensitivity to survey platforms (planes/boats)	Taxonomic Group (e.g. black-backed gulls, medium terns, large terns)	Species	Individual	Sexes Distinct	Age Class is Distinct	Seasonal Variation
	Stenella	*frontalis*	Atlantic spotted Dolphin	R	R	A	R	A	A	A	A	A	A	A	A	DD	NL	NL	G5	6 min (max)	unknown	5	low	Mostly	Sometimes	Rarely	No	No	No
	Stenella	*longirostris*	Spinner Dolphin	R	R	A	R	A	A	A	A	A	A	A	A	DD	NL	NL	G5	unknown	unknown	unknown	low	Mostly	Sometimes	Rarely	No	No	No
	Stenella	*clymene*	Clymene Dolphin	R	R	R	R	R	R	R	R	R	A	A	R	DD	NL	NL	G4	unknown	unknown	unknown	low	Mostly	Sometimes	Rarely	No	No	No
PHOCOENIDAE																													
	Phocoena	*phocoena*	Harbor Porpoise	A	A	A	A	A	R	R	A	R	R	R	R	NE	NL	NL	G4	5.35 min (max)	unknown	4	unknown	Mostly	Sometimes	Rarely	No	No	No
DERMOCHELYIDAE																													
	Dermochelys	*coriacea*	Leatherback Sea Turtle	R	A	A	R	R	A	A	R	A	A	A	A	CR	E	NL	G2	11.2 min	4.2 min	6	unknown	Mostly	Mostly	Rarely	Yes	No	No
CHELONIIDAE																													
	Chelonia	*mydas*	Green Turtle	R	A	A	R	R	A	A	R	A	A	A	A	EN	E	NL	G3	25 min	unknown	7	unknown	Mostly	Sometimes	Rarely	Yes	No	No
	Caretta	*caretta*	Loggerhead Sea Turtle	R	A	A	R	A	A	A	A	A	A	A	A	EN	T	NL	G3	42.8 min	unknown	8	unknown	Mostly	Sometimes	Rarely	Yes	No	No
	Eretmochelys	*imbricita*	Hawksbill Sea Turtle	R	A	A	R	R	A	A	R	A	A	A	A	CR	E	NL	G3	38 min	unknown	8	unknown	Mostly	Sometimes	Rarely	Yes	No	No
	Lepidochelys	*kempii*	Kemp's Ridley Sea Turtle	R	A	A	R	A	A	A	R	A	A	A	A	CR	E	NL	G1	30 min	unknown	7	unknown	Mostly	Sometimes	Rarely	Yes	No	No

Ainley et al. 2002
American Oystercatcher Working Group 2012
Austin et al. 1998
Ball 1994
Bordage and Savard 1995
Brown and Fredrickson 1997
Butler and Buckley 2002
Byrkjedal et al. 1995
Cairns 1992
Cramp et al. 1977
Crook et al. 2009
Dow 1964
Eadie et al. 1995
Eadie et al. 2000
ESS Group, Inc. 2005
Fjeldsa 1973
Garthe and Hüppop 2004
Gaston and Hipfner 2000
Gauthier 1993
Goudie et al. 2000
Guillemette et al. 2007
Harding et al. 2009
Hatch and Nettleship 1998
Hatch and Weseloh 1999
Hatch et al. 2000
Hays et al. 2001
Houghton et al. 2008
Howell 2012
IUCN 2010
Jenni and Gambs 1974
Johnsgard 1987
Kessel et al. 2002
Lavers et al. 2009
Lee and Haney 1996
Longcore et al. 2000
Lovvorn and Jones 1991
Lowther et al. 2002
McIntyre 1978
Michot et al. 2006
Montevecchi and Stenhouse 2002
Morton et al. 1989
Mowbray 2002
NatureServe 2012
NOAA 2012c
Nocera and Burgess 2002
Olsen and Larsson 2003
Palmer 1976
Poulton et al. 2002
Renaud 1995
Renaud and Carpenter 1994
Richman and Lovvorn 2008
Robertson and Goudie 1999
Robertson and Savard 2002
Rodway 1998
Ronconi and St. Clair 2002
Ruddock and Whitfield 2007
Savard et al. 1998
Scott and Chivers 2009
Sibley 2000
Simons and Hodges 1998
Southwood et al. 1999
Stedman 2000
Stout and Nuechterlein 1999
Sutherland 2009
Suydam 2000
Systad et al. 2000
Titman 1999
Tremblay et al. 2003
USFWS 2012
Westgate et al. 1995
Wiggins 2005
Woodin and Michot 2006
Woodin and Michot 2002
Wursig et al. 1998
Wynne and Schwartz 1999

6.5.2 Description of Terms, Categories, Scores, and Scoring Criteria within the Matrix

Occurrence describes the spatiotemporal distribution of each species within the AOCS region of interest (see above). The overall region is split into three subregions (Northeast, Midatlantic, Southeast), corresponding to the three BOEM planning regions that comprise the AOCS study region of interest. Within each subregion, abundances of each taxon are given for each of four seasons (winter, spring, summer, fall) defined by the solstices and equinoxes as per Northern Hemisphere convention. Crude abundance scores (A = abundant, R = rare) are given for each species in each subregion for each season, based on synthesis of a geospatial information sources listed in the footnote to the table.

Listing status includes the conservation/protected listing status of each species as classified by the following organizations, and with the following listing classifications.

International Union for the Conservation of Nature (IUCN) (Global Conservation Status)

The IUCN uses five criteria to determine if a taxa is threatened: (a) a declining population (past, present, and/or projected); (b) geographic range size, and fragmentation, decline or fluctuations; (c) small population size and fragmentation, decline, or fluctuations; (d) very small population or very restricted distribution; (e) quantitative analysis of extinction risk (e.g., population viability analysis). List categories and explanations as stated in the Red List Guidelines (IUCN 2010) are as follows:

Extinct (EX)—When there is no reasonable doubt that the last individual has died.

Extinct in the Wild (EW)—When a taxon is known only to survive in cultivations, in captivity, or as a naturalized populations (or populations) well outside the past range.

Critically Endangered (CR)—When the best available evidence indicates that it meets any of the criteria A to E for Critically Endangered, and it is therefore considered to be facing an extremely high risk of extinction in the wild.

Endangered (EN)—When the best available evidence indicates that it meets any of the criteria (a) to (e) for Endangered, and it is therefore considered to be facing a very high risk of extinction in the wild.

Vulnerable (VU)—When the best available evidence indicates that it meets any of the criteria (a) to (e) for Vulnerable, and it is therefore considered to facing a high risk of extinction in the wild.

Near Threatened (NT)—A taxon has been evaluated against the criteria but does not qualify for Critically Endangered, Endangered, or Vulnerable now, but it is close to qualifying for is likely to qualify for a threatened category in the near future.

Least Concern (LC)—A taxon has been evaluated against the criteria and does not qualify for Critically Endangered, Endangered, Vulnerable, or Near Threatened. Widespread and abundant taxa are included in this category.

Data Deficient (DD)—There is inadequate information of a taxon to make a direct, or indirect, assessment of its risk of extinction based on its distribution and/or population status.

Not Evaluated (NE)—A taxon has not yet been evaluated against the criteria.

NatureServe (Global Conservation Status)

Global ranking is established by NatureServe to assess the relative risk facing a species and does not imply that any specific action or legal status is needed to assure its survival. Ranking categories include:

GX—Presumed extinct (species) or eliminated (ecological communities)

GH—Possibly extinct (species) or eliminated (ecological communities)

G1—Critically imperiled: at very high risk of extinction due to extreme rarity (often 5 or fewer populations), very steep declines, or other factors.

G2—Imperiled: at high risk of extinction or elimination due to very restricted range, very few populations, steep declines, or other factors.

G3—Vulnerable: at moderate risk of extinction or elimination due to a restricted range, relatively few populations, recent and widespread declines, or other factors.

G4—Apparently secure: uncommon but not rare; some cause for long-term concern due to declines or other factors.

G5—Secure: Common; widespread and abundant.

G#G#—Range rank: used to indicate the range of uncertainty about the exact status of a taxon or ecosystem type.

Federal (US National Protected Status),

This column describes the status of species according to the US Endangered Species Act (ESA), with listing categories as follows,

NL = not listed

E = Endangered

T = Threatened

C = Candidate for listing (not currently listed)

State (US State Listing Status)

In this column, state-specific listing status is presented. Individual states in which species are listed are shown with the two-letter USPS abbreviations for US states. Listing designations are as follows:

NL = Not listed

E = Endangered

T = Threatened

SSC = Species of special concern

Diving Behavior Affecting Aerial Detectability

This set of four columns describes the amount of time that the species spends at water depths that render the animal undetectable to an aerial imaging camera, as follows:

Dive Times

Average durations of individual dives are reported here for species where such information is available in literature (see Table 6–16 note for information sources). The term surface feeder is used to describe many bird species whose diving behavior, if they dive at all, is restricted either to shallow dives (within 5 m of the surface, e.g., terns) or deeper, but very short duration dives (e.g., sulids). These species are not likely to be undetectable to aerial imaging cameras for significant periods of time. A bird diving deeper than 5 m may disappear from view for the duration of its dive time. Birds with longer dive times are more likely to be missed by aerial imaging, as the plane could pass by before they resurface. Marine mammals and turtles are only likely to be visible to aerial imaging cameras when they are close to the surface (generally within 5 m). Dive times for birds reflect averages of nonbreeding times for males and females together, and are an average of time ranges found in literature or are already presented as averages in literature (see Table 6–16 note for information sources). Maximum dive times are listed instead of average dive times for two species of cetaceans (Atlantic Spotted Dolphin and Harbor Porpoise) as no average or range of dive times was found. Dive times are listed as unknown for species for which no information on dive times was available in literature. Dive time for Loggerhead Sea Turtle represents a year-round average as reported by Renaud and Carpenter (1994), who noted that seasonal variation in diving behavior is present. We note that seasonal variation in diving behavior is not well known for most species of marine birds, mammals, or turtles, and may affect the results of aerial high-resolution imaging surveys.

Dive Pause Times

The amount of time that a diving animal is invisible to aerial cameras is a function not only of the duration of individual dives, but also the frequency of dives over the course of a day. The interval between dives is represented in this column (Table 6–16), reflecting the amount of time an animal spends on the surface in between dives, where such information is available. We note that this information is very poorly known for most species, particularly with respect to variation in diving frequency over the course of seasons, days, sexes, age classes, habitats, and weather conditions.

Visibility Scale

This is a scale we developed to reflect overall aerial visibility. It is based most strongly on the duration of individual dives, as such information is the most widely available information for most species. A score of 1 was assigned to species that do not dive under the water but are surface feeders,

as defined above for dive times. A score of 2 was assigned to diving birds whose individual average dive durations are typically less than 30 seconds. A score of 3 was assigned to species whose individual average dive durations were between 30 seconds and 1 minute. A score of 4 was assigned to species whose individual average dive durations were between 1 and 5 minutes. A score of 5 was assigned to species whose individual average dive durations were between 5 and 10 minutes. Scores of 6 through 9 reflect increasing individual average dive durations, roughly in increments of 10 minutes, where a score of 9 represents species whose individual average dive durations exceed 40 minutes. A score of 10 indicates species that are virtually never visible from the air. Exact dive times for some shearwater species were not found in literature, but based on the known dive time of the Manx Shearwater, all shearwaters were given a score of 2 on the visibility scale due to the fact that this group of birds are capable of diving and spending time under the surface. Likewise, all gadfly petrel species in the table were assigned surface feeder status based on information available for several congeners that occur outside of the AOCS region (Dark-rumped and Bonin Petrels, see Table 6–16 note)

6.5.3 Relative Sensitivity to Platforms

Some marine wildlife species may be difficult to survey accurately using conventional methods because these animals are known to be either attracted to, or repelled by, boats and/or low flying aircraft. For species with high or moderate sensitivity, aerial imaging surveys flown at higher altitudes are likely to represent a significant improvement over conventional survey methods, and possibly the only effective survey method for some species. The bird species most affected by conventional survey platforms include many species that spend much of their time sitting on the surface, such as sea ducks, loons, and alcids (Wiggins 2005; ESS Group 2005; Garthe 2004). Species were scored as unknown if no information on sensitivity to conventional survey platforms was available. Sensitivities for marine mammals were based primarily on studies involving low flying planes (Wursig 1998) and boats (Wynne 1999).

Taxonomic Depth of High-resolution Identification

This set of three columns describes the expected level of taxonomic depth that can potentially be achieved using high-resolution aerial imaging survey data. This level of depth is a function of the distinctiveness of appearance characteristics visible on the dorsal surface of animals. Scores of mostly, sometimes, rarely, or never are listed for three taxonomic levels as follows: group (greater than species-level appearance group, i.e., Black-backed Gulls, medium-sized terns, Chelonid turtles); species; and individual. Scores of sometimes at the species level mean that a species may possibly be confused with another. This includes most of the gulls, terns, skuas, jaegers, and alcids that are more difficult to distinguish between. Sometimes scores are also given in cases where there is distinct sexual, age-related, or seasonal variation in appearance features (see next set of columns Table 6–16). For example, King Eider and Common Eider males are visually distinct but females of the two species may be difficult to distinguish from one another, so both are recorded as sometimes identifiable to species level because of this. Mostly means a species will almost always be able to be identified and is not easily confused with other species. Examples of species that are mostly identifiable at the species level include Magnificent Frigatebird, Brown Pelican, Osprey, Bald Eagle, White-tailed and Red-billed Tropicbirds, and Leatherback sea turtles, as these species have unmistakable body shapes and/or color patterns visible in dorsal views that make them relatively easy to identify using aerial imagery. Rarely indicates that the taxon is very difficult to distinguish

from another. At the species level, this includes many of the female ducks. For example, female scoters look extremely similar in dorsal view, as do goldeneyes, many petrels, and storm-petrels. Behavioral considerations are also factored into expected identification frequency scores. For example, the male White-winged Scoter is given a sometimes score at the species level because the key feature by which it can be distinguished from other scoters—a white patch on the wing—is only visible to aerial viewing when the bird is in flight. Other patterns on species like wing stripes or colors on undertail coverts will not be visible in aerial images unless the bird species spends most of its time in flight. The identification of individual animals from aerial images will usually be impossible for birds, but it may be possible to observe features such as fluke patterns of Humpback Whales, scars on individual marine mammals, or barnacle patterns on sea turtles that enable the identification of a particular animal's individual identity.

Other Features Exhibiting Diagnostic Appearance Variation

This set of three columns indicates additional information that may be gathered under some circumstances using high-resolution aerial imaging for each species. Some bird, mammal, and turtle species exhibit distinct seasonal, sexual, or age-related patterns of variation in appearance features that are likely to be visible in aerial high-resolution imagery. Hence, this method can be used to gather useful data on these biological features for these species. Among the taxa in this matrix, sexual dimorphism occurs predominately in sea ducks, although sexual dimorphism in dorsal fin shape and tail length and thickness may be used to distinguish between sexes of killer whales and sea turtles, respectively, in some cases. Many sea ducks and gulls have age-distinct plumages that could potentially be used to derive useful information on these species, although complex patterns of variation and similarities among species may limit the extent of useful age-related information gathering from aerial imagery. Some birds exhibit seasonal variation in visible appearance features that may be discernible from aerial survey images. Examples include breeding versus nonbreeding plumages in loons and grebes, hood coloration in some terns and gulls, and bill color changes in gulls and terns, although the latter may be difficult to discern from aerial images.

7 Literature Cited

Ainley, D. G., Nettleship,D. N., Carter, H. R. and Storey, A. E. 2002. Common Murre (Uria aalge), The Birds of North America Online (Poole, A., Ed.). Ithaca: Cornell Lab of Ornithology; Retrieved from the Birds of North America Online: http://bna.birds.cornell.edu.bnaproxy.birds.cornell.edu/bna/species/666

Allison, T. D., Jedrey, E., Perkins, S. 2008. Avian issues for offshore wind development. Marine Technology Society Journal: 42:28–38.

American National Standards Institute (ANSI). 2000. Photography—Electronic still-picture cameras—Resolution measurements. ISO 12233–2000. http://webstore.ansi.org/RecordDetail.aspx?sku=ISO+12233%3a2000&source=google&adgroup=iso3&keyword=iso%2012233&gclid=CJ-_xYH137ICFQqZ4AodD1QAiw.

American Oystercatcher Working Group, Nol, E. and Humphrey, R. C. 2012. American Oystercatcher (Haematopus palliatus), The Birds of North America Online (Poole, A., Ed.). Ithaca: Cornell Lab of Ornithology; Retrieved from the Birds of North America Online: http://bna.birds.cornell.edu.bnaproxy.birds.cornell.edu/bna/species/082

Austin, J. E., Custer, C. M. and Afton, A. D. 1998. Lesser Scaup (Aythya affinis), The Birds of North America Online (Poole, A., Ed.). Ithaca: Cornell Lab of Ornithology; Retrieved from the Birds of North America Online: http://bna.birds.cornell.edu.bnaproxy.birds.cornell.edu/bna/species/338

Baayen, R. H., Davidson, D. J., Bates, D. M. (2008). Mixed-effects modeling with crossed random effects for subjects and items. Journal of Memory and Language, 59, 390–412.

Ball, J. P. 1994. Prey choice of omnivorous Canvasbacks: Imperfectly optimal ducks? Oikos, 70(2): 233–244.

Barton T. R., Barton C., Webb A. and Carter I. C. 1994. Seabird distribution in inshore waters of the western United Kingdom between Wick and St. David's Head from aerial surveys in 1987–1991. Joint Nature Cons. Comm. Rep. No. 183, Aberdeen.

Bates, D. M. and Maechler, M. (2009). lme4: Linear mixed-effects models using S4 classes. R package version 0.999375–32.

Begg, G. S., Reid, J. B., Tasker, M. L. and Webb A. 1997. Assessing the vulnerability of seabirds to oil pollution: sensitivity to spatial scale. Colonial Waterbirds 20: 339–352.

Blake B. F., Tasker M. L., Jones P. H., Dixon T. J., Mitchell R. and Langslow D. R. 1984. Seabird Distribution in the North Sea. Nature Conservancy Council, Huntingdon.

Boertmann, D., Olsen, K. and Due Nielsen , R. 2009. Seabirds and marine mammals in northeast Greenland. NERI Technical Report no. 721.

Bordage, D. and Savard, J. P. L. 1995. Black Scoter (Melanitta americana), The Birds of North America Online (Poole, A. Ed.). Ithaca: Cornell Lab of Ornithology; Retrieved from the Birds of North America Online: http://bna.birds.cornell.edu.bnaproxy.birds.cornell.edu/bna/species/177

Bräger, S. 1990. Results of waterfowl aerial surveys on the Baltic coast of Schleswig-Holstein in 1986–1990. Summ. lect. Joint Meeting IWRB's West. Pal. Seaduck Database. IWRB Newsletter December 1990: 20.

Brown, P. W. and Fredrickson, L. W. 1997. White-winged Scoter (Melanitta fusca), The Birds of North America Online (Poole, A., Ed.). Ithaca: Cornell Lab of Ornithology; Retrieved from the Birds of North America Online: http://bna.birds.cornell.edu.bnaproxy.birds.cornell.edu/bna/species/274

Brown, R. G. B., Nettleship D. N., Germain P., Tull C. E. and Davis T. 1975. Atlas of Eastern Canadian Seabirds. Can. Wildl. Serv., Bedford Inst. Ocean., Dartmouth.

Buckland, S. T., Anderson, D. R., Burnham, K. P. and Laake, J. L. 1993. Distance sampling: estimating abundance of biological populations. New York: Chapman and Hall. 446 pp.

Buckland, S. T., Anderson, D. R., Burnham, K. P., Laake, J. L., Borschers, D. L. and Thomas, L. 2001. Introduction to Distance Sampling. Estimating the abundance of biological populations. University Press, Oxford.

Buckland, S. T., Burt, M. L., Rexstad, E. A., Mellor, M., Williams, A. E. and Woodward, R. 2012. Aerial surveys of seabirds: the advent of digital methods. Journal of Applied Ecology doi: 10.1111/j.1365–2664.2012.02150.x

Burnham, K. P.,and Anderson, D. R., 2002. Model selection and multimodel inference: a practical information-theoretic approach. Springer-Verlag, New York.

Burt, L., Rexstad, E. and Buckland, S. 2009. Comparison of visual and digital aerial survey results of avian abundance for Round 3, Norfolk Region. Centre for Research into Ecological and Environmental Modelling, University of St. Andrews. Report Commissioned by Cowrie Ltd.

Burt, M. L., Rexstad, E. and Buckland, S. T. 2010. Comparison of design- and model-based estimates of seabird abundance derived from visual, digital still and digital video aerial surveys in Carmarthen Bay. Centre for Research into Ecological and Environmental Modelling, University of St. Andrews. Report Commissioned by Cowrie Ltd.

Burt, M. L., Rexstad, E. and S. T. Buckland. 2009. Comparison of visual and digital aerial survey results of avian abundance for Round 3, Norfolk Region. COWRIE Ltd.

Butler, R. G. and Buckley, D. E. 2002. Black Guillemot (Cepphus grylle), The Birds of North America Online (Poole, A. Ed.). Ithaca: Cornell Lab of Ornithology; Retrieved from the Birds of North America Online: http://bna.birds.cornell.edu.bnaproxy.birds.cornell.edu/bna/species/675

Byrkjedal, I., Eldoy, S., Grundetjern, S. and Loyning, M. K. 1995. Feeding Associations Between Red-Necked Grebes *Podiceps griseigena* and Velvet Scoters *Melanitta fusca* in Winter. Ibis, 139(1): 45–50.

Cairns, D. K. 1992. Diving behavior of black guillemots in northeastern Hudson Bay. Colonial Waterbirds, 15(2): 245–248.

Camphuysen, C. J. and Leopold, M. F. 1994. Atlas of seabirds in the southern North Sea. IBN Research report 94/6, NIOZ-Report 1994–8, Institute for Forestry and Nature Research, Netherlands Institute for Sea Research and Dutch Seabird Group, Texel.

Camphuysen, K. J., Fox, A. D., Leopold, M. F. and Petersen, I. K. 2004. Towards standardised seabirds at sea census techniques in connection with environmental impact assessments for offshore wind farms in the U.K.: a comparison of ship and aerial sampling methods for marine birds, and their applicability to offshore wind farm assessments (PDF, 2.7 mb), NIOZ report to COWRIE (BAM – 02–2002), Texel, 37pp.

Carter, I. C., Williams, J. M., Webb, A. and Tasker, M. L. 1993. Seabird concentrations in the North Sea: an atlas of vulnerability to surface pollutants. Joint Nature Conservation Committee, Aberdeen, 39pp.

Certain, G., and Bretagnolle, V. 2008. Monitoring seabirds population in marine ecosystem: The use of strip-transect aerial surveys. Remote Sensing of Environment. 112(8):3314–3322.

Clark, H. H. 1973. The language-as-fixed-effect fallacy: A critique of language statistics in psychological research. Journal of Verbal Learning and Verbal Behavior, 12, 335–359.

Cramp, S., Simmons, K. E. L., Ferguson-Lees, I. J., Gillmor, R., Hollom, P. A. D., Hudson, R., Nicholson, E. M., Ogilvie, M. A., Olney, P. J. S., Voous, K. H. and Wattel, J. 1977. Handbook of the Birds of Europe, the Middle East, and North Africa: The Birds of the Western Palearctic: Volume I Ostrich to Ducks. Oxford University Press, Oxford.

Crook, S. L., Conway, W. C., Mason, C. D. and Kraai, K. J. 2009. Winter Time-Activity Budgets of Diving Ducks on Eastern Texas Reservoirs. Waterbirds, 32(4): 548–558.

Dean, B. J., Webb, A., McSorley, C. A. and Reid, J. B. 2003. Aerial surveys of UK inshore areas for wintering seaduck, divers and grebes: 2000/01 and 2001/02. JNCC Report No. 333, Joint Nature Conservation Committee, Peterborough.

Degraer, S., Brabant, R. and Rumes, B., Eds. 2010. Offshore wind farms in the Belgian part of the North Sea: Early environmental impact assessment and spatio-temporal variability. Royal Belgian Institute of Natural Sciences, Management Unit of the North Sea Mathematical Models. Marine ecosystem management unit. 184 pp. + annexes

Desholm, M., and Kahlert, J. 2005. Avian collision risk at an offshore wind farm. Biology Letters 1:296–298.

Diederichs, A., Nehls, G. and Petersen, I. K. 2002. Flugzeugzählungen zur großflächigen Erfassung von Seevögeln und marinen Säugern als Grundlage für Umweltverträglichkeitsstudien im Offshorebereich. Seevögel 23: 38–46.

Doerffer, R., Schiller, H.; Fischer, J.; Preusker, R.; Bouvet, M. 2008. The Impact of Sun Glint on the Retrieval of Water Parameters and Possibilities for the Correction of MERIS Scenes. In Proceedings of the 2nd MERIS-(A)ATSR workshop, Frascati, Italy, September 22–26, 2008.

Dow, D. D. 1964. Diving times of wintering water birds. The Auk 81(4): 556–558.

Drewitt, A. L., and Langston, R. H. W. 2006. Assessing the impacts of wind farms on birds. IBIS 148(s1):29–42.

Durinck, J., Skov, H., Jensen, F. P. and Pihl, S. 1994. Important Marine Areas for Wintering Birds in the Baltic Sea. Ornis Consult report to the European Commission. 110 pp.

Eadie, J. M., Mallory, M. L. and Lumsden, H. G. 1995. Common Goldeneye (Bucephala clangula), The Birds of North America Online (Poole, A., Ed.). Ithaca: Cornell Lab of Ornithology; Retrieved from the Birds of North America Online: http://bna.birds.cornell.edu.bnaproxy.birds.cornell.edu/bna/species/170

Eadie, J. M., Savard, J. P. L. and Mallory, M. L. 2000. Barrow's Goldeneye (Bucephala islandica), The Birds of North America Online (Poole, A., Ed.). Ithaca: Cornell Lab of Ornithology; Retrieved from the Birds of North America Online: http://bna.birds.cornell.edu.bnaproxy.birds.cornell.edu/bna/species/548

ESS Group, Inc. 2005. Winter/Nocturnal Duck Survey Nantucket Sound, Massachusetts. ESS Group, Inc.

Fjeldsa, J. 1973. Feeding and habitat selection of the Horned Grebe, Podiceps auritus (Aves), in the breeding season. Vidensk Medd Dan Naturhist Foren 136: 57–95.

Garthe, S., and Hüppop, O. 2004. Scaling possible adverse effects of marine wind farms on seabirds: developing and applying a vulnerability index. Journal of Applied Ecology 41(4): 724–734.

Gaston, A. J. and Hipfner, J. M. 2000. Thick-billed Murre (Uria lomvia), The Birds of North America Online (Poole, A., Ed.). Ithaca: Cornell Lab of Ornithology; Retrieved from the Birds of North America Online: http://bna.birds.cornell.edu.bnaproxy.birds.cornell.edu/bna/species/497

Gauthier, G. 1993. Bufflehead (Bucephala albeola), The Birds of North America Online (Poole, A., Ed.). Ithaca: Cornell Lab of Ornithology; Retrieved from the Birds of North America Online: http://bna.birds.cornell.edu.bnaproxy.birds.cornell.edu/bna/species/067

Gill, A. B., Gloyne-Phillips, I., Neal, K. J. & Kimber, J. A. 2005. The potential effects of electromagnetic fields generated by sub-sea power cables associated with offshore wind farm developments on electrically and magnetically sensitive marine organisms – a review. Cowrie Report COWRIE-EM FIELD 2-06-2004

Goudie, R. I., Robertson, G. J. and Reed, A. 2000. Common Eider (Somateria mollissima), The Birds of North America Online (Poole, A., Ed.). Ithaca: Cornell Lab of Ornithology; Retrieved from the Birds of North America Online: http://bna.birds.cornell.edu.bnaproxy.birds.cornell.edu/bna/species/546

Groom, G. B., Petersen, I.K. and Fox, T. 2007. Sea bird distribution data with object based mapping of high spatial resolution image data. In: Mills, J. and Williams, M. (Eds.): Challenges for earth observation—scientific, technical and commercial. Proceedings of the Remote Sensing and Photogrammetry Society Annual Conference 2007, 11th–14th September 2007, Newcastle University, Nottingham, UK. The Remote Sensing and Photogrammetry Society. Paper 168.

Groom, G., Petersen, I. K. and Anderson, M. D. In press. Numbers and distribution of Lesser Flamingos analyzed with object based mapping of high spatial resolution image data. In: Harebottle, D. M. Craig, A. J. F. K., Anderson, M. D., Rakotomanana, H. and Muchai,

M. (Eds). Proceedings of the 12th Pan-African Ornithological Congress, 2008. Cape Town, Animal Demography Unit

Groom, G., Petersen, I. K., Anderson, M. D., and Fox, A. D. 2011. Using object-based analysis of image data to count birds: mapping of lesser flamingo at Kamfers Dam, Northern Cape, South Africa. International Journal of remote Sensing 32: 4611–4639. Doi: 10.1080/01431161.2010.489068

Guillemette, M., Pelletier, D., Grandbois, J. M., Butler, P. J. 2007. Flightlessness and the energetic cost of wing molt in a large sea duck. Ecology, 88. 11: 2936–2945

Hammer, Ø., Harper, D. A. T. and Ryan, P. D. 2001. PAST: Paleontological Statistics software package for education and data analysis. Paleontologica Electronica 4(1): 9 pp.

Hammond, P. S. 1995. Estimating abundance of marinine mammals: a North Atlantic Perspective. In Whales, Seals, Fish and Man. Proceedings of the International Symposium on the Biology of Marine Mammals in the North East Atlantic. 29 November – 1 December 1994.

Harding, A. M. A., Egevang, C., Walkusz, W., Merkel, F., Blanc, S. and Gremillet, D. 2009. Estimating Prey Capture Rates of a Planktivorous Seabird, the Little Auk (*Alle alle*), using Diet, Diving Behaviour, and Energy Consumption. Polar Biol, 32: 785–796.

Hatch, J. J. and Weseloh, D. V. 1999. Double-crested Cormorant (Phalacrocorax auritus), The Birds of North America Online (Poole, A., Ed.). Ithaca: Cornell Lab of Ornithology; Retrieved from the Birds of North America Online: http://bna.birds.cornell.edu.bnaproxy.birds.cornell.edu/bna/species/441

Hatch, J. J., Brown, K. M., Hogan, G. G. and Morris, R. D. 2000. Great Cormorant (Phalacrocorax carbo), The Birds of North America Online (Poole, A., Ed.). Ithaca: Cornell Lab of Ornithology; Retrieved from the Birds of North America Online: http://bna.birds.cornell.edu.bnaproxy.birds.cornell.edu/bna/species/553

Hatch, S. A. and Nettleship, D. N. 1998. Northern Fulmar (Fulmarus glacialis), The Birds of North America Online (Poole, A., Ed.). Ithaca: Cornell Lab of Ornithology; Retrieved from the Birds of North America Online: http://bna.birds.cornell.edu.bnaproxy.birds.cornell.edu/bna/species/361

Hays, G. C., Akesson, S., Broderick, A. C., Glen, F., Godley, B. J., Luschi, P., Martin, C., Metcalfe, J. D. and Papi, F. 2001. The diving behavior of green turtles undertaking oceanic migration to and from Ascension Island: dive durations, dive profiles and depth distribution. The Journal of Experimental Biology, 204: 4093–4098.

Hedley, J. D., Harborne, A. R. and Mumby, P.J. 2005. Simple and robust removal of sun glint for mapping shallow-water benthos. International Journal of Remote Sensing 26(10):2107–2112.

Heikkila, J., and Silven, O. 1997. A Four-step Camera Calibration Procedure with Implicit Image Correction. Proc. IEEE Computer Society Conference on Computer Vision and Pattern Recognition, San Juan, Puerto Rico, p. 1106–1112.

Henkel, L. A., Ford, R. G., Tyler, W. B. and Davis, J. N. 2007. Comparison of aerial and boat-based survey methods for Marbled Murrelets Brachyramphus marmoratus and other marine birds. Marine ornithology 35: 145–151.

Hexter, R. 2009a. High Resolution Video Survey of Seabirds and Mammals in the Norfolk Area. HiDef Aerial Surveying Limited, Report Commissioned by Cowrie Ltd.

Hexter, R. 2009b. High Resolution Video Survey of Seabirds and Mammals in the Rhyl Flats Area. HiDef Aerial Surveying Limited, Report Commissioned by Cowrie Ltd.

Hochberg, E. J., Andrefouet, S. and Tyler, M. R. 2003. Sea surface correction of high spatial resolution Ikonos images to improve bottom mapping in near-shore environments. IEEE Transactions on Geoscience and Remote Sensing, 41, pp. 1724–1729.

Houghton, J. D. R., Cedras, A., Myers, A. E., Liebsch, N., Metcalfe, J. D., Mortimer, J. A., Hays, G. C. 2008. Measuring the state of consciousness in a free-living diving sea turtle. Journal of Experimental Marine Biology and Ecology 356: 115–120.

Howell, S. 2012. Petrels, Albatrosses and Storm-Petrels of North America: A Photographic Guide. Princeton University Press, New Jersey.

Hyrenbach, K. D., Henry, M. F., Morgan, K. H., Welch, D. W., and Sydeman, W. J., 2007. Optimizing the width of strip transects for seabird surveys from vessels of opportunity. Marine Ornithology 35:29–38.

Image Science and Analysis Laboratory, NASA-Johnson Space Center. 2012. The Gateway to Astronaut Photography of Earth. <http://eol.jsc.nasa.gov/>10/05/2012 10:51:27.

Inger, R., Atrrill, M. J., Bearhop, S., Broderick, A. C., Grecian, W. J., Hodgson, D. J., Mills, C., Sheehan, E., Votier, S. C., Witt, M. J., and Godley, B. J. 2009. Marine renewable energy: potential benefits to biodiversity? An urgent call for research. Journal of Applied Ecology 46:1145–1153.

IUCN Standards and Petitions Subcommittee. 2010. Guidelines for using the IUCN Red List categories and criteria. Version 8.1. Prepared by the Standards and Petitions Subcommittee in March 2010. Downloadable from http://intranet.iucn.org/webfiles/doc/SSC/RedList/RedListGuidelines.pdf.

Jenni, D. A. and Gambs, R. D. 1974. Diving times of grebes and masked ducks. The Auk 91(2): 415–417.

Joensen, A. H. 1968. Wildfowl Counts in Denmark in November 1967 and January 1968. Danish Review of Game Biology 5: 1–72.

Joensen, A. H. 1973. Moult migration and wing-feather moult of seaducks in Denmark. Danish Review of Game Biology 8: 1–42.

Joensen, A. H. 1974. Waterfowl populations in Denmark 1965–73. Danish Review of Game Biology 9: 1–206

Johnsgard, P. A. 1987. Diving Birds of North America: Species Accounts—Loons (Gaviidae). University of Nebraska-Lincoln.

Joint Nature Conservation Committee (JNCC). 2012. Seabirds at Sea. http://jncc.defra.gov.uk/page-1547

Kay, S., Hedley, J. D., Lavender, S., 2009. Sun glint correction of high and low spatial resolution images of aquatic scenes: a review of methods for visible and near infrared wavelengths. Remote Sensing 1, 697e730.

Kessel, B., Rocque, D. A. and Barclay, J. S. 2002. Greater Scaup (Aythya marila), The Birds of North America Online (Poole, A., Ed.). Ithaca: Cornell Lab of Ornithology; Retrieved from the Birds of North America Online: http://bna.birds.cornell.edu.bnaproxy.birds.cornell.edu/bna/species/650

Komdeur, J., Bertelsen, J. and Cracknell, G. (eds) 1992. Manual for Aeroplane and Ship Surveys of Waterfowl and Seabirds. IWRB Special Publ. No. 19, National Environmental Research Institute Kalø.

Krijgsveld, K. L., Fijn, R. C., Japink, M., Van Horssen, P. W., Heunks, C., Collier, M. P., Poot, M. J. M., Beuker, D., Dirksen, S. 2011. Effect studies Offshore Wind Farm Egmond aan Zee: Final report on fluxes, flight altitudes and behaviour of flying birds. NoordzeeWind report nr OWEZ_R_231_T1_20111114_flux&flight, Bureau Waardenburg report nr 10–219.

Laake, J. L. and Borchers, D. L. 2004. Methods for incomplete detection at distance zero. 108–189 in Buckland, S.T., Anderson D.R., Burnham, K.P., Laake, J.L., Borchers, D.L. and Thomas, L. Advanced Distance Sampling. Oxford University Press, Oxford. Laake and Borchers (2004)

Laist, D., Knowlton, A., Mead, J., Collet, A., and Podesta, M. 2001. Collisions between ships and whales. Marine Mammal Science, 17(1), 35–75.

Langston, R. H. W. 2010. Offshore wind farms and birds: Round 3 zones, extensions to Round 1 and Round 2 sites and Scottish Territorial Waters. RSPB Research Report No. 39.

Larsen, J. K., and Guillemette, M. 2007. Effects of wind turbines on flight behaviours of wintering common eiders: implications for habitat use and collision risk. Journal of Applied Ecology 44:516–522.

Laursen, K., Frikke, J., Kahlert, J. 2008. Accuracy of total counts of waterbirds from aircraft in coastal waters. Wildlife Biology, 14(2):165–175.

Laursen, K., Pihl, S., Durinck, J., Hansen, M., Skov, H., Frikke, J. and Danielsen, F. 1997. Numbers and distribution of waterbirds in Denmark 1987–89. Danish Review of Game Biology 15: 1–181.

Lavers, J., Hipfner, M., Chapdelaine, G. and Hipfner, J. M. 2009. Razorbill (Alca torda), The Birds of North America Online (Poole, A., Ed.). Ithaca: Cornell Lab of Ornithology; Retrieved from the Birds of North America Online: http://bna.birds.cornell.edu.bnaproxy.birds.cornell.edu/bna/species/635

Lee, D. S. and Haney, J. C. 1996. Manx Shearwater (Puffinus puffinus), The Birds of North America Online (Poole, A., Ed.). Ithaca: Cornell Lab of Ornithology; Retrieved from the

Birds of North America Online: http://bna.birds.cornell.edu.bnaproxy.birds.cornell.edu/bna/species/257

Longcore, J. R., Mcauley, D. G., Hepp, G. R. and Rhymer, J. M. 2000. American Black Duck (Anas rubripes), The Birds of North America Online (Poole, A., Ed.). Ithaca: Cornell Lab of Ornithology; Retrieved from the Birds of North America Online: http://bna.birds.cornell.edu.bnaproxy.birds.cornell.edu/bna/species/481

Lovvorn, J. R. and Jones, D. R. 1991. Effects of body size, body fat, and change in pressure with depth on buoyancy and costs of diving in ducks (Aythya spp.) *Can. J. Zool*. **69:** 2879–2887.

Lowther, P. E., Diamond, A. W., Kress, S. W., Robertson, G. J. and Russell, K. 2002. Atlantic Puffin (Fratercula arctica), The Birds of North America Online (Poole, A., Ed.). Ithaca: Cornell Lab of Ornithology; Retrieved from the Birds of North America Online: http://bna.birds.cornell.edu.bnaproxy.birds.cornell.edu/bna/species/709

Maclean, I. M. D, Wright, L. J., Showler, D. A. and Rehfisch, M. M. 2009. A Review of Assessment Methodologies for Offshore Windfarms. British Trust for Ornithology Report Commissioned by Cowrie Ltd.

Maes, F., Cliquet, A., Seys, J., Meire, P. and Offringa, H. 2000. Limited Atlas of the Belgian part of the North Sea. Federal Office for Scientific, Technical, and Cultural Affairs, Brussels, 1–31.

McIntyre, J. W. 1978. Wintering Behavior of Common Loons. The Auk, 95(2): 396–403.

Mellor, M. and Maher, M. 2008. Full Scale Trial of High Definition Video Survey for Offshore Windfarm Sites. HiDef Aerial Surveying Limited, Report commissioned by COWRIE.

Mellor, M., Craig, T., Baillie, D. and Woolaghan, P. 2007. Trial of High Definition Video Survey and its Applicability to Survey of Offshore Windfarm Sites. HiDef Aerial Surveying Limited, Report commissioned by COWRIE.

Melsheimer, C., and Kwoh, L. K. 2001. Sun glitter in SPOT images and the visibility of oceanic phenomena, Paper presented at the 22nd Asian Conference on Remote Sensing, 5–9 November 2001, Singapore.

Michot, T. C., Woodin, M. C., Adair, S. E. and Moser, E. B. 2006. Diurnal Time-activity Budgets of Redheads (*Aythya americana*) Wintering in Seagrass Beds and Coastal Ponds in Louisiana and Texas. Hydrobiologia, 567: 113–128.

Montevecchi, W. A. and Stenhouse, I. J. 2002. Dovekie (Alle alle), The Birds of North America Online (Poole, A., Ed.). Ithaca: Cornell Lab of Ornithology; Retrieved from the Birds of North America Online: http://bna.birds.cornell.edu.bnaproxy.birds.cornell.edu/bna/species/701

Morton, J. M., Fowler, A. C. and Kirpatrick, R. L. 1989. Time and Energy Budgets of American Black Ducks in Winter. The Journal of Wildlife Management, 53(2): 401–410.

Mowbray, T. B. 2002. Canvasback (Aythya valisineria), The Birds of North America Online (Poole, A., Ed.). Ithaca: Cornell Lab of Ornithology; Retrieved from the Birds of North America Online: http://bna.birds.cornell.edu.bnaproxy.birds.cornell.edu/bna/species/659

National Oceanic and Atmospheric Administration (NOAA). 2012a. Marine Multipurpose Cadastre: http://www.marinecadastre.gov/default.aspx).

National Oceanic and Atmospheric Administration (NOAA). 2012b. Earth System Research Laboratory Monitoring Division. http://www.esrl.noaa.gov/gmd/grad/solcalc. Accessed on March 26, 2012.

National Oceanic and Atmospheric Administration (NOAA). 2012c. Fisheries. Species Under the Endangered Species Act (ESA). www.nmfs.noaa.gov/pr/species/esa/

NatureServe. 2012. NatureServe Explorer. http://www.natureserve.org/explorer/

Nedwell, J. R., Parvin, S. J., Edwards, B., Workman, R., Brooker, A. G. and Kynoch, J. E. 2007. Measurement and interpretation of underwater noise during construction and operation of offshore windfarms in UK waters. Subacoustech Report No. 544R0738 to COWRIE Ltd.

New Jersey Department of Environmental Protection (NJDEP), Office of Science. 2010. Ocean/wind power ecological baseline studies, Vol. II: avian studies. Prepared by Geo-Marine, Inc., Trenton, New Jersey, USA.

Nocera, J. J. and Burgess, N. M. 2002. Diving schedules of Common Loons in varying environments. Can. J. Zool. 80: 1643–1648.

Normandeau Associates, Inc. 2011. New insights and new tools regarding risk to Roseate Terns, Piping Plovers, and Red Knots from wind facility operations on the Atlantic Outer Continental Shelf. A final report for the U. S. Department of the Interior, Bureau of Ocean Energy Management, Regulation and Enforcement, Report # BOEMRE 048-2011. Contract # M08PC20060. 287 pp.

O'Connell, A. F., Gardner, B., Gilbert, A. T., and Laurent, K. 2009. Compendium of avian occurrence information for the continental shelf waters along the atlantic coast of the united states, final report (database section—seabirds). Prepared by the USGS Patuxent Wildlife Research Center, Beltsville, MD. U.S. Department of the Interior, Geological Survey, and Bureau of Ocean Energy Management Headquarters, OCS Study BOEM 2012–076.

O'Connell, A., Spiegel, C. S., and Johnson, S. 2011. Compendium of avian occurrence information for the continental shelf waters along the atlantic coast of the united states, final report (database section—shorebirds). Prepared by the U.S. Fish and Wildlife Service, Hadley, MD for the USGS Patuxent Wildlife Research Center, Beltsville, MD. U.S. Department of the Interior, Geological Survey, and Bureau of Ocean Energy Management Headquarters, OCS Study BOEM 2012–076.

Olsen, K. and Larsson, H. 2003. Gulls of Europe, Asia and North America. Christopher Helm, London.

Palmer, R. S. 1976. Handbook of North American Birds. Vol. 3. Yale Univ. Press, New Haven, CT.

Paton, P., Winiarski, K., Trocki, C., McWilliams, S. 2010. Spatial Distribution, Abundance, and Flight Ecology of Birds in Nearshore and Offshore Waters of Rhode Island. Interim

Technical Report for the Rhode Island Ocean Special Area Management Plan 2010. http://www.crmc.ri.gov/samp_ocean/11-PatonAvianReptV3_reduced.pdf

Petersen, I. K. 2007. Modelling total numbers and distribution of Common Scoter *Melanitta nigra* at Horns Rev. National Environmental Research Institute University of Aarhus, Denmark, Report Commissioned by DONG Energy.

Petersen, I. K., MacKenzie, M. L., Rexstad, E., Wisz, M. S. and Fox, A. D. 2011. Comparing pre- and post-construction distributions of long-tailed ducks *Clangula hyemalis* in and around the Nysted offshore wind farm, Denmark : a quasi-designed experiment accounting for imperfect detection, local surface features and autocorrelation University of St Andrews. 16 p. (CREEM Technical Report; 2011–1)

Plonczkier, P. and Simms, I. C. 2012. Radar monitoring of migrating Pink-footed Geese: behavioural responses to offshore wind farm development. Journal of Applied Ecology 49(5)1187–1194.

Pollock, C. M., Mavor, R., Weir, C., Reid, A., White, R. W., Tasker, M. L., Webb, A. and Reid, J. B. 2000. The distribution of seabirds and marine mammals in the Atlantic Frontier, north and west of Scotland. Seabirds and Cetaceans, Joint Nature Conservation Committee, Aberdeen.

Poulton, V. K., Lovvorn, J. R., Takekawa, J. Y. 2002. Clam Density and Scaup Feeding Behavior in San Pablo Bay, California. The Condor, 104(3): 518–527.

Powers, K. D. 1982. A comparison of two methods of counting birds at sea. Journal of Field Ornithology 53: 209–222.

R Development Core Team. 2011. R: A language and environment of statistical computing. R Foundation for Statistical Computing. Vienna, Austria. http://www.R-project.org.

Renaud, M. L. 1995. Movements and Submergence Patterns of Kemp's Ridley Turtles (Lepidochelys kempii). Journal of Herpetology, 29(3): 370–374.

Renaud, M. L. and Carpenter, J. A. 1994. Movements and Submergence Patterns of Loggerhead Turtles (Caretta caretta) in the Gulf of Mexico Determined Through Satellite Telemetry. Bulletin of Marine Science, 55(1): 1–15.

Rexstad, E. and Buckland, S. T. 2009. Comparison of aerial survey methods for estimating abundance of common scoters. Final report submitted to Defra, July 2009. http://research-repository.st-andrews.ac.uk/bitstream/10023/784/1/CREEM%20technical%20report%202009-1.pdf

Richman, S. E. and Lovvorn, J. R. 2008. Costs of diving by wing and foot propulsion in a sea duck, the white-winged scoter. *Journal of Comparative Physiology* B 178:321–332

Robertson, G. J. and Goudie, R. I. 1999. Harlequin Duck (Histrionicus histrionicus), The Birds of North America Online (Poole, A., Ed.). Ithaca: Cornell Lab of Ornithology; Retrieved from the Birds of North America Online: http://bna.birds.cornell.edu.bnaproxy.birds.cornell.edu/bna/species/466

Robertson, G. J. and Savard, J. P. L. 2002. Long-tailed Duck (Clangula hyemalis), The Birds of North America Online (Poole, A., Ed.). Ithaca: Cornell Lab of Ornithology; Retrieved

from the Birds of North America Online: http://bna.birds.cornell.edu.bnaproxy.birds.cornell.edu/bna/species/651

Rodway, M. S. 1998. Activity patterns, diet, and feeding efficiency of Harlequin Ducks breeding in northern Labrador. Canadian Journal of Zoology 76(5): 902–909.

Ronconi, R. A. and St. Clair., C. C. 2002. Management options to reduce boat disturbance on foraging black guillemots (*Cepphus grylle*) in the Bay of Fundy. Biological Conservation 108, 265–271.

Ruddock, M., and Whitfield, D. P. 2007. A Review of Disturbance in Selected Bird Species. Natural Research (Projects) Ltd to Scottish Natural Heritage.

Savard, J. P. L., Bordage, D. and Reed, A. 1998. Surf Scoter (Melanitta perspicillata), The Birds of North America Online (Poole, A., Ed.). Ithaca: Cornell Lab of Ornithology; Retrieved from the Birds of North America Online: http://bna.birds.cornell.edu.bnaproxy.birds.cornell.edu/bna/species/363

Scott, M. and Chivers, S. 2009. Movements and Diving Behavior of Pelagic Spotted Dolphins. Publications, Agencies and Staff of the U.S. Department of Commerce. Paper 46.

Seys, J. 2001. Sea- and coastal bird data as tools in the policy and management of Belgian marine waters. PhD thesis, University of Gent, 133+69 pp.

Shoop, C. R., and Kenney, R. D. 1992. Seasonal distributions and abundances of loggerhead and leatherback sea turtles in waters of the northeastern United States. Herpetological Monographs, 6, 1992, 43–67.

Sibley, D. A. 2000. The Sibley Guide to Birds. Chanticleer Press, Inc., New York.

Simons, T. R. and Hodges, C. N. 1998. Dark-rumped Petrel (Pterodroma phaeopygia), The Birds of North America Online (Poole, A., Ed.). Ithaca: Cornell Lab of Ornithology; Retrieved from the Birds of North America Online: http://bna.birds.cornell.edu.bnaproxy.birds.cornell.edu/bna/species/345doi:10.2173/bna.345

Skov, H., Durinck, J., Leopold, M. F. and Tasker, M. L. 1995. Important bird areas for seabirds in the North Sea, including the Channel and the Kattegat. Birdlife International, Cambridge, 156pp.

Skov, H., Upton, A. J., Reid, J. B., Webb, A., Taylor, S. J. and Durinck, J. 2002. Dispersion and vulnerability of marine birds and cetaceans in Faroese waters. Joint Nature Conservation Committee, Peterborough.

Southwood, A. L., Andrews, R. D., Lutcavage, M. E., Paladino, F. V., West, N. H., George, R. H. and Jones, D. R. 1999. Heart rates and diving behavior of leatherback sea turtles in the Eastern Pacific Ocean. The Journal of Experimental Biology 202: 1115–1125.

Stedman, S. J. 2000. Horned Grebe (Podiceps auritus), The Birds of North America Online (Poole, A., Ed.). Ithaca: Cornell Lab of Ornithology; Retrieved from the Birds of North America Online: http://bna.birds.cornell.edu.bnaproxy.birds.cornell.edu/bna/species/505

Stone, C. J., Webb, A., Barton, C., Ratcliffe, N., Reed, T. C., Tasker, M. L., Camphuysen, C. J. and Pienkowski, M. W. 1995. An atlas of seabird distribution in north-west European waters. Joint Nature Conservation Committee Report, Peterborough.

Stout, B. E. and Nuechterlein, G. L. 1999. Red-necked Grebe (Podiceps grisegena), The Birds of North America Online (Poole, A., Ed.). Ithaca: Cornell Lab of Ornithology; Retrieved from the Birds of North America Online: http://bna.birds.cornell.edu.bnaproxy.birds.cornell.edu/bna/species/465

Sutherland, I. T. 2009. Foraging behavior of wild Tufted Duck Aythya fuligula in winter. Wildfowl 59: 53–61.

Suydam, R. S. 2000. King Eider (Somateria spectabilis), The Birds of North America Online (Poole, A., Ed.). Ithaca: Cornell Lab of Ornithology; Retrieved from the Birds of North America Online: http://bna.birds.cornell.edu.bnaproxy.birds.cornell.edu/bna/species/491

Systad, G. H., Bustnes, J. O.,Erikstad, K. E. 2000. Behavioral responses to decreasing day length in wintering sea ducks. The Auk, 117: 33–40.

Tasker, M. L., Jones P. H., Dixon T. J. and Blake B. F. 1984. Counting seabirds at sea from ships: a review of methods employed and a suggestion for a standardized approach. Auk 101: 567–577.

Tasker, M. L., Webb, A., Hall, A. J., Pienkowski, M. W. and Langslow, D. R. 1987. Seabirds in the North Sea. Nature Conserv. Council, Peterborough.

Tasker, M. L., Webb, A., Harrison, N. M. and Pienkowski, M. W. 1990. Vulnerable concentrations of marine birds west of Britain. Nature Conservancy Council, Peterborough: 1–45.

Taylor, S. J. and Reid, J. B. 2001. The distribution of seabirds and cetaceans around the Faroe Islands. Joint Nature Conservation Committee, Peterborough, 68pp.

Thaxter, C. B. and Burton, N. H. K. 2009. High Definition Imagery for Surveying Seabirds and Marine Mammals: A Review of Recent Trials and Development of Protocols. British Trust for Ornithology Report Commissioned by Cowrie Ltd.

Thaxter, C. B., Daunt, F., Hamer, K. C., Watanuki, Y., Harris, M. P., Grémillet, D., Peters, G. and Wanless, S. 2009. Sex-specific food provisioning in a monomorphic seabird, the common guillemot *Uria aalge*: nest defence, foraging efficiency or parental effort? Journal of Avian Biology 40: 75–84.

Thaxter, C. B., Wanless, S., Daunt, F., Harris, M. P., Benvenuti, S., Watanuki, Y., Grémillet, D. and Hamer, K. C. 2010. Influence of wing loading on trade-off between pursuit-diving and flight in common guillemots and razorbills. Journal of Experimental Biology 213: 1018–1025.

Thomas, L., Laake, J. L., Rexstad, E., Strindberg, S., Marques, F. F. C., Buckland, S. T., Borchers, D. L., Anderson, D. R., Burnham, K. P., Burt, M. L., Hedley, S. L., Pollard, J. H., Bishop, J. R. B. and Marques, T. A. 2009. Distance 6.0. Release 2. Research Unit for Wildlife Population Assessment, University of St. Andrews, UK. http://www.ruwpa.st-and.ac.uk/distance

Thomsen, F. 2010. Sound impacts. In Huddleston, J. (ed). Understanding the environmental impacts of offshore windfarms. COWRIE. Pp 32–43.

Titman, R. D. 1999. Red-breasted Merganser (Mergus serrator), The Birds of North America Online (Poole, A., Ed.). Ithaca: Cornell Lab of Ornithology; Retrieved from the Birds of North America Online: http://bna.birds.cornell.edu.bnaproxy.birds.cornell.edu/bna/species/443

Tremblay, Y., Cherel, Y., Oremus, M., Tveraa, T. and Chastel, O. 2003. Unconventional Ventral Attachment of Time-depth Recorders as a New Method for Investigating Time Budget and Diving Behavior of Seabirds. The Journal of Experimental Biology, 206: 1929–1940.

U.S. Department of Energy (USDOE). 2008. 20% wind energy by 2030: increasing wind energy's contribution to U.S. Electricity Supply. USDOE report # DOE/GO-102008-2567

U.S. Fish and Wildlife Service (USFWS). 2012. Endangered Species Program. http://www.fws.gov/endangered/.

Webb A., Stronach A., Tasker M.L., Stone C.J. and Pienkowski M.W. 1995. Seabird concentrations around south and west Britain—an atlas of vulnerability to oil and other surface pollutants. Joint Nature Conservation Committee, Aberdeen, 38pp.

Weng, J., Cohen, P., Herniou, M. 1992. Camera Calibration with Distortion Models and Accuracy Evaluation. Proc. IEEE Transactions on Pattern Analysis and Machine Intelligence, Vol. 14, No. 10, pp. 965–980.

Westgate, A. J., Read, A. J., Berggren, P., Koopman, H. N., Gaskin, D. E. 1995. Diving behaviour of harbour porpoise, *Phocoena phocoena*. Can. Fish. Aquat. Sci. 52: 1064–1073.

Wiggins, D. A. 2005. Harlequin Duck (*Histrionicus histrionicus*): A technical conservation assessment. USDA Forest Service, Rocky Mountain Region.

Wilson, B. Batty, R. S., Daunt, F. and Carter, C. 2007. Collision risks between marine renewable energy devices and mammals, fish and diving birds. Report to the Scottish Executive. Scottish Association for Marine Science, Oban, Scotland, PA37 1QA.

Wilson, J., Elliott, M., Cutts, N., Mander, L., Mendão, V., Perez-Dominguez, R., and Phelps, A. 2010. Coastal and Offshore Wind Energy Generation: Is It Environmentally Benign? Energies 3:1383–1422; doi:10.3390/en3071383

Wiltschko, W., and Wiltschko, R. 2005. Magnetic orientation and magnetoreception in birds and other animals. Journal of Comparative Physiology A, 191(8), 675–693.

Woodin, M. C. and Michot, T. C. 2002. Redhead (Aythya americana), The Birds of North America Online (Poole, A., Ed.). Ithaca: Cornell Lab of Ornithology; Retrieved from the Birds of North America Online: http://bna.birds.cornell.edu.bnaproxy.birds.cornell.edu/bna/species/695

Woodin, M. C. and Michot, T. C. 2006. Foraging behavior of redheads (*Aythya Americana*) wintering in Texas and Louisiana. *Hydrobiologia.* 567:129–141

Wursig, B., Lynn, S. K., Jefferson, T. A. and Mullin, K. D. 1998. Behavior of cetaceans in the northern Gulf of Mexico relative to survey ships and aircraft. Aquatic Mammals 24.1: 41–50.

Wynne, K. and Schwartz, M. 1999. Guide to Marine Mammals and Turtles of the U.S. Atlantic and Gulf of Mexico. Rhode Island Sea Grant, University of Rhode Island, Narragansett, RI.

The Department of the Interior Mission

As the Nation's principal conservation agency, the Department of the Interior has responsibility for most of our nationally owned public lands and natural resources. This includes fostering the sound use of our land and water resources, protecting our fish, wildlife and biological diversity; preserving the environmental and cultural values of our national parks and historical places; and providing for the enjoyment of life through outdoor recreation. The Department assesses our energy and mineral resources and works to ensure that their development is in the best interests of all our people by encouraging stewardship and citizen participation in their care. The Department also has a major responsibility for American Indian reservation communities and for people who live in island communities.

The Bureau of Ocean Energy Management

The Bureau of Ocean Energy Management (BOEM) works to manage the exploration and development of the nation's offshore resources in a way that appropriately balances economic development, energy independence, and environmental protection through oil and gas leases, renewable energy development and environmental reviews and studies.

www.boem.gov